AER/AGS Open File Report 2020-06

New Evidence for Cretaceous Depositional Changes in the Alberta Foreland Basin Triggered by Tectonism in the Southern Canadian Rocky Mountains

AER/AGS Open File Report 2020-06

New Evidence for Cretaceous Depositional Changes in the Alberta Foreland Basin Triggered by Tectonism in the Southern Canadian Rocky Mountains

D.I. Pană[1] and P.E. Smith[2]

[1]Alberta Energy Regulator
Alberta Geological Survey

[2]TerraChron Corp.

March 2021

ISBN 978-1-4601-4929-4

If you use information from this publication in other publications or presentations, please acknowledge the AER/AGS. We recommend the following reference format:

Pană, D.I. and Smith, P.E. (2021): New evidence for Cretaceous depositional changes in the Alberta foreland basin triggered by tectonism in the Southern Canadian Rocky Mountains; Alberta Energy Regulator / Alberta Geological Survey, AER/AGS Open File Report 2020-06, 121 p.

Publications in this series have undergone only limited review and are released essentially as submitted by the author.

Author address:
P.E. Smith
TerraChron Corp.
University of Toronto
Suite 331
60 St. George Street
Toronto, ON M5S 1A7
Canada
Tel: 416.978.2947
Email: psmith@physics.utoronto.ca

Published March 2021 by:
Alberta Energy Regulator
Alberta Geological Survey
4th Floor, Twin Atria Building
4999 – 98th Avenue
Edmonton, AB T6B 2X3
Canada

Tel: 780.638.4491
Fax: 780.422.1459
Email: AGS-Info@aer.ca
Website: www.ags.aer.ca

Contents

Tables

Figures

Acknowledgements

We thank Dean Rokosh, Chris Filewich, and Matt Grobe for critical review and editing of the original manuscript.

Abstract

A new set of muscovite, biotite, feldspar, and whole rock $^{40}Ar/^{39}Ar$ ages has been obtained from the Rocky Mountain fold-and-thrust belt (RM-FTB) and from its western margin along the northern segment of the Southern Rocky Mountain Trench (SRMT). Two phyllonite samples from the Monarch and Moose Pass thrusts in the Main Ranges of the Rockies yielded less well constrained $^{40}Ar/^{39}Ar$ ages of ca. 131 Ma (whole rock) and ca. 135 Ma (muscovite), respectively. The classical $^{40}Ar/^{39}Ar$ dating technique proved inefficient in providing age dates in poorly recrystallized fault rocks of the shallower thrusts in the Alberta Rockies to the east. Thus, the sheared rocks of the McConnell and Burnt Timber Creek thrust faults yielded erroneous dates (mixed between detrital and tectonic ages). A feldspar grain from a sheared and slickensided sandstone sample of the Brazeau Formation in front of the Brazeau thrust yielded a well constrained plateau age of 130 Ma, likely representing the source crystallization/cooling age. Deeper faults on the western margin of the Rocky Mountains are generally marked by phyllonite, more amenable to classical $^{40}Ar/^{39}Ar$ dating. Four sericite samples from the oblique compression Bear Foot thrust and the associated Valemount strain zone in its footwall yielded exclusively late Campanian-earliest Maastrichtian ages (ca. 73–71 Ma). One biotite sample from the eastern margin of this zone yielded a biotite plateau age of 87 Ma. Four samples from the strike-slip Walker Creek fault zone yielded Early Cretaceous (ca. 133–124 Ma), mid-Cretaceous (ca. 111–96 Ma), and weak Late Cretaceous (ca. 85–68 Ma) pulses. These fault zones merge with the northern segment of the SRMT. Nine $^{40}Ar/^{39}Ar$ ages from phyllite and phyllonite with conspicuous subhorizontal stretching lineation and steeply dipping foliation collected along 200 km of this segment, indicate two Early Cretaceous (ca. 135 and ca. 125 Ma), two mid-Cretaceous (ca. 115–111 Ma and ca. 101–96 Ma), and two Late Cretaceous (ca. 85 Ma and ca. 74–72 Ma) peaks of transpressional tectonism and define the Southern Rocky Mountain Trench shear zone (SRMTSZ).

The new structural and geochronological data from the Main Ranges and from the three, merging strike- and oblique-slip shear/fault zones at the western margin of the Rockies indicate protracted Cretaceous deformation, apparently as distinct pulses of mainly orogen-parallel tectonism. The tectonic pulses identified in this study are consistent with tectonothermal events previously reported from the eastern Omineca belt and document the kinematic link inferred, but not documented between the Foreland belt and its hinterland. More importantly, the tectonic pulses are contemporaneous with important depositional changes in the Alberta foreland basin. Thus, the Early Cretaceous phyllonite ages suggest a previously unrecognized out-of-sequence thrusting pulse in the western RM-FTB contemporaneous and kinematically linked to the initial transpression along the SRMTSZ. Valanginian ages of ca. 135–131 Ma may record a phase of tectonic loading of the North American margin accompanied by the development of a forebulge that corresponds to the extensive pre-Cadomin–pre-Mannville (“sub-Cretaceous”) unconformity in the foreland basin. The early Aptian ages of 128–123 Ma may record the subsequent orogenic uplift accompanied and outlasted by vigorous erosion in the proto-Rockies and deposition of extensive Cadomin gravel sheets in the proximal portion of the foreland. The late Aptian–earliest Albian ages of 115–111 Ma are contemporaneous with the Moosebar sea transgression, which suggests a new phase of tectonic loading that triggered downwarping of the foreland basin floor (i.e., creation of accommodation space). The mid-Cretaceous tectonic pulse (101–96 Ma) is quasi-contemporaneous with the development of the Dunvegan fluvial system. Finally, the latest Cretaceous compressional pulses at the western margin of the Rockies (79–71 Ma)—best recorded by the Bear Foot thrust and the Valemount strain zone—are contemporaneous with major Campanian thrusting in the Front Ranges (tectonic loading), that triggered crustal down-warping accompanied by the last major transgression (Bearpaw sea) in the Alberta Basin.

1 Introduction

Stratigraphic sequences in the Mesozoic Alberta foreland basin have resulted from tectonic loading events (i.e., emplacement of thrust sheets) in the Rocky Mountains, triggered by terrane accretion and changes in plate boundary dynamics. Understanding the tectonic/structural evolution of the Rocky Mountain fold-and-thrust belt (RM-FTB), particularly the timing of the tectonic pulses is critical in defining the stratigraphic sequences and their rank in the Alberta foreland basin.

Radiometric ages from regionally distributed thrust-fault gouge collected in the Alberta portion of the RM-FTB have shown that the eastward propagation of the RM-FTB occurred in four orogenic pulses (Late Jurassic, mid-Cretaceous, Late Cretaceous, and late Paleocene-early Eocene) that correlate with tectonic events of the Cordilleran interior and with depositional patterns in the adjacent foreland (Pană and van der Pluijm, 2015). There are however, major depositional events (e.g., the extensive Aptian Cadomin gravel sheets) and long non-depositional periods (the "sub-Cretaceous" unconformity) in the Alberta Basin that are not yet directly related to contemporaneous Cordilleran tectonic events. It is reasonable to assume that the record of tectonic events corresponding to such depositional anomalies exist in the still untested western portion of the RM-FTB.

This report includes new results of $^{40}Ar/^{39}Ar$ dating on gouge and phyllonite collected from the RM-FTB. We have sampled a cataclastic silt from the shallow Burnt Timber Creek thrust and a striated Brazeau sandstone in front of the Brazeau thrust in the Foothills, and highly sheared shales in the immediate hanging wall of the McConnell thrust that marks the boundary between Foothills and Front Ranges of the Alberta Rockies. From the Main Ranges, west of the town of Jasper, we analyzed poorly recrystallized phyllonite samples from the Monarch and Moose Pass thrusts, two major thrusts that straddle the Alberta–British Columbia Border. In addition, we have collected and tested phyllonite samples from several tectonic discontinuities farther west: specifically, from the dextral oblique thrust known as the Bear Foot thrust and its immediate footwall (the "Valemount strain zone"); from phyllite and phyllonite samples collected along the northern 200 km stretch of the 600 km long Southern Rocky Mountain Trench (SRMT), between the Kinbasket Lake (52°42'N), and Walker Creek (53°47'N), and lastly from the Walker Creek fault zone (McMechan, 2000), which is the kinematic link between the SRMT and the Northern Rocky Mountain Trench (NRMT) (Roddick, 1967; Price and Carmichael, 1986; Struik, 1993) (Figure 1).

Our structural and geochronological data indicate protracted tectonic activity, which started in the Early Cretaceous (ca. 135 Ma) as a kilometres-wide zone of orogen-parallel crustal yielding in the northern segment of the SRMTSZ and was kinematically linked to at least the Monarch and Moose Pass thrusts in the Main Ranges of the RM-FTB. This tectonic event may correspond to the "sub-Cretaceous" unconformity followed by the extensive deposition of gravel sheets of the late Early Cretaceous Cadomin Formation in the Alberta Basin. Over time, strike-slip strain gradually concentrated into narrower mid- and Late Cretaceous belts within the SRMTSZ and the adjacent Walker Creek fault zone and into the mainly Campanian Valemount dextral oblique compression strain zone. This event coincides with the emplacement of several major thrusts in the Front Ranges and with the westward transgression of the Bearpaw sea in the Alberta Basin.

2 Regional Geology

The RM-FTB in the eastern portion of the Canadian Cordilleran orogen stretches from 49°N (Canada–U.S. border) to 60°N latitude (Liard River) in western Canada and consists of overlapping thrust sheets and detached folds. To the west, the RM-FTB is bound by the Northern Rocky Mountain Trench (NRMT) in northeastern British Columbia and the Southern Rocky Mountain Trench (SRMT) from southeastern British Columbia into Montana. The two segments of the Trench form a continental scale physiographic feature consisting of a chain of valleys about 1600 km long by 5–15 km wide (inset in Figure 1).

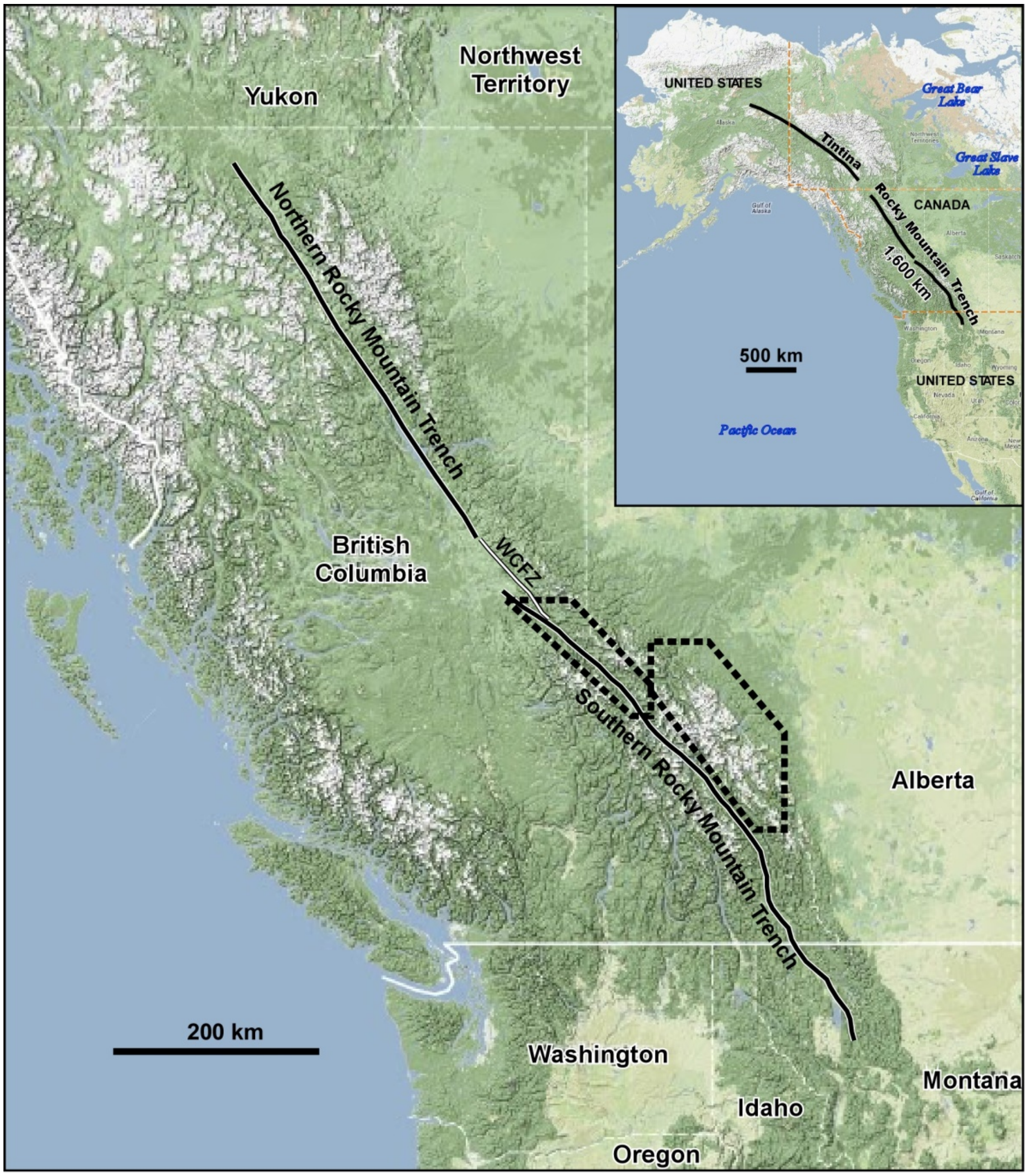

Figure 1. Location of the investigated areas (black outlined areas) relative to the Rocky Mountain Trench in the Canadian Cordillera.

The eastern boundary of the RM-FTB in Alberta, from 49°N to the British Columbia border (Figure 2), is the elusive "eastern limit of Cordilleran deformation," arbitrarily traced east of the easternmost deformed strata known in outcrop and/or subsurface (Pană and Elgr, 2013).

The SRMT separates the RM-FTB to the east from the Omineca belt and the Purcell Anticlinorium (the latter is geologically part of the RM-FT; McMechan and Thompson, 1989; 1992) of the southern Canadian Cordillera to the west. Compressional deformation structures are dominant on either side of the Rocky Mountain Trench and record protracted interaction between North America and the Pacific oceanic lithosphere and its island arcs. The craton moved northwestward during 240–180 Ma, westerly between 180–160 Ma northward until ~140 Ma and then southwestward until present with an interval of westerly movement between 120–60 Ma (Monger and Gibson, 2019).

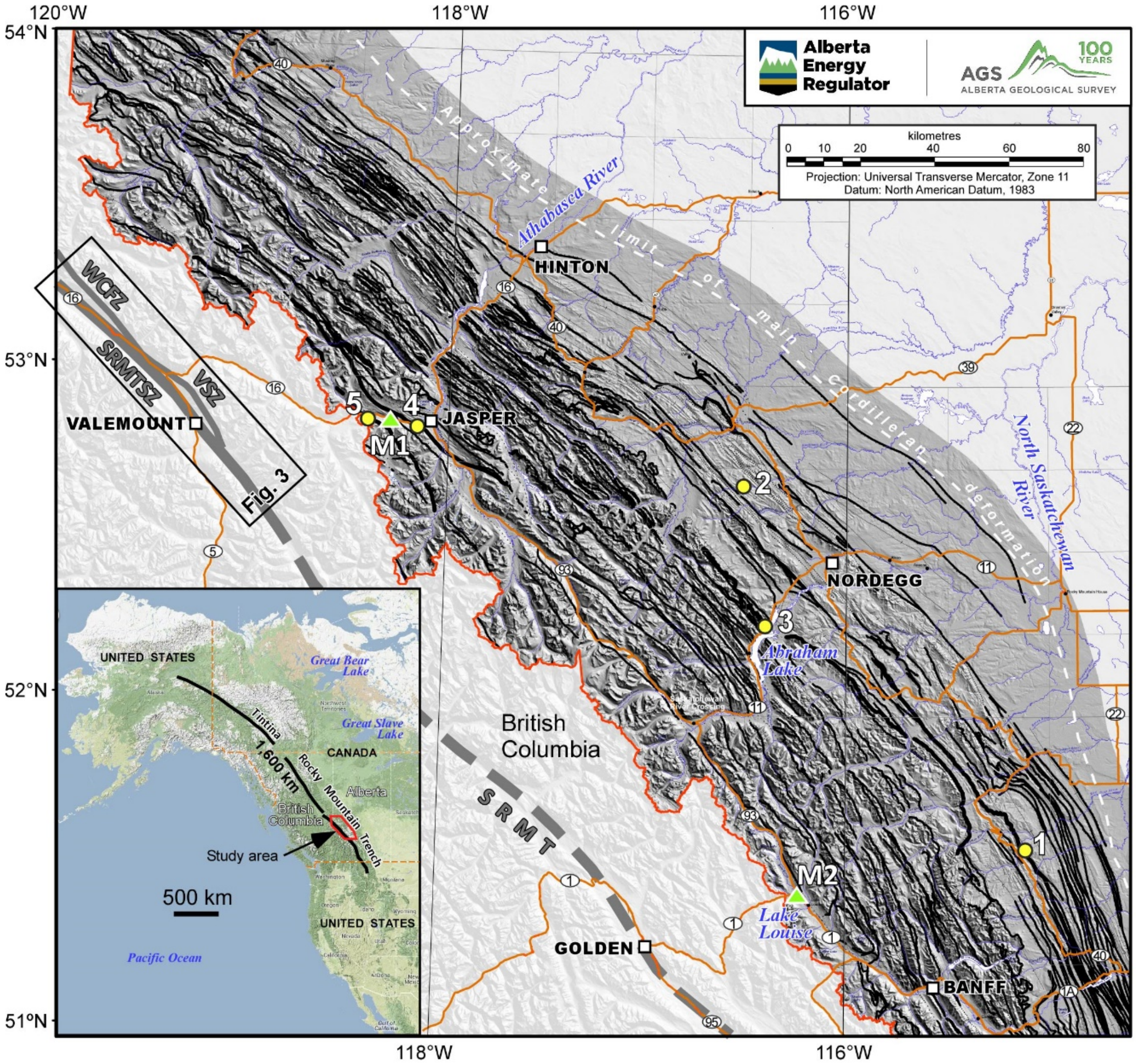

Figure 2. Sample location map of the Rocky Mountain fold-and thrust-belt, simplified after Pană and Elgr (2013). SRMT = Southern Rocky Mountain Trench; SRMTSZ = Southern Rocky Mountain shear zone; WCFZ = Walker Creek fault zone; VSZ = Valemount strain zone. Numbers 1 to 5, and M1 and M2 represent sample locations.

On the west side of the SRMT at the latitude of our study is the Omineca belt, the region of overlap between ancestral North America and, from east to west, pericratonic (marginal or "suspect" Kootenay), accreted oceanic (Slide Mountain), and fringing arc (Quesnellia-Stikinia) terranes. The imbrication and overthrust of terranes onto North America are inferred to have started during the Pliensbachian–Toarcian (ca. 187–173 Ma; Nixon et al., 1993; 1997; 2020; Murphy et al., 1995) and lasted into the early Eocene. Compressional tectonism resulted in a zone of penetrative shortening and metamorphism that trends approximately north-northwest across the Selkirk-Cariboo-Monashee mountains of the southeastern Omineca belt (e.g., Okulitch, 1984; Monger et al., 1982; 1986; Ghent and Simony, 2005). The Omineca belt is locally overprinted by Eocene extensional deformation (e.g., Monger and Price, 2002; Evenchick et al., 2007).

Middle Jurassic shortening and crustal thickening up to 50–55 km in the Omineca belt involved tectonic wedging, basement-cover detachment, and complex deformation of the detached supracrustal rocks (e.g., Simony et al., 1980; Price, 1986; Brown et al., 1986; Brown and Journeay, 1987; Murphy, 1987; Struik, 1988; Colpron et al., 1996; 1998; Gibson et al., 2008). Southwest-verging overturned or recumbent folds, nappes and thrusts accompanied by regional metamorphism involved mainly the Neoproterozoic Windermere Supergroup and latest Neoproterozoic–lower Cambrian Hamill Group and the lower Paleozoic Lardeau Group. At the latitude of our study, the intensity of Jurassic metamorphism reached upper amphibolite facies in the western Selkirk Mountains (Colpron et al., 1996; Gibson et al., 2008), and decreased northwesterly to low-grade in the northern Monashee Mountains (Raeside and Simony, 1983), to low- and very low-grade in the Cariboo Mountains (Reid et al., 2002). Major structures formed during the Jurassic contraction are sealed by the 174 Ma Hobson pluton in the Cariboo Mountains (Gerasimoff, 1988) and by the 167 Ma Adamant pluton in the Selkirk Mountains (Gibson et al., 2008).

Subsequent recurrent tectonothermal events in the Selkirk-Monashee-Cariboo mountains (the SMC metamorphic complex of Crowley et al., 2000) of the southeastern Omineca belt reached peak metamorphic conditions in different areas at different times: from Early Cretaceous in southeastern Cariboo Mountains (Currie, 1988), to mid-Cretaceous in the northern Monashee Mountains (Sevigny et al., 1990; Scammell, 1991; 1992; 1993), to Late Cretaceous and Paleocene in distinct linear domains of the northeastern Monashee Mountains near the SRMT (Crowley et al., 2000), and to Paleocene in the northwestern Monashee Mountains (Digel et al., 1998).

Paleoproterozoic "autochthonous" North American basement in the Omineca belt is exposed in tectonic windows in structural culminations such as the Monashee and Malton complexes; these structural culminations also expose the décollement at the interface between basement and its "parautochthonous" cover represented by Neoproterozoic Windermere Supergroup and Paleozoic formations (e.g., Parrish and Armstrong, 1983; Brown et al., 1986; Carr, 1995; Johnson and Brown, 1996; Johnson, 2006). The east-verging structures (F2 and F3) in the southeastern Omineca belt were inferred to be Late Jurassic to Paleocene and congruent with the structures across the central segment of the SRMT in the western RM-FTB (Currie, 1988; Residae and Simony, 1983; Sevigny and Simony, 1989; Gibson et al., 2008).

On the east side of the SRMT, the Canadian RM-FTB consists of east-verging overlapping thrust sheets and detached folds formed between Late Jurassic and early Eocene within an easterly-tapering wedge of Middle Proterozoic to early Cenozoic sedimentary (with minor igneous) rocks that were deposited on the ancestral western margin of North America (Price, 1981; McMechan and Thompson, 1992; Pană and van der Pluijm, 2015; Pană et al., 2018a, b). A profound unconformity separates the sedimentary cover from the normal thickness or attenuated Paleoproterozoic and older crystalline crust of ancestral North America (e.g., Price, 1994).

Orthogneiss cores of easterly overturned or recumbent folds (the Yellowjacket, Bulldog, Blackman, and Hugh Allan gneiss bodies) exposed in thrust slices of the westernmost RM-FTB along the east side of the SRMT (Figures 2, 3) have been also interpreted as slices of North American basement (Oke and Simony, 1981; McDonough and Simony, 1984; 1986; 1988b; McDonough and Parrish, 1991). Their relationships with the adjacent stratigraphy of the RM-FTB are discussed in the next section.

3 Geology of the Investigated Western Margin of the Rocky Mountains

Our study area includes a portion of the RM-FTB and the northern segment of the SRMT between 52°42'N and 53°47'N latitude with a focus on the western margin of the Rocky Mountains mostly underlain by the Neoproterozoic Windermere Supergroup (Figures 1–3). The Windermere Supergroup includes the Horsethief Creek, Kaza, Cariboo, and Miette groups deposited on the western passive margin of ancestral North America (e.g., Campbell, 1968; 1970; 1973; Campbell et al. 1973; 1982; Carey and Simony, 1985; Pell and Simony, 1987; Ross, 1991; Ross and Arnott, 2007; McMechan, 2015). These stratigraphic units consist of southeastward-tapering granule conglomerate, pelite, and carbonate, and indicate crustal thinning and stretching, processes initiated with the 800–700 Ma emplacement of alkaline and carbonatite intrusions during the breakup of Rodinia (e.g., Millonig et al., 2012).

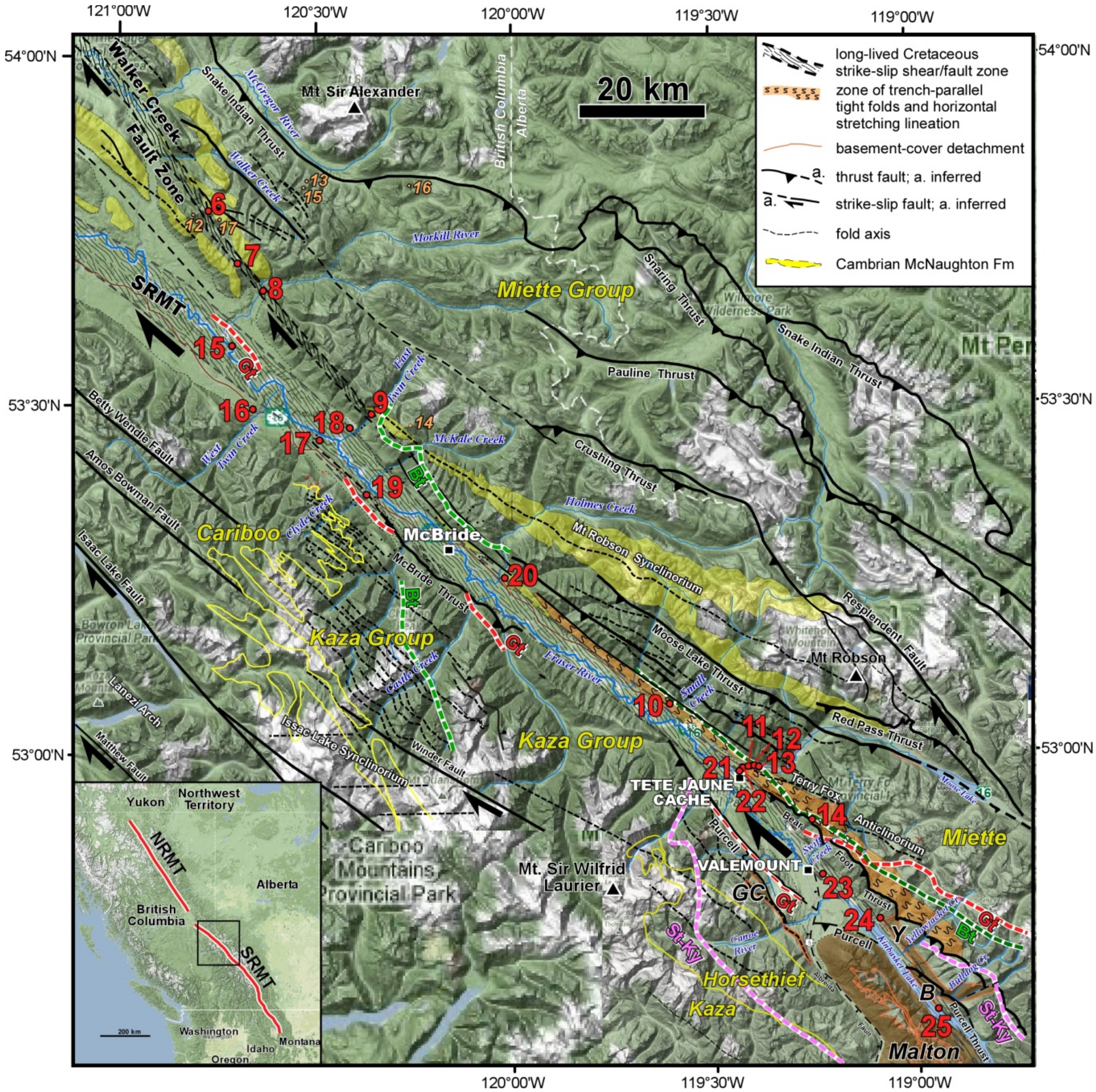

Figure 3. Sample location map of the northern segment of the Southern Rocky Mountain Trench (SRMT) area between Walker Creek and northern Kinbasket Lake (northern rectangle in Figure 1). Orange dots are sample locations dated by K-Ar with numbers representing the last two digits of the Sample ID as in Table 1. Red dots are locations of samples analyzed in this study with numbers as in Table 2. The green, red, and pink dashed lines represent biotite (Bt), garnet (Gt) and staurolite-Kyanite (St-Ky) isogrades. The yellow solid line represents group contacts. Simplified geology compiled from Mountjoy (1980), McDonough and Murphy (1994), Ross and Ferguson (2003), Ferguson and Ross (2003), McMechan (1996), and Reid et al. (2002). B – Bulldog orthogneiss; GC – Gold Creek orthogneiss; NRMT – Northern Rocky Mountain Trench; Y – Yellowjacket orthogneiss.

In the Rocky Mountains, the Neoproterozoic strata are assigned to the Miette Group. Very similar lithological assemblages have been recognized on either side of the investigated segment of the SRMT (Figure 3). The Miette Group of the RM-FTB is partly correlative with the Kaza Group of the Omineca belt in the McBride area (McMechan, 1996; Ferguson and Ross, 2003), and with parts of Horsethief Group of the Omineca belt in the Kinbasket Lake area (McDonough and Simony, 1988a; 1989).

North of Valemount, the east flank of the Trench is underlain by the Neoproterozoic Miette Group (Windermere Supergroup) with a sliver of Cambrian McNaughton quartzite between Holmes Creek and McBride (Figure 3) (Mountjoy, 1980; McDonough and Murphy, 1994; Ferguson and Ross, 2003). The Old Fort Point Formation mapped in the middle Miette Group in the Rocky Mountains (McDonough and Murphy, 1994; Ferguson and Ross, 2003) has been also recognized across the SRMT between the middle and upper Kaza in the Cariboo Mountains (Ferguson and Ross, 2003). The Walker Creek fault zone on the east side of the Trench, merges with the Trench south of the town of McBride; farther south along the east side of the Trench between Holmes Creek and Tête Jaune Cache, we have observed subhorizontal lineation within a 2–3 km wide zone of tight folds initially identified by Mountjoy (1980) (Figure 3). This belt projects to the southeast into the pre- to synmetamorphic Bear Foot thrust and its footwall "Valemount strain zone" (McDonough and Simony, 1989; McDonough and Murphy, 1994).

South of Valemount on the east side of the SRMT (here occupied by the Kinbasket Lake), several Paleoproterozoic orthogneiss slices are exposed in thrust sheets on the western slopes of the Selwyn Range (part of the Main Ranges of the Rocky Mountains) (Figures 2, 3). From north to south these are the structurally lower Yellowjacket gneiss carried in the hanging wall of the synmetamorphic Bear Foot thrust and the overlying Bulldog gneiss carried by the postmetamorphic Purcell thrust (McDonough, 1984; McDonough and Simony, 1988a, b; 1989). Across the Trench at the north end of the Monashee Mountains, the Malton gneiss complex consists of the Paleoproterozoic Malton orthogneiss and its metasedimentary cover (e.g., Morrison, 1979; 1982). McDonough and Simony (1984; 1988a, b, 1989) interpreted the Malton orthogneiss in the Omineca and the Yellowjacket-Bulldog gneiss units across the Trench as slices of the same gneiss complex, despite apparent geochemical and geophysical dissimilarities identified by Chamberlain and Lambert (1985a, b) and Chamberlain et al. (1979; 1980). Some 30 km south of Bulldog Creek, the Mount Blackman gneiss is underlain by a premetamorphic shear zone and overlain by the postmetamorphic Purcell thrust, which carries the Hugh Allan Creek gneiss (Oke and Simony, 1981; Oke, 1982; Mountjoy et al., 1984, Mountjoy and Forest, 1986, Mountjoy, 1988).

All the thrust sheets on the east side of Kinbasket Lake (west margin of the Rockies) have been described to consist of orthogneiss infrastructure overlain by decollement zones carrying parautochtonous metasedimentary cover (Oke and Simony, 1981; McDonough, 1984; McDonough and Simony, 1988b; 1989). The more micaceous gneiss and micaschist were typically interpreted as metasedimentary cover and assigned to the Neoproterozoic lower Miette Group, partly equivalent with the Horsethief Creek Group of the southeastern Omineca (McDonough and Simony, 1988a; 1989). The micaceous sequences commonly assigned to the cover are often intercalated with orthogneiss and have variable thickness and lithological composition in different thrust sheets.

Along the trunk road on east side of northern Kinbasket Lake, Murphy (1990) reported a vertical shear zone with subhorizontal lineation in the Yellowjacket gneiss, showing dextral displacement parallel to the Trench. Trench-parallel subhorizontal lineation was subsequently mapped throughout the Bulldog and Yellowjacket units (McDonough and Murphy, 1994). Farther south, the Hugh Allen Creek gneiss contains a subvertical strike-slip shear zone with a 10°SE plunging lineation, which parallels the local trend of the Trench (Oke and Simony, 1981).

From north to south in the investigated area, biotite, garnet, and staurolite-kyanite isogrades crosscut the tectonic contacts from the metasedimentary cover of the orthogneiss nappes and thrusts into the underlying Miette strata homotaxial with the stratigraphy of the western Rockies (McDonough at al., 1991a, b; McDonough and Murphy, 1994). Although the isograds are difficult to trace across the Trench, the metamorphic zonation in the Rockies appears to roughly correspond to that of the adjacent Omineca belt. Farther south, between the Selkirk Mountains of the Omineca belt and Solitude Range of the western Rockies, models of pre- and postmetamorphic thrusting are compatible with late, southwest dipping normal faulting along the trench (Gal et al., 1989; Gal and Ghent, 1990).

The controversy over the nature and magnitude of faulting in the SRMT leading to the variety of interpretations (Murphy, 1984, 1990, 2007; Mattauer et al., 1983; van den Driessche and Malusky, 1986;

Price and Carmichael 1986; McDonough and Murphy, 1994; McMechan, 2000) reflects, in part, the paucity of outcrop in the floor of much of the SRMT. Between the towns of McBride and Valemount, the SRMT is a flat area up to 10 km wide largely covered by Quaternary alluvial and lacustrine deposits. The few isolated outcrops within the trench expose highly sheared and transposed equivalents of Neoproterozoic Cariboo Group sedimentary units mapped in the Cariboo Mountains (Ross and Ferguson, 2003). Around Valemount, the floor of the trench is overlain mostly by post-glacial sand dunes. To the southeast, for more than 185 km, the trench floor is occupied by Kinbasket Lake, which hinders the examination of field relationships between the orthogneiss slices in the Rockies and the Malton orthogneiss, as well as the relationships between their metamorphosed cover sequences; specifically, Miette Group of the Rockies and the Horsethief Group of the Omineca belt.

4 Previous Geochronological Data

4.1 Rocky Mountains

Unlike many other fold-and-thrust belts where the age of thrusting can be inferred from field relationships (e.g., age of hanging wall and footwall formations, dated igneous rocks plugging thrusts and/or stratigraphic units of well-constrained age sealing the thrusts), thrusting in the RM-FTB could only be indirectly deduced based on depositional features in the Alberta basin or involvement of the youngest strata in deformation. Thus, the RM-FTB was considered to have evolved between the first record of westerly derived clastic sediments from the Cordilleran orogen deposited in the Kimmeridgian strata of the upper Fernie Formation (McMechan et al., 2006; Raines et al., 2013; Quinn et al., 2016) and the latest record of compression recorded by the involvement of Paleocene–earliest Eocene Paskapoo Formation in the Foothills deformation (e.g., Entrance, Grease Creek, Williams Creek synclines; Ancona and Brewster Creek thrusts). The cessation of compression must have predated the earliest record of extension: early Oligocene graben fill (Kishenehn Formation) in the hanging wall of the Flathead fault in the southernmost Canadian Rockies.

Several apatite fission track studies hinted to uplift, erosion, and cooling of the RM-FTB above 70 to 110°C for typical apatite (using the number of fission events produced from the spontaneous decay of uranium-238 in common accessory minerals to date the time of rock cooling below closure temperature), and about 230 to 250°C for zircon during the Paleocene: 65–60 Ma (Donelick and Beaumont, 1990); 60 Ma (McDonough et al., 1995); 59 Ma (Sears, 2001); 74–59 Ma (Hoffman et al., 1976); 60–55 Ma (Kalkreuth and McMechan, 1988, 1996); 59 Ma (Arne and Zentilli, 1994). Direct dating of fault gouge collected from individual thrusts documented four orogenic pulses (Late Jurassic, mid-Cretaceous, Late Cretaceous, and early Eocene) separated by relatively long periods of tectonic quiescence (van der Pluijm et al., 2006; Pană and van der Pluijm, 2015).

4.2 Western Margin of the Rockies and the Southern Rocky Mountain Trench

On the western margin of the Rockies, the Yellowjacket granodiorite orthogneiss samples yielded U-Pb emplacement ages of ca. 1870 Ma (zircon and allanite) and ca. 1872 Ma (zircon) with imprecise Permian lower intercept ages; two leocogranite samples from the Bulldog Creek gneiss unit yielded ages of 1870 Ma and 1866 Ma (McDonough and Parrish, 1991). Well-defined arrays in the Yellowjacket and Bulldog Creek orthogneiss samples indicate contemporaneous emplacement of the granitoid protoliths at ca. 1870 Ma with some Archean component [$\varepsilon Nd_{(1870\ Ma)}$ values of -3.4 and -2.6], whereas the lower intercepts appear to record a period of Pb loss in monazite from migmatitic schist possibly related to late Paleozoic, post-Antler tectonometamorphic events in the latest Mississippian (326 ±36 Ma) and Permian (276 ±19 Ma; 259 ±34 Ma; McDonough and Parrish, 1991). A felsic gneiss from the Mount Blackman unit yielded a U-Pb zircon age of 1950 Ma and an amphibolite produced a whole-rock Rb-Sr age of 1860 ±50 Ma (Chamberlain and Lambert, 1985b) in the 1870–1860 Ma range of the Yellowjacket and Bulldog Creek gneisses. The Hugh Allan Creek orthogneiss, the only gneiss body affected by polyphase migmatization

(Oke and Simony, 1981), yielded Rb-Sr ages of 900 Ma and 805 ±11 Ma (Chamberlain et al., 1979; Chamberlain and Lambert, 1985b), and a leucogranite yielded a U-Pb zircon crystallization age of ca. 736 Ma, with an imprecise Jurassic lower intercept age of 173 ±78 Ma (McDonough and Parrish, 1991).

Instead, a K-Ar biotite age of 72 ±5 Ma was reported from a retrogressed, foliated and lineated Bulldog biotite gneiss along the road on the eastern side of northern Kinbasket Lake—just a few kilometres south along strike from Murphy's (1990) strike-slip shear zone—and "may date an important tectonic and metamorphic episode in the Late Cretaceous near the Rocky Mountain Trench" (Wanless et al., 1967). A Late Cretaceous "orogenesis" (low-grade metamorphism accompanied by folding, cleavage development, thrust and strike-slip faulting) propagating from the trench was proposed by Charlesworth et al. (1967). These authors reported whole-rock and muscovite K-Ar ages from arenaceous rocks and slates of the Neoproterozoic Miette Group collected along Highway 16, ranging from 69 Ma (age of orogenesis) near the Rocky Mountain Trench (Tête Jaune Cache) to 1770 Ma (age of the muscovite source rocks), eastwards towards the town of Jasper.

Van den Driessche and Maluski (1986) reported $^{40}Ar/^{39}Ar$ ages of 78 ±2 Ma from muscovite and 100 ±2 Ma from biotite recovered from a sample of sheared Miette conglomerate collected at an unspecified location near Tête Jaune Cache. The authors proposed a mid-Cretaceous (?) age for the syn- to late-tectonic metamorphic minerals in their orogen-parallel zone of high strain along the Trench, which is roughly coincident with the mapped trace of the Purcell thrust.

North of McBride, McMechan and Roddick (1991) produced whole rock K-Ar ages using the less than 1 µm size fraction in an attempt to date the very low- to low-grade tectonometamorphic imprint on the Neoproterozoic Miette Group and Cambrian McNaughton Formation of the western Rocky Mountains. They reported ages ranging from 261 to 141 Ma, which have limited—if any—geological significance (Table 1).

Across the Trench in the Malton gneiss complex, the Precambrian age of the orthogneiss was initially inferred based on discordant U-Pb zircon dates of ca. 2500 Ma and 1300–1200 Ma, and Rb-Sr ages of ca. 1767 ±20 Ma, possibly with Archean components as suggested by a Rb-Sr errorchron of 3235 ±258 Ma (Chamberlain, 1983). A lineated granodioritic augen gneiss produced a well-defined discordia array with an upper intercept age of 1987 Ma and an imprecise lower intercept of 93 ±142 Ma (McDonough and Parrish, 1991) in the range of other Cretaceous ages of metamorphism recognized in the northern Monashee Mountains (Sevigny et al., 1989, 1990; Crowley et al., 2000) but absent in the sampled orthogneiss units on the east side of the trench.

Table 1. Summary of previous K-Ar and $^{40}Ar/^{39}Ar$ ages in the investigated region.

Sample ID	UTM Location, Zone 10 (Easting/Northing)	Stratigraphic Unit	Rock Type		K-Ar Age (Ma)	$^{40}Ar/^{39}Ar$ Age (Ma)
GSC 91-17	651050 / 5960300	McNaughton Fm.	Argillite; phyllitic, cleaved		181.0 ±4.8	
GSC 91-12	646700 / 5960900	Upper Miette Gp.	Phyllite; weakly crenulated		152.9 ±2.6	
GSC 91-14	682400 / 5928400	Upper Miette Gp.	Phyllite; laminate, weakly crenulated		140.9 ±2.4	
GSC 91-16	681200 / 5966700	Upper Miette Gp.	Argillite; phyllitic, laminated		261.4 ±5.7	
GSC 91-13	664950 / 5967150	Middle Miette Gp.	Argillite; silty, cleaved		226.0 ±3.0	
GSC 91-15	664500 / 5966050	Middle Miette Gp.	Argillite; silty, poorly cleaved		178.3 ±4.6	
GSC 91-18	696900 / 5933350	Middle Miette Gp.	Phyllite; fine crenulation cleavage		231.9 ±3.7	
GSC 65-24*	1.6 km NW of Bulldog Cr.	Bulldog gneiss	Chl-retrogressed, lineated gneiss		72 ±2	
TO28**	Tête Jaune Cache	Middle Miette Gp.	Conglomerate.with horizontal stretching parallel to SRMT	muscovite		78 ±2
				biotite		100 ±2

Note: Samples labelled GSC91- are from McMechan and Roddick (1991); sample marked * is from Wanless et al. (1967) and that marked ** is from Van der Driessche and Malusky (1986).

Zircon analyses from a second lineated augen gneiss are not collinear, but instead yielded individual $^{207}Pb/^{206}Pb$ ages of 2062–2069 Ma. εNd values for these gneisses are -2.6 (T=1990 Ma) and -1.8 (T=2060 Ma) (McDonough and Parrish, 1991). Immediately to the north in the southeastern Cariboo Mountains, similar ages of ca. 2080 Ma have been reported from the Gold Creek orthogneiss (Murphy et al., 1991), a tectonic sliver intercalated into the amphibolite facies Mica Creek succession of the lower Kaza Group (Figure 3).

5 New Samples

Two samples were collected from highly strained rocks near thrust faults in the Foothills and one from the immediate hanging wall of the McConnell thrust that marks the boundary between the Foothills and the Front Ranges of the Rockies. Two more samples have been collected along Highway 16, west of Jasper from phyllonite of the Monarch and Moose Pass thrusts in the Main Ranges. From the western margin of the Rockies, five samples were collected from the Bear Foot thrust and its strained footwall known as the Valemount strain zone (VSZ), and four samples were collected along the Walker Creek fault zone (WCFZ). Eleven more samples were collected along the SRMT that separates the RM-FTB from its hinterland, the Omineca belt.

In an attempt to distinguish between syntectonic muscovite/sericite ages in phyllonite and the detrital muscovite of the protolith, we have collected two samples of less or non-sheared Miette Group: one sandstone from the Lower Miette along Highway 16 (Sample M1; Figure 2) and one pelite, just south of the intersection of Highway 1 and Highway 93 (Sample M2; Figure 2).

The locations of analyzed phyllite and phyllonite samples are shown in Figures 2 and 3. Table 2 includes the UTM coordinates of the samples and a summary of their stratigraphic and structural context. Samples in the Rocky Mountain fold-and-thrust belt have intermediate dips (30–60°), whereas most samples near the SRMT were collected from rocks with steeply dipping foliation and subhorizontal stretching lineation or mullions. Approaching the Trench, both from the Cariboo Mountains to the west and from the Rocky Mountains to the east, within 1–3 km, bedding is gradually transposed by a foliation steeply dipping into the SRMT, with subhorizontal mullions, fold axes, and stretching lineation paralleling the SRMT. Although the deformation is complex and polyphase, there is a common denominator: the structural trends are consistently subparallel or rotated into parallelism to the local trend of the Trench. Detailed structural analyses of the dextral WCFZ can be found in McMechan (2000), and of the oblique dextral strike-slip Valemount strain zone (VSZ) in van den Driessche and Malusky (1986) and McDonough and Simony (1989). Photographs of the outcrops examined and sampled for this study, which show the characteristic structural elements of the three zones of strain concentration are included in Appendices 1 and 2.

6 Analytical Technique

The $^{40}Ar/^{39}Ar$ analyses have been carried out in the Argon Geochronology Laboratory of TerraChron Corp. of the Department of Physics, University of Toronto, and by GeochronEx Analytical Services Ltd. Full step-by-step analytical results are presented in Appendix 3. Because the main objective of this study was to derive ages of tectonism, sampling focused on the selection of secondary micas, free of detrital minerals (except for the two non- or slightly sheared Miette Group samples analyzed for detrital muscovite). We examined the general appearance and physical characteristics of the samples, and then the selected portions were gently crushed and examined under the binocular microscope to identify the most recent mica generations and to select grains for irradiation. Thus, the analyses are on material that represents our best efforts to physically separate the most recent generation of muscovite (sericite) from the previous generations of mica in the samples. However, this was not always a straightforward undertaking, and it may not have been achieved in all samples. Particularly difficult was the separation of datable material near the shallow thrust faults of the Foothills. Moreover, some samples were undersized in order to ensure their purity, which limited the number of heating steps.

Table 2. $^{40}Ar/^{39}Ar$ sample locations and their stratigraphic and structural context.

Sample No.	Site	Easting	Northing	Location	Stratigraphic Unit	Strat. Age	Structural Measurements
Burnt Timber							
1	DP8-199	627708	5719314	NW side of road along Timber River	Cadomin/Paskapoo fms	LCret/Paleocene	S=242°/35°
Brazeau thrust							
2	DP9-548	471105	5909602	NW of bridge across Chungo Creek	Brazeau Fm.	UCretaceous	B=28°/55°
McConnell thrust							
3	DP7-6A	541546	5790286	NW side of Hwy 11 vis-à-vis Abraham L.	Eldon/Luscar	Cambr/Cret	S=212°/37°
Miette Group							
M1	DP16-359	412372	5858915	S side of Hwy 16 (Corral Ck W of Jasper)	Middle Miette (m-M)	Proterozoic	B=245°/40°
M2	DP8-1202A	555617	5699184	SE of Hwy 1-Hwy 93 intersection	Miette shale/siltstone	Proterozoic	L=333°/3° (intersection)
Monarch thrust							
4	DP11-123	418092	5721106	Small outcrop on S side of Hwy 16	Middle/Upper Miette	Proterozoic	S=256°/35°
Moose Pass thrust							
5	DP11-125b	402584	5863798	Outcrop, S side of Hwy 16, AB/BC border	Middle/Upper Miette	Proterozoic	S=250°/33°
Walker Creek fault zone							
6	DP12-110	251753	5968349	W-E ridge - Walker Creek watershed	Mural Fm./Mahto Fm.	Cambrian	S=236°/65°
7	DP12-112	257569	5957609	Saddle north of Morkill River	Yankee or Isaac Fm.	Proterozoic	
8	DP11-136	262183	5952477	Morkill River quarry	McNaughton Fm.	Cambrian	S=226°/90°; L=316°/2°
9	DP12-70	278439	5931853	East Twin Creek strike-slip fault	East Twin Fm.	Proterozoic	S=60°/80°; L=133°/35°
Valemount strain zone							
10	DP12-105	325451	5882603	Zone of tight isoclinal folding	Middle Miette Gp.	Proterozoic	S=230°/50°; L=305°/30°
11	DP10-4x	337449	5872343	Tête Jaune Cache (Hwy 16)	Middle Miette Gp.	Proterozoic	S=220°/87°; L=318°/12°
12	DP12-125	337523	5872332	Tête Jaune Cache (Hwy 16)	Middle Miette Gp.	Proterozoic	Mullion L=305°/3°
13	DP16-362	339541	5872607	NE side of Hwy 16, ~ 2 km E of Trench	Lower Miette (l-M)	Proterozoic	B=245°/3°; S=245°/87°
14	DP12-87b	337449	5872343	Bear Foot thrust (S of Swift Creek)	Yellowjacket-Miette	Proterozoic	S=230°/64°; L=300°/32°
Southern Rocky Mountain Trench shear zone							
15	DP11-133	257293	5943432	Fraser River Bridge to Morkill River	Greenish-grey phyllonite	Proterozoic	S=228°/90°; L312°/5°
16	DP11-137	266408	5926253	Yellowhead Hwy (W of Twin Creek)	Upper Kaza	Proterozoic	S=215°/60°; L=300°/4°
17	DP12-80	269534	5928262	N of McBride (within SRMT)	Yankee-Cunningham	Proterozoic	S=227°/83°; L=310°/5°
18	DP12-77	274869	5929798	N of East Twin Creek (NE side of SRMT)	East Twin Fm.	Proterozoic	S=205°/55°; L=295°/12°
19	DP12-81	276428	5919472	Hwy 16 (Clyde Creek, SW side of SRMT)	Middle Kaza Gp.	Proterozoic	S=230°/63°; L=304°/5°
20	DP11-146	298738	5904332	Holmes Creek quarry (NE side of SRMT)	McNaughton Fm.	Cambrian	mullion L=132°/5°
21	DP12-94	336552	5872121	Tête Jaune Cache (W bank of Fraser R.)	Middle Miette Gp.	Proterozoic	S=34°/83°; L_1=320°/40°; L_2=300°/5
22	DP10-2x	337067	5872187	Tête Jaune Cache (N turn of Hwy 16)	Middle Miette Gp.	Proterozoic	S=210°/85°; L=300°/6°
23	DP11-173	349490	5854225	Valemount townsite	Cunningham Fm.	Proterozoic?	
24	DP10-8x	356161	5848425	E of north end of Kinbasket Lake	Yellowjacket cover, retrogr. crenulated Gt-micaschist	Proterozoic	
25	DP11-161	367977	5831437	E of Kinbasket Lake	Bulldog cover, retrogr.	Proterozoic	S=215°/63°

Note: All structural measurement orientations are dip direction/dip angle; Gt – garnet

The selected grains were packaged in aluminum foil and loaded into an aluminum canister, together with a number of grains of the sanidine standard TCR and the hornblende standard Hb3gr, and irradiated in the McMaster Nuclear Reactor, Hamilton, Ontario. The samples were irradiated for a total of 48 Megawatt-hours (approx. 16 hours in the reactor).

Once the canister was returned to Toronto, the samples and standards were placed into holes in an aluminum disk and loaded into the ultra-high vacuum sample chamber within the mass spectrometer inlet system. After pumping down, the sample chamber and gas extraction line were baked for at least 12 hours at 150°C to achieve low argon blank levels.

The first stage in analysis was to fuse each of the standards in a single heating step, using a Lee Laser Nd-YAG laser operated with frequency doubling, to produce green light of 532 nm wavelength. The evolved gas was then purified by an SAES type 707 Ti-Fe-Zr getter held at 250°C to remove all reactive gases. The remaining noble gas component was let into a VG1200 mass spectrometer equipped with an ion multiplier for analysis of argon. The mass spectrometer was operated in static mode, isolated from the pumps during the analysis. All five natural and irradiation-produced argon isotopes (^{36}Ar through ^{40}Ar) were measured in 20 to 40 successive cycles over about a one-hour period, followed by pumping out of the mass spectrometer. Procedural blanks (in which all steps except the laser heating were followed) were performed before each analysis. The resulting argon isotope measurements were reduced using software developed in-house at the TerraChron Laboratory of the University of Toronto, which includes correction for atmospheric contamination, mass discrimination, and for interfering nuclear reactions resulting from the irradiation, as well as appropriate statistical analysis of the data, including a detailed treatment of error propagation. The J value (essentially the efficiency of ^{39}Ar production from ^{39}K) was calculated for each standard, using an age of 28.32 Ma for the TCR standard, (the Hb3gr standard with assumed age of 1071 Ma is also monitored). The J value varies with position in the container during irradiation, and standards are distributed along the length of the container. Each sample analyzed was assigned an appropriate J value for the irradiation, depending on its own position in the irradiation container.

The samples were analyzed by an identical procedure, except that for the unknown samples the gas release was done in a series of heating steps. In each heating step, the sample was heated by the laser, generally for 30 seconds, followed by the gas purification and analysis steps as above. In successive heating steps the laser power was gradually increased until the sample was fused in the final step.

The samples analyzed by GeochronEx were wrapped in Al foil and loaded into an evacuated and sealed quartz vial with K and Ca salts, and packets of LP-6 biotite interspersed with the samples to be used as a flux monitor. The samples were irradiated in the nuclear reactor for 48 hours. The flux monitors were placed between every two samples, thereby allowing precise determination of the flux gradients within the tube. After the flux monitors were run, J values were calculated for each sample, using the measured flux gradient. LP-6 biotite has an assumed age of 128.1 Ma. The neutron gradient did not exceed 0.5% on sample size. The Ar isotope composition was measured in a Micromass 5400 static mass spectrometer. 1200ºC blank of ^{40}Ar did not exceed n*10^{-10} cc Standard Temperature and Pressure (STP).

7 Analytical Results

The step-heating ^{40}Ar/^{39}Ar analyses were performed on mineral separates that represent our best efforts to physically select the most recent generation of muscovite (sericite) from the detrital mineral phases in the samples in order to derive ages of tectonism. The argon data have been carefully examined and the analytical results for each sample are discussed based on interpretive tools such as age spectra and isochron plots for indications of meaningful ages. Raw data were delivered by the TerraChron Laboratory of the University of Toronto and by GeochronEx (Appendix 3). The next section includes a discussion of the results of our detailed step-heating ^{40}Ar/^{39}Ar analyses from each thrust fault, fault/shear zone. A summary of the results obtained in this study is included in Tables 2 and 3.

Table 3. Summary of $^{40}Ar/^{39}Ar$ analytical results.

Sample No.	Lab Analysis ID	Type of Material	No. of Steps	Integrated Age (Ma)	Preferred Age (Ma)	Method†	Fraction(s) Used	% ^{39}Ar	$^{40}Ar/^{36}Ar$	ΣS *(n-f)
Burnt Timber thrust										
1	YK-223s	muscovite	7	166.7 ±1.9						
Brazeau thrust (striated sandstone ~1000 m in front of thrust)										
2	YK-220	feldspar	8	135.9 ±1.5	135.1 ±1.5	plateau	5--8	~70	182 ±7	
					138.6 ±1.5	isochron				
McConnell thrust (carbonatic shale, hanging wall, ~20 m above thrust surface)										
3	YK-216	sericite - illite	7	291.1 ±3.0						
Miette Group detrital muscovite										
M1	YK-G418	muscovite	10	1549.3 ±33.2	1647±14.0	plateau	5	67.8		
M2	YK-220m	muscovite	12	1486.6 ±11.7	1593 ±12.3	WM	3	~35		
	YK-220s	sericite	12	1066.2 ±9.3	1234.3 ±10.3	WM	3	~40		
Monarch thrust										
4	P57-004	biotite	8	704.0 ±5.2	620 ±58	isochron	3-7	84.3	1870 ±970	2.24
	P57-007	whole rock	15	273.7 ±0.9	134.5 ±8.1	*low*	3	2.1		
					624.0 ±4.9	*high*	15	2.9		
Moose Pass thrust										
5	P57-009	amphibole	10	326.3 ±1.3	452 ±5.1	*high*	10	6.6		
	P57-002	muscovite	22	289.9 ±0.8	134.8 ±1.8	*low*	1-3	8.1		
					421.0 ±4.8	*high*	22	2.0		
Walker Creek fault zone										
6	P59-081	muscovite	17	171.9 ±0.8	85.3 ±0.9	plateau	1-3	5.8		0.05
7	P59-068	muscovite	18	135.4 ±0.6	123.7 ±0.7	plateau	5-9	22.8		3.05
					132.5 ±2.5	isochron	10-16	63.5	1847 ±544	
8	P57-030	muscovite	16	106.1 ±0.3	96.1 ±1.0	*low*	4	24.3		
					168.3 ±2.3	*high*	16	0.7		
9	P59-017	muscovite	12	92.4 ±0.5	79.0 ±0.6	plateau	1-3	17.8		
					95.9 ±5.1	plateau	4-12	82.2		
Valemount strain zone										
10	P63-055	muscovite	10	84.2 ±0.7	77.1 ±0.7	*low*	2	18.2		
					96.5 ±0.8	*high*	9, 10	19.3		0.36
11	P54-019	sericite	15	70.2 ±0.5	72.6 ±0.4	plateau	13-15	45.7		0.10
12	P59-080	muscovite	12	71.2 ±0.4	68.3 ±0.7	isochron	1-5	15.1	282.4 ±7.1	0.77
					71.4 ±0.7	isochron	6-12	84.9	305.3 ±4.8	12.83
					421.0 ±4.8	*high*	22	2.0		
13	YK-G421b	biotite	10	77.5 ±1.6	87.02 ±0,66	plateau	6	72.6		
	YK--G421m	muscovite	10	127.4 ±2.6						
14	P59-026	muscovite	15	71.9 ±0.3	68.8 ±1.1	plateau	1-4	1.7		0.13
					67.3 ±5.9	isochron	1-8			
					72.0 ±0.4	plateau	5-15	98.3		4.37
Southern Rocky Mountain Trench shear zone										
15	P57-041	muscovite	12	119.4 ±0.4	87.9 ±5.0	*low*	1	1.7		
					160.5 ±5.7	*high*	12	2.1		
16	P57-029	muscovite	11	120.9 ±0.8	135.9 ±1.1	*high*	9-11	25.8		
17	P59-007	muscovite	11	122.3 ±0.6	123.2 ±3.6	plateau	7-9	68.1		13.94
18	P59-020	muscovite	11	99.4 ±0.9	99.3 ±4.4	plateau	1-11	100		19.59
19	P59-008	muscovite	13	123.3 ±0.6	128.0 ±1.5	plateau	9-13	56.2		4.88
20	P57-015	biotite	12	101.8 ±0.3	85.2 ±0.6	*low*	8	8.9		
	P57-010	muscovite	9	105.9 ±0.6	88.8 ±1.7	*low*	1-3	9.8		
					155 ±23	*high*	9	1.0		
21	P59-070	plagioclase	6	176 ±12	98.2 ±10.1	plateau	1-4	87.3		0.22
	P59-218	muscovite	17	71.4 ±0.3	71.9 ±0.7	plateau	8-15	83.9		10.97
	P59-072	biotite	11	103.1 ±0.6	101.5 ±0.6	isochron	4-10	87.6	327.0 ±5.0	0.66
22	P54-004	sericite	6	74.9 ±0.3	71.7 ±0.4		3,4	20.5		
	P54-028	sericite	30	92.1 ±0.3	77.7 ±3.1	isochron	21-30	36.5	7417 ±524	0.26
23	P57-023	whole rock	16	138.9 ±0.9	85.4 ±0.5	plateau	12-17	39.2		0.48
24	P54-034	sericite	23	71.2 ±0.3	74.3 ±0.4	plateau	22, 23	14.3		0.02
25	P57-028	K-feldspar	6	272 ±16	219 ±28	isochron	1-6	100.	618 ±274	0.60
	P57-025	muscovite	12	121.8 ±0.8	75.0 ±0.7	isochron	3-8	65.3	600 ±33	0.97

Notes: * Goodness-of-fit parameter; *f* is degrees of freedom: *f* = 1 for plateaus, *f* = 2 for isochrons; WM – weighted mean age; † ages marked *low* and *high* represent limiting ages from low-temperature and high-temperature portions of age spectrum

7.1 Foothills, Front and Main Ranges of the Rocky Mountains

7.1.1 Burnt Timber Thrust

Sample 1 is from a sheared dark grey to black cataclastic siltstone collected at the base of the Cadomin conglomerate (Figure 2; Tables 2, 3). The rock is a cataclasite that consists of angular to sub-angular quartz clasts with weakly granulated grain boundaries in a matrix/cement of amorphous Fe-stained clays. Poorly crystalline, very fine-grained interstitial sericite/illite nucleated on the dark clays. Minor biotite locally replaced sericite/illite aggregates. Several fragmented accessory minerals (ilmenite, rutile, zircon, apatite, pyrite, and hematite) are disseminated through the rock matrix. The matrix micas and clays are most likely syndepositional in origin and appear to cement the quartz clasts. A few needle-shaped muscovite grains (0.015–0.3 mm) are partly deformed and may be detrital as they do not line up along a fabric, although a syntectonic origin cannot be precluded.

The sericite separated from this sample (YK-223s) yielded a discordant age spectrum with an integrate age (IA) of 166.7 ±1.9 Ma (Figure 4a). The Ca/K spectrum suggests that argon was released from at least two minerals, one sericite and the other Ca-bearing. On the Inverse Isochron Plot, points scatter along the X-axis and do not form any linear regression. The 500ºC step characterized by 62% of ^{39}Ar, yielded an age of 149.6 ±1.7 Ma. This age is older than the age of the formations on either side of the thrust (hanging wall: Cadomin <125 Ma, and footwall: Paskapoo <66 Ma), hence neither the time of siltstone diagenesis nor the time of thrusting can be accurately approximated. Because the textural relationships suggest the growth of syn- and postdepositional sericite at the expense of amorphous clay masses, the ca. 150 Ma age, if geologically meaningful, can only represent a detrital muscovite/sericite component, possibly the age of the bent, slender muscovite needles (Appendix 2).

7.1.2 Striated Brazeau Sandstone

Sample 2 was collected from a small outcrop along the trunk road just north of the bridge on Chungo Creek (Figure 2; Tables 2, 3), approximately 1 km E of the Brazeau thrust (here not exposed). An anorthoclase crystal (K-Na feldspar) separated from this sample (YK-220) yielded an age spectrum with a low-temperature two-step hump followed by a four-step plateau of 135.1 ±1.5 Ma (69% of ^{39}Ar) labeled WMPA (weighted mean plateau age) (Figure 4b). On the Inverse Isochron Plot (not shown), plateau points form a linear trend characterized by an age value of 138.6 ±1.7 Ma, mean squared weighted deviation (MSWD) = 19 and low $(^{40}Ar/^{36}Ar)_0$ = 182 ±7. The high MSWD value suggests the linear trend is likely an errorchron.

7.1.3 McConnell Thrust

Sample 3 is a sheared shale/siltstone collected within 20–25 m above the thrust surface from the Cambrian Eldon Formation along Highway 11 on the west side of Abraham Lake (Figure 2; Tables 2, 3). At this location, the McConnell thrust is not exposed. A concentrate of illite/smectite/sericite? (YK-216) yielded a complex hump-shaped age spectrum (Figure 4c) starting from a low temperature step characterized by 43% of ^{39}Ar, with an age value of 187.6 ±2.0 Ma; at higher temperature, it climbed to 600 Ma and decreased to about 450 Ma at fusion temperature. The ca. 188 Ma age corresponds to a flat segment on the Ca/K spectrum suggesting argon release from a homogeneous component of the analyzed mineral separate. At higher temperature steps, the Ca/K ratio varied, probably indicating that the mineral separate included other mineral generations. The youngest age of ca. 188 Ma, if geologically meaningful, roughly coincides with the Early Jurassic age of initiation of tectonic loading of the North American continent. No isochron can be plotted for this sample.

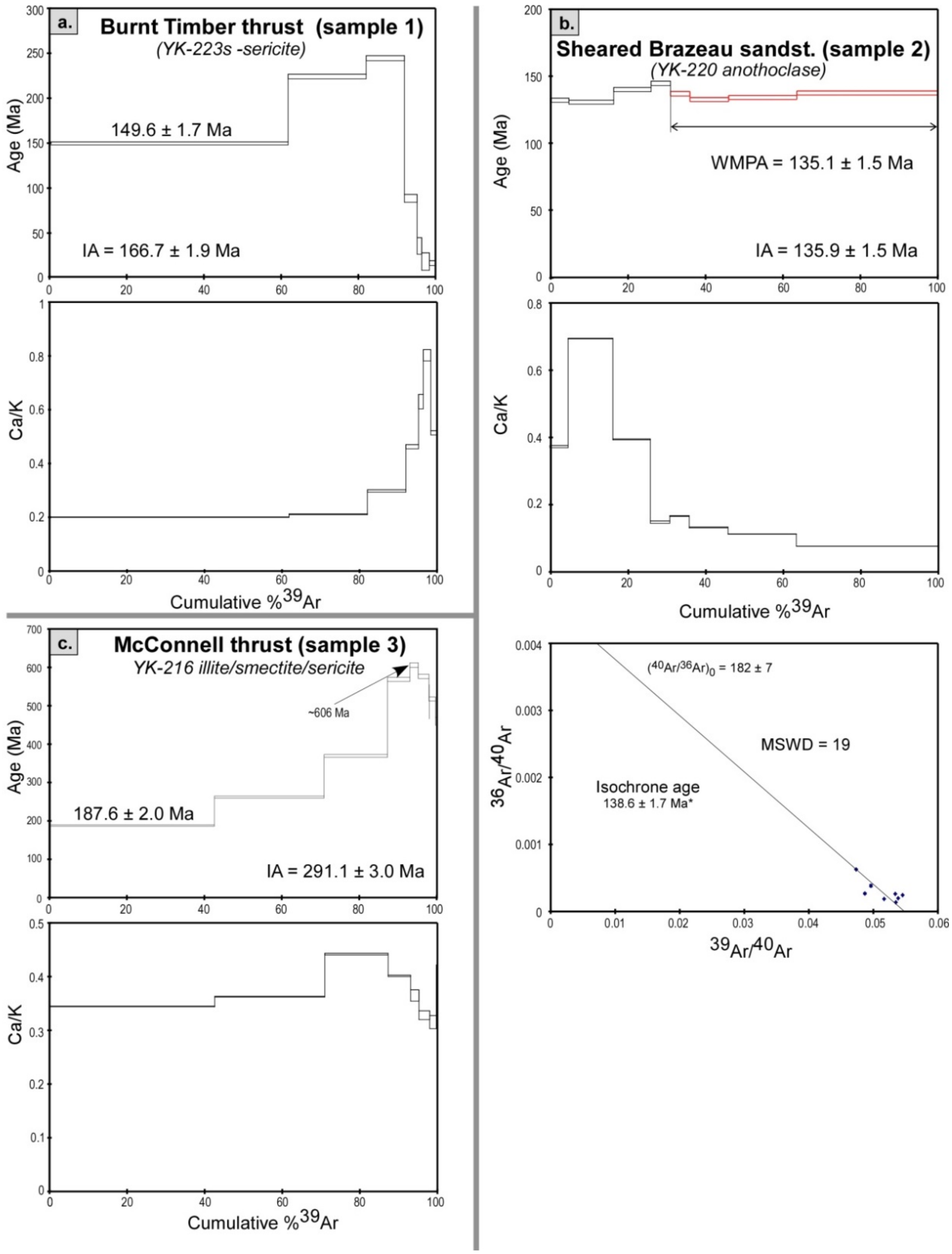

Figure 4. $^{40}Ar/^{39}Ar$ age and apparent K/Ca spectra for thrust faults in the Foothills and Main Ranges of the Rocky Mountain fold-and-thrust belt. a) the black gouge at the base of the Cadomin conglomerate within the Burnt Timber thrust; b) shared carbonate shale within 20 m above McConnell thrust on the west side of Abraham Lake; c) $^{39}Ar/^{40}Ar$, Ca/K spectra and the isochron diagram for a feldspar grain separated from sheared and striated Brazeau sandstone exposed on the trunk road south of Chungo Creek. Analytical uncertainties (2σ, intralaboratory) are represented by vertical width of bars. Experimental temperatures increase from left to right. Plateau and/or integrated ages, together with other possibly significant ages are discussed in the text, and are listed on each diagram. The symbol * indicates isochron age. Abbreviations: IA, integrated age; MSWD, mean squared weighted deviation; WMPA, weighted mean plateau age.

7.1.4 Miette Group Detrital Muscovite

Faults to the west in the Main Ranges and particularly along the western margin of the Rockies, overprinted mostly Neoproterozoic Miette Group rocks which commonly contain detrital muscovite. The age of the detrital muscovite provides a reference framework for the newly formed, syntectonic white mica (muscovite/sericite). To confidently date detrital muscovite, we selected two Miette rock samples away from faults to be compared with syntectonic white mica (sericite) formed along zones of strain concentration (fault and/or shear zones) that affected the Miette Group during Cordilleran tectonism.

Sample M1 was collected from a coarse Miette sandstone/grit on the south side of Highway 16, west of Jasper (Figure 2; Tables 2, 3). A coarse muscovite separate (YK-G418) yielded a plateau age of 1647 ±14 Ma from 67.8% of the ^{39}Ar (Figure 5a). The Ca/K spectrum shows a high Ca/K ratio mineral phase for the first three steps, followed by a very low and flat portion corresponding to a single mineral phase that generated the plateau age.

Sample M2 is a silty shale overprinted by very low-grade metamorphism collected from the large outcrop on the east side of Highway 1 at the intersection with Highway 93 (Figure 2; Tables 2, 3). Detrital muscovite and secondary sericite have been separated. The muscovite separate (YK-220m) yielded a discordant age spectrum with a low, rising temperature staircase and a three-step intermediate plateau with an age value of 1593.2 ±12.3 Ma characterized by 39% of ^{39}Ar (Figure 5b). On the Inverse Isochron Plot (not shown), points scatter along the X-axis and do not form any linear regression. The Ca/K – Age diagram shows a negative trend between Ca/K and Age values, likely evidence of superposition of argon from at least two minerals, one Ca-bearing and the other sericite. The sericite separate (YK-220s) yielded a discordant age spectrum with a rising, low temperature staircase and a three-step intermediate plateau with an age value of 1234.3 ±10.3 Ma, characterized by 39% of ^{39}Ar (Figure 5c). The Ca/K – Age diagram shows a negative trend between Ca/K and Age values, likely evidence of superposition of argon from at least two minerals, one Ca-bearing and the other sericite. On the Inverse Isochron Plot (not shown), points scatter along the X-axis and do not form any linear regression.

7.1.5 Monarch Thrust

Sample 4 was collected from a small outcrop of phyllonite from the Monarch thrust (Figure 2; Tables 2, 3) on the south side of Highway 16 west of the town of Jasper. A small biotite crystal (P57-004, Figure 6a), run in eight steps, gives an integrated age (IA) of 703.0 ±5.2 Ma, with an integrated Ca/K ratio of 0.24 ±0.05. Its age spectrum climbs rapidly from an imprecise age of 90 ±70 Ma to ages in the 700 to 800 Ma range before closing at 614 ±19 Ma. There is no obvious plateau. The Ca/K spectrum is uniformly flat as would be expected in the analysis of a pure single phase. On the $^{39}Ar/^{40}Ar$ vs. $^{36}Ar/^{40}Ar$ plot the points are somewhat clustered near the $^{39}Ar/^{40}Ar$ axis. Nonetheless, fractions 3 to 7 [with 84.3% ^{39}Ar] fit a line corresponding to an isochron age of 620 ±58 Ma, with an elevated initial $^{40}Ar/^{36}Ar$ ratio of 1870 ±970 [$S/(n\text{-}2) = 2.24$]. The high initial ratio can account for the apparent raggedness of the plateau on the age spectrum, and 620 Ma provides the best formation age estimate for this biotite.

From this sample (originally selected for muscovite but the high Ca/K ratios suggest that it was contaminated with plagioclase feldspar), a whole rock analysis (P57-007, Figure 6b), run in 15 steps gives a Permian IA of 273.7 ±0.9 Ma, with an integrated Ca/K ratio of 14.01 ±0.05. On the age spectrum the pattern plunges from an initial age of 625 ±22 Ma (likely explained by excess argon) to the minimum age of 131.3 ±7.9 Ma (fraction 3), which may hint to the last Ar-loss event affecting the sample. The next temperature steps climb to a mid-temperature Antler-age peak at 367.5 ±0.9 Ma (fraction 9). From there, the spectrum falls slightly and then proceeds to climb to a final age of 624.0 ±4.9 Ma in fraction 15.

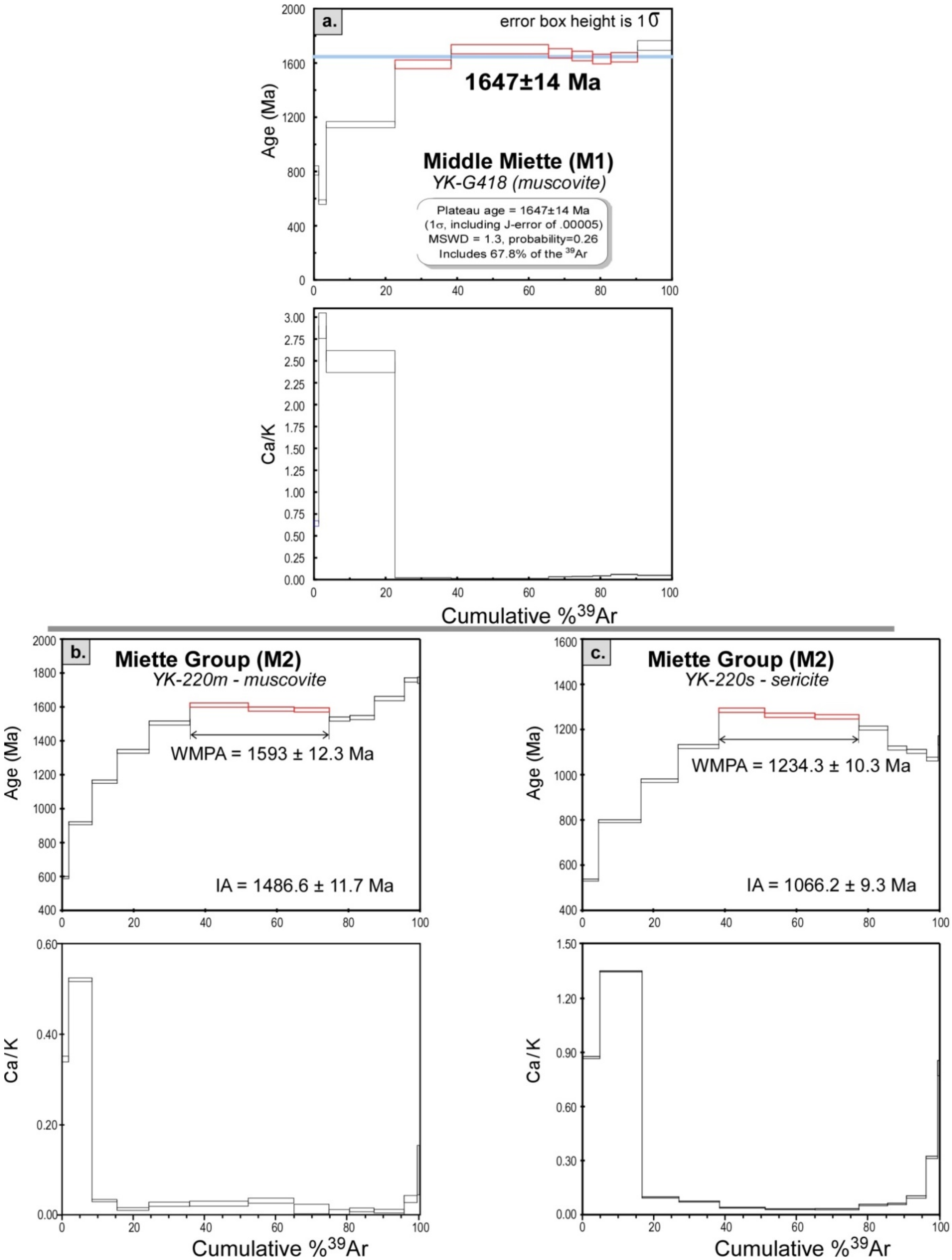

Figure 5. $^{40}Ar/^{39}Ar$ age and apparent K/Ca spectra for detrital mica in the Miette Group. Data plotted as in Figure 4.

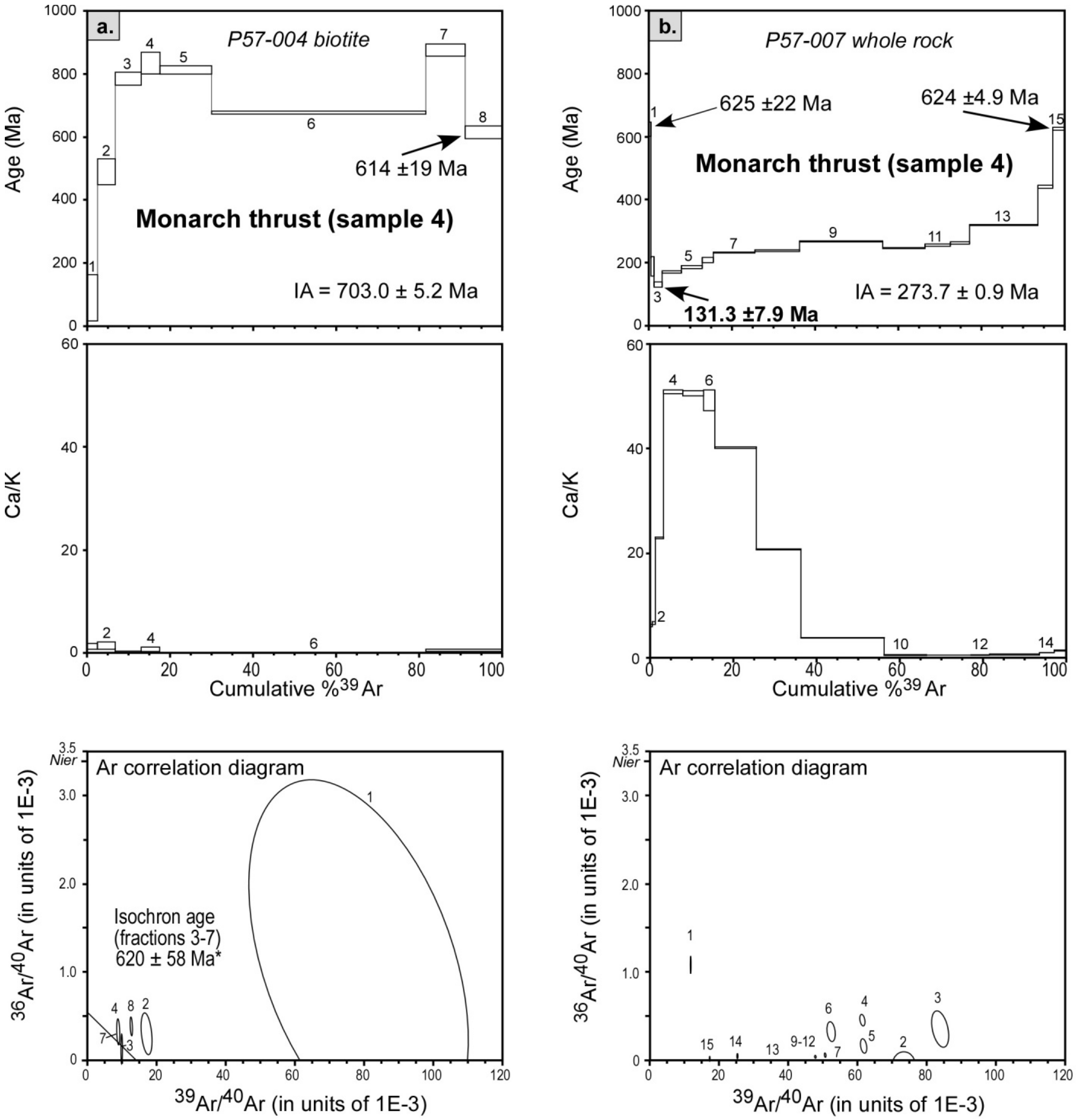

Figure 6. $^{39}Ar/^{40}Ar$, Ca/K spectra, and the argon correlation diagrams for a biotite grain (a) and a whole rock sample (b) collected from poorly recrystallized phyllonite of the Monarch thrust just south of Highway 16, west of the town of Jasper. Data plotted as in Figure 4.

Its Ca/K spectrum starts at a ratio of 6.2 ±0.2, then climbs rapidly to a maximum of 50.7 ±0.3 (fractions 4 to 6, with 13.1% of the total ^{39}Ar). This portion of the spectrum probably corresponds to the degassing of plagioclase. At mid-temperature the Ca/K pattern falls to a low of 0.55 ±0.04 (fractions 10 to 13) before rising slightly to an average of 1.1 ±0.1 in the final 2 fractions. The low Ca/K ratios characterizing the latter portion most likely signify the higher temperature degassing of the muscovite.

During heating, argon retention in muscovite is expected to be higher than that of associated biotite. On the other hand, the blocking temperature of plagioclase is lower than that of both muscovite and biotite. Thus, the younger apparent ages of the whole rock analysis relative to those of the biotite may reflect less argon retention in the plagioclase, or they may result from new growth of muscovite/plagioclase during tectonism. The final fusion ages of both analyses are coincident at ~620 Ma, correspond to the isochron age of 620 ±58 Ma obtained from 84% of the ^{39}Ar in biotite and provide the best estimate for the age of this mica.

7.1.6 Moose Pass Thrust

Sample 5 was collected from the Moose Pass thrust on the south side of Highway 16 at the Alberta–British Columbia border (Figure 2; Tables 2, 3). A small amphibole crystal (P57-009*,* Figure 7a), run in 10 steps, gives an IA of 326.3 ±1.3 Ma, with an integrated Ca/K ratio of 1.93 ±0.02. Its age spectrum starts at 218 ±10 Ma and climbs to a mid-temperature high averaging 384.3 ±1.6 Ma (fractions 5 and 6 with 34.4% of the total ^{39}Ar). At higher temperature, the pattern drops to 340.2 ±3.6 Ma before climbing again to the final age of 452.0 ±5.1 Ma (fraction 10). There are no significant lines on the ^{39}Ar/^{40}Ar vs. ^{36}Ar/^{40}Ar plot.

A muscovite crystal (P57-002, Figure 7b), run in 22 steps, gives an IA of 289.9 ±0.8 Ma, with an integrated Ca/K ratio of 0.012 ±0.004. On the age spectrum, low temperature fractions 1 to 3 [with 8.1% of the total ^{39}Ar, $S/(n\text{-}1) = 0.10$] yield a mean age of 134.8 ±1.8 Ma. Ensuing fractions increase in age progressively to 293.6 ±1.7 Ma (fraction 11). The next fractions at mid-temperature increase in age very gently and there is a plateau-like portion averaging 324.2 ±1.2 Ma [fractions 14 to 16 with 23.7% of the total ^{39}Ar, $S/(n\text{-}1) = 0.37$]. At higher temperature the pattern jumps up to 395.3 ±1.9 Ma in fraction 19, and then gently rises to the final age of 421.0 ±4.8 Ma (fraction 22).

On the ^{39}Ar/^{40}Ar vs. ^{36}Ar/^{40}Ar plot the stepwise increase in apparent age of the fractions 4 to 22 on the age spectrum is shown as a progressively leftward march of these points along the ^{39}Ar/^{40}Ar axis.

The complicated spectral patterns from both amphibole and muscovite samples are not easily interpreted. The muscovite age spectrum may indicate a very complex history of argon loss and/or multiple-aged components for this sample. The coincidence of the most recent imprint evident from the lowest temperature fractions, estimated at ca. 135 Ma, with the ca. 131 Ma minimum age registered in the Monarch whole rock sample may be geologically significant.

7.2 Western Rockies

7.2.1 Walker Creek Fault Zone

Four samples (6 to 9) were collected along the Walker Creek fault zone (Figure 3; Tables 2, 3; Appendix 1): sample 6 is from a ridge that exposes Cambrian phyllite/phyllonite; sample 7 is a phyllonite from a saddle north of the Morkill River; sample 8 from the south side of the Morkill River is a muscovite-quartzite from a small quarry in the Cambrian McNaughton Formation with subvertical foliation and conspicuous lineation; and sample 9 from a wide (>100 m) phyllonite zone exposed along the south side of First Twin Creek, about 1 km east of the SRMT margin. All four spectra are complex and the pattern of climbing ages may indicate that the samples have undergone periods of substantial argon loss, with the youngest ages possibly recording the last tectonic overprint.

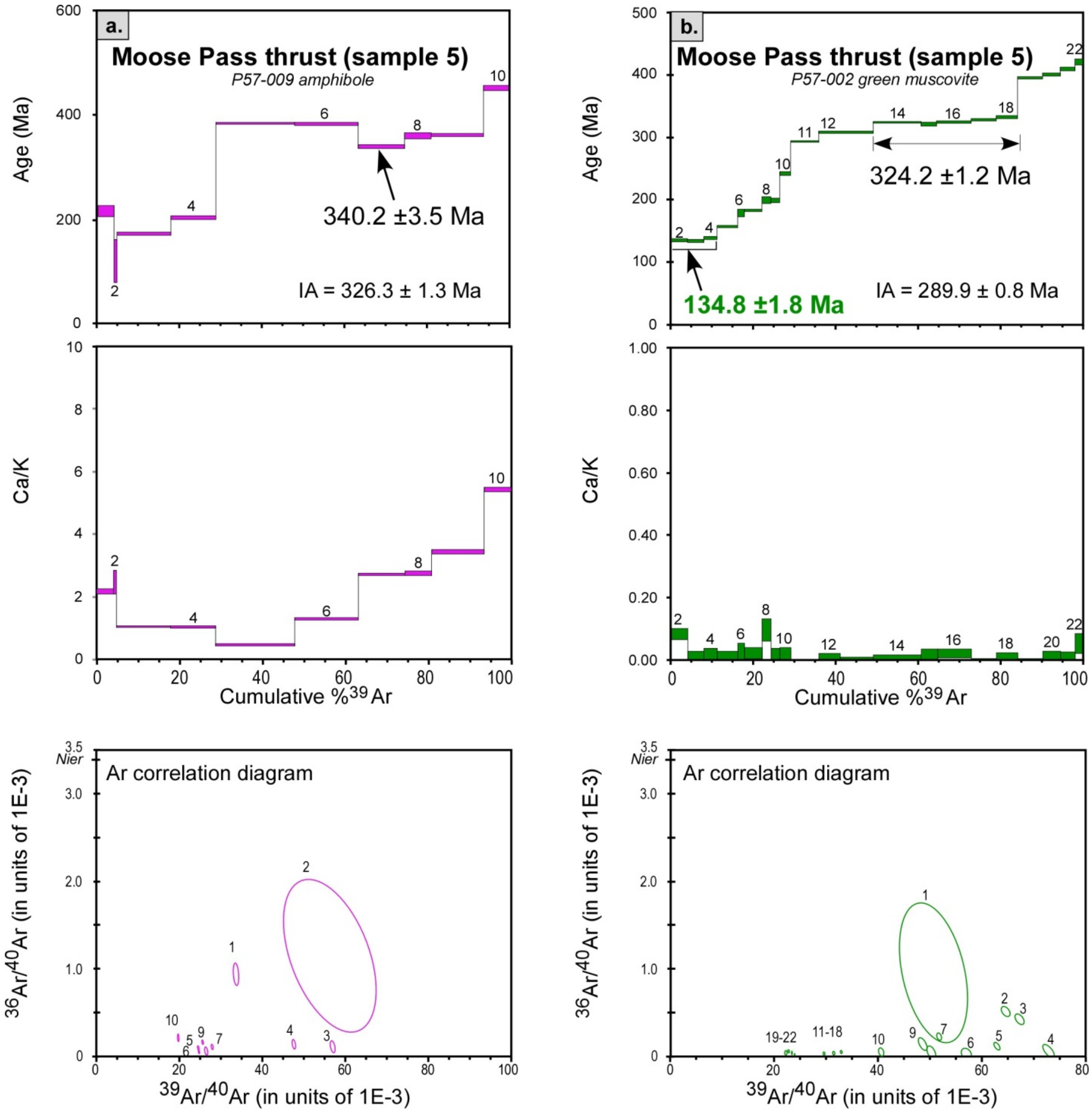

Figure 7. $^{40}Ar/^{39}Ar$ age and apparent K/Ca spectra for poorly recrystallized phyllonite from the Moose Pass thrust fault. Data plotted as in Figure 4.

The oldest ages preserved are Permian (sample 6, Figure 8a) and Middle Jurassic (sample 8, Figure 9a) fusion ages that resulted from minor amounts of ^{39}Ar and are considered irrelevant. They indicate however, that subsequent tectonothermal events have not completely reset the argon system in detrital muscovite of the Cambrian formations. The 184 Ma weighted average age obtained from the mid-temperature range in sample 6, if geologically accurate, corresponds to the inferred Early Jurassic initial tectonic loading of North America. The Jurassic ages, including the inclined plateau averaging 184 Ma and the IA of 172 Ma in this sample are comparable to the previously published K-Ar ages of ca. 181 Ma and 178 Ma (McMechan and Roddick, 1991), and consistent with a tectonothermal event during the Toarcian loading of North America (Murphy et al., 1995; Nixon et al., 1993, 2020). The final temperature age of 168 Ma in sample 8 (Figure 8a) is close to the K-Ar age of 153 Ma previously reported from an Upper Miette phyllite (McMechan and Roddick, 1991). Although correlations to the Jurassic tectonothermal events documented in the SMC metamorphic complex to the south (e.g., Currie, 1988; Gibson et al., 2008) are tempting, none of the K-Ar and incremental ^{40}Ar/^{39}Ar step ages permit solid arguments.

The 139.0 ±4.8 Ma well-defined plateau age (68.2% ^{39}Ar, fractions 10 to 16), and the 123.7 Ma (22.8% ^{39}Ar, fractions 6 to 9) lower temperature plateau-like segment in sample 7, appear to be distinct Early Cretaceous (Valanginian and Aptian) tectonic phases rather than one continuous phase (Figure 8b). The isochron treatment of fractions 10–16 compensates for at least some of the excess argon, hence the best estimate for the high-temperature data is given by the isochron result of 132.5 ±2.5 Ma (see Appendix 3).

Total gas ages of 106 Ma and 92 Ma obtained from samples 8 and 9, respectively, suggest a mid-Cretaceous tectonic event (Figure 9). In more detail, the inclined plateau age of 95.9 Ma (82.2% ^{39}Ar) includes a maximum age of 100 Ma and a minimum age of 91 Ma (Figure 9b), and can be considered good evidence for a mid-Cretaceous argon-loss event. Low- and mid-temperature ages obtained from sample 8 are also consistent with a mid-Cretaceous (Cenomanian) event.

The youngest ages in these samples vary from 111 Ma (sample 7), to 85 Ma (sample 6), 79 Ma (sample 9), to as young as 68 Ma (sample 8), but their interpretation as the youngest tectonic events that affected the Ar system in white mica is speculative. We retain however, the ca. 79 Ma age obtained at low temperature steps 1 to 3 in sample 9, confirmed by the argon correlation plot for the same steps (Figure 9b), as a record of Campanian tectonism along the WCFZ. Taken together, the dates obtained from the WCFZ indicate that it was tectonically active since the Valanginian and Aptian (ca. 133 Ma and ca. 124 Ma), experienced a mid-Cretaceous (Albian-Cenomanian) pulse that peaked during the Cenomanian (ca. 96 Ma), with several discrete apparently weak Late Cretaceous pulses (85 Ma, 79 Ma, and 68 Ma).

7.2.2 Bear Foot Thrust and the Valemount Strain Zone

Three samples from the Valemount strain zone (Figure 3; Tables 2, 3) yielded remarkably consistent late Campanian-earliest Maastrichtian ages (73 Ma to 71 Ma). The Ar system in the Neoproterozoic Middle Miette rocks appears to have been almost completely reset by the Late Cretaceous tectonometamorphic event. Only the sericite fusion age of 175 Ma in sample 12 (Figure 10) collected near the eastern margin of the strain zone along Highway 16, suggest a pre-Cretaceous history (may have preserved the memory of the Toarcian tectonism). Thus, the oblique compression identified by van der Driessche and Malusky (1986), and further documented by McDonough and Simony (1989) along the Bear Foot thrust and its footwall, the Valemount strain zone, are contemporaneous with the Campanian major strike-slip displacement along the Tête Jaune Cache-Kinbasket segment of the SRMTSZ (see next section).

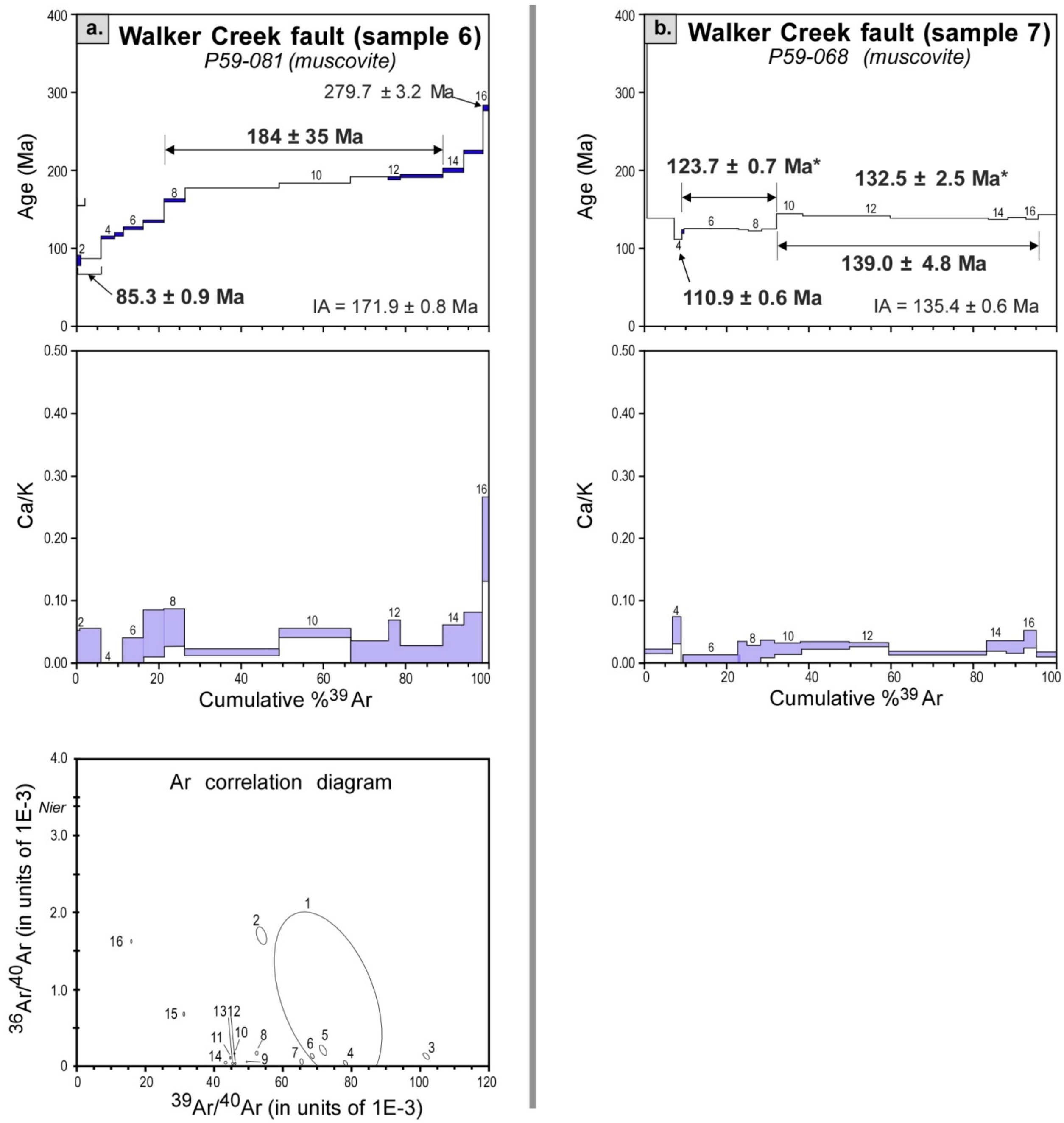

Figure 8. $^{40}Ar/^{39}Ar$ age and apparent K/Ca spectra for muscovite crystals from phyllite/phyllonite samples collected along Walker Creek fault zone. Data plotted as in Figure 4.

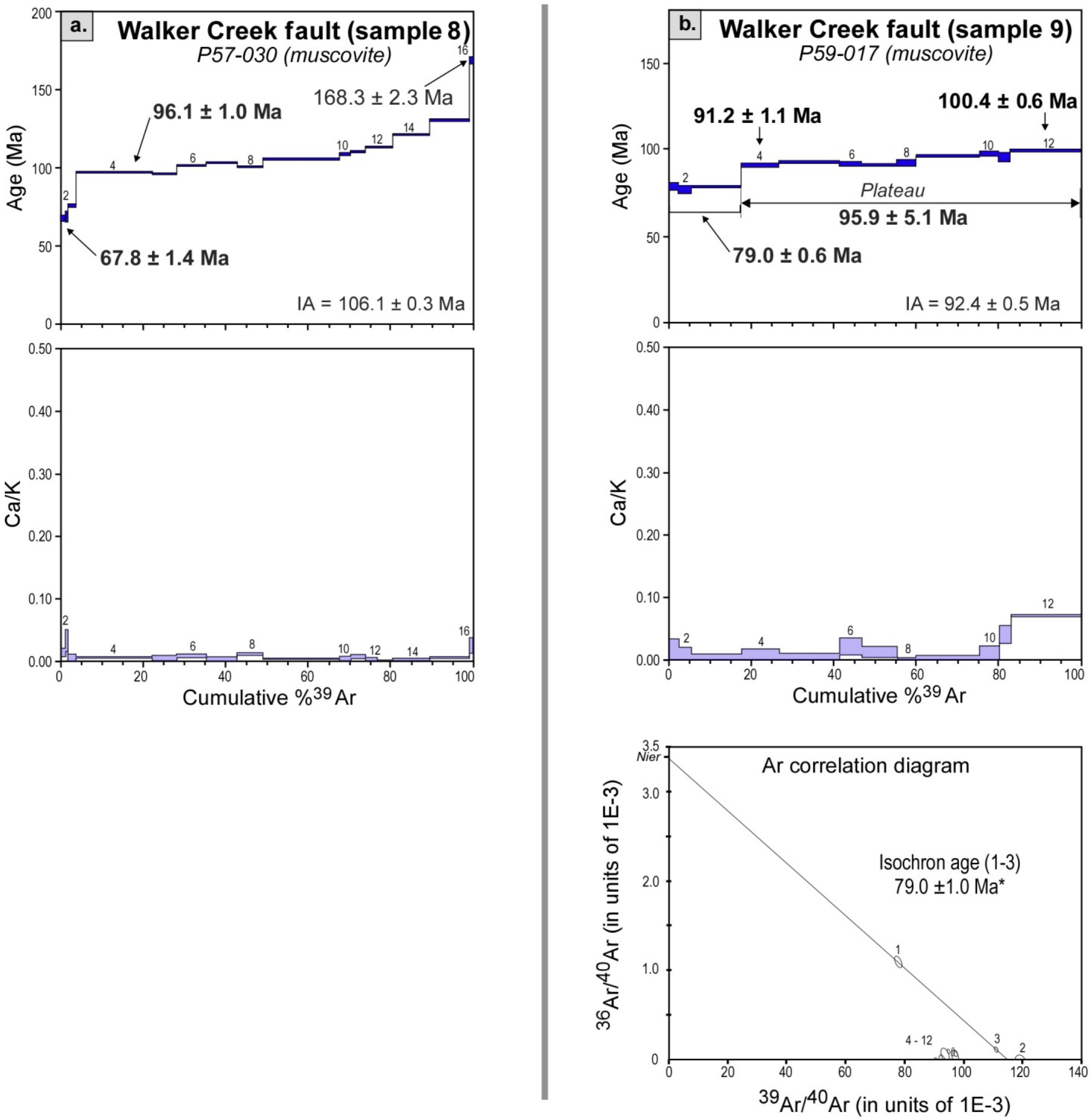

Figure 9. $^{40}Ar/^{39}Ar$ age and apparent K/Ca spectra for muscovite crystals from phyllite/phyllonite samples collected along the Walker Creek fault zone. Data plotted as in Figure 4.

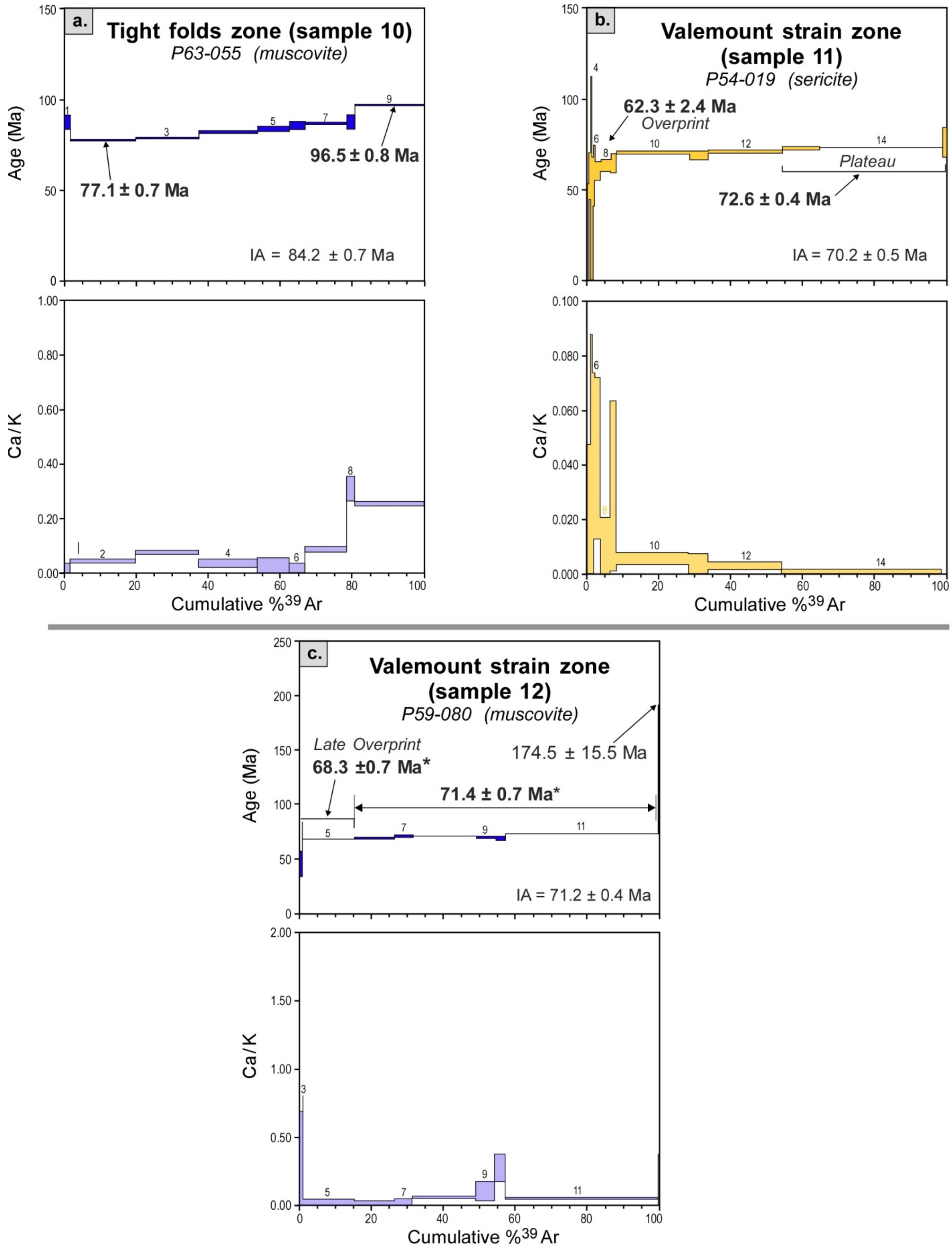

Figure 10. $^{40}Ar/^{39}Ar$ **age and apparent K/Ca spectra for muscovite/sericite crystals from phyllite/phyllonite samples collected from the Valemount strain zone and the Bear Foot thrust. Data plotted as in Figure 4.**

Sample 13 was collected near the eastern limit of the Valemount strain zone on the northwest side of Highway 16 from Lower Miette sandstone, and yielded a biotite and a muscovite concentrate. The well-exposed thick-bedded massive sandstone is subhorizontal but overprinted by a 2 to 10 cm spaced subvertical foliation. A biotite separate (YK-G421b, Figure 11a) yields a well-constrained middle to high-temperature plateau age of 87 ±0.66 Ma (fractions 3 to 8) that corresponds for the most part to an almost constant Ca/K ratio. The muscovite separate (YK-G421m, Figure 11b) from the same sample yields a complex spectrum that may represent Jurassic to Late Cretaceous disturbances of the ca. 1600 Ma detrital muscovite age recognized in other Miette samples.

Sample 14 was collected from the mapped trace of the Bear Foot thrust northwest of the town of Valemount (Appendix 1). A muscovite separate (P59-026), run in 15 steps, yields an IA of 71.9 ±0.3 Ma, with an integrated Ca/K ratio of 0.0097 ±0.0005. An initial low-temperature age of 68.8 ±1.2 Ma is given by fractions 1 to 4 with only 1.7% of the total ^{39}Ar [$S/(n-1) = 0.13$]. The dominant proportion of the age spectrum given by fractions 5 to 15 [with 98.3% the total ^{39}Ar, $S/(n-1) = 4.37$] yields an average age of 72.0 ±0.4 Ma (Figure 11c). The age spectrum of this sample indicates a simple history and yields a confident estimate at 72.0 ±0.4 Ma. The Ca/K spectrum is uniformly low and flat indicating a single homogenous phase. On the ^{39}Ar/^{40}Ar vs. ^{36}Ar/^{40}Ar correlation plot low-temperature fractions 1 to 8 fit a line [$S/(n-2) = 0.66$] corresponding to an isochron age of 67.3 ±5.9 Ma (which may record a late Maastrichtian tectonic disturbance) with an imprecise initial ^{40}Ar/^{36}Ar ratio of 750 ±750. The remainder of the points is clustered near the ^{39}Ar/^{40}Ar axis.

7.2.3 Shear Zone within the Northern Segment of the Southern Rocky Mountain Trench

The samples collected from the northern segment of the SRMT and its flanks (Figure 3; Tables 2, 3) yielded complex ^{40}Ar/^{39}Ar spectra dominated by Cretaceous ages. In the McBride area the age groups (Figures 12–14) are the same as those obtained from the WCFZ. To the south, particularly near Tête Jaune Cache and at the northern end of Kinbasket Lake, an additional Campanian record is dominant.

From sample 15, a muscovite crystal (P57-041), run in 12 steps, gives an IA of 119.4 ±0.4 Ma (Figure 12a). The age spectrum begins with an age of 87.9 ±5.0 Ma (fraction 1 with 1.7% of the total ^{39}Ar) followed by progressively older ages in successive fractions with increasing temperature up to a final fusion age of 160.5 ±5.7 Ma. On the ^{39}Ar/^{40}Ar vs. ^{36}Ar/^{40}Ar plot, fractions 1 to 3 fit a line corresponding to an isochron age of 96.2 ±1.4 Ma, with an initial ^{40}Ar/^{36}Ar ratio of 285.8 ±6.2. The remainder of the points forms an arcuate pattern below and to the left of this line.

This sample contained ~0.1 mm sized pristine garnet crystals. Two of these crystals were run in single fusion steps to see if the timing of their metamorphic growth could be determined. However, their argon gas yields were very small, and their mean total fusion age of 360 ±90 Ma is too imprecise to be of much use.

A muscovite crystal (P57-029) from sample 16 run in 11 steps gives an IA of 120.9 ±0.8 Ma, with an integrated Ca/K ratio of 0.012 ±0.006 (Figure 12b). The first 2 imprecise and very small steps are followed by a large third step (with 32.6% of the total ^{39}Ar) with an apparent age of 107.1 ±0.8 Ma. The pattern then climbs to 135.9 ±1.1 Ma (fractions 9 to 11 with 25.8% of the total ^{39}Ar). A weighted average age of 125 Ma can be calculated from the mid-temperature fractions 4 to 8 (% ^{39}Ar) with similar ages. The large gas evolved in fraction 3, combined with the overall climbing nature of the age spectrum renders low-temperature age information imprecise.

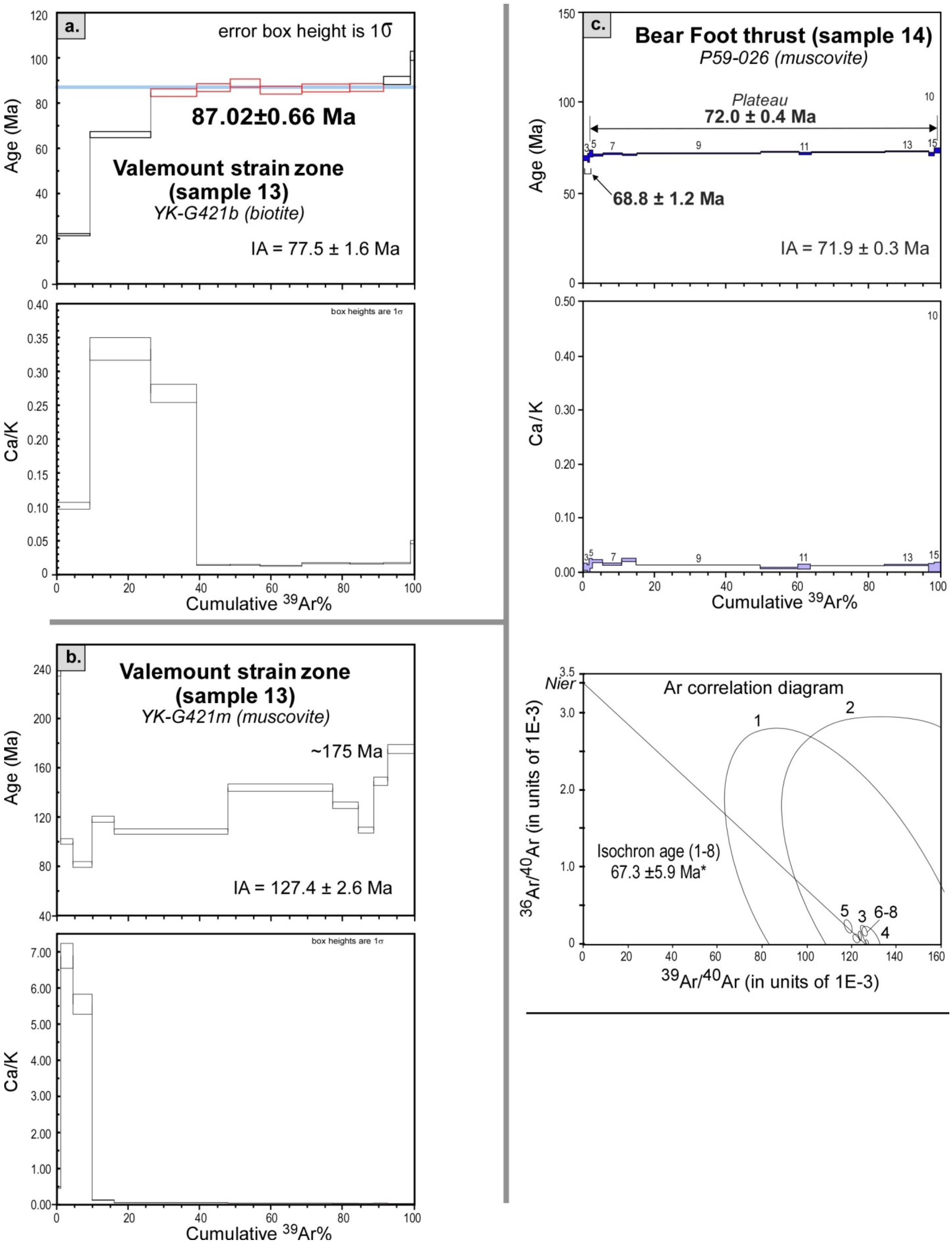

Figure 11. $^{40}Ar/^{39}Ar$ age and apparent K/Ca spectra for muscovite/sericite crystals from phyllite/phyllonite samples collected along the Valemount strain zone. Data plotted as in Figure 4.

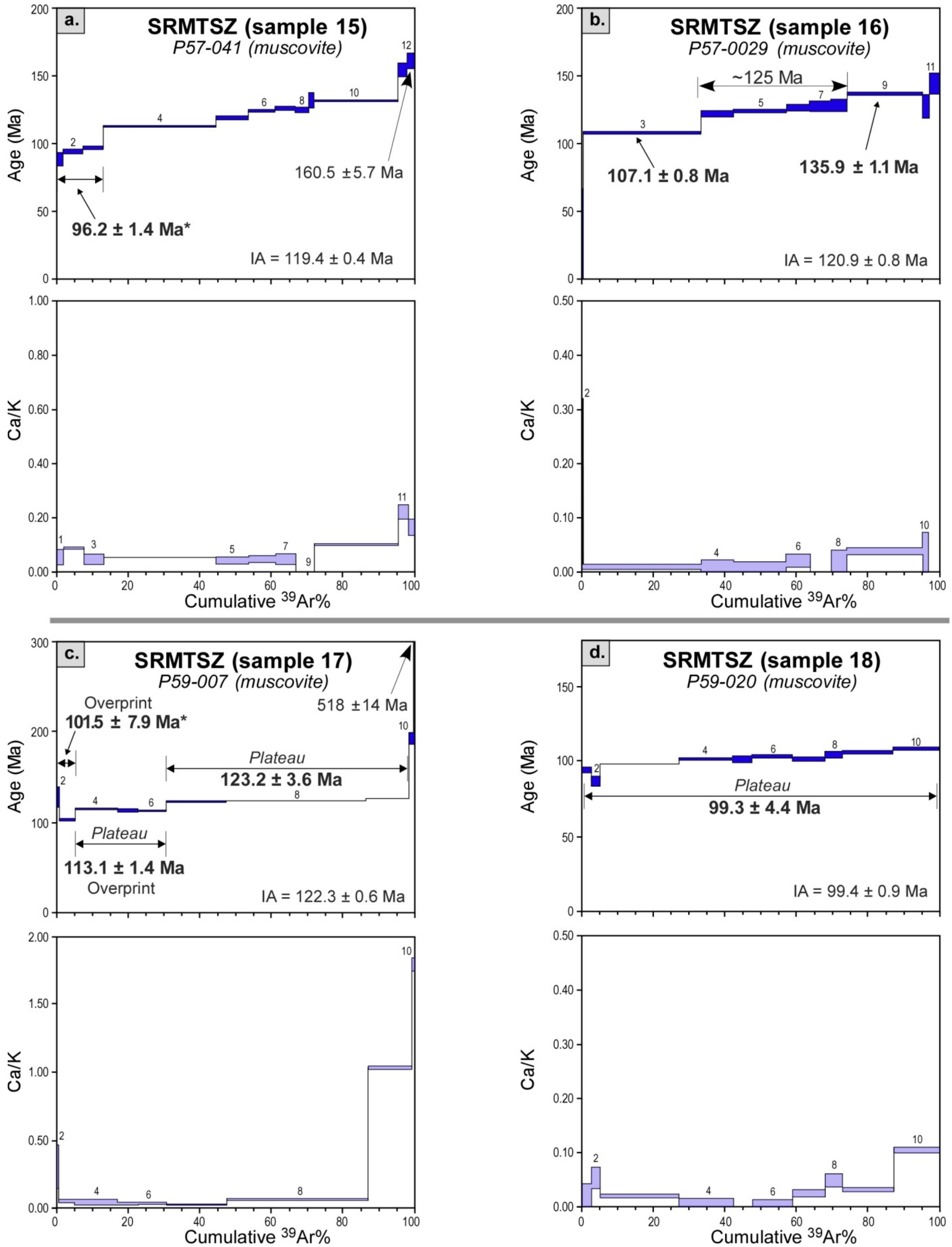

Figure 12. ^{40}Ar/^{39}Ar age and apparent K/Ca spectra for muscovite crystals from phyllite/phyllonite samples collected along the Southern Rocky Mountain Trench north of McBride. Data plotted as in Figure 4.

From sample 17, a muscovite (P59-007), run in 11 steps yields an IA of 122.3 ±0.6 Ma from low but non-uniform Ca/K ratios (Figure 12c). At low temperature, a plateau-like segment averaging 113.1 ±1.4 Ma is formed by fractions 4 to 6 (with 25.2% of the total ^{39}Ar). This is followed by a high-temperature plateau-like portion (fractions 7 to 9) averaging 123.2 ±3.6 Ma (with 68.1% of the total ^{39}Ar). These ages correspond to a predominantly flat portion of the Ca/K spectrum. At the highest temperature, the pattern steps up steeply to an apparent age of 518 ±14 Ma (fraction 11) from a mineral phase with significantly higher Ca/K values—likely from a relic phase in the muscovite—that degassed at high temperature. On the ^{39}Ar/^{40}Ar vs. ^{36}Ar/^{40}Ar correlation plot, fractions 1 to 3 yield an apparent isochron age of 101.5 ±7.9 Ma with an elevated but imprecise initial ^{36}Ar/^{40}Ar ratio of 1450 ±1840. Ensuing points are clustered near the ^{39}Ar/^{40}Ar axis. Thus, the best estimate for this sample's age is given by the plateau portion averaging 123.2 ±3.6 Ma that is recorded before degassing of the anomalously old impurity.

A muscovite (P59-020) recovered from sample 18, run in 11 steps, yielded an IA of 99.4 ±0.9 Ma from a predominantly flat spectrum (with the exception of the penultimate fraction 10) (Figure 12d). Its age spectrum is slightly inclined upwards climbing from a low-temperature age of 93.7 ±2.0 Ma to the high-temperature age of 106.9 ±0.9 Ma (fraction 10), and gives a plateau age of 99.3 ±4 Ma. The very small fraction 11 yields an imprecise final fusion age of 164 ±47 Ma.

Sample 19 provided both muscovite and very small, pristine, pink, gem quality, garnet crystals. Muscovite (P59-008), run in 13 steps, yielded an IA of 123.3 ±0.6 Ma, given by relatively uniform low Ca/K values (Figure 13a). The complex low-temperature portion of its age spectrum starts at 55.3 ±2.7 Ma and climbs to a maximum age of 128.6 ±0.3 Ma (fraction 5). The pattern oscillates before settling down to a plateau sequence for fractions 9 to 13 with an average age of 128.0 ±1.5 Ma (with 56.2% of the total ^{39}Ar).

Total-fusion ages for the very small garnet crystals separated from this sample (Table 4) are more precise compared to those attempted for sample 13. The apparent ages and Ca/K ratios show wide variation that probably reflects different inclusions trapped during the growth of the garnet.

Assuming that no argon has been lost from the garnet crystals, their youngest apparent age of 135.2 ±4.8 Ma may provide a maximum estimate for the growth of the garnet. This age is very close to the muscovite plateau age of 128.0 ±1.5 Ma from this sample, which implies approximately synchronous blocking of the K-Ar systems in the two minerals. The other garnet crystals yield apparent ages that are significantly older than the associated muscovite. Their apparent ages and Ca/K ratios show wide variation that probably reflects different inclusions trapped during the growth of the garnet as old as ca 2.4 Ga (209-00c), and points to the old ages of their host rocks as indicated by the anomalously old apparent ages in the high-temperature portions of some muscovite age spectra.

Table 4. Total-fusion ages and Ca/K ratios for garnet crystals from sample 19.

Analysis	Age (Ma)	Ca/K
209-00a	135.2 ±4.8	38.7 ±0.3
209-00b	630 ±27	103.2 ±3.8
209-00c	2441 ±42	116.2 ±4.9
209-00d	200.4 ±7.5	150.2 ±1.3
214-00	260 ±16	0.2 ±0.6

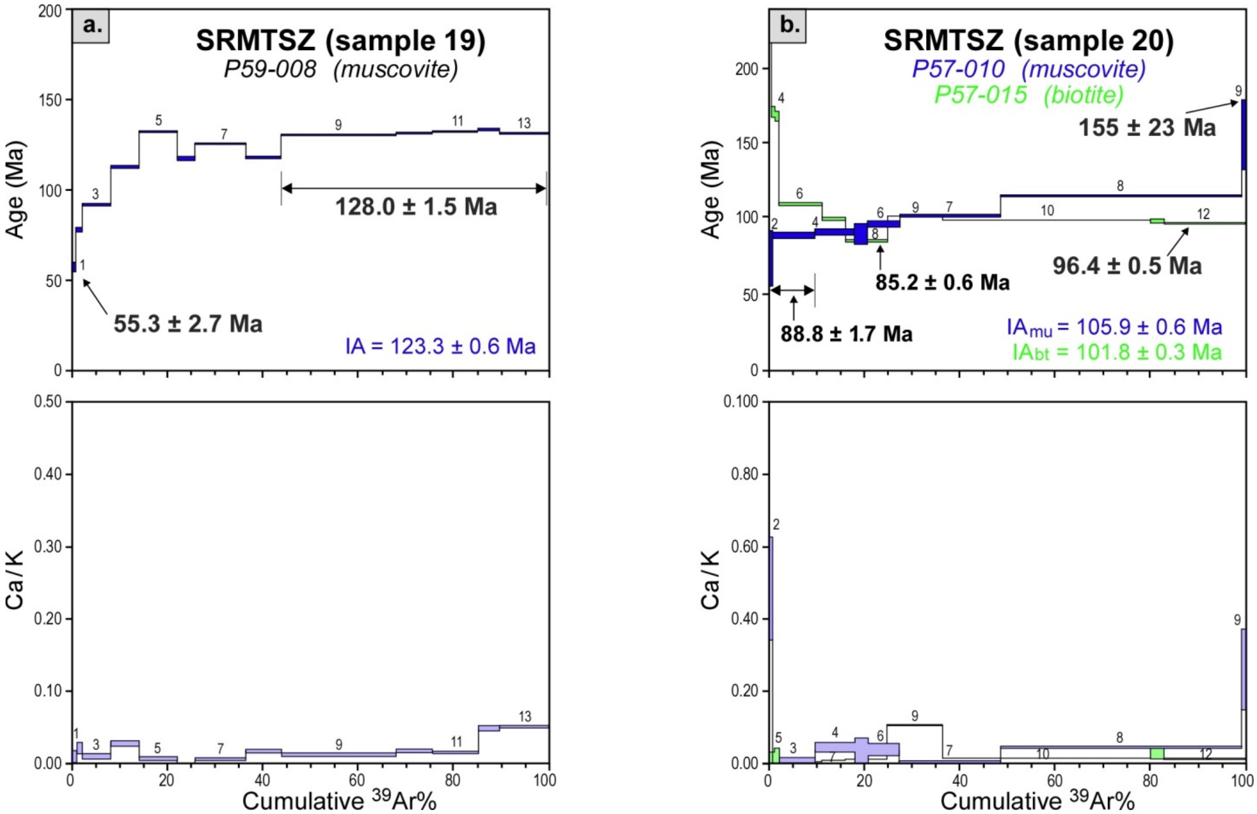

Figure 13. ^{40}**Ar/**^{39}**Ar age and apparent K/Ca spectra for muscovite and/or biotite or plagioclase crystals from phyllite/phyllonite samples collected along the Southern Rocky Mountain Trench near Tête Jaune Cache. Data plotted as in Figure 4.**

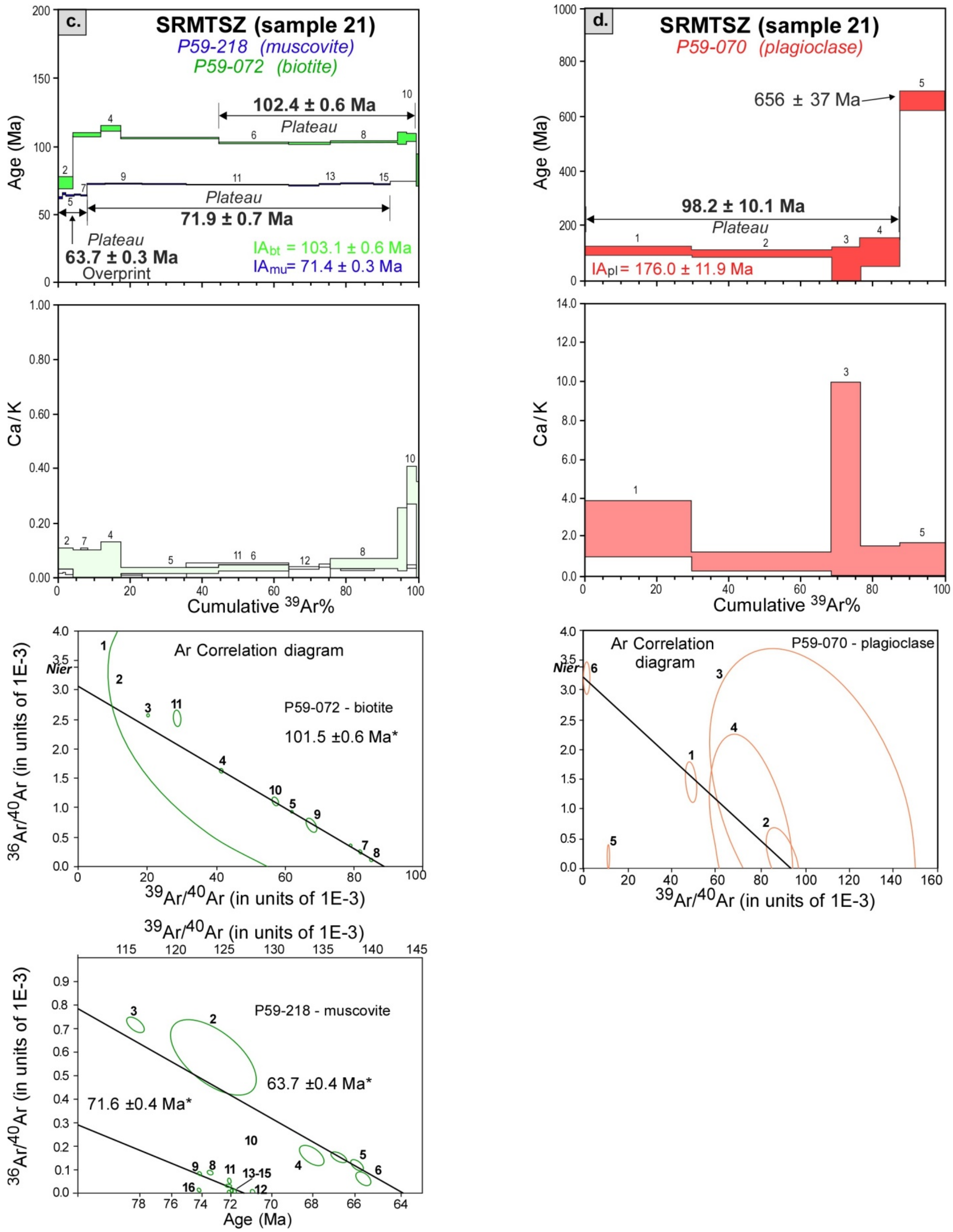

Figure 13 (continued). $^{40}Ar/^{39}Ar$ age and apparent K/Ca spectra for muscovite and/or biotite or plagioclase crystals from phyllite/phyllonite samples collected along the Southern Rocky Mountain Trench near Tête Jaune Cache. Data plotted as in Figure 4.

From sample 20 both muscovite and biotite separates were obtained. A muscovite crystal (P57-010), run in 9 steps, gives an IA of 105.9 ±0.6 Ma (Figure 13b). From a low-temperature age of 88.8 ±1.7 Ma for fractions 1 to 3 (with 9.8% of the total ^{39}Ar), the pattern climbs to an age of 115.0 ±0.4 Ma in fraction 8 (with 50% of the total ^{39}Ar). The final fraction has an apparent age of 155 ±23 Ma that correspond to a higher Ca/K ratio. Biotite (P57-015) run in 12 steps gives an IA of 101.8 ±0.3 Ma (Figure 13b), with an integrated Ca/K ratio of 0.0230 ±0.0007. Its age spectrum plunges from 683 ±43 Ma down to the minimum of 85.2 ±0.06 Ma (fraction 8), before climbing again and finishing at an age of 96.4 ±0.5 Ma in the final fraction. Fractions 9 to 12 representing 75% of the total ^{39}Ar form a slightly down-sloping plateau-like segment with a weighted average age of 100.4 ±2.6 Ma. The climbing age spectrum of the muscovite contrasts with that of the biotite, which shows excess argon in its low temperature fractions. Nonetheless, the muscovite low-temperature age estimate of 88.8 ±1.7 Ma is in fair agreement with the minimum age of 85.2 ±0.6 Ma for the biotite, especially considering that both are estimates of the late overprint for the sample.

Five more samples (21 to 25) were collected between Tête Jaune Cache and at the northern end of Kinbasket Lake (Figure 2).

Fractions of muscovite, biotite, and plagioclase have been obtained from sample 21. Muscovite (P59-218), run in 17 steps, yields an IA of 71.4 ±0.3 Ma from low and relatively constant Ca/K values indicating a single homogenous phase. Its age spectrum (Figure 13c) shows a subordinate low-temperature plateau averaging 63.7 ±0.3 Ma for fractions 1 to 7 (with 2.2% of the total ^{39}Ar). This is followed by a broad plateau averaging 71.9 ±0.7 Ma for fractions 8 to 15 (with 83.9% of the total ^{39}Ar). The final fractions 16 and 17 are slightly older. The discrete partitioning of the muscovite data into two separate plateaus as indicated on its age spectrum is also quite apparent on the ^{39}Ar/^{40}Ar vs. ^{36}Ar/^{40}Ar correlation plot. The plot shows a blow-up near the ^{39}Ar/^{40}Ar axis. The upper line shows the data for fractions 1 to 7 that corresponds to an isochron age of 63.7 ±0.4 Ma. The isochron for higher temperature data points 8 to 15 plots beneath the low-temperature isochron and yields an isochron age of 71.6 ±0.4 Ma, with an imprecise initial ^{40}Ar/^{36}Ar ratio of 460 ±100. Neither isochron result is significantly different from the ages calculated from their respective plateaus.

Apart from a slightly younger ~64 Ma overprint evident in the low-temperature fractions, the data indicate a relatively undisturbed K-Ar system of this mica, and yield a crystallization estimate of 71.9 ±0.7 Ma.

Biotite (P59-072), run in 11 steps, yields an IA of 103.1 ±0.6 Ma from uniform values except the final fraction with a slightly higher ratio. Its age spectrum (Figure 13c) features a starting age of 72.9 ±4.3 Ma, followed by a maximum age of 113.1 ±2.0 Ma (fraction 4). This gives way to a plateau averaging 102.4 ±0.6 Ma for fractions 6 to 10 (with 54.9% of the total ^{39}Ar). The biotite data points are well spread out on the ^{39}Ar/^{40}Ar vs. ^{36}Ar/^{40}Ar correlation plot. Fractions 4 to 10 (with 87.7% of the total ^{39}Ar) fit a line within experimental uncertainties that corresponds to an isochron age of 101.5 ±0.6 Ma, with an initial ^{40}Ar/^{36}Ar ratio of 327.0 ±5.0.

A very small unaltered plagioclase crystal (P59-070), run in six steps, yields an IA of 176.0 ±11.9 Ma (Figure 13d). Its age spectrum consists of a plateau averaging 98.2 ±10.1 Ma for fractions 1 to 4 (with 53.2% of the total ^{39}Ar). Fraction 5 jumps to a significantly older age of 656 ±37 Ma. This high-temperature fraction explains the somewhat high IA and may reflect the presence of relict material within the crystal. The age signature from the major portion of gas from the crystal (plateau age of 98.2 ±10.1 Ma) is indistinguishable from the biotite age.

The analysis of both biotite and muscovite in this sample allows additional insight into the deformation history and timing of mineral growth in this rock. The age of the biotite is ~30 Ma older than that of the associated muscovite. This result is inconsistent with a picture of simple cooling of the rock through the micas' blocking temperatures. Since the closure temperature of muscovite (300–350°C) is significantly higher than biotite's (~250°C), simple slow cooling should render the muscovite's age at least as old as the biotite. Instead, the age pattern of the micas suggests that the biotite, and possibly the plagioclase, represent earlier phases in the crystallization history of the rock, and confirms that the younger muscovite has grown during later tectonism. Indeed, the age of 72.8 ±4.3 Ma recorded from the lowest temperature steps (fractions 1 and 2) of the biotite also appears to be imprinted with the age of the muscovite growth.

Thus, the main muscovite plateau age of 71.9 ±0.7 Ma provides the best estimate for the age of tectonism associated with the growth of this mineral. The younger age at 63.7 ±0.3 Ma given by the low-temperature fractions may represent a younger, gentler overprint on this mica.

Two sericite separates were obtained from sample 22. Sericite P54-004, run in six steps, gives an IA of 74.9 ±0.3 Ma, with an integrated Ca/K ratio of 0.0033 ±0.0009 (s1 in Figure 14a). The age spectrum features a mid-temperature minimum age of 71.7 ±0.4 Ma for fractions 3 and 4 (with a total of 20.5% ^{39}Ar). Higher ages of 77.5 ±0.3 Ma and 88.2 ±6.0 Ma for high and low temperature fractions 1 and 6, respectively, suggest that the sample may contain excess argon. If indeed excess argon has been mixed in with the radiogenic argon of this crystal, the minimum age of 71.7 Ma would provide a maximum age estimate for this sample.

The second sericite grain (P54-028) was run in more detail. The analysis was divided into 30 steps and yields a significantly higher IA of 92.1 ±0.3 Ma, but with a similar integrated Ca/K ratio of 0.0058 ±0.0004 (s2 in Figure 14a). Its age spectrum also shows signs of excess argon, having low and high temperature age maxima at 1277 ±23 Ma (fraction 1) and 3050 ±49 Ma (fraction 30), respectively. Its Ca/K spectrum is uniformly low, except for a slight increase in the last three fractions. On the age spectrum there is a low-temperature minimum age of 59.5 ±1.6 Ma for fractions 6 to 8 (with a total of 1.4% ^{39}Ar). Following this, the spectrum climbs to a pattern that oscillates between average ages of 75.5 ±0.3 Ma (fractions 13, 16, and 17) with a total of 23.5% ^{39}Ar) and a lower age of 71.5 ±0.6 Ma (fraction 15). Ensuing fractions then climb at first gradually (fractions 19 to 24) and then more steeply to the high temperature age maximum. On the argon correlation plot the data form a roughly oval distribution, trending from low ^{39}Ar/^{40}Ar ratios to the highest ratios in fractions 6 to 8, before plunging to higher ratios of ^{36}Ar/^{40}Ar. High-temperature fractions 21 to 30 (with a total of 36.5% of the ^{39}Ar) form an array that trends back to fractions 1 with very low ^{39}Ar/^{40}Ar value. This array is linear within experimental uncertainties and corresponds to an isochron age of 77.7 ±3.1 Ma, with a very high initial ^{40}Ar/^{36}Ar ratio of 7417 ±524.

Assuming that excess argon has affected these samples, the lowest points on their age spectra are least affected and can provide approximations to their crystallization ages. Although the two analyses have different quantities of excess argon, as shown by their variable integrated ages, the age of ~71.5 Ma is a mid-temperature low common to both spectra and may be significant. On the other hand, a more refined estimate that corrects for the excess argon (as reflected in the high initial ^{40}Ar/^{36}Ar ratio compared to the modern value of 295.5 ["NIER"]),(Nier, 1950; Lee et al., 2006; Quan et al., 2014) and includes more of the overall data, is given by the isochron age of 77.7 ±3.1 Ma. The age of 59.5 ±1.6 Ma taken at very low temperature represents a very small fraction of the age spectrum (<2% 39Ar). This is the lowest apparent age and may represent a mild overprint on the mica.

Sample 23 is a whole rock chip (P57-023) run in 16 steps gives an IA of 138.9 ±0.9 Ma, with an integrated Ca/K ratio of 48.8 ±0.5 (Figure 14b). Its age spectrum begins at an extreme average age of 3002 ±56 Ma (fractions 1 and 2), then descends precipitously to a plateau averaging 85.4±0.5 Ma for fractions 12 to 17 (with 39.2% of the total 39Ar). The high ages in the low-temperature portion of the age spectrum are matched by high Ca/K ratios (usually indicative of liquid inclusions). The Ca/K spectrum drops from a maximum of 388 ±5 (fractions 5 and 6) to an average of 0.41 ±0.18 in the plateau steps 12 to 17. By fraction 12, the excess argon characterizing the low to mid-temperature fractions appears to have been quantitatively separated from the high temperature, low Ca/K fractions. Thus, the best estimate of the sample's age is high-temperature plateau result of 85.4±0.5 Ma. On the ^{39}Ar/^{40}Ar vs. ^{36}Ar/^{40}Ar plot the high-temperature points are clustered near the 39Ar/40Ar axis and do not offer additional age information.

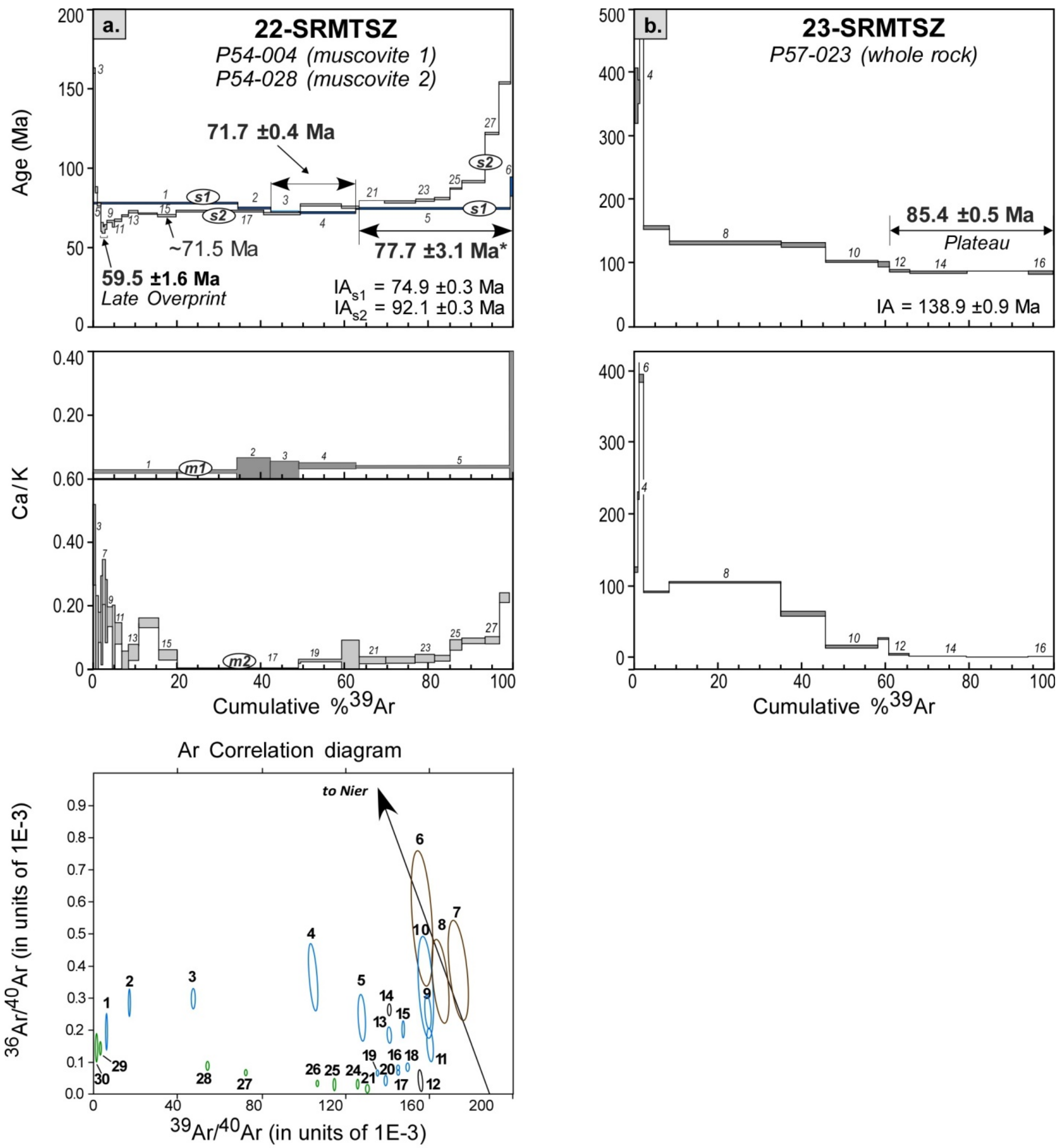

Figure 14. $^{40}Ar/^{39}Ar$ age and apparent K/Ca spectra for muscovite/sericite, and K-feldspar crystals or whole rock chips from phyllite/phyllonite samples collected along the Southern Rocky Mountain Trench from Tête Jaune Cache to the northeast side of Kinbasket Lake. Data plotted as in Figure 4.

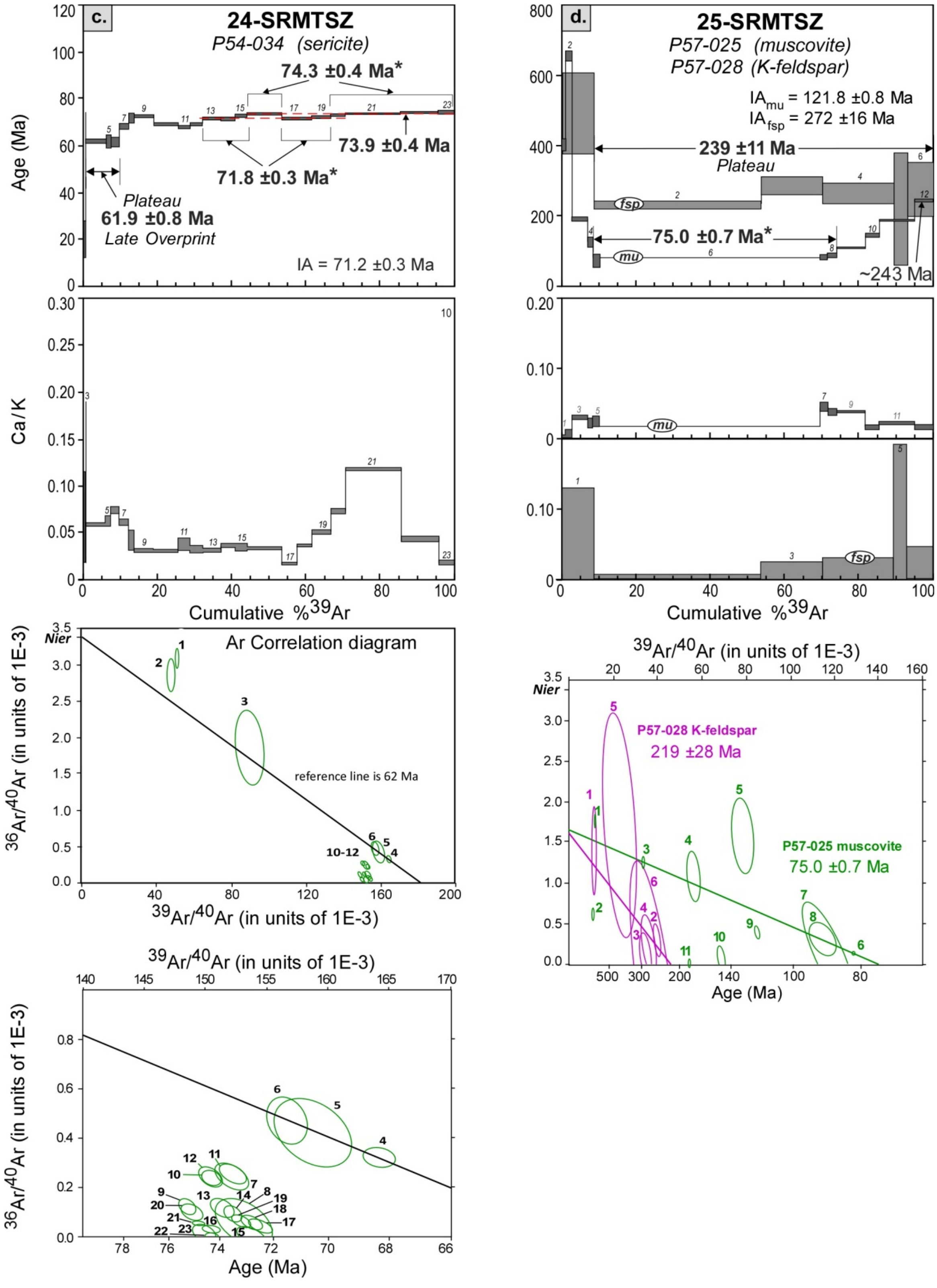

Figure 14 (continued). $^{40}Ar/^{39}Ar$ **age and apparent K/Ca spectra for muscovite/sericite, and K-feldspar crystals or whole rock chips from phyllite/phyllonite samples collected along the Southern Rocky Mountain Trench from Tête Jaune Cache to the northeast side of Kinbasket Lake. Data plotted as in Figure 4.**

A sericite grain (P54-034) from sample 24, run in 23 steps, gives an IA of 71.2 ±0.3 Ma, with an integrated Ca/K ratio of 0.0514 ±0.0006 (Figure 14c). Its Ca/K spectrum features a high-temperature peak in fraction 21. The complex age spectrum begins at an age of 20 ±8 Ma and is followed by a climb to a mini-plateau averaging 61.9 ±0.8 Ma (with 9.1% of the total ^{39}Ar). The remaining fractions oscillate between ages of 68.0 ±0.7 Ma (fraction 11) and 73.7 ±0.4 Ma (fraction 16), before making a final climb from fraction 17 to a high-temperature age of 74.3 ±0.4 Ma (fractions 22 and 23, with 14.3% of the total ^{39}Ar). On the argon correlation plot the data trend to increasing values of ^{39}Ar/^{40}Ar until fraction 6. Ensuing points are more radiogenic and cluster below the 62 Ma reference isochron for fractions 3 to 6. After fraction 12, the data partition into 2 separate clusters with apparent ages of 71.8 ±0.3 Ma (fractions 13 to 15, and 17 to 19); and 73.9 ±0.4 Ma (fractions 20 to 23 and 16). This pattern may reflect mixing of 72 and 74 Ma components within the sample.

A K-feldspar and a muscovite grain were separated from sample 25. A minute K-feldspar fragment (P57-028), run in 6 steps, gives an IA of 272 ±16 Ma, with an integrated Ca/K ratio of 1 ±1 (Figure 14d). Fractions 2 to 6 (with 91.2% of the total ^{39}Ar) yield a plateau age of 239 ±11 Ma. On the ^{39}Ar/^{40}Ar vs. ^{36}Ar/^{40}Ar plot all fractions fit a line within experimental uncertainties, which corresponds to an isochron age of 219 ±28 Ma, with an initial ^{40}Ar/^{36}Ar ratio of 618 ±274.

The muscovite crystal (P57-025) from the same sample 25, run in 12 steps, gives a much lower IA of 121.8 ±0.8 Ma, with an integrated Ca/K ratio of 0.181 ±0.004 (Figure 14d). Its age spectrum is U-shaped given by a mid-temperature plateau averaging 78.2 ± 0.3 Ma for fractions 5 to 8 (with 65.3% of the total ^{39}Ar) between age extremes of 1654 ±15 Ma (fraction 1) and 243.4 ±4.1 Ma (fraction 12). On the ^{39}Ar/^{40}Ar vs. ^{36}Ar/^{40}Ar plot fractions 3 to 8 (with 65.3% of the total ^{39}Ar) yield a slightly younger age of 75.0 ±0.7 Ma, with an initial ^{40}Ar/^{36}Ar ratio of 600 ±33. The isochron age of 75 Ma accommodates the excess argon evident in the plateau on the age spectrum and therefore is the preferred estimate for the muscovite’s age.

The younger age for the muscovite probably reflects its growth during a rejuvenation of the rock, although the high-temperature portion of its age spectrum climbs to 243 Ma, which is within uncertainty of the K-feldspar plateau age. Accordingly, older ages in the higher temperature portion of the muscovite spectrum may reflect incomplete resetting of its K-Ar system, or the presence of relicts in the crystal. Thus, the age of 240 Ma may be close to the formation (or cooling) age of the rock.

The ~518 Ma muscovite fusion age in sample 17 and the plagioclase high-temperature age of ~656 Ma in sample 21 are the only hints to old protolith ages or pre-Cretaceous tectonothermal events overprinting the analyzed Precambrian to Cambrian phyllite/phyllonite samples in the SRMTSZ. The Middle Triassic feldspar plateau age of 240 Ma was recovered from a garnet micaschist on the east side of Kinbasket Lake (sample 25, Figure 3) interpreted by McDonough and Simony (1989) as part of the metamorphosed cover (Miette Group equivalent) of the Bulldog gneiss. The Jurassic event inferred on either side of the Trench at this latitude appears largely obliterated in the phyllonite samples from the SRMTSZ, with the only hints of Late Jurassic tectonism represented by the muscovite fusion ages of 161 Ma (sample 15) and 155 Ma (sample 20).

Samples from the McBride area show Early to mid-Cretaceous integrated ages: 123 Ma (sample 19); 122 Ma (sample 17); 121 Ma (sample 16); 119 Ma (sample 15); 106 Ma muscovite and 102 Ma biotite (sample 20); 103 Ma (sample 21) and 99 Ma (sample 18) (Figures 12, 13). Although these ages represent total gas ages equivalent to K-Ar dates, we note that the ages vary within a limited range and thus may be geologically significant. In detail, individual spectra show a muscovite high-temperature age of 136 Ma (sample 16) that matches a ^{40}Ar/^{39}Ar garnet age of 135 Ma (sample 19), as well as well-defined high temperature plateau ages of 128 Ma (sample 19) and 123 Ma (sample 17). These ages may record distinct Valanginian (136–135 Ma) and Barremian–Aptian (128–123 Ma) events in the SRMTSZ, which appear to be quasi-contemporaneous with those identified in the WCFZ (133 Ma and 124 Ma, respectively).

A mid-Cretaceous event is recorded by the low temperature plateau age of 113 Ma (sample 17) with a low-temperature isochron age of 102 Ma (fractions 1, 2, and 3) as well as the low-temperature age of

107 Ma (sample 16), the well-defined high-temperature biotite plateau age of 102 Ma (sample 21), the full-spectrum, inclined plateau of 99 Ma (sample 18), the well-defined feldspar plateau age of 98 Ma (sample 21), the isochron age of 96 Ma (sample 15), and the 96 Ma high-temperature age of biotite (sample 20). Biotite integrated ages of 102 Ma and 103 Ma from two samples, 30 km apart (sample 20 and 21, respectively) correlate well with the 106 Ma integrated age of muscovite from sample 20, strengthening the argument for a mid-Cretaceous tectonic event. Moreover, the biotite plateau age of 102.4 ±0.6 Ma from sample 21 is close to the 100 ±2 Ma biotite $^{40}Ar/^{39}Ar$ age reported from the same location by Van der Driessche and Malusky (1986). The mid-Cretaceous tectonic event along SRMTSZ may have started during early Albian (113 Ma) and peaked during the late Albian–Cenomanian (102–98 Ma), as suggested by the best-defined plateau ages identified in samples 18 (Figure 12d), 20, and 21 (Figure 13b–d). These ages are similar to those obtained from the WCFZ (111–96 Ma). The identification of a high-temperature muscovite plateau age of 85 Ma (sample 23) in the SRMTSZ, which is identical with the 85 Ma age recorded in the WCFZ (sample 6), makes a strong argument for a kinematic link between the two lineaments of strain.

A sericite isochron age of 78 Ma (sample 22, Figure 14a), and several muscovite ages including the 75 Ma mid-temperature plateau age (sample 25, Figure 14d), the high-temperature mini-plateau age of 74 Ma (sample 24, Figure 14c), the well-defined 72 Ma muscovite plateau age (sample 21, Figure 13c), and the ca. 71.5 Ma mid-temperature low of two muscovite grains in the same sample (sample 22) indicate middle Campanian to earliest Maastrichtian tectonism along the eastern flank of the SRMTSZ between Tête Jaune Cache and northern Kinbasket Lake. All three phyllonite samples with ages in the 75 to 72 Ma range, yield a narrow error-weighted age estimate of 72.5 ±0.3 Ma.

In the case of samples 22 (SRMTSZ) and 11 (VSZ), the ages presumably correspond to the crystallization of the white mica associated with the phyllonitization of the Miette Group. Similar ages recovered from samples 24 (74 Ma) and 25 (75 Ma) in the SRMTSZ on the east (Rockies) side of Kinbasket Lake are associated with the retrograde metamorphic event generating the thin films of sericite on K-feldspar porphyroclasts in gneiss.

This mainly Campanian age range overlaps with previously reported 78 Ma $^{40}Ar/^{39}Ar$ muscovite age from Tête Jaune Cache (van den Driessche and Malusky, 1986) and the 72 Ma biotite K-Ar age from the mylonitized Bulldog gneiss (Wanless et al., 1967).

Muscovite low temperature ages of 60 Ma (sample 22, Figure 14a), and the muscovite mini-plateau ages of 62 Ma (samples 24, Figure 14c) and 64 Ma (sample 21, Figure 13c) hint to slightly early Paleocene rejuvenation in the northern SRMTSZ, between Tête Jaune Cache and Kinbasket Lake. To the north along the McBride segment of the Trench, the latest Cretaceous and Paleocene rejuvenation has not been identified, yet.

8 Regional Correlations

The age groups identified in this study (Table 5) are roughly coincident with the five periods of metamorphism, deformation, and plutonism (175–160, 140–120, 110, 100–90, and 75–50 Ma) previously identified in different parts of the southern Omineca belt (Parrish, 1995). More importantly, the same age groups have been recognized in the Selkirk-Monashee-Cariboo (SMC) metamorphic complex of the southeastern Omineca belt, directly south and west of the investigated area (e.g., Sevigny et al., 1990; Colpron et al., 1996; Crowley et al., 2000; Gibson, 2008). In particular, the recovery of roughly the same five age groups (~163, 122, 110, 99–93, and 72–58 Ma; Crowley et al., 2000) from the relatively small Mica Dam area near the SRMTSZ (Figure 15) suggests a direct correlation of the tectonothermal events in the SMC metamorphic complex to the high strain zones overprinting the western Rocky Mountains examined in this study. Moreover, the age groups identified in this study along the northern segment of the SRMTSZ and within the SMC (published data) overlap with the ages of the main pulses of thrusting identified in the adjacent Rocky Mountain fold-and-thrust belt (Pană and van der Pluijm, 2015). Here we review existing dates and explore the possible kinematic links.

Table 5. Summary of age intervals obtained from phyllonite samples from the three zones of strain concentration at the western margin of the Rocky Mountain fold-and-thrust belt.

Tectonic Lineament	Sample No.	Field Site	Analysis	Pre-Jurassic	Jurassic	Early Cretaceous	Mid-Cretaceous	Late Cretaceous		Early Cenozoic
							Albian-Cenomanian	*Coniacian-Santon.*	*Campan.-Maastrich*	
Monarch thrust	**4**	**DP11-123**	**P57-004 (bt)**	620 ±58 (isochron)						
			P57-007 (wr)	624.0 ±4.9 (FS)		134.5 ±8.1 (low)				
Moose Pass thrust	**5**	**DP11-125b**	**P57-009 (am)**	326.3 ±1.3 (IA)						
				452 ±5.1 (FS)						
			P57-002 (mu)	289.9 ±0.8 (IA)		134.8 ±1.8 (low)				
				421.0 ±4.8 (FS)						
Walker Creek fault zone	**6**	**DP12-110**	**P59-081 (mu)**	279.7 ±3.2 (FS)	171.9 ±0.8 (IA)			85.3 ±0.9 (PA)		
					184 ±35 (PA)					
	7	**DP12-112**	**P59-068 (mu)**			123.7 ±0.7 (PA)	110.9 ±0.6 (min)			
						132.5 ±2.5 (isochron)				
	8	**DP11-136**	**P57-030 (mu)**		168.3 ±2.3 (FS)		96.1 ±1.0 (low)		67.8 ±1.4 (1.9 %)	
	9	**DP12-70**	**P59-017 (mu)**				95.9 ±5.1 (PA)		79.0 ±0.6 (PA)	
Valemount strain zone	**10**	**DP12-105**	**P63-055 (mu)**				96.5 ±0.8 (FS; 19%)	84.2 ±0.7 (IA)	77.1 ±0.7 (low; 18%)	
	11	**DP12-92**	**P54-019 (ser)**						72.6 ±0.4 (PA)	62.3 ±2.4 (mPA)
	12	**DP10-4x**	**P59-080 (mu)**	421.0 ±4.8 (high)	175 ±16 (FS, 0.4%)				71.4 ±0.7 (isochron)	
									68.3 ±0.7 (isochron)	
	13	**DP16-362**	**YK-G421(bt)**				101 (FS)	87.02 ± 0.66 (PA)		
			YK-G421(mu)		~175 (FS)					
	14	**DP12-125**	**P59-026 (mu)**						72.0 ±0.4 (PA)	
									68.8 ±1.1 (mPA), 1.7%)	
Southern Rocky Mountain Trench shear zone	**15**	**DP11-133**	**P57-041 (mu)**		160.5 ±5.7 (high)		96.2 ±1.4 (isochron)	87.9 ±5.0 (lowT, 1.7%)		
			P57-036 (gt)	360 ±90						
	16	**DP11-137**	**P57-029 (mu)**			135.9 ±1.1 (high, 25%)	107.1 ±0.8 (low 32%)			
	17	**DP12-80**	**P59-007 (mu)**	518 ±14 (FS)		123.2 ±3.6 (PA)	113.1 ±1.4 (low, 25%)			
	18	**DP12-77**	**P59-020 (mu)**				99.3 ±4.4 (PA)			
	19	**DP12-81**	**P59-008 (mu)**			128.0 ±1.5 (PA)				55.3 ±2.7
			209-00a (gt)			135.2 ±4.8				
			209-00d,b,c (gt)	200; 630; 2441						
			214-00 (gt)	260						
	20	**DP11-146**	**P57-010 (mu)**		155 ±23 (high)		115.0 ±0.4	88.8 ±1.7 (lowT, 9.8%)		
			P57-015 (bt)				96.4 ±0.5 (FS)	85.2 ±0.6 (low T)		
	21	**DP12-94**	**P59-218 (mu)**						71.9 ±0.7 (PA)	63.7 ±0.3 (mPA, 2.2%)
			P59-072 (bt)	656 ±37			101.5 ±0.6 (isochron)		72.9 ±4.3 (low)	
			P59-070 (pl)				98.2 ±10.1 (PA)			
	22	**DP10-2x**	**P54-004 (ser)**						71.7 ±0.4 (min)	
			P54-028 (ser)						71.5 ±0.6 (min)	59.5 ±1.6 (min, 1.4%)
									77.7 ±3.1 (isochron)	
	23	**DP11-173**	**P57-023 (wr)**					85.4 ±0.5 (PA)		
	24	**DP10-8x**	**P54-034 (ser)**						74.3 ±0.4 (PA)	61.9 ±0.8 (mPA, 9.1%)
	25	**DP11-161**	**P57-025 (mu)**	243.4 ±4.1 (FS)					75.0 ±0.7 (isochron)	
			P57-028 (Kf)	239 ±11 (plateau)						
				219 ±28 (isochron)						

Notes: FS - final (fusion) heating step, percentage of ^{39}Ar released; PA - plateau age; mPA - mini plateau age; IA - total gas age; min - minimum age within complex-pattern spectrum; mu - muscovite; ser - sericite; bt - biotite; gt - garnet; Kf - potassic feldspar ; pl - pagioclase; wr - whole rock

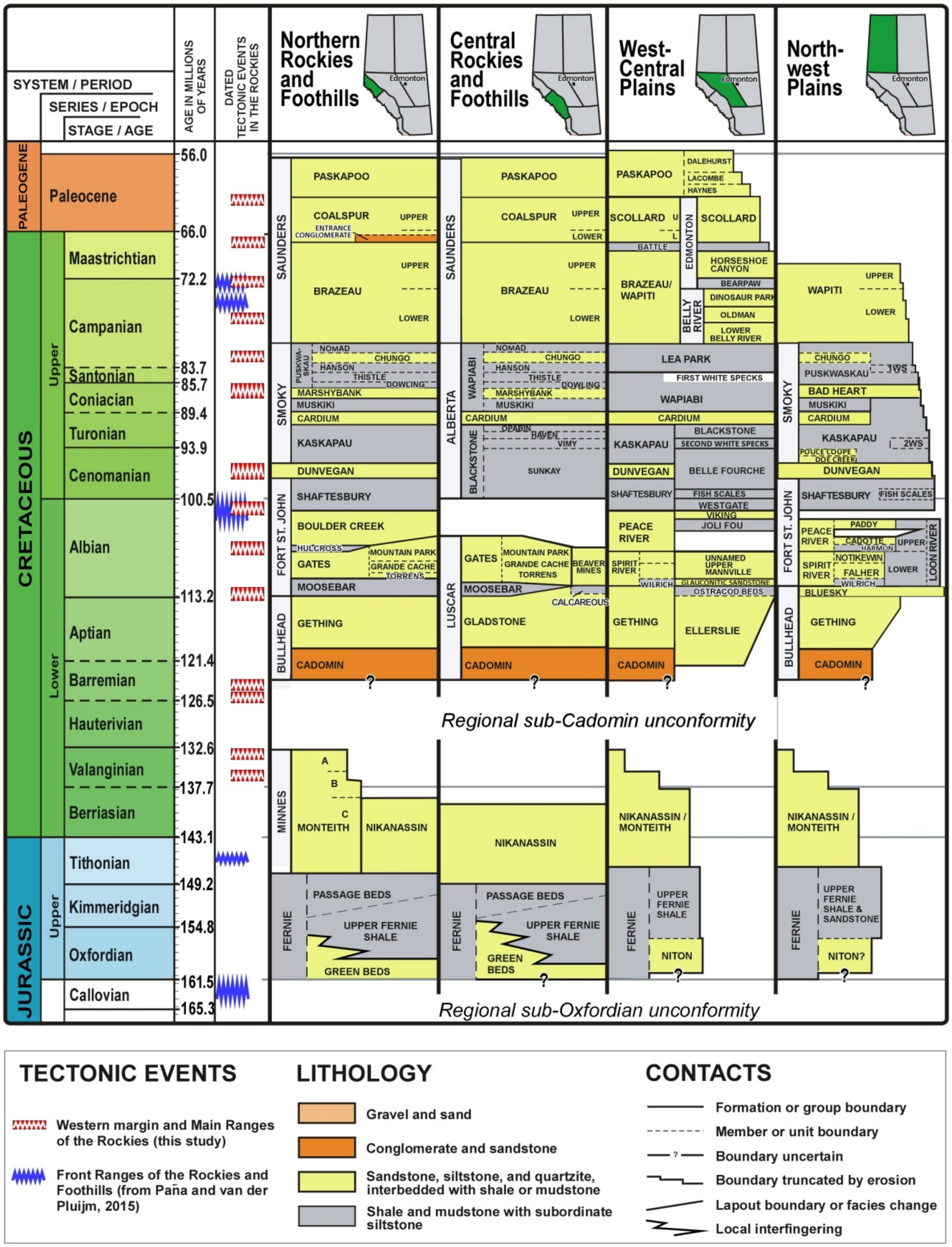

Figure 15. Time-correlation of Cretaceous tectonic pulses in the Foreland belt (Rocky Mountain fold-and-thrust belt, red zig-zag lines) with major depositional changes in the foreland basin (Alberta Basin); stratigraphy simplified after the Alberta Table of Formations (https://ags.aer.ca/activities/table-of-formation.html) and Pană et al. (2018a, b). Geological time scale from Gradstein et al. (2020). Tectonic pulses in the Rockies (blue zig-zag lines) from Pană and van der Pluijm (2015).

Directly south and west of the investigated area, on the west side of the SRMTSZ, metamorphic rocks of the Neoproterozoic Horsethief, Kaza, and Cariboo groups, and of the lower Paleozoic Lardeau Group, which encompass parts of the Selkirk, Monashee, and Cariboo mountains have been referred to as the SMC metamorphic complex (Crawley et al., 2000). Xenoblastic monazite grains with highly embayed boundaries of internal zoning indicate significant dissolution and multiple periods of growth. Peak metamorphic conditions were reached in different areas at different times, from the late Early Jurassic to early Cenozoic time (Crowley et al., 2000). In spite of these complexities, a set of northwest trending regional isograds appear roughly parallel to the regional structural grain in the central part of the SMC complex (Figure 15). Within the wide region dominated by the occurrence of sillimanite (generally fibrous, locally coarse-grained and prismatic), the metamorphic grade increases in a southwesterly direction from the sillimanite-*in*, through the kyanite-*out* isograd (that coincides for the most part with the first appearance of peraluminous granites), to the metamorphic culmination defined by muscovite-*out* isograd (i.e., disappearance of muscovite in the presence of quartz) (Figure 15). The isograds are oblique to the F2 folds towards the northern (northern Monashee and southern Cariboo mountains; Currie, 1988; Sevigny and Simony, 1989) and southern (south of the Bigmouth pluton in the Selkirk Mountains; Gibson et al., 2008) extremities of the SMC metamorphic complex (Figure 15) suggesting metamorphic conditions outlasted F2 deformation.

A single Barrovian metamorphic zonation (lack of intersecting isograds) and the apparent geological continuity (same fold generations and the Neoproterozoic Windermere stratigraphy) suggest the Jurassic through Cenozoic tectonothermal events were mostly cospatial.

On the western margin of the Rockies, south of Valemount, although somewhat disturbed by faulting in the vicinity of the SRMTSZ, a regular succession of Barrovian isograds from staurolite-kyanite, garnet, and biotite can be traced in the Neoproterozoic Miette Group and lower Paleozoic strata. The biotite-*in* isograd, although not mapped, in the region northeast of Kinbasket Lake, is mentioned by Charlesworth and Price (1972) just west of the Rocky Mountain divide along Highway 16 between Jasper and Tête Jaune Cache. A second biotite-*in* isograd mapped by McDonough and Murphy (1994) across the garnet isograd in the Miette Group east of Valemount is here interpreted as the result of shear zone metamorphism along the SRMTSZ and VSZ contemporaneous with the greenschist facies retrogression of the orthogneiss and amphibolite-facies paragneiss east of the trench. It is worth noticing that Rocky Mountains stratigraphy is only metamorphosed vis-à-vis the SMC metamorphic complex in the Omineca belt, suggesting limited, probably within 100 km, translations along the SRMT after the Barrovian metamorphic overprint.

8.1.1 Pre-Jurassic Ages

The oldest preserved dates are muscovite plateau ages of 1.65–1.59 Ga in the Miette Group which may record formation and/or cooling of the muscovite-bearing source rocks. The Miette (Windermere) clastic deposits were largely sourced from the adjacent Canadian Shield and the Middle Proterozoic Belt-Purcell Supergroup underlaying Windermere strata to the south. We note that no tectonothermal event contemporaneous with the Miette deposition is known on the immediate Canadian Shield and the muscovite age interval largely overlaps with the North American magmatic gap (NAMG: 1610–1490 Ma). Therefore, the ages of the detrital muscovite in the Miette Group more likely represent cooling ages during the slow uplift and erosion of the adjacent Paleoproterozoic crystalline basement. Because in the nearest exposed Canadian Shield muscovite-bearing rocks are rare, the reworking of muscovite from the Belt-Purcell Supergroup (with an interpreted source in now tectonically removed ca. 1.7 Ga western basement; Ross and Villeneuve, 2003) appears as a reasonable alternative source.

Zircons from the Hugh Allan leucogranitic orthogneiss yielded a colinear array with an upper intercept of 736 Ma and lower intercept of 173 Ma (McDonough and Parish, 1991). The upper intercept age represents an emplacement age in the range of several other felsic and alkaline igneous rocks or carbonatite intrusions, which may record igneous activity associated with extensional tectonics of the protocontinental margin (Parrish, 1995; Millonig et al., 2012). Pre-Jurassic tectonothermal event(s) affecting the Windermere Supergroup could include late Paleozoic (McDonough and Parrish, 1991) and Triassic (Murphy et al., 1995) events, but their areal extent and intensity is unknown.

An uppermost Mississippian zircon lower intercept age of 326 ±36 Ma from a foliated leucogranitic Bulldog gneiss sample on the east side of the RM trench (northern Kinbasket Lake) is very close to the Late Devonian–mid-Mississippian (between 335–375 Ma) emplacement age of the granitic protoliths of two orthogneiss bodies near Quesnel Lake in the Barkerville terrane in the western Cariboo Mountains (Mortensen et al., 1987). This time interval partly overlaps with Antler tectonism.

A K-Ar date of 261.4 ±5.7 Ma from a phyllitic argillite in the Upper Miette east of the northernmost segment of the SRMT (McMechan and Roddick, 1991) and an imprecise Permian monazite upper intercept age of ca. 276 Ma from the SMC complex in the Mica Dam area (Crowley et al., 2000) are within the range of 279 ±25 Ma and 259 ±34 Ma zircon lower intercept ages reported from the foliated leucogranitic Bulldog orthogneiss and granodioritic Yellowjacket orthogneiss, respectively (McDonough and Parish, 1991) and may hint to a mid-Permian tectonothermal event. However, allanite from one of the two Yellowjacket samples shows the same degree of Pb loss as zircon, and the similar $^{207}Pb/^{206}Pb$ ages suggests that Mesozoic metamorphism, although significant, has not been sufficiently severe to reset the allanite U-Pb system.

The ca. 239 Ma feldspar age obtained from the garnet micaschist of the SRMTSZ (sample 25) may point to a Triassic event, also suggested by previous K-Ar dates of ca. 232 Ma, and 226 Ma (McMechan and Roddick, 1991).

8.1.2 Jurassic Tectonism

Several $^{40}Ar/^{39}Ar$ spectra from phyllonites of all three tectonic lineaments investigated for this report show step ages in the ca. 185–155 Ma range and hint to Jurassic tectonism. This Jurassic range of $^{40}Ar/^{39}Ar$ ages encompasses the K-Ar ages of ca. 181 Ma and 178 Ma previously reported from the Rocky Mountains northeast of McBride (McMechan and Roddick, 1991).

The imprecise lower intercept age of 173 Ma obtained from the Hugh Allen orthogneiss was suggested to represent Pb loss associated with a Jurassic tectonometamorphic event (McDonough and Parish, 1991).

In the Omineca belt, the Jurassic tectonothermal event is defined by the initial development of kilometre-scale, southwest-verging recumbent, isoclinal folds (F1) and nappes, such as the Scrip nappe in the northern Selkirk and Monashee mountains (Residae and Simony, 1983), the Carnes nappe in the western Selkirk Mountains (Brown and Lane, 1988), and the Riondel nappe in the Kootenay Arc (Höy, 1976). The timing of F1 is uncertain. In the south-central Cariboo Mountains, upright and southwest-verging map-scale folds formed before the 174 ±1 Ma emplacement of the Hobson Lake pluton (Gerasimoff, 1988; Reid et al., 2002), and in the Selkirk Mountains west-verging structures formed between 173-168 Ma (Colpron et al., 1996) or 172–167 Ma (Gibson et al., 2005). Note however that Mortensen et al. (1987) interpreted a U-Pb age of 174 ±4 Ma for metamorphic sphene from one of the orthogneiss bodies in the Barkerville terrane (near Quesnel Lake) as dating the end of the second phase of deformation (F2) in southwestern Cariboo Mountains.

Metamorphic conditions during the Jurassic tectonothermal event increased southeastwards: from non-metamorphic in the northern Cariboo (Reid et al., 2002), to amphibolite facies in the southern Cariboo and northern Monashee, and to upper amphibolite facies in the northern Selkirk mountains (Colpron et al., 1996; Gibson et al., 2008).

The Late Jurassic tectonothermal event is recorded in the southeastern Cariboo Mountains by a K-Ar hornblende age of 156 Ma and a 154 Ma zircon age from pegmatite intrusions in the Kaza Group (Currie, 1988). In the immediately adjacent Malton complex of the northernmost Monashee Mountains, a K-Ar hornblende age of 156 Ma from a sample with biotite ages of 59 and 54 Ma (McDonough et al., 1991a) suggests that the hornblende age is likely related to Late Jurassic postmetamorphic cooling, whereas the ca. 100 Ma younger biotite age matches the 55 Ma K-Ar biotite cooling dates related to Eocene regional exhumation of the northern Monashee Mountains (Sevigny et al., 1990). Just south of the Malton basement complex, the ca. 496 Ma Cambrian Little Chicago carbonatite intruded into the Horsethief Creek (Windermere) cover and was subject to a ca. 156 Ma overprint (Millonig et al., 2012). The ca. 156 Ma ages indicate that both basement and cover shared a common Late Jurassic evolution (Figures 15, 16).

Evidence for the Jurassic tectonothermal event appears to have been obliterated during the metamorphic culmination of the northern Monashee Mountains (Sevigny et al., 1990), but it is preserved to the east in the Mica Dam area by 163 Ma garnet, by 166-160 Ma primary monazite and xenotime, and pegmatite emplacement (Crowley et al., 2000). SHRIMP spot dates of 183 Ma ($^{206}Pb/^{238}U$) and 173 Ma ($^{208}Pb/^{232}Th$) from monazite inclusions in garnet are the oldest Jurassic ages recovered in this area (Crowley et al., 2000).

Farther south, the Jurassic tectonothermal event is well preserved in the west flank of the Selkirk fan, a peculiar structure in the Selkirk Mountains, where folds on either side of a northwesterly trending fan axis have opposite vergence (Figure 16). At the northern end of the fan, outcrop-scale southwest-verging isoclinal folds (interpreted as F2 folds) developed during the high-grade metamorphic peak (172–167 Ma) and were sealed by the emplacement of the late kinematic 167 Ma Adamant and Bigmouth plutons, and the 156 Ma post F2 tonalite dykes (Gibson et al., 2005). Immediately to the south in the Illecillewaet synclinorium, the same high-grade metamorphism accompanied by southwest-verging folding and thrusting (173–168 Ma) led to rapid decompression (exhumation), which was completed by the late Middle Jurassic time (165 Ma, Colpron et al., 1996).

The 184–155 Ma range of $^{40}Ar/^{39}Ar$ dates obtained from phyllonites along the northern segment of the SRMTSZ coincides with the 183–154 Ma range of U-(Th)-Pb dates reported so far from the SMC metamorphic complex of the adjacent eastern Omineca belt.

8.1.3 Early Cretaceous–Early Eocene Tectonism

The garnet age of ca. 135 Ma recognized on the west flank of the SRMTSZ (sample 19) and the ca. 133 Ma muscovite isochron age found in the WCFZ (sample 7) testify for an early Cretaceous tectonic pulse at the western margin of the Rockies (Figures 15, 16) and are similar to Valanginian ages recognized to the south in the SMC metamorphic complex. Thus, in the southern Cariboo Mountains, just west of the Malton basement complex, the amphibolite facies metamorphic peak was attained at ca. 135 ±4 Ma (Currie, 1988). In the northern Monashee Mountains, zircon and monazite ages of 136 ±2 Ma were reported from leucogranite (Scammell, 1991, 1992, 1993). Farther to southeast in the northern Selkirk Mountains, a zircon lower intercept age of 138 Ma was reported from Trident Mountain syenite (Pell, 1994), while SHRIMP monazite ages of 144 Ma and 131 Ma record Berriasian-Valanginian peak prograde metamorphism in kyanite- and staurolite-bearing micaschists, respectively, in the east flank of the Selkirk fan (Gibson, 2003; Gibson et al., 2004).

The Barremian range of 128–123 Ma $^{40}Ar/^{39}Ar$ ages identified in the phyllite and phyllonite of the SRMTSZ and CWFZ (samples 2, 6, 7, and 9) encompass the 125 Ma U-Pb monazite and zircon age of a pegmatitic phase in the southeastern Cariboo Mountains (Currie, 1988). Quasi-contemporaneous is the metamorphic monazite of 129 Ma reported from high-grade metamorphic rocks in the footwall of the Albreda-North Thompson normal fault in the northern Monashee Mountains (J.H. Sevigny, cf. Parrish 1995). An Aptian leucogranite crystallization age of 122 Ma was reported from the Mica Dam area (Crawley et al., 2000), and U-Pb ages (ID-TIMS) in the Barremian-Aptian range have been reported for peak metamorphism of staurolite (127 Ma) and kyanite (124 Ma) bearing migmatite schist units from the east flank of the Selkirk fan (Gibson et al., 2008). This event corresponds to the inferred initiation of the widespread sheets of Cadomin gravel deposition (Figure 15).

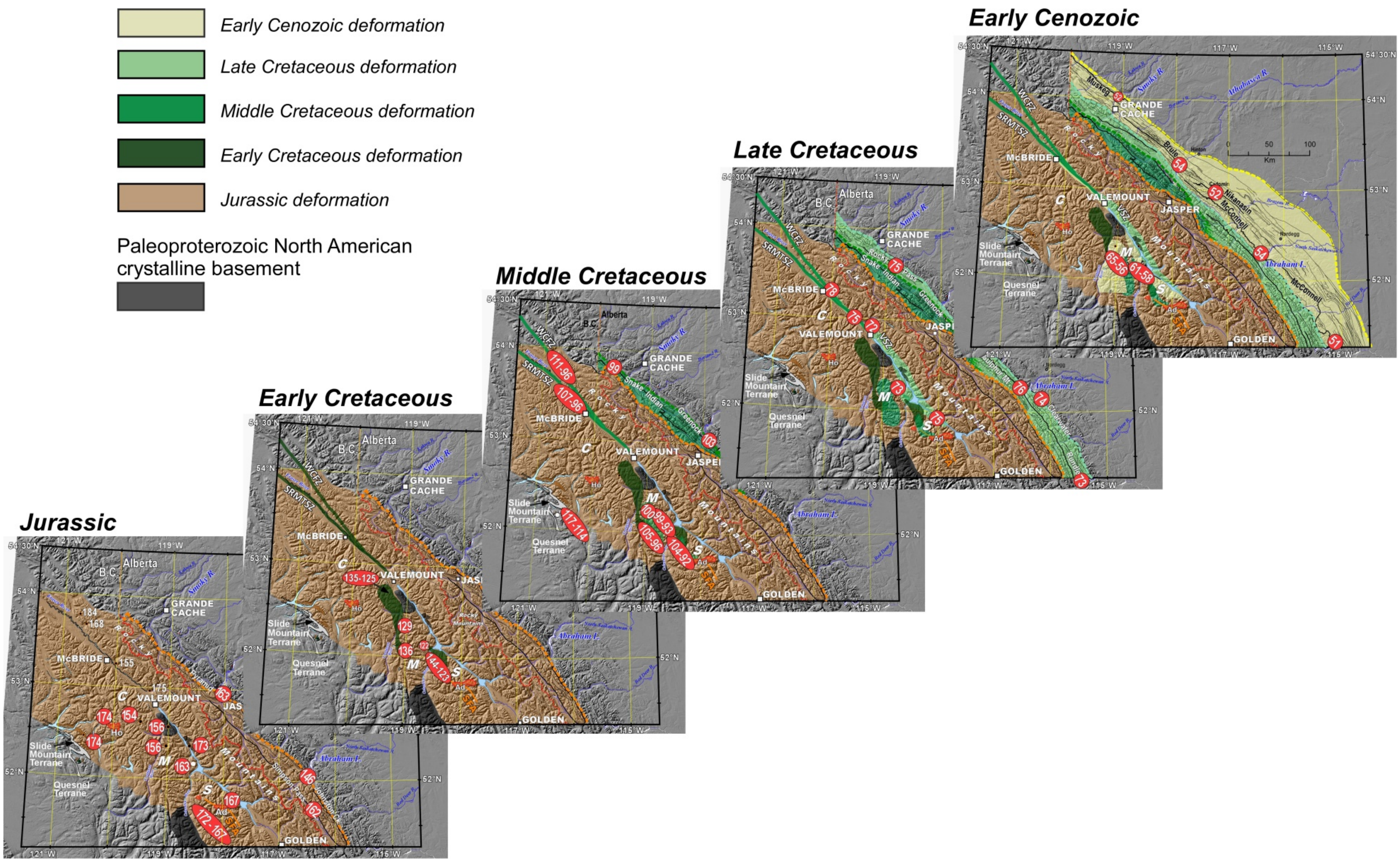

Figure 16. Schematic representation of the main phases of Jurassic–Cretaceous tectonic evolution and deformation at the latitude of the Northern Monashee Mountains along the interface between the Foreland and Omineca belts, and the contemporaneous thrusting pulses in the Rocky Mountain fold-and-thrust belt (adapted from Price, 1994). S – Selkirk Mountains, M – Monashee Mountains, C – Cariboo Mountains; Ad – Adamant pluton, Ho - Hobson pluton. SRMTSZ = Southern Rocky Mountain shear zone; WCFZ = Walker Creek fault zone; VSZ = Valmont strain zone, SFA = Selkirk fan axis.

Our mid-Cretaceous age range of 113–96 Ma $^{40}Ar/^{39}Ar$ ages, with convincing 102–98 Ma plateau ages obtained from the SRMTSZ (samples 15 to 18, 20, 21), and the ca. 96 Ma ages obtained from WCFZ (samples 6, 7) and VSZ (sample 10), testify for a mid-Cretaceous event (Figure 15), and is quasi-contemporaneous with several ages in the adjacent Omineca hinterland. Thus, directly west of our study area on the southwest side of the Cariboo Mountains, two nearly concordant U-Pb ages of 117 and 114 Ma for monazite from Paleozoic granitic orthogneiss suggest a relatively young shearing and (or) metamorphic event that locally affected the Barkerville terrane (Mortensen et al., 1987).

To the south in the northern Monashee Mountains, the mid-Cretaceous age range of tectonism identified in this study along the western margin of the Rockies encompasses the 100 Ma amphibolite facies metamorphic peak accompanied synkinematic emplacement of dikes, sills, and two-mica granite sheets, the latter up to 50 m thick, within the sillimanite zone of the Adams River area (Sevigny et al., 1990). The synkinematic granites yielded U-Pb zircon ages of 100.4 ± 0.3 Ma and monazites ages of 99 ±1.0 Ma (Sevigny et al., 1990). In an adjacent area to the south, synmetamorphic peak leucogranite were emplaced at ca. 105–96 Ma (Scammell, 1991, 1992). Farther south, in the Mica Dam area, 110 Ma monazite inclusions in garnet, and 99-93 Ma ages of monazite growth and/or overgrowth apparently record two mid-Cretaceous tectonothermal events (Crowley et al., 2000). A lineated Malton orthogneiss yielded a discordia array with a precise upper intercept age of 1987 Ma and an imprecise lower intercept age of 93 Ma (McDonough and Parrish, 1991). A minor 91 Ma thermal overprint was reported from the northern part of the west flank of the Selkirk fan (Gibson et al., 2005). To the southwest and farther away from the SRMTSZ in the Illecillewaet synclinorium, the evidence for a Cretaceous metamorphic overprint is lacking (Colpron et al., 1996). Instead, farther south along the Kootenay Arc, a well constrained tectonometamorphic event contemporaneous with the mid-Cretaceous tectonic phase described in this report is recorded by mostly lower Paleozoic sequences in front of the Omineca belt by a belt of Barrovian isogrades (peak metamorphism between 143–134 Ma) and by the 118-94 Ma Bayonne plutonic suite (Moynihan, 2012; Moynihan and Pattison, 2013; Webster et al., 2017).

The Coniacian–Santonian $^{40}Ar/^{39}Ar$ ages obtained in this study from phyllonite of the SRMTSZ (89–85 Ma) and WCFZ (85 Ma) are quasi-contemporaneous with a tectonometamorphic event along the eastern side of the SMC metamorphic complex recorded by the 90 Ma growth of secondary monazite in the Mica Dam area (Crowley et al., 2000) and by the 87 Ma and 84 Ma ages of monazite growth during prograde metamorphism in kyanite-bearing migmatitic schists in the east flank of the Selkirk fan (Gibson et al., 2008). A Maastrichtian late overprint is present in phyllonite of the Bear Foot thrust and in its VSZ footwall by the muscovite low-temperature isochron ages of 67.3 Ma (sample 14) and 68.3 (sample 12), respectively. This event may be recorded by the apparent age average of 67.8 Ma from minor fractions 1 and 2 (sample 6) along the WCFZ, but it has no record within the SRMTSZ. If real, the 67–68 Ma time interval encompasses the late Maastrichtian deposition of the Entrance conglomerate directly to the east of the Bear Foot/VSZ, in the Hinton region (Figures 1, 15).

The "important tectonic and metamorphic episode in the late Cretaceous near the Rocky Mountain Trench" inferred by Wanless et al. (1967) and locally documented by Murphy (1990) is fully confirmed by our work.

Similarly, the Campanian–Maastrichtian $^{40}Ar/^{39}Ar$ ages obtained from the SRMTSZ (78–72 Ma), WCFZ (79 Ma), and VSZ (77–68 Ma) have also been reported from the Mica Dam area, where 73 Ma inclusions of monazite in kyanite, a 72 Ma pegmatite dyke emplacement, the 70 Ma growth of monazite and xenotime (Crowley et al., 2000), and from kyanite-bearing migmatitic schists (75, 73, and 71 Ma) on the eastern flank of the Selkirk fan (Gibson et al., 2008).

Finally, phyllonites from the SRMTSZ and VSZ yielded Paleocene–early Eocene $^{40}Ar/^{39}Ar$ ages (64–55 Ma). The 736 Ma Hugh Allen orthogneiss sample also yielded a biotite K-Ar age of 52 Ma, whereas another Hugh Allan gneiss in the trench yielded K-Ar dates of 67 Ma from biotite and 60 Ma from muscovite (McDonough et al, 1991b). This age interval encompasses the 63 Ma second phase of anatectic granite emplacement in the Adams River area of the northern Monashee Mountains (Sevigny et al., 1990) and is in the range of 66-60 monazite growth, the 64 Ma emplacement of deformed pegmatite, 61 Ma leucosome crystallization, and the 58 Ma postkinematic emplacement of pegmatite in the Mica Dam area (Crowley et al., 2000). Monazite ages of 65 Ma (ID-TIMS) and 62 Ma, and 57 Ma to 56 Ma (SHRIMP) obtained from the migmatitic schists on the east flank of the Selkirk fan may represent final monazite growth during retrograde metamorphism (Gibson et al., 2008), likely contemporaneous with partial chlorite overprint in a domain nearest to the SRMTSZ in the Mica Dam area (Crawley et al., 2000). The 359 Ma Trident Mountain nepheline-syenite located near the SRMTSZ just south of the Mica Dam area yielded a pyrochlor age of 60 Ma (Pell, 1994) and a 15-zircon grain weighted average age of 57 Ma, which indicates late Paleocene metamorphic resetting (Millonig et al., 2012).

Subsequent to the F1 westerly directed folds, nappes, and thrusts, the structures in the eastern Omineca belt were eastward directed and are congruent with those on the western margin of the Rockies. Thus, Cretaceous tectonism is largely responsible for the second generation of structures; specifically, the northeast-verging isoclinal and commonly tight F2 folds developed regionally in the SMC complex. In the southeastern Cariboo Mountains, the F2 formed sometime between the Late Jurassic and Early Cretaceous (160–131 Ma) and were outlasted by the thermal event (Currie, 1988). In the northern Monashee Mountains, F2 developed during peak-metamorphism at 100 Ma and were outlasted by the thermal event (Simony et al., 1980; Sevigny et al., 1989; 1990; Sevigny and Simony, 1989). There, syn- and postkinematic dikes, sills, and two-mica granites sheets up to 50 m thick, derived by low degree partial melting of Late Proterozoic Horsethief Creek Group metapelites (Sevigny et al., 1990), occur within the sillimanite zone. The garnet- and sillimanite-bearing syn-kinematic granites yielded U-Pb zircon ages of 100.4 ±0.3 Ma and monazites ages of 99 ±1.0 Ma. Post-kinematic granites that locally contain garnet, have 62.5 ±0.2 Ma zircon ages and 63.4 ±0.1 Ma monazite ages (Sevigny et al., 1989; 1990). A similar time interval (122–58 Ma) for the F2 folds development was inferred farther south in the Monashee Mountains near Mica Dam (Crawley et al., 2000).

On the west flank of the Selkirk fan, outcrop scale isoclinal folds, interpreted as F2 folds, formed between 172–167 Ma (Gibson et al., 2008). In the east flank of the Selkirk fan, F2 folds are coaxial with late syn- to post-peak metamorphic northeast-verging mid-Cretaceous F3 folds constrained to 104–84 Ma. These southwest dipping axial surfaces become progressively shallower and are accompanied by thrusts towards the trench, a style of deformation congruent with folding and thrusting in the adjacent Rocky Mountains (e.g., Simony et al., 1980; Gibson et al., 2008).

Thus, the Cretaceous tectonometamorphic events recognized in the SMC metamorphic complex appear to have propagated northward and concentrated into the SRMTSZ and the associated lineaments of strain analyzed in this study.

8.1.4 Exhumation of the Selkirk-Monashee-Cariboo Metamorphic Complex

Although the spatial relationships between the Foreland and Omineca belts may have changed during large-scale Cordilleran latitudinal translations, the Windermere Supergroup unifies the two deformation belts at the margin of ancient North America. The Horsethief and Kaza groups in the SMC, and the Miette Group in the Rockies are partly correlative. The most likely source of sediment for the foreland basin is the Foreland belt and its immediate hinterland, the Omineca belt, specifically the SMC. The orogenic evolution of the SMC is thus very significant to the depositional processes in the Alberta Basin.

At least parts of the SMC complex were buried and metamorphosed at lower to middle crustal levels during the Jurassic. The west flank of the Selkirk fan was exhumed to upper crustal levels (above10–12 km depth) by the late Middle Jurassic and in part reburied during the Cretaceous tectonothermal event (Colpron et al., 1996; Gibson et al., 2008), whereas the eastern flank of the fan remained at deeper crustal levels (>20–30 km depth) throughout the Cretaceous and appears to have been progressively or episodically reworked and recrystallized between the earliest Cretaceous (144 Ma) and Maastrichtian (70 Ma) (Crowley et al., 2000; Gibson et al., 2008).

The rest of the SMC metamorphic complex may have remained at lower to mid-crustal levels throughout the Jurassic to early Cenozoic. The 154 Ma pegmatite emplacement in the southeastern Cariboo Mountains, the 156 Ma hornblende ages in the southeastern Cariboo and northernmost Monashee mountains, and the 163 Ma garnet and 157–155 Ma primary monazite growth in the Mica Dam area testify for at least a mid-crustal level residence into the Late Jurassic. The ca. 76 Ma K-Ar hornblende cooling ages in the northern Monashee Mountains (Sevigny et al., 1990) suggest that this portion of the SMC complex may have been uplifted above the 550°C isotherm only during Campanian time.

The residence of the northern portion of the SMC complex at deep structural levels through Early and mid-Cretaceous time is documented by the 134 Ma peak staurolite-kyanite metamorphism with 125 Ma pegmatite emplacement in the southeastern Cariboo Mountains (Currie, 1988), by a 129 Ma metamorphic monazite from upper amphibolite facies rocks in the northern Monashee Mountains (J.H. Sevigny, cf. Parrish 1995), by the PT estimates for the peak metamorphism that outlasted the 100 Ma sillimanite and garnet-bearing anatectic granitoids in the Adams River area (Sevigny et al., 1990), by U-Pb zircon and monazite ages of 136 ±2 Ma and a 105–96 Ma leucogranite associated with mid-Cretaceous peak metamorphism in an area immediately to the south (Scammell, 1991, 1992, 1993), and finally, the ca. 122 Ma emplacement of leucogranite and the 110-90 Ma polyphase growth or overgrowth of secondary monazite in the Mica Dam area (Crowley et al., 2000).

Postmetamorphic 63 Ma anatectic granitic sheets and dikes which locally contain garnet (Sevigny et al., 1989), and voluminous 67–57 Ma granites (Scammell, 1991, 1992) identified in in the northern Monashee Mountains were emplaced at a higher structural level, but below the 350°C isotherm (muscovite closure temperature), which was reached only at ca. 51 Ma (Sevigny et al., 1990). In the Mica Dam area, multiple phases of monazite growth (73 Ma, 70 Ma, 67 Ma), pegmatite emplacement (64 Ma, 63 Ma and 58 Ma), and crystallization of leucosome (61 Ma) corroborate with the post 73 Ma kyanite growth (age of monazite inclusions in kyanite) and the presence of kyanite in 61 Ma leucosome, thus documenting the residence of the easternmost portion of the SMC complex at mid-crustal levels through the Late Cretaceous-Paleocene (Crowley et al., 2000). All these data indicate a significant pre-Cenozoic orogen on the west side of the SRMT, the immediately adjacent hinterland to the RMFTB.

Late Cretaceous to Eocene postmetamorphic thermal relaxation in the northern Monashee Mountains is tracked by K-Ar cooling ages (mean age and standard deviation) of 76.3 ±5.8 Ma from hornblende, of 51.4 ±3.5 Ma from muscovite, and by apatite fission-track ages of 45.0 ±2.9 Ma (Sevigny et al., 1990).

9 Summary and Conclusions

The spatial and temporal relationships of the tectonic features examined in this study indicate kinematic links between shallow dipping Early Cretaceous thrusts in the Main Ranges (Monarch and Moose Pass thrusts) of the Alberta Rockies and three zones of dextral strike- to oblique-slip lineaments overprinting the western margin of the Rockies (SRMTSZ, WCFZ, and VSZ-Bear Foot thrust). The ca. 135 Ma age of detrital feldspar in the Brazeau Formation testifies for contemporaneous igneous activity in the Cordillera.

The SRMTSZ and WCFZ consist of steeply dipping phyllite and phyllonite belts with conspicuous subhorizontal stretching lineation, whereas the VSZ and Bear Foot thrust include moderately dipping phyllonite with oblique stretching; together they define a Cretaceous zone of transpression and metamorphism along the western margin of the Rocky Mountains, at this latitude. Detailed step-heating $^{40}Ar/^{39}Ar$ analyses unraveled protracted tectonism along the SRMTSZ, and its subsidiaries (WCFZ and VSZ) with apparent episodic pulses throughout Cretaceous time with a subtle early Cenozoic overprint (Table 3):

- Valanginian (ca. 136–133 Ma),
- Aptian (ca. 128–123 Ma),
- Albian–Cenomanian (ca. 113–96 Ma),
- Santonian (ca. 89–85 Ma),

- Campanian–Maastrichtian (ca. 79–68 Ma),
- early Cenozoic local and weaker rejuvenations (ca. 64–55 Ma).

Behind the veil of predominantly Cretaceous ages of tectonism, the analyzed minerals preserved vague memories of older events. The oldest preserved dates are latest Paleoproterozoic muscovite plateau ages of 1.65–1.59 Ga in the Miette Group, which record formation and/or cooling of the muscovite-bearing source rocks. Although less well constrained, Neoproterozoic fusion ages (656–614 Ma) were sporadically identified in phyllonite samples with Miette protoliths and, if geologically meaningful, they may be related to extensional tectonics during the Miette deposition. A step age of 340 Ma and a plateau-like age of 324 Ma may record a Mississippian event, possibly a late phase of the Antler tectonism. Scattered Permian (280 Ma), Triassic (239 Ma and 219 Ma) and Jurassic (175 Ma; 168 Ma; 161 Ma; Figure 16) muscovite fusion dates are unlikely to date significant tectonic events, such as the protolith age of 239 Ma to a Triassic event. Although roughly coincident with the Pliensbachian initial thrusting at the western margin of North America, the interpretation of the muscovite plateau-like age of 188 Ma and the low-temperature date of 184 Ma as meaningful ages remains speculative.

Our structural and geochronological data indicate protracted tectonic activity, which started in *Early Cretaceous* (ca. 135 Ma) as a kilometres-wide zone of orogen-parallel crustal yielding in the northern segment of the SRMT (Figure 16). The shear zone was identified in isolated outcrops of the trench floor along its east side (samples 18, 20, 21; Figure 3), but probably occupies most of the 5–8 km wide trench floor now covered by flat laying Quaternary to Recent sediments (samples 15, 17; Figure 3). The spatial distribution of ages suggests that this zone of strain was wider (samples 7, 16, 17, 19; Figure 3) than the present trench. The Early Cretaceous transpression along the SRMTSZ resulted in eastward thrusting but was apparently limited to the trench proximity and parts of the Main Ranges. Thus, the Monarch and Moose Pass thrusts are kinematically linked to tectonism along the SRMTSZ and are “out-of-sequence” within the RM-FTB, as older thrusts are known to the east (e.g., Late Jurassic Pyramid and Simpson Pass thrusts; Pană and van der Pluijm, 2015). Early Cretaceous tectonic loading in the proto-Rockies is quasi-contemporaneous with the extensive sub-Cadomin–sub-Mannville unconformity that records uplift and erosion in the orogenic foreland. Phyllonite ages in the 128–123 Ma range record transpression along the SRMTSZ and WCFZ which likely triggered the rising of the proto-Rockies accompanied and outlasted by vigorous erosion in the mountains and deposition of the extensive Cadomin sheets of gravel in the proximal foreland basin. Ages of 115–111 Ma along the same belts of strain concentration are contemporaneous, within error, with the southward transgression of the Moosebar sea, which suggests that this late Aptian–early Albian event along the western Rockies triggered tectonic loading and downwarping of the North American plate.

Over time, strike-slip strain along the western margin of the Rockies gradually concentrated into narrower mid- and Late Cretaceous belts within the SRMTSZ, the WCFZ and the VSZ. The WCFZ and the VSZ merge with the SRMTSZ and appear to have been tectonically active during different phases of strike-slip displacement along the SRMTSZ. The WCSZ to the east and north records the same tectonic pulses as the SRMTSZ with a weak Campanian–Maastrichtian pulse and no apparent early Cenozoic rejuvenation. In contrast, the VSZ (including the Bear Foot thrust) records only a Late Cretaceous (mainly Campanian–earliest Maastrichtian) pulse of oblique compression—due to either a single tectonic pulse or a pulse that was severe enough to completely obliterate previous records—with minor early Paleocene reactivation.

The mid-Cretaceous tectonic activity along the SRMTSZ (peak at ca. 102–98 Ma) and WCFZ (peak at ca. 96 Ma) is quasi-contemporaneous and kinematically linked to thrusting in the Alberta Rockies at the same latitude (103 Ma Greenock, 99 Ma Snake Indian thrusts; Pană and van der Pluijm, 2015)(Figures 15, 16). The mid-Cretaceous tectonism along the WCFZ extended to the north into the conterminous NRMT, where dextral transpression accompanied by granitoid intrusions apparently built up the Northern Rockies orogenic belt (e.g., McMechan, 2000; Gabrielse et al., 2006). This orogenic phase is contemporaneous with, and likely triggered, the mid-Cenomanian establishment of a vast fluvial system draining from the

Northern Rocky Mountains and depositing proximal alluvial conglomerate and more distal sands of the Dunvegan Formation in the foreland in northeastern British Columbia and northwestern Alberta.

Late Cretaceous tectonism was recorded in all fault and shear zones along the western margin of the Rockies (Figures 15, 16). Campanian–Maastrichtian $^{40}Ar/^{39}Ar$ ages were obtained from the SRMTSZ (78–72 Ma), WCFZ (79 Ma), and VSZ (77–68 Ma). It seems however, that Early and mid-Cretaceous links between the SRMTSZ, WCFZ and Monarch and Moose Pass thrusts of the Rockies were replaced by Campanian kinematic links between the SRMTSZ and the VSZ. A strong, mainly Campanian, pulse was identified in the Bear Foot thrust and the VSZ (73–71 Ma). Oblique compression on these structures was probably driven by the Campanian–Maastrichtian tectonic reactivation of the Tête Jaune Cache–Valemount segment of the SRMTSZ. This event coincides with the emplacement of several major Campanian thrusts in the Front Ranges (e.g., Rocky Pass, Sulphur Mountain, Clearwater, Rundle thrusts) and with the westward transgression of the Bearpaw sea in the Alberta Basin (Pană and van der Pluijm, 2015).

This intriguing synchronicity of tectonic events suggests a kinematic link between oblique compression along the shear- and fault-zone network at the western margin of the Rocky Mountain fold-and-thrust belt and major thrusting events within the belt (Figure 16).

The Cretaceous network of dextral orogen-parallel shear/fault zones in the examined portion of the western Rockies projects southward into the wider Cretaceous tectonometamorphic zone along the SRMTSZ, previously documented on either side of Kinbasket Lake, which encompasses both the western Rockies, and the eastern Omineca belt. We infer that this wide linear zone of mainly Cretaceous strain and metamorphism is part of a complex regional kinematic link between Cretaceous oblique compression in the hinterland and major thrusting in the foreland.

10 References

Arne, D. and Zentilli, M. (1994): Apatite fission track thermochronology integrated with vitrinite reflectance; Chapter 16 *in* Vitrinite Reflectance as a Maturity Parameter: Applications and Limitations, P.K., Mukhopadhyay and W.G. Dow (ed.), Washington, D.C., American Chemical Society, Symposium Series, v. 570, p. 249–268, doi:10.1021/bk-1994-0570.ch016

Brown, R.L. and Journeay, J.M. (1987): Tectonic denudation of the Shuswap metamorphic terrane of southeastern British Columbia; Geology, v. 15, p. 142–146.

Brown, R.L. and Lane L.S. (1988): Tectonic interpretation of west-verging folds in the Selkirk Allochthon of the southern Canadian Cordillera; Canadian Journal of Earth Sciences, v. 25, p. 292–300.

Brown, R.L., Journeay, J.M., Lane, L.S., Murphy, D.C. and Rees, C.J. (1986): Obduction, backfolding and piggyback thrusting in the metamorphic hinterland of the southeastern Canadian Cordillera; Journal of Structural Geology, v. 8, p. 255–268.

Campbell, R.B. (1968): Canoe River (83 D), British Columbia; Geological Survey of Canada, Map 15 - 1967, scale 1: 253 440.

Campbell, R.B. (1970): Structural and metamorphic transitions from infrastructure to suprastructure, Cariboo Mountains, British Columbia; Geological Association of Canada, Special Paper 6, p. 67–72.

Campbell, R.B. (1973): Structural cross-section and tectonic model of the southeastern Canadian Cordillera; Canadian Journal of Earth Sciences, v. 10, p. 1607–1620.

Campbell, R.B., Mountjoy, E.W. and Young, F.G. (1973): Geology of the McBride map-area, British Columbia; Geological Survey of Canada, Paper 72-35.

Campbell, R.B., Mountjoy, E.W. and Struik, L.C. (1982): Structural cross-section through south-central Rocky and Cariboo mountains to the Coast Range; Geological Survey of Canada, Open File 844.

Carr, S.D. (1995): The southern Omineca belt, British Columbia; new perspectives from the Lithoprobe Geoscience Program; Canadian Journal of Earth Science, v. 32, p. 1720–1739.

Carey, J.A. and Simony, P.S. (1985): Stratigraphy, sedimentology and structure of late Proterozoic Miette Group, Cushing Creek area, British Columbia; Bulletin of Canadian Petroleum Geology, v. 33, p. 184–203.

Chamberlain, V.E. (1983): The geochemistry and geochronology of the Malton Gneiss Complex, British Columbia; Ph.D. thesis, University of Alberta, Edmonton, Alta., 212 p.

Chamberlain, V.E. and Lambert, R.ST.J. (1985a): Cordilleria, a newly defined Canadian microcontinent; Nature, v. 314, p. 707–713.

Chamberlain, V.E. and Lambert, R.ST J. (1985b): Geochemistry and geochronology of the gneisses east of the Southern Rocky Mountain Trench, near Valemount, British Columbia; Canadian Journal of Earth Sciences, v. 22, p. 980–991.

Chamberlain, V.E., Lambert, R.ST J., Baadsgaard, H. and Gale, N.H. (1979): Geochronology of the Malton Gneiss Complex of British Columbia; *in* Current research, part B; Geological Survey of Canada, Paper 79-1B, p. 45–50.

Chamberlain, V.E., Lambert, R.ST J. and Holland, J.G. (1980): The Malton Gneiss: Archean gneisses in British Columbia; Precambrian Research, v. 11, p. 297–306.

Charlesworth, H.A.K. and Price, R.A. (1972): Rocky Mountain Main Ranges to Monashee and Cariboo Mountains-Yellowhead Pass section, 9 p.

Charlesworth, H.A.K., Weiner, J.L., Akehurst, A.J., Bielenstein, H.U., Evans, C.R., Griffiths, R.E., Remington, D.B., Stauffer, M.R. and Steiner, J. (1967): Precambrian geology of the Jasper region, Alberta; Research Council of Alberta, Bulletin 23.

Colpron, M., Price, R.A., Archibald, D.A. and Carmichael, D.M. (1996): Middle Jurassic exhumation along the western flank of the Selkirk fan structure: Thermobarometric and thermochronometric constraints from the Illecillewaet synclinorium, southeastern British Columbia; Geological Society of America Bulletin, v. 108, p. 1372–1392, doi:10.1130/0016-7606(1996)108<1372:MJEATW>2.3.CO;2

Colpron, M., Warren, M.J. and Price, R.A. (1998): Selkirk fan structure, southeastern Canadian Cordillera: Tectonic wedging against an inherited basement ramp; Geological Society of America Bulletin, v. 110, p. 1060–1074, doi:10.1130/0016-7606(1998)110<1060:SFSSCC>2.3.CO;2

Crowley, J.L., Ghent, E.D., Carr, S.D., Simony, P.S. and Hamilton, M.A. (2000): Multiple thermotectonic events in a continuous metamorphic sequence, Mica Creek area, southeastern Canadian Cordillera; Geol. Mater. Res., 2, p. 1–45.

Currie, L.D. (1988): Geology of the Allan Creek area, Cariboo Mountains, British Columbia; M.Sc. Thesis, University of Calgary, Alberta.

Digel, S.G., Ghent, E.D., Carr, S.D. and Simony, P.S. (1998): Early Cretaceous kyanite–sillimanite metamorphism and Paleocene sillimanite overprint near Mount Cheadle, southeastern British Columbia: geometry, geochronology, and metamorphic implications; Canadian Journal of Earth Sciences, v. 35, p. 1070–1087.

Donelick, R.A. and Beaumont, C. (1990): Late Cretaceous–early Tertiary cooling of the Brazeau thrust sheet, central Foothills, Alberta: Implications for the timing of the end of Laramide thrusting in the region; Geological Association of Canada Programs with Abstracts, v. 15, p. A34.

Eisbacher, G.H. (1985): Pericollisional strike-slip faults and synorogenic basins, Canadian Cordillera: *in* Strike-slip deformation, basin formation and sedimentation; K.T. Biddle and N. Christie-Blick (ed.) Society of Economic Paleontologists and Mineralogists, Special Publication v. 37, p. 265–282.

Evenchick, C.A., McMechan, M.E., McNicoll, V.J. and Carr, S.D. (2007): A synthesis of the Jurassic–Cretaceous tectonic evolution of the central and southeastern Canadian Cordillera: Exploring links across the orogen; *in* L.W. Sears, T.A. Harms and C.A. Evenchick (ed.), Whence the Mountains? Inquiries into the Evolution of Orogenic Systems: A Volume in Honor of Raymond A. Price: Geological Society of America Special Paper 433, p. 117–145, doi:10.1130/2007.2433(06)

Ferguson, C.A. and Ross, G.M. (2003): Geology and structure cross-sections, McBride, British Columbia; Geological Survey of Canada, "A" Series Map 2004A (93H08), scale 1:50 000.

Gabrielse, H. (1985): Major dextral transcurrent displacements along the Northern Rocky Mountain Trench and related lineaments in north-central British Columbia; Geological Society of America Bulletin, v. 96, p. 1–14.

Gabrielse, H., Murphy, D.C. and Mortensen, J.K. (2006): Cretaceous and Cenozoic dextral orogen-parallel displacements, magmatism, and paleogeography, north-central Canadian Cordillera; *in* Paleogeography of the North American Cordillera: Evidence for and against large-scale displacements, J.W. Haggart, R.J. Enkin and J.W.H. Monger (ed.), Geological Association of Canada, Special Paper 46, p. 255–276.

Gal, L.P. and Ghent, E.D. (1990): Metamorphism in the Solitude Range, southwestern Rocky Mountains, British Columbia: comparison with adjacent Omineca Belt rocks and tectonometamorphic implications for the Purcell Thrust; Canadian Journal of Earth Sciences, v. 27, p. 1511–1520.

Gal, L.P., Ghent, E.D. and Simony, P.S. (1989): Geology of the northern Solitude Range, western Rocky Mountains, British Columbia; *in* Current Research, part D, Geological Survey of Canada, Paper 89-1D, p. 55–60.

Gerasimoff, M.D. (1988): The Hobson Lake pluton, Cariboo Mountains, British Columbia, and its significance to Mesozoic and early Cenozoic Cordilleran tectonics; M.Sc. thesis, 196 p., Queens University, Kingston, Ontario,

Ghent, E.D., and Simony, P.S. (2005): Geometry of isogradic, isothermal, and isobaric surfaces: Interpretation and application; Canadian Mineralogist, v. 43, p. 295–310, doi:10.2113/gscanmin.43.1.295

Gibson, H.D. (2003): Structural and thermal evolution of the northern Selkirk Mountains, southeastern Canadian Cordillera: Tectonic development of a regional-scale composite structural fan; Ph.D. Thesis, 298 p., Carleton University, Ottawa.

Gibson, H.D., Carr, S.D., Hamilton, M.A. and Brown, R.L. (2004): Correlations between chemical and age domains in monazite, and metamorphic reactions involving major pelitic phases: An integration of ID-TIMS and SHRIMP geochronology with YTh-U X-ray mapping; Chemical Geology, v. 211, p. 237–260, doi:10.1016/j.chemgeo.2004.06.028

Gibson, H.D., Brown, R.L. and Carr, S.D. (2005): U-Th-Pb geochronologic constraints on the structural evolution of the Selkirk fan, northern Selkirk Mountains, southern Canadian Cordillera, Journal of Structural Geology, v. 27, p. 1899–1924, doi:10.1016/j.jsg.2005.05.014

Gibson, D.H., Brown, R.L. and Carr, S.D. (2008): Tectonic evolution of the Selkirk fan, southeastern Canadian Cordillera: A composite Middle Jurassic-Cretaceous orogenic structure; Tectonics, v. 27, p. 1–14.

Gradstein, F.M., Ogg, J.G., Schmitz, M.D. and Ogg, G.M. (2020): Geologic time scale 2020; Elsevier, 1280 p.

Hoffman, J., Hower, J. and Aronson, J.L. (1976): Radiometric dating of the time of thrusting in the disturbed belt of Montana; Geology, v. 4, p. 16–20.

Höy, T. (1976): Calc-silicate isograds in the Riondel area, southeastern British Columbia; Canadian Journal of Earth Sciences, v. 13, p. 1093–1104, doi:10.1139/e76-112

Johnson, J. (2006): Extensional shear zones, granitic melts, and linkage of overstepping normal faults bounding the Shuswap metamorphic core complex, British Columbia; Geological Society of America Bulletin, v. 118 (3-4), p. 366–382, doi:10.1130/B25800.1

Johnson, B.J. and Brown, R.L. (1996): Crustal structure and early Tertiary extensional tectonics of the Omineca belt at 51°N latitude, southern Canadian Cordillera; Canadian Journal of Earth Sciences, v. 33, p. 1596–1611.

Kalkreuth, W. and McMechan, M. (1988): Burial history and thermal maturity, Rocky Mountain Front Ranges, Foothills, and Foreland, east-central British Columbia and adjacent Alberta, Canada; American Association of Petroleum Geologists Bulletin, v. 72, no. 11, p. 1395–1410.

Kalkreuth, W. and McMechan, M. (1996): Coal rank and burial history of Cretaceous–Tertiary strata in the Grande Cache and Hinton areas, Alberta, Canada: Implications for fossil fuel exploration; Canadian Journal of Earth Sciences, v. 33, p. 938–957, doi:10.1139/e96-071

Kendall, B.S., Creaser, R.A., Ross, G.M. and Selby, D. (2004): Constraints on the timing of Marinoan ''Snowball Earth'' glaciation by ^{187}Re–^{187}Os dating of a Neoproterozoic, post-glacial black shale in Western Canada; Earth and Planetary Science Letters, v. 222, p. 729–740.

Lee, J-Y, Marti, K., Severinghaus, J.P., Kawamura, K., Yoo, H-S., Lee, J.B. and Kim, J.S. (2006): A redetermination of the isotopic abundances of atmospheric Ar; Geochemica and Cosmochemica Acta, v. 70, p. 4507-4512, doi:10.1016/j.gca.2006.06.1563

Mattauer, M., Collot, B. and van den Driessche, J. (1983): Alpine model for the internal metamorphic zones of the North American Cordillera; Geology, v. 11, p. 11–15.

McDonough, M.R. (1984): Structural evolution and metamorphism of basement gneisses and Hadrynian cover, Bulldog Creek area, British Columbia; M.Sc. thesis, The University of Calgary, Calgary, Alberta.

McDonough, M.R. and Simony, P.S. (1984): Basement gneisses and Hadrynian metasediments near Bulldog Creek, Selwyn Range, British Columbia; *in* Current Research, part A; Geological Survey of Canada, Paper 84-1A, p. 99–102.

McDonough, M.R. and Simony, P.S. (1986): Geology of the northern Selwyn Range, western Main Ranges, Rocky Mountains, British Columbia: preliminary report: *in* Current Research, part A; Geological Survey of Canada, Paper 86-1A, p. 619–626.

McDonough, M.R. and Simony, P.S. (1988a): Stratigraphy and structure of late Proterozoic Miette Group, northern Selwyn Range, Rocky Mountains, British Columbia; *in* Current Research, part D. Geological Survey of Canada, Paper 88-1D, p. 105–113.

McDonough, M.R. and Simony, P.S. (1988b): Structural evolution of basement gneisses and Hadrynian cover, Bulldog Creek area, Rocky Mountains, British Columbia; Canadian Journal of Earth Sciences, v. 25, p. 1687–1702.

McDonough, M.R. and Simony, P.S. (1989): Valemount strain zone: a dextral-oblique thrust system linking the Rocky Mountain and Omineca belts of the southern Canadian Cordillera; Geology, v. 17, p. 237-240.

McDonough, M.R. and Parrish R.R. (1991): Proterozoic gneisses of the Malton Complex, near Valemount, British Columbia: U–Pb ages and Nd isotopic signatures; Canadian Journal of Earth Sciences, v. 28/8, p. 1202-1216, doi:10.1139/e91-108

McDonough, M R. and Murphy, D.C. (1994): Geology, Valemount, West of the Sixth Meridian, British Columbia; Geological Survey of Canada, "A" Series Map, 1843A

McDonough, M.R., Simony, P.S., Morrison, M.L., Oke, C., Sevigny, J.H., Robbins, D.B., Digel, S.G., and Grasby, S.E. (1991a): Howard Creek, British Columbia (83D/7); Geological Survey of Canada, Open File Report, scale 1:50 000.

McDonough, M.R., Morrison, M.L., Currie, L.D., Walker, R.T., Pell, J. and Murphy, D.C. (1991b): Canoe Mountain, British Columbia (83D/11); Geological Survey of Canada, Preliminary Map 1991, scale 1:50 000.

McDonough, M.R., Stockmal, G.S., Issler, D.R., Grist, A.M., Zentilli, M. and Archibald, D.A. (1995): Apatite fission track and ^{40}Ar-^{39}Ar analysis of the external zone of the Canadian Rockies near Jasper, Alberta: implications for thermal maturity in Proceedings of the oil and gas forum ’95, Energy from sediments; J.S. Bell, T.D. Bird, T.L. Hillier and P.L. Greener (ed.), Geological Survey of Canada Open File 3058, p. 83–88.

McMechan, M.E. (1996): Geology and structure cross-section, Walker Creek, British Columbia; Geological Survey of Canada, Map 1839A, scale 1: 50 000.

McMechan, M.E. (2000): Walker Creek fault zone, central Rocky Mountains, British Columbia—southern continuation of the Northern Rocky Mountain Trench fault zone; Canadian Journal of Earth Sciences, v. 37, p. 1259–1273.

McMechan, M.E. (2015): The Neoproterozoic succession of the central Rocky Mountains, Canada; Bulletin of Canadian Petroleum Geology, v. 63, p. 243–273.

McMechan M.E. and Roddick, C. (1991): Seven whole rock radiometric ages from the western Rocky Mountains near 54 N; *in* Radiogenic age and isotopic studies. Report 5; Geological Survey of Canada, Paper 91-2, p. 212–214.

McMechan, M.E. and Thompson, R.I. (1989): Structural style and history of the Rocky Mountain fold and thrust belt; Chapter 4 *in* Western Canada Sedimentary Basin, A Case History, B.D. Ricketts (ed.), Canadian Society of Petroleum Geologists, p. 47–72.

McMechan, M.E. and Thompson, R.I. (1992): The Rocky Mountains; Chapter 17, Part E *in* Geology of the Cordilleran Orogen in Canada, Geological Survey of Canada, Geology of Canada, no.4, (also Geological Society of America, The Geology of North America, v. G-2), H. Gabrielse and C.J. Yorath (ed.), p. 635–642.

McMechan, M.E., Anderson, B., Creaser, R. and Ferri, F. (2006): Clasts from the past: Latest Jurassic–earliest Cretaceous foreland basin conglomerates, northeastern British Columbia and northwest Alberta; Geological Survey of Canada Open-File 5086, 1 sheet.

Millonig, L.J., Gerdes, A. and Groat, L.A. (2012): U-Th-Pb geochronology of meta-carbonatites and meta-alkaline rocks in the southern Canadian Cordillera: a geodynamic perspective; Lithos, v. 152, p. 202–217.

Monger, J.W.H., and Price, R.A. (2002): The Canadian Cordillera: Geology and tectonic evolution: Canadian Society of Exploration Geophysicists, Recorder, February 2002, p. 17–36.

Monger, J.W.H., Price, R.A. and Templeman-Kluit, D.J. (1982): Tectonic accretion and the origin of two major metamorphic and plutonic welts in the Canadian Cordillera; Geology, v. 10, p. 70–75.

Monger, J.W.H., Woodsworth, G.J., Price, R. A., Clowes, R.N., Ridihough, R.P., Currie, R., Hoy, T., Preto, V.A. G., Simony, P.S., Snavely, P.D. and Yorath, C.J. (1986): Transect B2. Southern Canadian Cordillera, North American continent-ocean transects; Geological Society of America, Decade of North American Geology Program.

Monger, J.W.H. and Gibson, H.D. (2019): Mesozoic-Cenozoic deformation in the Canadian Cordillera: The record of a "Continental Bulldozer"? Tectonophysics, v. 757, p. 153-167, 12.02.

Morrison, M.L. (1979): Structure and petrology of the southern portion of the Malton Gneiss, British Columbia; *in* Current research, part B; Geological Survey of Canada, Paper 79-1B, p. 407–410.

Morrison, M.L. (1982): Structure and petrology of the Malton Gneiss Complex; Ph.D. thesis, The University of Calgary, Calgary, Alberta.

Mortensen, J.K., Montgomery, J.R. and Fillipone, J. (1987): U-Pb zircon, monazite, and sphene ages for granitic orthogneiss of the Barkerville terrane, east-central British Columbia; Canadian Journal of Earth Sciences, v. 24, p. 1261–1266.

Mountjoy, E.W. (1980): Mount Robson, Alberta - British Columbia; Geological Survey of Canada, Map 1499A, scale 1:250 000.

Mountjoy, E.W. (1988): The Hugh Allan (Purcell) fault (a low-angle west-dipping thrust) at Hugh Allan Creek, British Columbia; *in* Current Research, Part E, Geological Survey of Canada, Paper 88-1E, p. 97–104.

Mountjoy, E.W. and Price, R.A. (1985): Jasper, Alberta (83 D/16); Geological Survey of Canada, Map 1611A, scale 1:50 000.

Mountjoy, E.W. and Forest, R. (1986): Revised structural interpretation, Selwyn Range between Ptarmigan and Hugh Allan creeks, British Columbia – an antiformal stack of thrusts; *in* Current research part A, Geological Survey of Canada, Paper 86-1A, p. 177–183.

Mountjoy, E.W., Leonard, R. and Forest, R. (1984): Non-basement involvement in the western Main Ranges, Jasper - Valemount, Alberta and British Columbia; Geological Society of America, Abstracts with Programs, 16, p. 602.

Moynihan, D.P. (2012): Metamorphism and deformation in the central Kootenay Arc, southeastern British Columbia; Ph.D. thesis, University of Calgary.

Moynihan, D.P. and Pattison, D.R.M. (2013): Barrovian metamorphism in the central Kootenay Arc, British Columbia: petrology and isograd geometry; Canadian Journal of Earth Sciences, v. 50, p. 769–794, doi:10.1139/cjes-2012-0083

Murphy, D.C. (1984): A note on faulting in the southern Rocky Mountain Trench between McBride and Canoe Reach, British Columbia; *in* Current Research, Part A, Geological Survey of Canada, Paper 84-1A, p. 627–630.

Murphy, D.C. (1987): Suprastructure/infrastructure transition, east-central Cariboo Mountains, British Columbia: geometry, kinematics and tectonic implications; Journal of Structural Geology, 9, p. 13–29.

Murphy, D.C. (1990): Direct evidence for dextral strike-slip displacement from mylonites in the southern Rocky Mountain Trench near Valemount, British Columbia; *in* Current Research, Part E, Geological Survey of Canada, Paper 90-1E, p. 91–95.

Murphy, D.C. (2007): Geology, Canoe River, British Columbia-Alberta; Geological Survey of Canada, "A" Series Map, 2110A (83D), scale 1:250 000.

Murphy, D.C., Walker, R.T. and Parrish, R.R. (1991): Age and geological setting of Gold Creek gneiss, crystalline basement of the Windermere Supergroup, Cariboo Mountains, British Columbia; Canadian Journal of Earth Sciences, v. 28, p. 1217–1231.

Murphy, D.C., van der Heyden, P., Parrish, R.R., Klepacki, D.W., McMillan, W., Struik, L.C. and Gabites, J. (1995): New geochronological constraints on Jurassic deformation of the western edge of North America, southeastern Canadian Cordillera; *in* Jurassic Magmatism and Tectonics of the North American Cordillera, D.M. Miller and C. Busby (ed.), Geological Society of America Special Paper 299, p. 159–171, doi:10.1130/SPE299-p159

Nier, A.O. (1950): A redetermination of the relative abundances of the isotopes of carbon, nitrogen, oxygen, argon, and potassium; Physical Reviews, v. 77, p. 789–793.

Nixon, G.T., Archibald, D.A. and Heaman, L.M. (1993): ^{40}Ar-^{39}Ar and U-Pb geochronometry of the Polaris Alaskan-type complex, British Columbia: Precise timing of Quesnellia–North America interaction; Geological Association of Canada Annual Meeting Abstracts, v. 18, p. A-76.

Nixon, G.T., Hammack, J.L., Ash, C.H., Cabri, L.J., Case, G., Connelly, J.N., Heaman, L.M., Laflamme, J.H.G., Nuttall, C., Paterson, W.P.E. and Wong, R.H. (1997): Geology and platinum-group-element mineralization of Alaskan-type ultramafic-mafic complexes in British Columbia: British Columbia Geological Survey, Bulletin 93, 142 p.

Nixon, G., Scheel, J.E.S., Scoates, J., Friedman, R.M., Wall, C.J., Gabites, J. and Jackson-Brown, S. (2020): Syn-accretionary multi-stage assembly of an Early Jurassic Alaskan-type intrusion in the Canadian Cordillera: U-Pb and ^{40}Ar/^{39}Ar geochronology of the Turnagain ultramafic-mafic intrusive complex, Yukon-Tanana terrane; Canadian Journal of Earth Sciences, v. 57, p. 575–600.

Oke, C. (1982): Structure and metamorphism of Precambrian basement and its cover in the Mount Blackman area, British Columbia; M.Sc. thesis, The University of Calgary, Calgary, Alberta.

Oke, C. and Simony, P.S. (1981): Basement gneisses of the western Rocky Mountains, Hugh Allan Creek area, British Columbia; *in* Current Research, part A. Geological Survey of Canada, Paper 81-1A, p. 181–184.

Okulitch, A.V. (1984): The role of the Shuswap Metamorphic Complex in Cordilleran tectonism: a review; Canadian Journal of Earth Sciences, v. 21, p. 1171–1193.

Pană, D.I. and Elgr, R. (2013): Geological Map of the Alberta Rocky Mountains and Foothills (NTS 82G, 82H, 82J, 82O, 82N, 83B, 83C, 83D, 83F, 83E, and 83L); Energy Resources Conservation Board, ERCB/ AGS Map 560, scale 1:500 000, URL <https://ags.aer.ca/publication/map-560>.

Pană, D.I. and van der Pluijm, B.A. (2015): Orogenic pulses in the Alberta Rocky Mountains: Radiometric dating of fault gouge from major thrusts and comparison with the regional tectono-stratigraphic record; Geological Society of America Bulletin, v. 127, p. 480–502, doi:10.1130/B31069.1

Pană, D.I., Poulton, T.P. and DuFrane, S.A. (2018a): U-Pb detrital zircon dating supports Early Jurassic initiation of the Cordilleran foreland basin in southwestern Canada; Geological Society of America Bulletin, p. 1–17, doi:10.1130/B31862.1

Pană, D.I., Poulton, T.P. and Heaman, L.M. (2018b): U-Pb zircon ages of volcanic ashes integrated with ammonite biostratigraphy, Fernie Formation (Jurassic), Western Canada, with implications for Cordilleran-Foreland basin connections and comments on the Jurassic time scale; Bulletin of Canadian Society of Petroleum Geologists, v. 66, no. 3, p. 595–622, URL <https://pubs.geoscienceworld.org/cspg/bcpg/article-pdf/66/3/595/4588416/595.pana66.3.pdf>.

Parrish, R.R. (1995): Thermal evolution of the southeastern Canadian Cordillera; Canadian Journal of Earth Sciences, v. 32, p. 1618–1642.

Parrish, R.R. and Armstrong, R.L. (1983): U -Pb zircon age and tectonic significance of gneisses in structural culminations of the Omineca Crystalline Belt, British Columbia; Geological Society of America, Abstracts with Programs, 15, p. 324.

Pell, J. (1994): Carbonatites, nepheline syenites, kimberlites and related rocks in British Columbia; British Columbia Ministry of Energy, Mines and Petroleum Resources Bulletin 88, 136 p.

Pell, J. and Simony, P.S. (1987): New correlations of Hadrynian strata, south-central British Columbia; Canadian Journal of Earth Sciences, v. 24/2, p. 302–313, doi:10.1139/e87-032

Pope, M.C. and Sears, J.W. (1997): Cassiar platform, north-central British Columbia: a miogeoclinal fragment from Idaho; Geology, v. 25, p. 515–518.

Price, R.A. (1981): The Cordilleran foreland thrust and fold belt in the southern Canadian Rocky Mountains; *in* Thrust and nappe tectonics, K.R. McClay and N. J. Price (ed.), Geological Society of London, Special Publication 9, p. 427–448.

Price, R.A. (1986): The southeastern Canadian Cordillera: Thrust faulting, tectonic wedging, and delamination of the lithosphere; Journal of Structural Geology, v. 8, p. 239–254, doi:10.1016/0191-8141(86)90046-5

Price, R.A. (1994): Cordilleran tectonics and the evolution of the Western Canada Sedimentary Basin; Chapter 2 *in* Geological atlas of the Western Canada Sedimentary Basin, G.D. Mossop and I. Shetsen (comp.), Canadian Society of Petroleum Geologists and Alberta Research Council, p. 13–24.

Price, R.A. and Carmichael, D.M. (1986): Geometric test for Late Cretaceous - Paleogene intracontinental transform faulting in the Canadian Cordillera; Geology, v. 14, p. 468–471.

Quan, W., Ji, J. and Zhou, J. (2014): Nier value and initial argon isotope ratio of K-Ar, $^{40}Ar/^{39}Ar$ dating technique; Chinese Journal of Geology, v. 50, issue 1, p. 213–221, doi:10.3969/j.issn.0563-5020.2015.01.013

Quinn, G.M., Hubbard, S.M., van Drecht, R., Guest, B., Matthews, W.A. and Hadlari, T. (2016): Record of orogenic cyclicity in the Alberta foreland basin, Canadian Cordillera; Lithosphere, p. 317–332, doi:10.1130/L531.1

Raeside, R.P. and Simony, P.S. (1983): Stratigraphy and deformational history of the Scrip Nappe, Monashee Mountains, British Columbia; Canadian Journal of Earth Sciences, v. 20, p. 639–650.

Raines, M.K., Hubbard, S.M., Kukulski, R.B., Leier, A.L. and Gehrels, G.E. (2013): Sediment dispersal in an evolving foreland: Detrital zircon geochronology from Upper Jurassic and lowermost Cretaceous strata, Alberta Basin, Canada; Geological Society of America Bulletin, v. 125, no. 5-6, p. 741–755, doi:10.1130/B30671.1

Reid, L.F., Simony, P.S. and Ross, G.M. (2002): Dextral strike-slip faulting in the Cariboo Mountains, British Columbia: a natural example of wrench tectonics in relation to Cordilleran tectonics; Canadian Journal of Earth Sciences, v. 39, p. 953–970, doi:10.1139/E02-017

Roddick, J.A. (1967): Tintina Trench; Journal of Geology, v. 75, p. 23–33.

Ross, G.M. (1991): Tectonic setting of the Windermere Supergroup revisited; Geology, v. 19, p. 1125–1128.

Ross, G.M. and Ferguson, C.A. (2003): Geology and structure cross-sections, Eddy, British Columbia; Geological Survey of Canada, "A" Series Map 1967A (93H01), scale 1:50 000.

Ross, G.M. and Villeneuve, M. (2003): Provenance of the Mesoproterozoic (1.45 Ga) Belt basin (western North America): another piece in the pre-Rodinia paleogeographic puzzle; Geological Society of America Bulletin, v. 115, no. 10, p. 1191–1217.

Ross, G. M. and Arnott, R. W. (2007): Regional geology of the Windermere Supergroup, southern Canadian Cordillera and stratigraphic setting of the Castle Creek study area; *in* Atlas of Deep-Water Outcrops, T.H. Nilsen, R.D. Shew, G.S. Steffens and J.R.J. Studlick (ed.), American Association of Petroleum Geologists, Studies in Geology 56, 16 p.

Scammell, R.J. (1991): Structure and U-Pb geochronometry of the southern Scrip Range, southern Omineca belt, British Columbia: a progress report; Lithoprobe Southern Canadian Cordillera Transect Report, p. 85–96.

Scammell, R.J. (1992): Composite deformation, intradefornational leucogranite magmatism and thermal history, northern Monashee Mountains, Omineca belt, British Columbia; Lithoprobe Southern Canadian Cordillera Transect Report 24, p. 5–11.

Scammell, R.J. (1993): Mid-Cretaceous to Tertiary thermotectonic history of former mid-crustal rocks, southern Omineca Belt, Canadian Cordillera; Ph.D. thesis, Queen’s University, Kingston, Ontario.

Sears, J.W. (2001): Emplacement and denudation history of the Lewis-Eldorado thrust slab in the northern Montana Cordillera, USA – Implications for steady-state orogenic processes; American Journal of Earth Sciences, v. 301, p. 359–373.

Sevigny, J. and Simony, P. (1989): Geometric relationship between the Scrip Nappe and metamorphic isograds in the northern Adams River area, Monashee Mountains, British Columbia; Canadian Journal of Earth Sciences, v. 26, p. 606–610.

Sevigny, J.H., Parrish, R.R. and Ghent, E.D. (1989): Petrogenesis of peraluminous granites, Monashee Mountains, southeastern Canadian Cordillera; Journal of Petrology, v. 30/3, p. 557–581.

Sevigny, J.H., Parrish, R.R., Donelick, R.A. and Ghent, E.D. (1990): Northern Monashee Mountains, Omineca Crystalline Belt, British Columbia: Timing of metamorphism, anatexis, and tectonic denudation; Geology, v. 18, p. 103–106.

Shaw, D. (1980): A concordant uranium-lead age for zircons in the Adamant Pluton, British Columbia; *in* Current Research, part C, Geological Survey of Canada, Paper 80-1C, p. 243–246.

Simony, P.S., Ghent, E.D., Craw, D., Mitchell, W. and Robbins, D.B. (1980): Structural and metamorphic evolution of northeast flank of Shuswap Complex, southern Canoe River area, British Columbia; *in* Cordilleran metamorphic core complexes, M.D. Crittenden, Jr., P.J. Coney and G.H. Davis (ed.), Geological Society of America, Memoir 153, p. 445–461.

Struik, L.C. (1988): Crustal evolution of the eastern Canadian Cordillera; Tectonics, v. 7, p. 727–747, doi:10.1029/TC007i004p00727

Struik, L.C. (1993): Intersecting intracontinental Tertiary transform fault systems in the North American Cordillera; Canadian Journal of Earth Sciences, v. 30, p. 1262–1274.

van den Driessche, J. and Malusky, H. (1986): Mise en évidence d'un cisaillement ductile dextre d'âge crétacé moyen dans la région de Tête Jaune Cache (nord-est du complexe métamorphique Shuswap, Colombie-Britannique); Canadian Journal of Earth Sciences, v. 23, p. 1331–1342.

van der Pluijm, B.A., Vrolijk, P.J., Pevear, D.R., Hall, C.M. and Solum, J. (2006): Fault dating in the Canadian Rocky Mountains: Evidence for Late Cretaceous and early Eocene orogenic pulses; Geology, v. 34, p. 837–840, doi:10.1130/G22610.1

Wanless, R.K., Stevens, R.D., Lachance, G.R. and Edmonds, C.M. (1967): Age determinations and geological studies, K-Ar isotopic ages, Report 7; Geological Survey of Canada, Paper 66-17, 120 p.

Webster, E.R., Pattison, D. and DuFrane, A.S. (2017): Geochronological constraints on magmatism and polyphase deformation and metamorphism in the southern Omineca Belt, British Columbia; Canadian Journal of Earth Sciences, v. 54, p. 529–549, doi:10.1139/cjes-2016-0126

Appendix 1 – Field Photos

Walker Creek Fault Zone

Sample 6

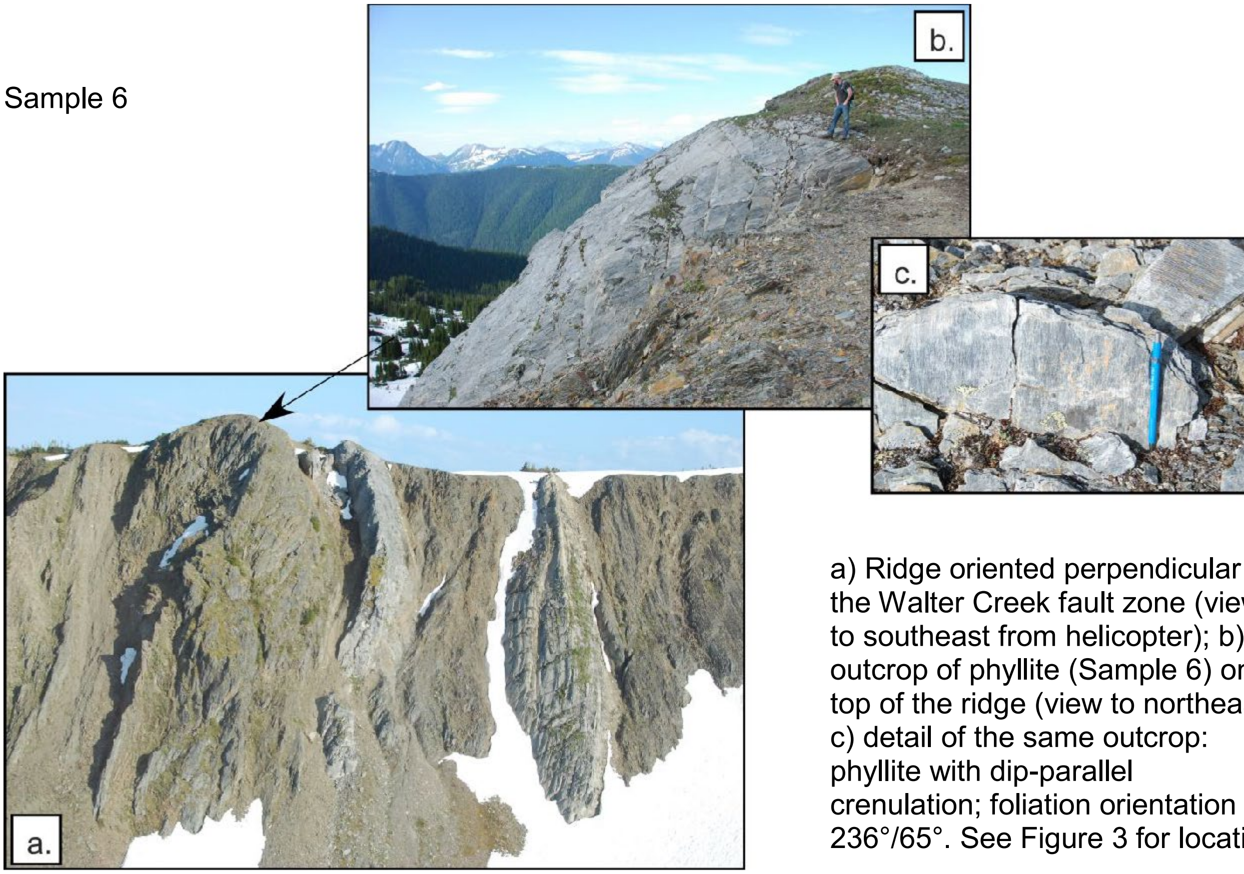

a) Ridge oriented perpendicular to the Walter Creek fault zone (view to southeast from helicopter); b) outcrop of phyllite (Sample 6) on top of the ridge (view to northeast); c) detail of the same outcrop: phyllite with dip-parallel crenulation; foliation orientation 236°/65°. See Figure 3 for location.

Sample 7

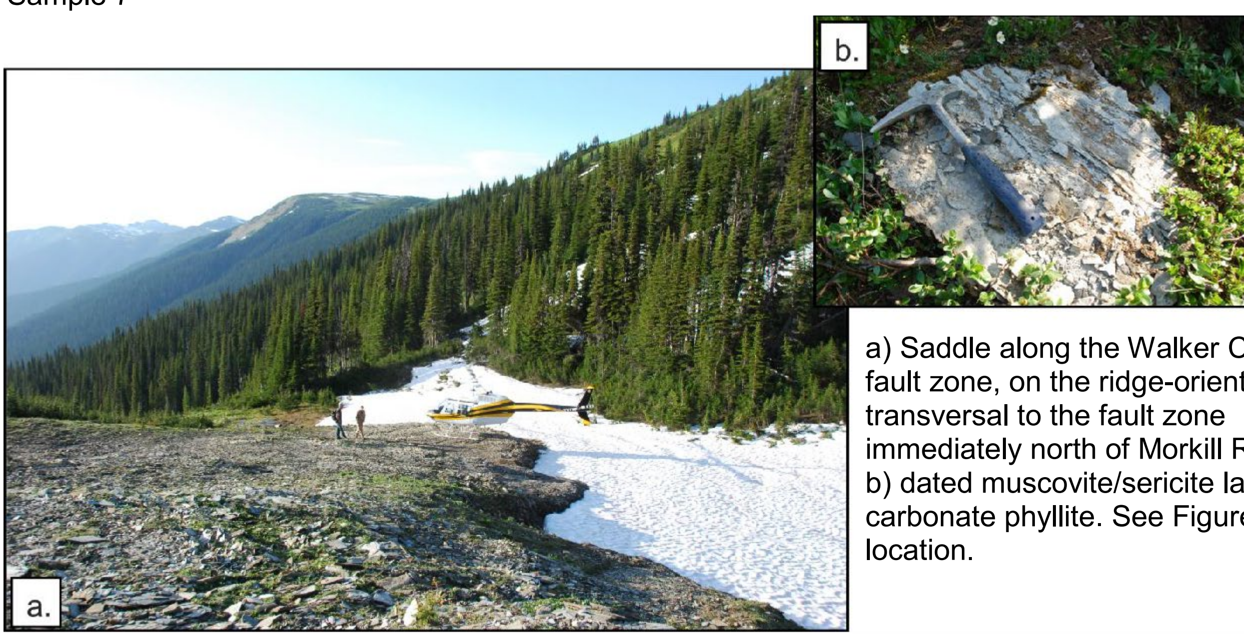

a) Saddle along the Walker Creek fault zone, on the ridge-oriented transversal to the fault zone immediately north of Morkill River; b) dated muscovite/sericite layer in a carbonate phyllite. See Figure 3 for location.

Sample 8

a) McNaughton Formation overprinted by the Walker Creek fault zone at the rip-rap quarry on south side of the Morkill River Forestry Service Road, about 6 km east (see map below) from the Southern Rocky Mountain Trench (UTM 262183E, 5952477N); foliation orientation 228°/87°, lineation 316°/2°; b) detail showing the sampled mica films. See Figure 3 for location.

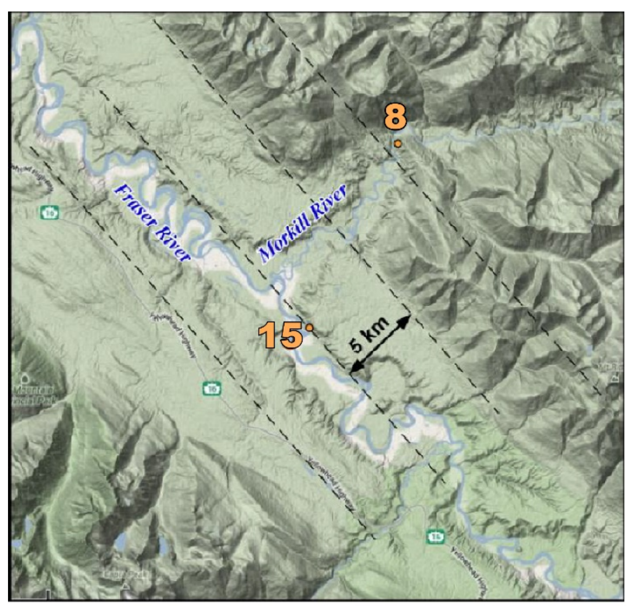

Topographic map showing the location of sample 8 along Walker Creek fault zone and of sample 15 near the middle of the Southern Rocky Mountain Trench. See Figure 3 for map context.

Southern Rocky Mountain Trench

Sample 15

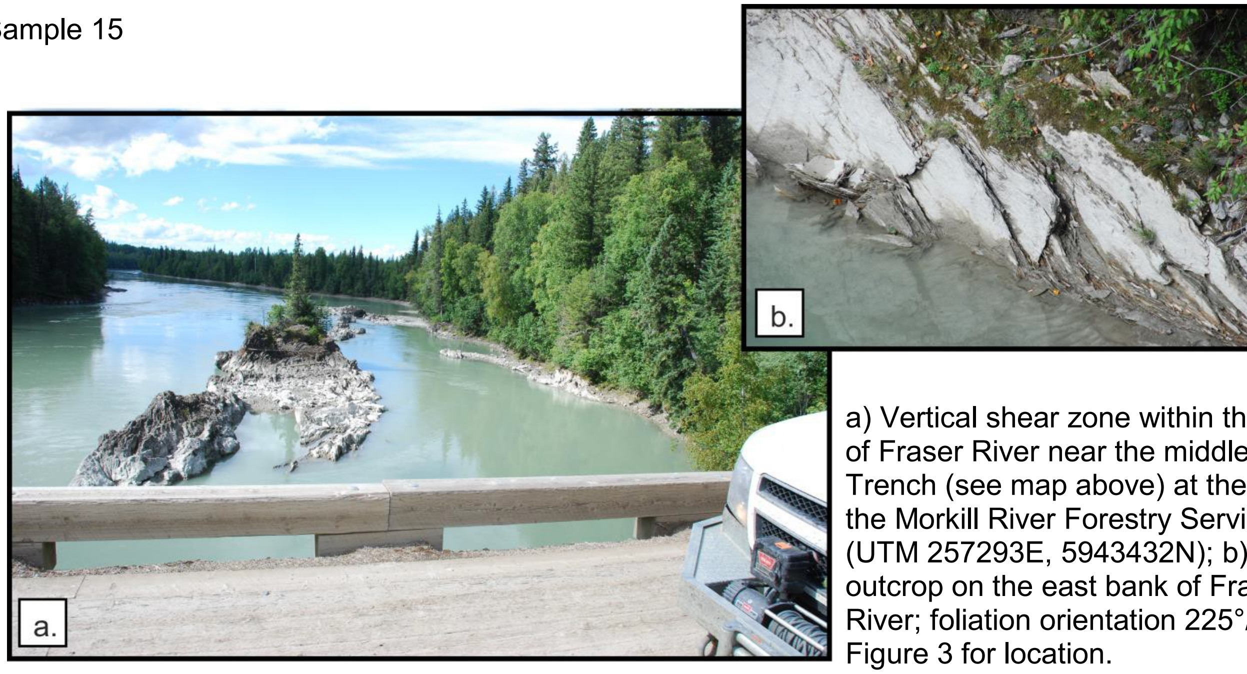

a) Vertical shear zone within the talweg of Fraser River near the middle of the Trench (see map above) at the bridge of the Morkill River Forestry Service Road (UTM 257293E, 5943432N); b) sampled outcrop on the east bank of Fraser River; foliation orientation 225°/87°. See Figure 3 for location.

Sample 16

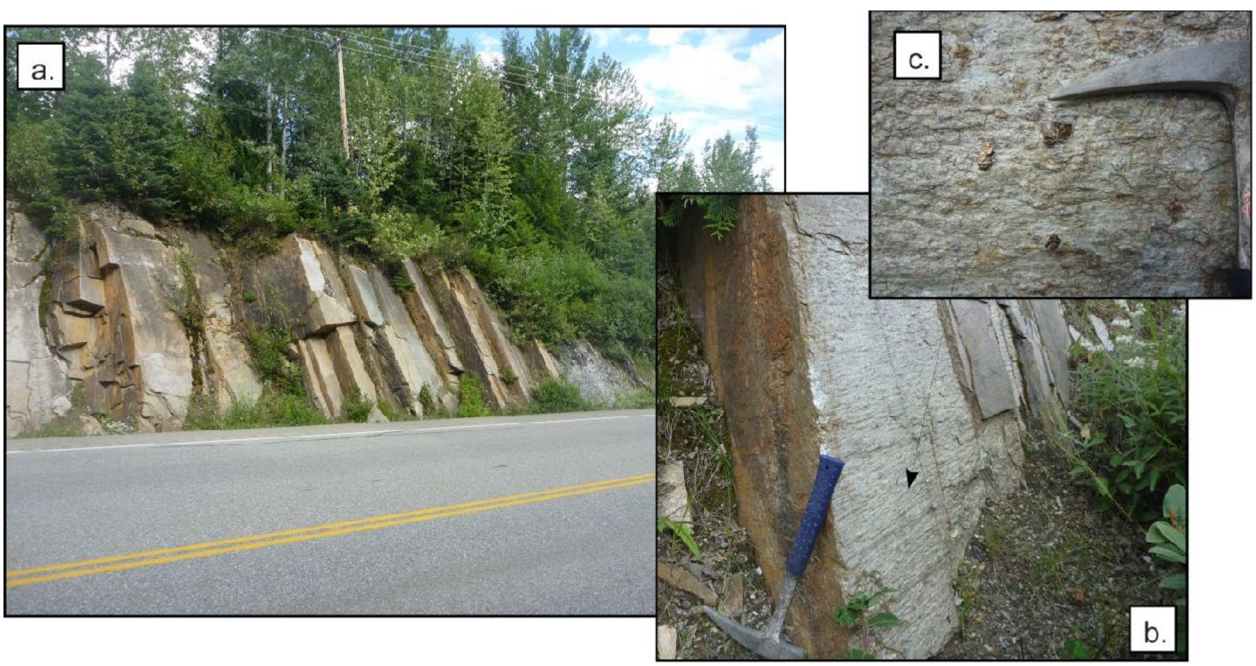

a) Kaza Group grit and pelite on west side of the Southern Rocky Mountain Trench, just north of West Twin Creek (UTM 266408E, 5926253N); b) Sample 16 collected from a muscovite/sericite layer with foliation orientation 215°/60° and stretching lineation 300°/4°; c) detail of bedding-parallel foliation with pyrite aggregate up to 2 cm diameter. See Figure 3 for location.

Sample 20

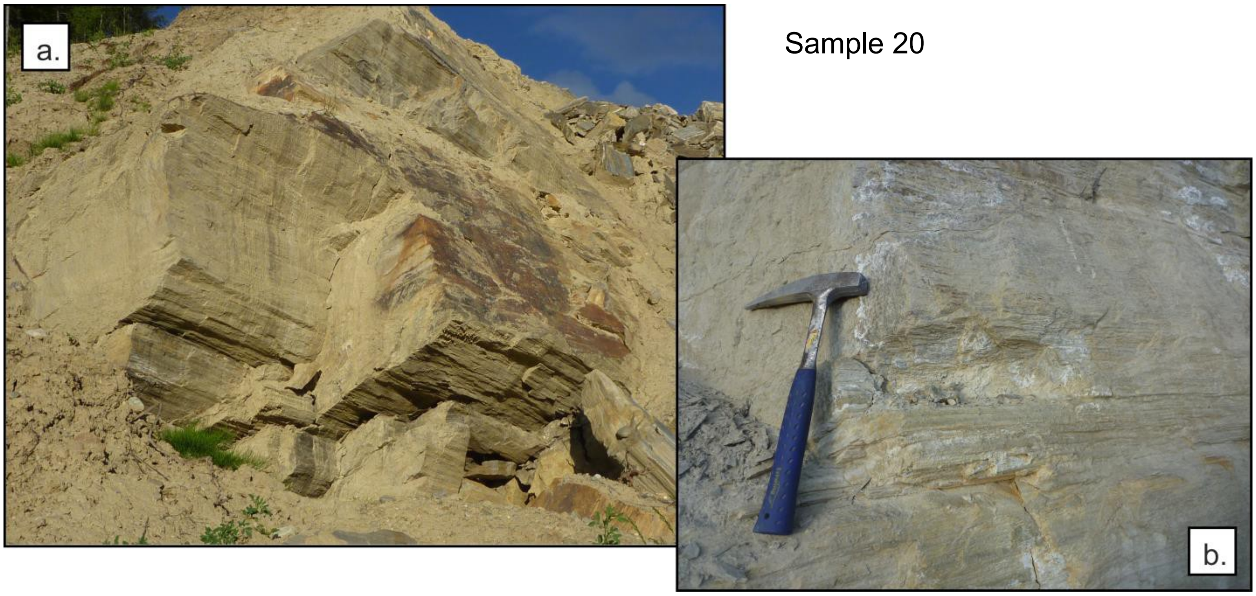

a) Miette grit and pelite near the contact with McNaughton Formation in quarry on east side of the Southern Rocky Mountain Trench near the mouth of Holmes Creek, 150 m east of Highway 16 (UTM 298738E, 5904332N); b) sample 20 collected from a muscovite/sericite layer; orientation of mullions and stretching lineation 132°/5°. See Figure 3 for location.

Sample 21

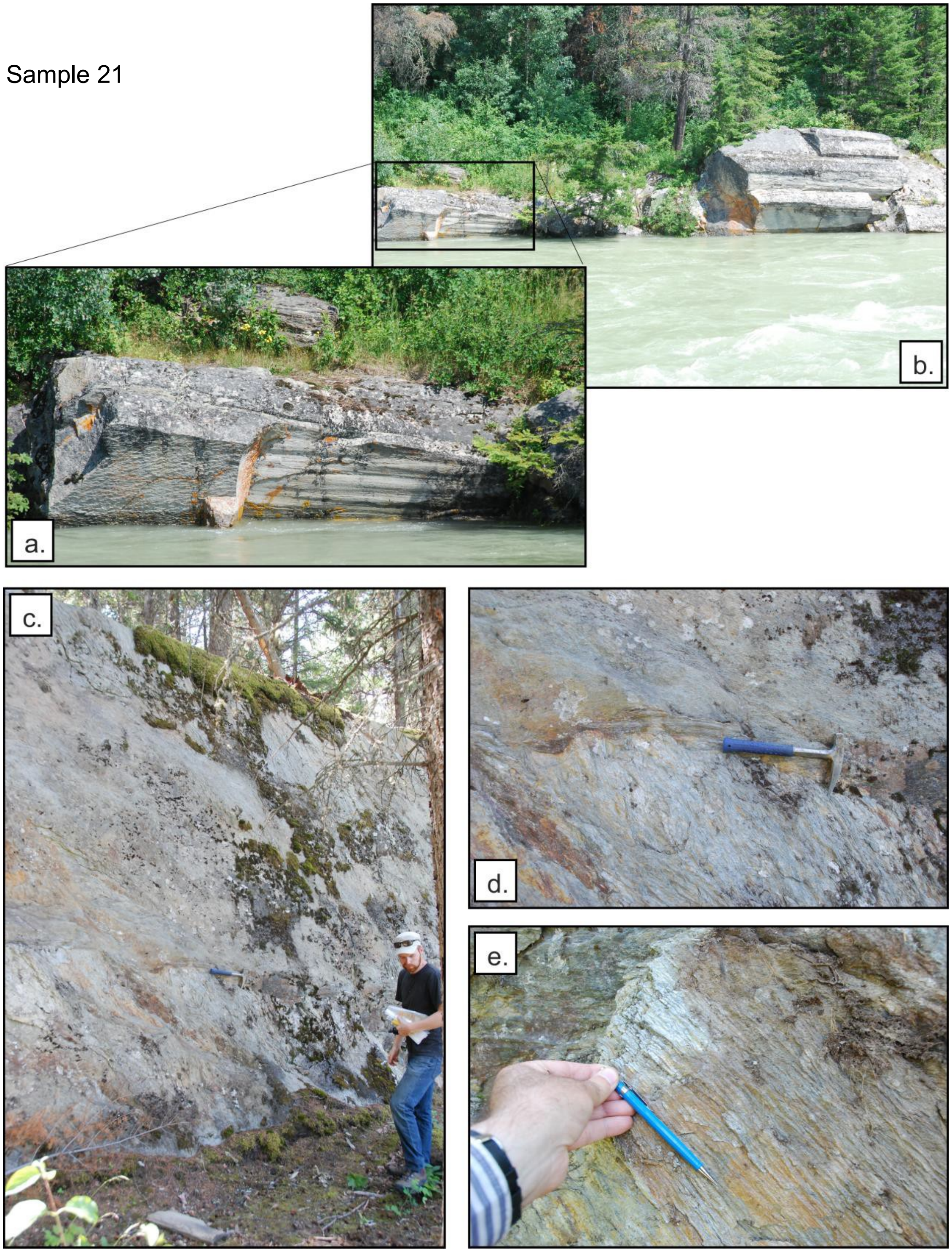

a) and b) Subhorizontal mullions in Miette grit and sandstone in the east bank of Fraser River at Tetê Jaune Cache; trend of mullions parallels the Trench; c) subvertical foliation (34°/83°) in the Miette phyllite and phyllonite in the west bank of Fraser River at the same location; d) detail of the subhorizontal stretching lineation (300°/5°) parallel to the mullions in coarser grained Miette rocks on the opposite bank of the river; e) detail of the crenulation lineation 320°/40°. See Figure 3 for location.

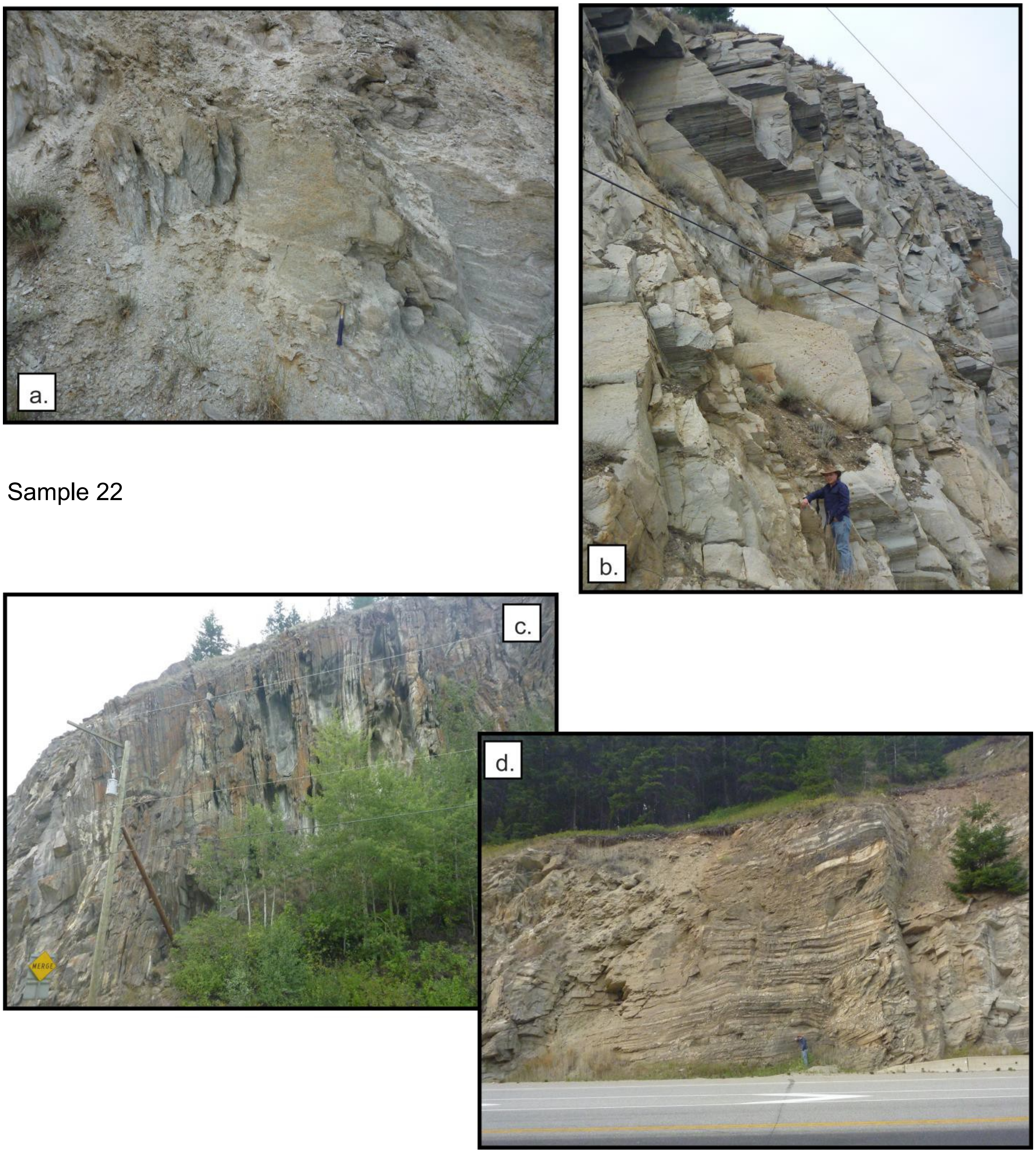

Sample 22

Shear zones overprinting Miette Group at Tête Jaune Cache, on the east side of the Southern Rocky Mountain Trench: a) site of phyllonite sample, about 50 m from the flat area in the Trench (UTM 337067E, 5872187N); foliation orientation of is 208°/87° and lineation 300°/06°; about 50 m to the east, consistent subhorizontal stretching lineation in both vertical and horizontal shear surfaces in the Miette sandstone and grit (best expressed in the top portion of photo) parallels the local trend of the Trench; c) 50 m farther east, vertical zone of shearing up to 50 m wide, subparallel to the local orientation of the trench; d) 100 m to the east on the north side of Highway 16 to Jasper (UTM 337260E, 5872327N), subhorizontal bedding in Miette Group. See Figure 3 for location.

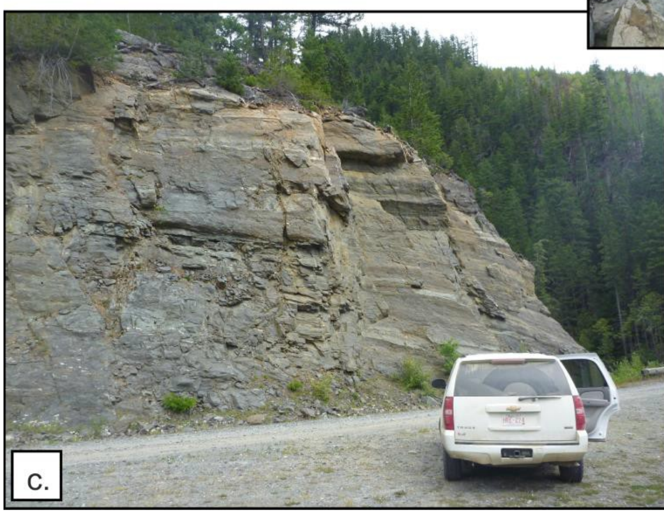

Subhorizontal mullions in gneiss and amphibolite along the trunk road on the east shore of Kinbasket Lake, indicating ductile stretching along the Southern Rocky Mountain Trench:

a) amphibolite gneiss (UTM 359332E, 5844648N);
b) granite gneiss (UTM 361517E, 5842728N); and
c) alternating amphibolite/gneiss succession just north of bridge over Bulldog Creek (UTM 366892E, 5833320N). See Figure 3 for location.

Sample 24

Retrogressed garnet micaschist with tight isoclinal folds (likely Lower Miette cover of the Yellowjacket orthogneiss in the Bear Foot thrust sheet) collected from mountain slope on east side of the trunk road at the north end of Kinbasket Lake (UTM 356161E, 5848425N).

See Figure 3 for location.

Sample 25

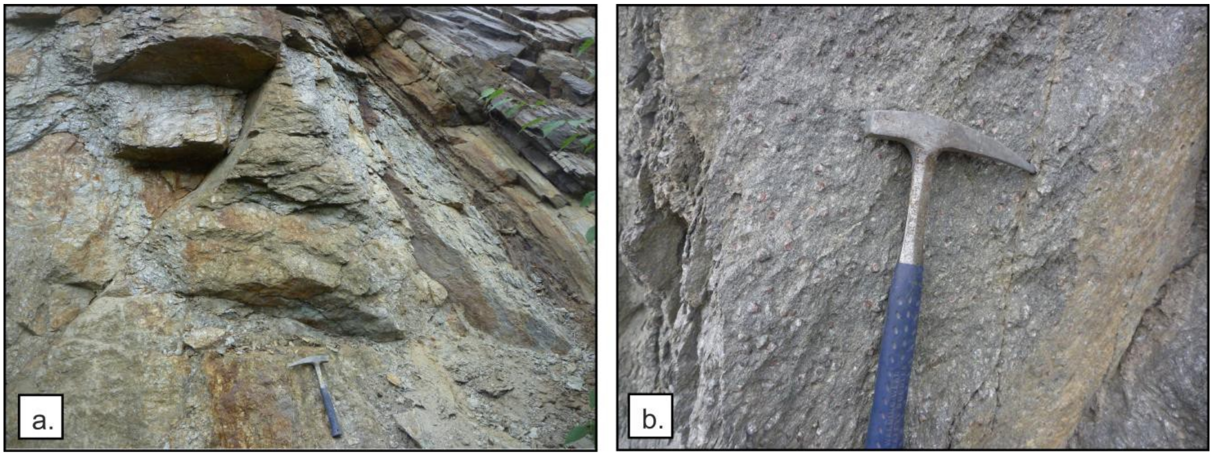

a) Sampled retrogressive shear zone 1–2 m wide (subparallel to the Trench) within garnet micaschist along the east side of Kinbasket Lake (UTM 367977E, 5831437N); the sense of movement, during retrogression and sericite neoformation is uncertain; rocks are overprinted by centimetre-thick gouge layers related to late west dipping normal faults; b) non-retrogressed garnet micaschist and gneiss protolith assigned to the metasedimentary cover (Lower Miette Group) of the Bulldog orthogneiss in the Purcell thrust sheet. See Figure 3 for location.

Valemount Strain Zone

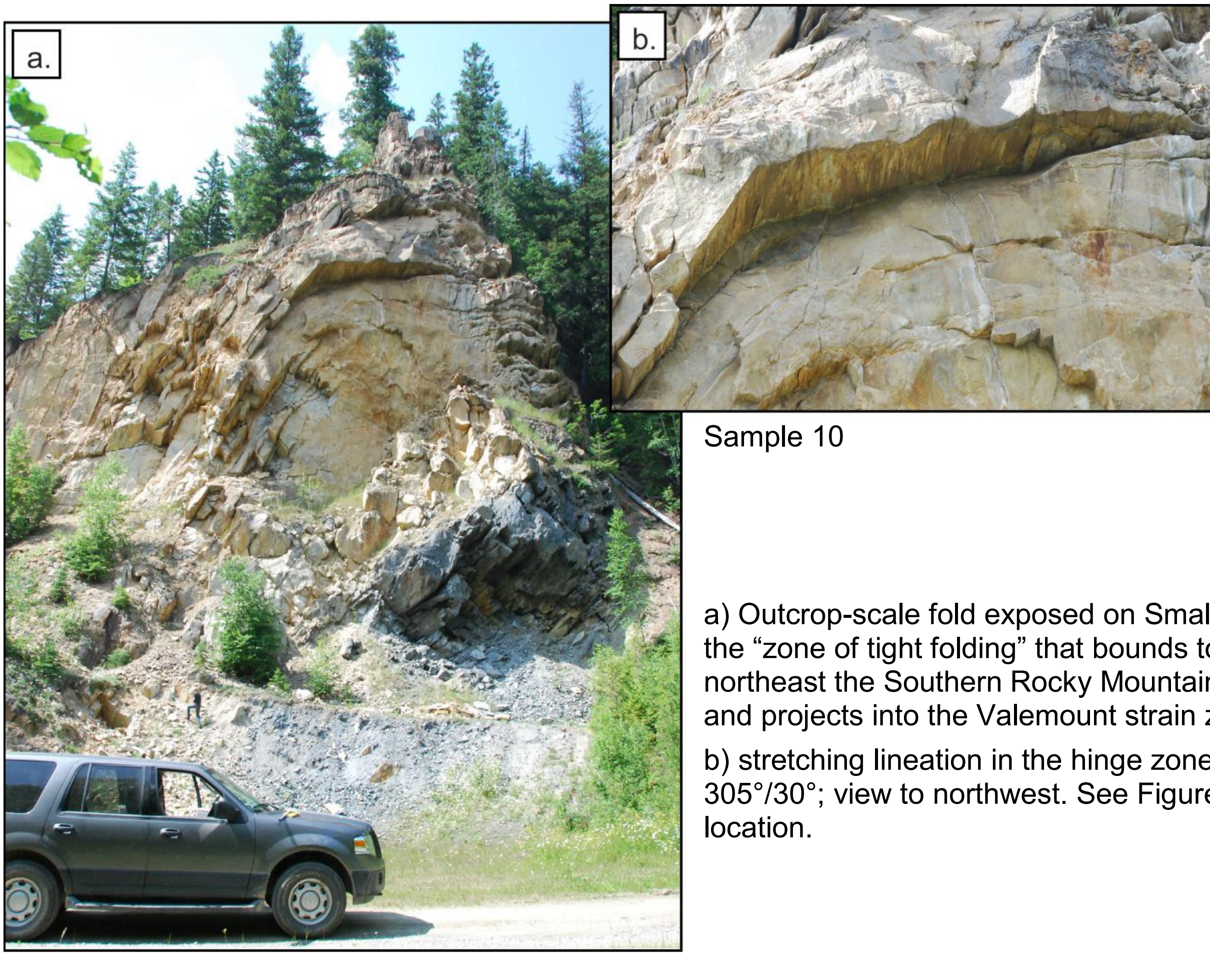

Sample 10

a) Outcrop-scale fold exposed on Small Creek in the “zone of tight folding” that bounds to the northeast the Southern Rocky Mountain Trench and projects into the Valemount strain zone.

b) stretching lineation in the hinge zone is oriented 305°/30°; view to northwest. See Figure 3 for location.

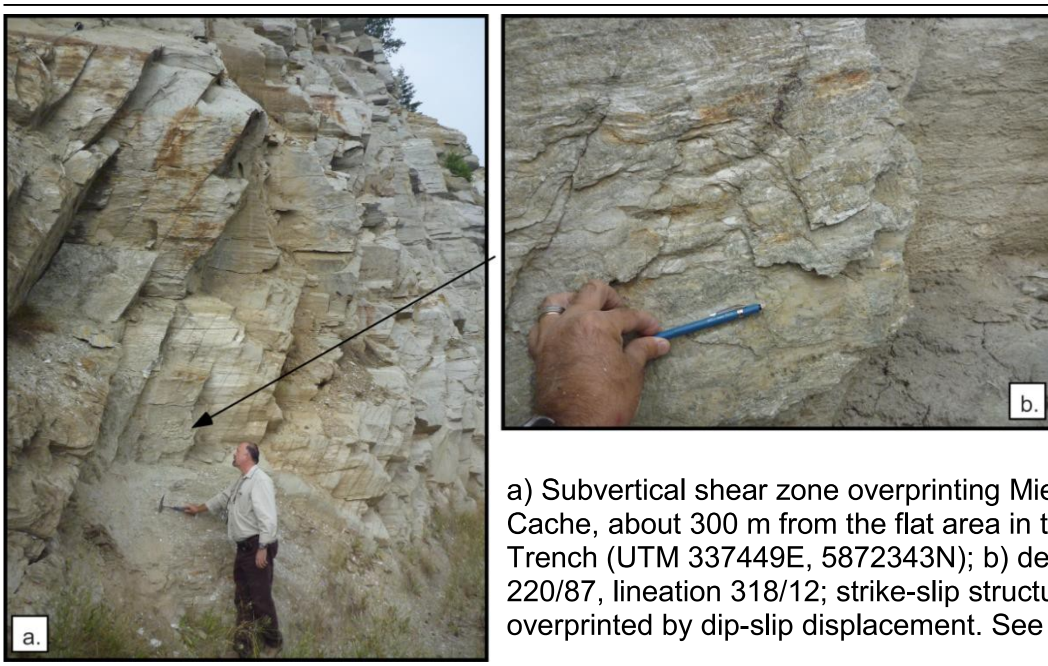

Sample 11

a) Subvertical shear zone overprinting Miette Group at Tête Jaune Cache, about 300 m from the flat area in the Rocky Mountain Trench (UTM 337449E, 5872343N); b) detail: foliation orientation 220/87, lineation 318/12; strike-slip structures are locally overprinted by dip-slip displacement. See Figure 3 for location.

Sample 12

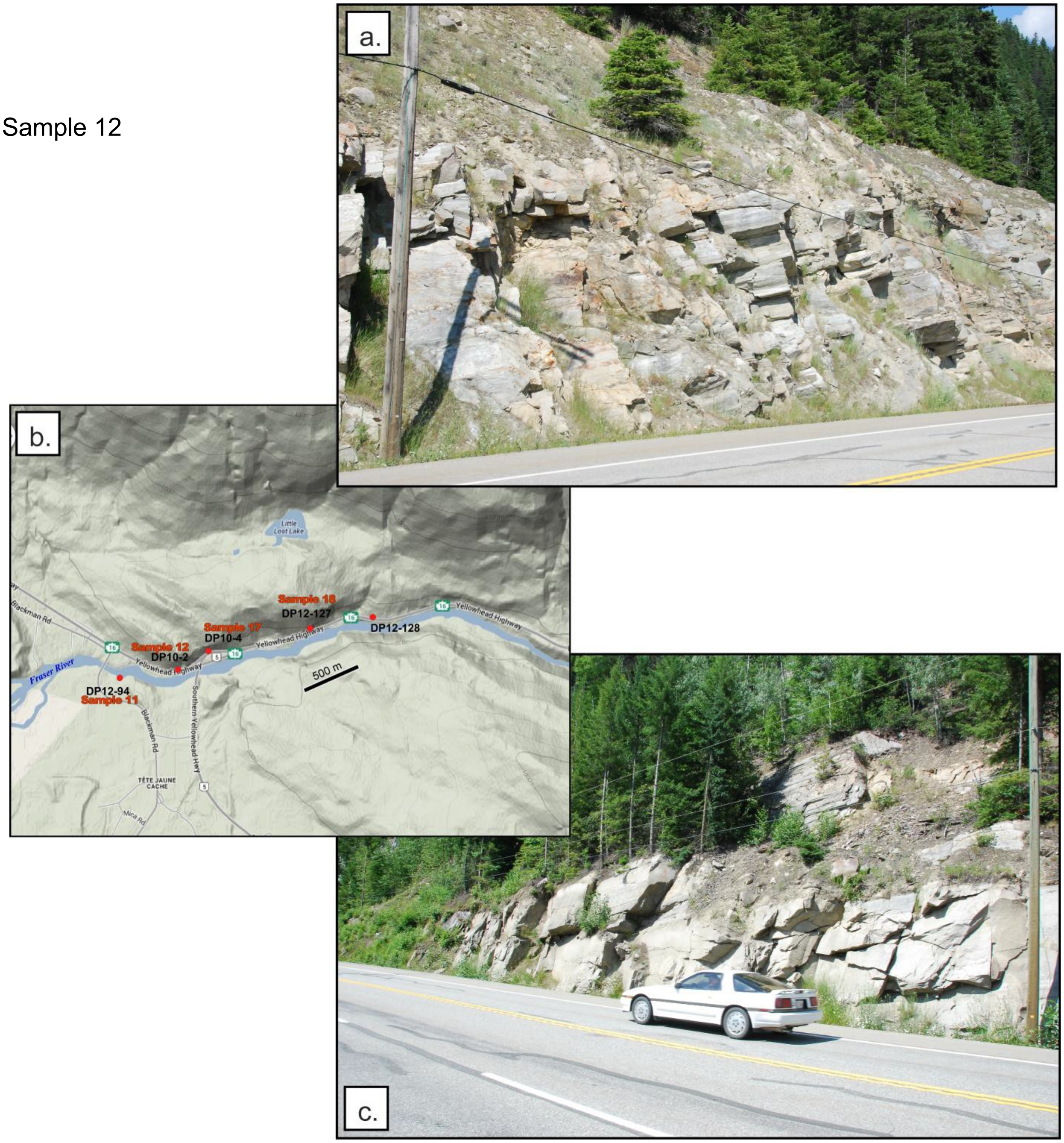

a) Subhorizontal mullions (305°/3°) within Miette sandstone and grit along Highway 16 east of Tête Jaune Cache are slightly oblique to the local trend of the Trench and project southeast into the Valemount strain zone; b) between 1.5 -2 km from the Trench, penetrative deformation (phylonite samples in red) grades into discrete deformation shown in c) thickly bedded Miette sandstone and grit is only locally overprinted by steeply dipping shear surfaces with subhorizontal stretching. See Figure 3 for location.

Sample 14

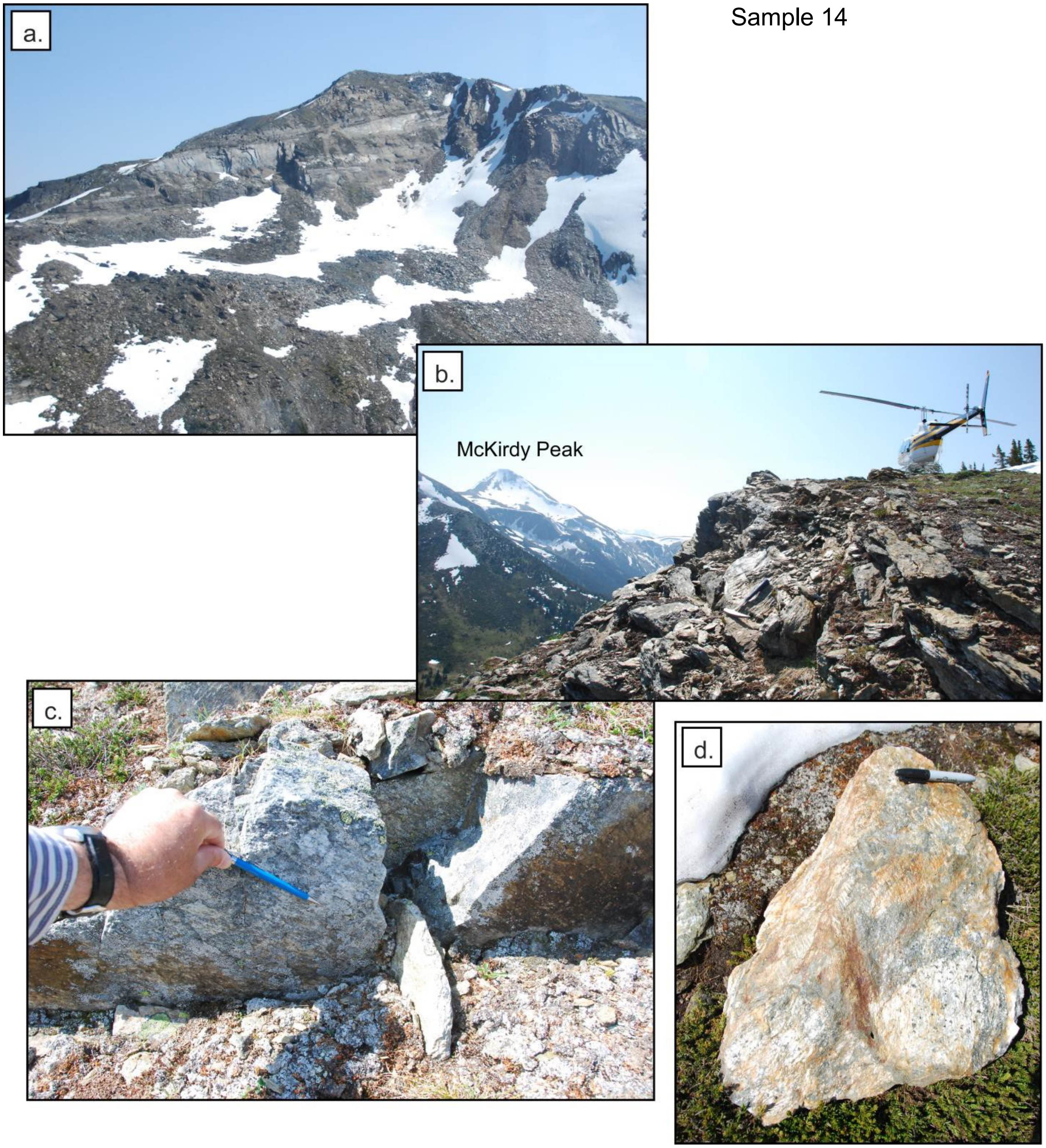

a) View to northeast and to southeast (b) across Valemount strain zone from the site of sample 14 within metres from Bear Foot thrust (traced on top of knob with helicopter in b); c) kinematic indicators in Miette grit below the thrust: foliation 230°/64°; stretching lineation 300°/32° (dextral); d) analyzed sample 19. See Figure 3 for location.

Appendix 2 – Micrographs

PLATE I

Burnt Timber thrust (Sample 1)

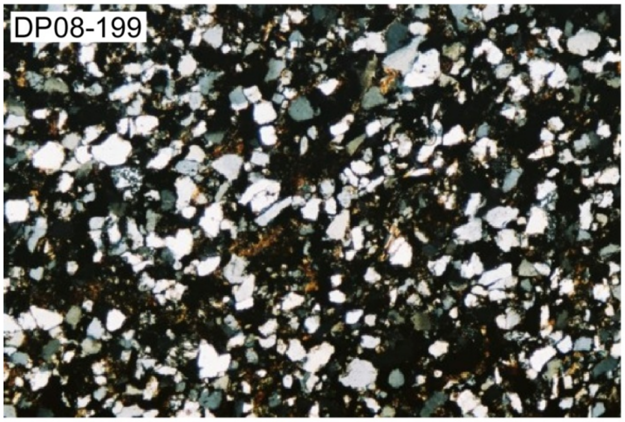

Quartz (white & gray) and interstitial Fe-stained dark matrix in fine-grained siltstone. X-axis of photo: 2.3 mm, N+.

Brazeau sandstone (Sample 2)

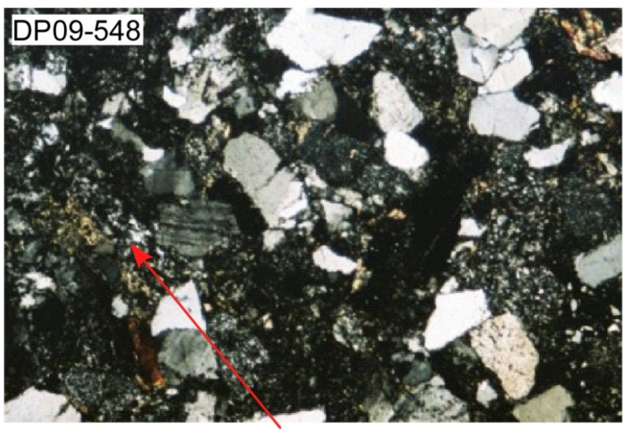

Angular quartz (light) and minor plagioclase (arrow) in wacke. The matrix (cement) consists mostly of fine-grained quartz and feldspars. X-axis of photo: 2.3 mm, N+.

McConnell thrust (Sample 3)

A. Large, stubby grain of biotite is interstitial to the matrix quartz and feldspars. X-axis of photo: 0.45 mm, N II.

B. Slender prisms of biotite (dark brown) are interstitial to the fine-grained matrix of quartz, feldspars and a large carbonate (in center). X-axis of photo: 2.3 mm, N II.

PLATE II

Miette Group (Sample M2)

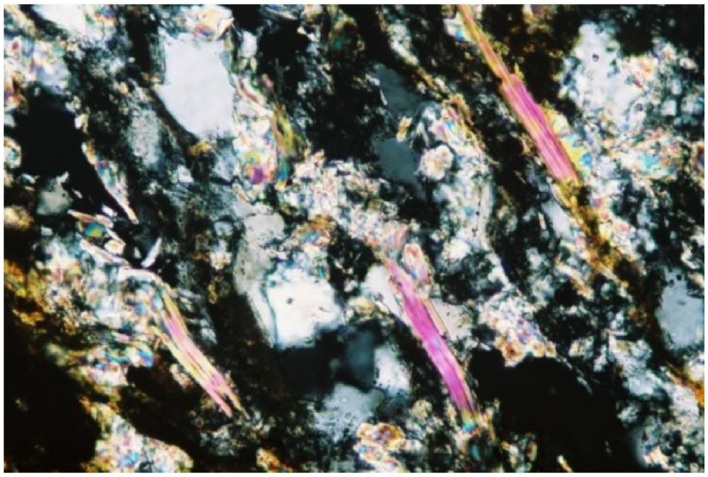

A. Fine-grained fibrous sericite aggregates (s) are interstitial to quartz, and slender prisms of muscovite (m) parallel the rock fabric. X-axis of photo: 0.45 mm, N+.

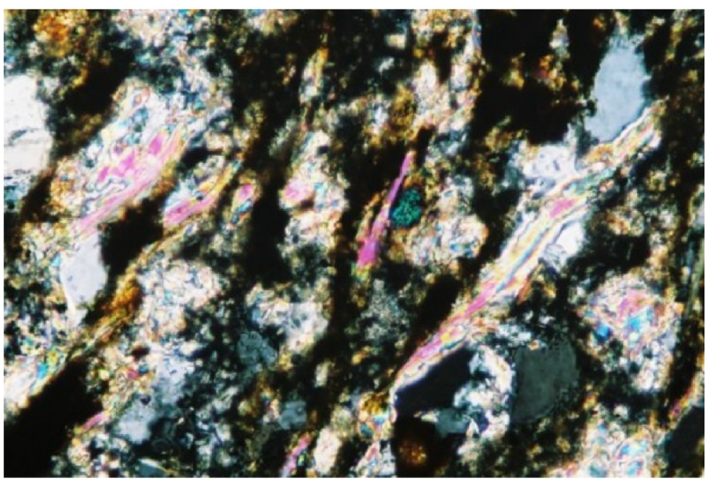

B. Fine-grained sericite and interstitial Fe-hydroxide (dark) that defines the rock fabric.X-axis of photo: 0.45 mm, N+.

PLATE III

Valemount Strain Zone
(Sample 13)

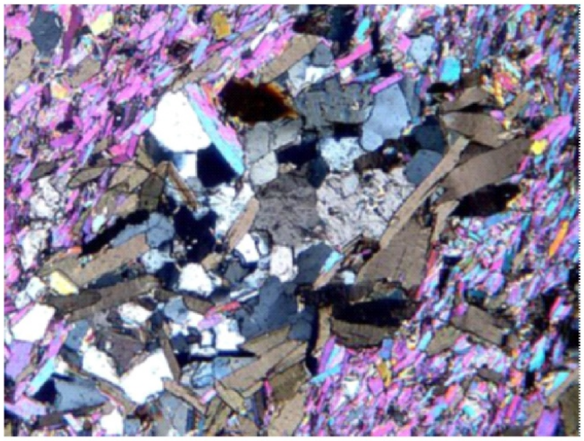

Muscovite (multi colour) - biotite (brown laths) schist
X - axis of photo: 1.6 mm, N+.

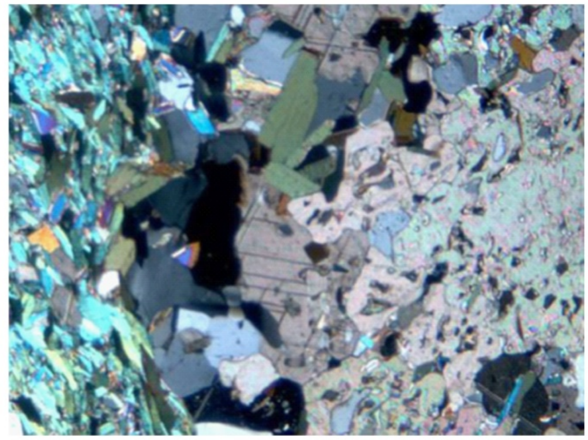

Carbonate aggregate (right half of photo) is rimmed by muscovite (green). X - axis of photo: 1.6 mm, N+.

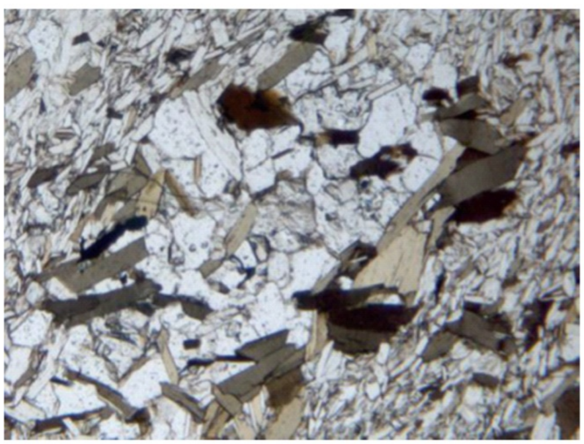

Same as above, with N II. Note brown and tan coloured biotite laths; muscovite grains are colourless.

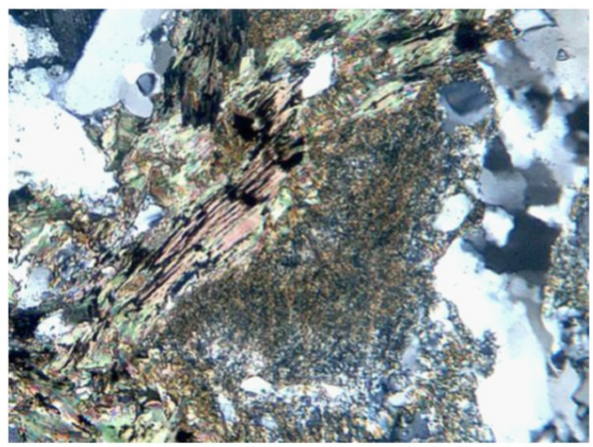

Biotite veinlet in muscovite-biotite schist
X - axis of photo: 0.64 mm, N+.

Appendix 3 – $^{40}Ar/^{39}Ar$ Raw Data

Table 6. Samples analyzed by GeochronEx Analytical Services Ltd.

Sample No.	Site	GeochronEx ID
1	DP08-199	YK-223s sericite
2	DP09-548	YK-220 anorthoclase
3	DP07-6A	YK-216 sericite/illite
M1	DP16-359	YK-G418
M2	DP08-1202A	YK-220m muscovite
		YK-220s sericite
13	DP16-362	YK-G421m muscovite
		YK-G421b biotite

Sample 1: DP08-199 (YK-223s sericite) **J=0.004425±0.000051**

T^0C	^{40}Ar (STP)	$^{40}Ar/^{39}Ar$	±1σ	$^{38}Ar/^{39}Ar$	±1σ	$^{37}Ar/^{39}Ar$	±1σ	$^{36}Ar/^{39}Ar$	±1σ	Ca/K	$\Sigma^{39}Ar$ (%)	Age (Ma)	±1σ
500	$316.62*e^{-9}$	20.484	0.011	0.0184	0.0001	0.0556	0.0003	0.0032	0.0002	0.20	61.8	149.6	1.7
550	$158.56*e^{-9}$	31.324	0.023	0.0183	0.0003	0.0586	0.0004	0.0049	0.0002	0.21	82.0	224.0	2.5
650	$85.47*e^{-9}$	34.471	0.027	0.0210	0.0007	0.0827	0.0013	0.0057	0.0004	0.30	91.9	244.5	2.8
750	$13.96*e^{-9}$	16.971	0.033	0.0256	0.0017	0.1284	0.0021	0.0189	0.0019	0.46	95.2	88.6	4.3
850	$4.17*e^{-9}$	13.821	0.088	0.0501	0.0059	0.1750	0.0075	0.0315	0.0040	0.63	96.4	35.6	9.2
1000	$4.54*e^{-9}$	9.263	0.021	0.0330	0.0039	0.2229	0.0059	0.0236	0.0041	0.80	98.4	18.3	9.7
1130	$3.14*e^{-9}$	7.847	0.021	0.0269	0.0016	0.1427	0.0022	0.0195	0.0011	0.51	100.0	16.6	2.6

Sample 2: DP09-548 (YK-220 anorthoclase) **J=0.004412 ± 0.000051**

T^0C	^{40}Ar (STP)	$^{40}Ar/^{39}Ar$	±1σ	$^{38}Ar/^{39}Ar$	±1σ	$^{37}Ar/^{39}Ar$	±1σ	$^{36}Ar/^{39}Ar$	±1σ	Ca/K	$\Sigma^{39}Ar$ (%)	Age (Ma)	±1σ
500	$94.03*e^{-9}$	21.128	0.011	0.02545	0.00035	0.10348	0.00091	0.01326	0.00015	0.373	4.7	132.0	1.5
600	$199.80*e^{-9}$	18.338	0.007	0.02313	0.00007	0.19278	0.00019	0.00448	0.00007	0.694	16.2	130.6	1.5
700	$176.87*e^{-9}$	19.356	0.007	0.02346	0.00011	0.10945	0.00041	0.00362	0.00008	0.394	25.9	140.0	1.6
800	$97.48*e^{-9}$	20.541	0.013	0.02385	0.00031	0.04115	0.00094	0.00549	0.00023	0.148	30.9	144.6	1.7
900	$95.52*e^{-9}$	20.152	0.017	0.02451	0.00039	0.04612	0.00035	0.00773	0.00035	0.166	36.0	136.9	1.7
1000	$177.00*e^{-9}$	18.728	0.008	0.02392	0.00009	0.03667	0.00042	0.00490	0.00010	0.132	46.0	132.5	1.5
1065	$309.11*e^{-9}$	18.573	0.009	0.02325	0.00007	0.03130	0.00013	0.00368	0.00005	0.113	63.6	134.1	1.5
1130	$642.88*e^{-9}$	18.697	0.009	0.02312	0.00003	0.02116	0.00005	0.00256	0.00002	0.076	100.0	137.4	1.5

Sample 3: DP07-6A (YK-216 illite/smectite/sericite) **J=0.004276 ± 0.000048**

T^0C	^{40}Ar (STP)	$^{40}Ar/^{39}Ar$	±1σ	$^{38}Ar/^{39}Ar$	±1σ	$^{37}Ar/^{39}Ar$	±1σ	$^{36}Ar/^{39}Ar$	±1σ	Ca/K	$\Sigma^{39}Ar$ (%)	Age (Ma)	±1σ
500	$717.50*e^{-9}$	26.893	0.014	0.02158	0.00006	0.09565	0.00016	0.00428	0.00005	0.344	42.6	187.6	2.0
550	$661.88*e^{-9}$	37.283	0.013	0.02117	0.00008	0.10071	0.00021	0.00248	0.00002	0.363	71.0	262.0	2.7
600	$554.51*e^{-9}$	54.203	0.022	0.02134	0.00013	0.12272	0.00043	0.00367	0.00011	0.442	87.3	369.3	3.8
650	$320.31*e^{-9}$	88.302	0.059	0.02125	0.00026	0.11147	0.00037	0.00565	0.00026	0.401	93.1	568.5	5.5
700	$131.21*e^{-9}$	97.162	0.126	0.02451	0.00047	0.10136	0.00291	0.01298	0.00123	0.365	95.2	605.8	6.2
800	$155.71*e^{-9}$	89.770	0.085	0.02113	0.00119	0.09110	0.00228	0.00590	0.00100	0.328	98.0	576.4	5.8
930	$87.32*e^{-9}$	82.498	0.118	0.02488	0.00160	0.08752	0.00339	0.01633	0.00117	0.315	99.7	517.4	5.5
1130	$15.58*e^{-9}$	83.390	0.428	0.04115	0.00638	0.10299	0.01406	0.05287	0.00500	0.371	100.0	459.1	10.1

Total fusion age, TFA= 166.7 ± 1.9 Ma (including J).

Sample M1: DP16-359 YK-G418 coarse muscovite J=0.004172±0.000083

T^0C	$^{36}Ar/^{40}Ar$	±1σ	$^{40}Ar/^{39}Ar$	±1σ	$^{38}Ar/^{39}Ar$	±1σ	$^{37}Ar/^{39}Ar$	±1σ	$^{36}Ar/^{39}Ar$	±1σ	Ca/K	$\Sigma^{39}Ar$ (%)	Age (Ma)	±1σ
508	0.002657	0.000215	0.001464	0.00005	0.788417	0.02937	0.175415	0.00654	1.815513	0.06761	0.64	1.3	807.7	34.2
585	0.001224	0.000026	0.007001	0.00014	0.711671	0.01501	0.792921	0.01672	0.174901	0.00370	2.90	3.4	574.4	16.7
692	0.001070	0.000003	0.003180	0.00000	0.128875	0.00033	0.680906	0.00170	0.336490	0.00085	2.49	22.6	1144.9	23.1
782	0.000077	0.000000	0.002875	0.00000	0.019747	0.00007	0.005699	0.00003	0.026676	0.00010	0.02	38.3	1590.0	32.2
833	0.000075	0.000000	0.002594	0.00000	0.019735	0.00004	0.003675	0.00001	0.028848	0.00006	0.01	65.5	1701.6	34.2
885	0.000246	0.000002	0.002526	0.00001	0.036166	0.00023	0.009192	0.00007	0.097300	0.00059	0.03	72.1	1671.1	34.9
940	0.000395	0.000003	0.002446	0.00001	0.050222	0.00038	0.009948	0.00008	0.161617	0.00117	0.04	77.8	1651.7	35.1
987	0.000501	0.000005	0.002407	0.00002	0.059381	0.00053	0.011872	0.00012	0.208101	0.00181	0.04	83.0	1629.5	35.5
1070	0.000685	0.000005	0.002224	0.00001	0.077094	0.00053	0.016140	0.00013	0.307993	0.00208	0.06	90.4	1642.0	34.6
1272	0.000502	0.000003	0.002196	0.00001	0.060799	0.00034	0.013391	0.00009	0.228595	0.00126	0.05	100.0	1729.4	35.9

Sample M2: DP08-1202A YK-220m muscovite J=0.004405±0.000051

T^0C	^{40}Ar (STP)	$^{40}Ar/^{39}Ar$	±1σ	$^{38}Ar/^{39}Ar$	±1σ	$^{37}Ar/^{39}Ar$	±1σ	$^{36}Ar/^{39}Ar$	±1σ	Ca/K	$\Sigma^{39}Ar$ (%)	Age (Ma)	±1σ
500	$57.40*e^{-9}$	90.421	0.272	0.0232	0.0011	0.0959	0.0018	0.0065	0.0020	0.35	1.9	594.0	6.9
600	$332.90*e^{-9}$	150.816	0.665	0.0199	0.0004	0.1445	0.0011	0.0035	0.0007	0.52	8.4	914.1	9.0
650	$484.57*e^{-9}$	204.953	0.254	0.0194	0.0009	0.0091	0.0007	0.0014	0.0007	0.03	15.4	1159.0	10.0
700	$754.55*e^{-9}$	250.207	0.221	0.0193	0.0003	0.0039	0.0009	0.0025	0.0003	0.01	24.3	1337.6	11.0
750	$1145.80*e^{-9}$	297.002	0.550	0.0192	0.0010	0.0069	0.0013	0.0046	0.0009	0.02	35.7	1504.5	12.0
800	$1810.00*e^{-9}$	327.934	0.256	0.0216	0.0007	0.0072	0.0016	0.0018	0.0011	0.03	52.0	1610.9	12.4
850	$1391.59*e^{-9}$	321.281	0.323	0.0238	0.0006	0.0091	0.0016	0.0042	0.0008	0.03	64.8	1586.8	12.3
900	$1086.99*e^{-9}$	326.746	0.544	0.0244	0.0013	0.0039	0.0029	0.0275	0.0015	0.01	74.7	1582.1	12.4
950	$587.36*e^{-9}$	303.792	0.311	0.0183	0.0010	0.0021	0.0015	0.0043	0.0006	0.01	80.4	1528.0	12.0
1000	$709.17*e^{-9}$	306.118	0.365	0.0192	0.0007	0.0034	0.0011	0.0028	0.0008	0,01	87.2	1537.5	12.1
1050	$965.67*e^{-9}$	339.759	0.317	0.0185	0.0005	0.0026	0.0011	0.0017	0.0004	0.01	95.6	1649.1	12.6
1090	$472.26*e^{-9}$	378.878	0.527	0.0193	0.0012	0.0101	0.0022	0.0132	0.0011	0.04	99.3	1759.4	13.1
1130	$88.73*e^{-9}$	388.870	3.632	0.0309	0.0078	0.0278	0.0151	0.0500	0.0090	0.10	100.0	1756.8	18.5

Total fusion age, TFA= 1486.6 ± 11.7 Ma (including J);

Weighted Mean Plateau Age = 1593.2 ± 12.3 Ma (including J).

Sample M2: DP08-1202A YK-220s sericite J=0.004417±0.000051

T^0C	^{40}Ar (STP)	$^{40}Ar/^{39}Ar$	±1σ	$^{38}Ar/^{39}Ar$	±1σ	$^{37}Ar/^{39}Ar$	±1σ	$^{36}Ar/^{39}Ar$	±1σ	Ca/K	$\sum^{39}Ar$ (%)	Age (Ma)	±1σ
500	$89.49*e^{-9}$	65.356	0.071	0.0226	0.0015	0.2429	0.0016	0.0111	0.0011	0.87	4.7	437.1	4.9
600	$388.26*e^{-9}$	112.112	0.062	0.0194	0.0004	0.3753	0.0008	0.0036	0.0005	1.35	16.5	720.1	6.9
650	$455.56*e^{-9}$	150.497	0.093	0.0200	0.0006	0.0277	0.0008	0.0034	0.0006	0.10	26.9	914.7	8.3
700	$617.19*e^{-9}$	185.914	0.130	0.0191	0.0004	0.0213	0.0008	0.0020	0.0006	0.08	38.3	1079.0	9.4
750	$851.17*e^{-9}$	227.436	0.194	0.0093	0.0002	0.0120	0.0006	0.0012	0.0007	0.04	51.1	1253.2	10.5
800	$905.06*e^{-9}$	221.202	0.167	0.0014	0.0000	0.0095	0.0007	0.0008	0.0006	0.03	65.1	1228.8	10.3
850	$789.91*e^{-9}$	219.804	0.176	0.0197	0.0005	0.0095	0.0009	0.0020	0.0007	0.03	77.4	1221.6	10.3
900	$487.30*e^{-9}$	207.291	0.146	0.0183	0.0006	0.0161	0.0011	0.0041	0.0006	0.06	85.5	1167.6	10.0
950	$285.28*e^{-9}$	185.078	0.202	0.0198	0.0007	0.0177	0.0012	0.0049	0.0010	0.06	90.8	1071.5	9.5
1000	$295.21*e^{-9}$	183.077	0.274	0.0195	0.0005	0.0284	0.0019	0.0105	0.0014	0.10	96.3	1055.3	9.5
1070	$166.35*e^{-9}$	174.852	0.218	0.0199	0.0011	0.0894	0.0018	0.0103	0.0012	0.32	99.5	1018.7	9.2
1130	$28.14*e^{-9}$	205.545	2.703	0.0330	0.0057	0.2267	0.0117	0.0456	0.0132	0.82	100.0	1108.3	22.1

Total fusion age, TFA= 1066.2 ± 9.3 Ma (including J);

Weighted Mean Plateau Age = 1234.3 ± 10.3 Ma (including J).

Sample 13: DP16-362 YK-G421m muscovite J=0.004184+/-0.000084

T^0C	$^{38}Ar/^{39}Ar$	±1σ	$^{37}Ar/^{39}Ar$	±1σ	$^{36}Ar/^{39}Ar$	±1σ	$^{39}Ar/^{40}Ar$	±1σ	$^{36}Ar/^{40}Ar$	±1σ	Ca/K	Cum% ^{39}Ar	Age (Ma)	±1σ
585.2	0.161494	0.006535	0.129187	0.005231	0.153673	0.006220	0.012419	0.000501	0.001908	0.000527	0.47	1.0	245.5	11.1
687.9	0.060650	0.000602	1.882647	0.018144	0.100095	0.000983	0.023029	0.000222	0.002305	0.000023	6.89	4.5	100.2	2.3
765.1	0.135565	0.000870	1.516508	0.009555	0.614862	0.003884	0.005150	0.000032	0.003167	0.000020	5.55	9.8	81.5	2.4
819.7	0.026022	0.000152	0.035301	0.000204	0.056101	0.000317	0.030438	0.000163	0.001708	0.000010	0.13	16.0	118.2	2.5
875.1	0.014965	0.000031	0.015184	0.000029	0.012801	0.000028	0.053911	0.000078	0.000690	0.000001	0.06	47.8	108.2	2.2
927.5	0.015777	0.000033	0.012059	0.000028	0.017366	0.000037	0.040058	0.000057	0.000696	0.000001	0.04	77.1	143.9	2.9
979.3	0.029962	0.000162	0.010946	0.000067	0.089164	0.000460	0.022573	0.000112	0.002013	0.000011	0.04	84.3	129.5	2.7
1033.4	0.054226	0.000403	0.010662	0.000094	0.210027	0.001523	0.012909	0.000093	0.002711	0.000020	0.04	88.6	109.4	2.4
1082.3	0.066084	0.000689	0.011537	0.000135	0.268273	0.002746	0.009957	0.000101	0.002671	0.000028	0.04	92.5	149.0	2.8
1197.6	0.058673	0.000273	0.008840	0.000052	0.235830	0.001054	0.010576	0.000047	0.002494	0.000012	0.03	100.0	175.2	2.9

Total fusion age, TFA= 127.4 ± 2.6 Ma (including J);

Sample 13: DP16-362 YK-G421b biotite J=0.004205+/-0.000084

T^0C	$^{38}Ar/^{39}Ar$	±1σ	$^{37}Ar/^{39}Ar$	±1σ	$^{36}Ar/^{39}Ar$	±1σ	$^{39}Ar/^{40}Ar$	±1σ	$^{36}Ar/^{40}Ar$	±1σ	Ca/K	Cum% ^{39}Ar	Age (Ma)	±1σ
623.3	0.158901	0.000183	0.027759	0.000037	0.051194	0.000062	0.055302	0.000061	0.002831	0.000677	0.10	9.2	21.8	0.5
720.4	0.048594	0.000050	0.091042	0.000093	0.016054	0.000018	0.073417	0.000066	0.001179	0.000001	0.33	26.2	66.0	1.3
794.6	0.027456	0.000027	0.073112	0.000072	0.011044	0.000013	0.068109	0.000059	0.000752	0.000001	0.27	39.1	84.6	1.7
848.4	0.022660	0.000020	0.003889	0.000006	0.007931	0.000009	0.071094	0.000038	0.000564	0.000000	0.01	48.5	86.8	1.7
921.3	0.022681	0.000020	0.003915	0.000008	0.007205	0.000010	0.070771	0.000041	0.000510	0.000000	0.01	56.8	88.9	1.8
1014.9	0.021617	0.000018	0.003515	0.000006	0.006410	0.000009	0.074322	0.000047	0.000476	0.000000	0.01	68.5	85.7	1.7
1071.3	0.024979	0.000020	0.004598	0.000006	0.009637	0.000011	0.068724	0.000043	0.000662	0.000001	0.02	81.9	86.7	1.7
1145.5	0.022906	0.000021	0.004430	0.000007	0.010374	0.000013	0.067577	0.000036	0.000701	0.000001	0.02	91.3	86.9	1.7
1186.2	0.023905	0.000024	0.004628	0.000009	0.021714	0.000023	0.053787	0.000032	0.001168	0.000001	0.02	98.9	90.0	1.8
1240.8	0.024195	0.000066	0.013099	0.000041	0.026088	0.000066	0.046712	0.000093	0.001219	0.000003	0.05	100.0	100.9	2.0

Total fusion age, TFA= 77.5 ± 1.6 Ma (including J);

Table 7. Samples analyzed by TerraChron Corp.

Site	Sample No.	TerraChron ID
DP10-2x	22	P54-004
		P54-028
DP10-4x	11	P54-019
DP10-8x	24	P54-034
DP11-123	4	P57-004
		P57-007
DP11-125b	5	P57-002
		P57-009
DP11-133	15	P57-041
		P57-036
DP11-136	8	P57-030
DP11-137	16	P57-029
DP11-146	20	P57-015
		P57-010
DP11-161	25	P57-028
		P57-025
DP11-173	23	P57-023
DP12-70	9	P59-017
DP12-77	18	P59-020
DP12-80	17	P59-007
DP12-81	19	P59-008
		P59-209
DP12-87b	14	P59-026
DP12-94	21	P59-070
		P59-072
		P59-218
DP12-105	10	P63-055
DP12-110	6	P59-081
DP12-125	12	P59-080

DP10-2x P54-004 sericite

Fractions:

No	Name	Temp	Cum 39K	Age	40Ar* / 39K
1	4-01 1.4W 22-Ma	1	0.34408	77.478 ± 0.309 Ma	6.929 ± 0.03
2	4-02 2.0W 22-Ma	3	0.42302	74.415 ± 0.692 Ma	6.649 ± 0.06
3	4-03 2.5W 22-Ma	4	0.49038	72.106 ± 0.613 Ma	6.439 ± 0.06
4	4-04 4.5W 20kHz	5	0.62753	71.552 ± 0.389 Ma	6.388 ± 0.04
5	4-05 4.5W 20kHz	6	0.99526	74.376 ± 0.145 Ma	6.646 ± 0.01
6	4-06 5.0W 20kHz	7	1.00000	88.198 ± 6.002 Ma	7.911 ± 0.55

No	Name	Cum 36S	40Ar / 36Ar	40ArAcc/g	37Ca / 39K
1	4-01 1.4W 22-Ma	0.55465	8221.48 ± 367.21	8.4E-0012	1.110 ± 0.191 m
2	4-02 2.0W 22-Ma	0.58550	31674.60 ± 26725.73	4.7E-0013	1.362 ± 2.099 m
3	4-03 2.5W 22-Ma	0.66524	10324.78 ± 2952.86	1.2E-0012	1.499 ± 1.506 m
4	4-04 4.5W 20kHz	0.77635	14835.65 ± 3547.23	1.7E-0012	2.014 ± 0.532 m
5	4-05 4.5W 20kHz	0.98553	21839.39 ± 2462.51	3.2E-0012	1.873 ± 0.153 m
6	4-06 5.0W 20kHz	1.00000	5071.79 ± 5633.05	2.2E-0013	0.421 ± 39.500 m

No	38Cl / 39K	40Ar* Vol ccNTP/g	Atm Cont	F1	F2
1	1.996 ± 0.306 m	226.44 ± 1.32 E-12 (0.6%)	3.5942%	-0.000001	0.000354
2	-315.874 ± 808.328 µ	49.86 ± 0.48 E-12 (1.0%)	0.9329%	-0.000001	0.001792
3	1.927 ± 0.572 m	41.19 ± 0.41 E-12 (1.0%)	2.8620%	-0.000001	0.000651
4	1.813 ± 0.365 m	83.22 ± 0.60 E-12 (0.7%)	1.9918%	-0.000001	0.001278
5	1.541 ± 0.127 m	232.12 ± 1.23 E-12 (0.5%)	1.3531%	-0.000001	0.001692
6	4.333 ± 8.413 m	3.56 ± 0.25 E-12 (6.9%)	5.8263%	-0.000000	0.000071

Integrated Results:

Age = 92.145 ± 0.335 MaWt. Mean Age = 88.220 ± 247.166 Ma (2825)

40Ar* / 39K = 8.275 ± 0.014

Total 39K Vol = 3.4535E-0010 ccNTP/g

Total 40Ar* Vol = 2.858 ± 0.004 E-9

(40Ar / 36Ar)sam = 11041.59 ± 328.64

Total Atm 40Ar Vol = 7.8580E-0011 ccNTP/g

(36Ar / 40Ar)sam = 0.00009057 ±0.00000376
(37Ar / 40Ar)sam = 0.00036895 ±0.00002281
(39Ar / 40Ar)sam = 0.11761865 ±0.00014432

Corr 36/40 & 39/40 ratios =-0.446581
Corr 36/40 & 37/40 ratios =-0.010557
Corr 37/40 & 39/40 ratios = 0.012315

37Ca / 39K = 3.137 ± 0.194 E-3
Ca / K = 5.756 ± 0.356 E-3
F1 = -2.238 E-6

38Cl / 39K = 1.923 ± 0.087 E-3
Cl / K = 4.038 ± 0.182 E-4
F2 = 1.135 E-3

DP10-2x P54-028 Sericite

Fractions:

No	Name			Temp	Cum 39K	Age				40Ar* / 39K		
1	28-01	1.5W	23-M	4	0.00048	1.277	±	0.023	Ga	162.532	±	4.15
2	28-02	1.5W	23-M	5	0.00272	534.497	±	5.732	Ma	54.450	±	0.67
3	28-03	1.8W	23-M	6	0.00795	208.194	±	2.122	Ma	19.315	±	0.21
4	28-04	2.0W	23-M	7	0.01222	95.337	±	2.820	Ma	8.569	±	0.26
5	28-05	2.1W	23-M	8	0.02124	81.329	±	1.681	Ma	7.281	±	0.15
6	28-06	2.1W	23-M	9	0.02493	60.256	±	4.043	Ma	5.363	±	0.37
7	28-07	2.2W	23-M	10	0.02978	57.303	±	2.544	Ma	5.096	±	0.23
8	28-08	2.2W	23-M	11	0.03487	61.018	±	2.220	Ma	5.432	±	0.20
9	28-09	2.5W	24-M	13	0.04832	65.335	±	0.910	Ma	5.823	±	0.08
10	28-10	2.5W	24-M	14	0.05294	64.174	±	3.102	Ma	5.718	±	0.28
11	28-11	2.8W	24-M	15	0.06917	66.935	±	0.864	Ma	5.969	±	0.08
12	28-12	3.5W	24-M	16	0.08509	71.111	±	0.617	Ma	6.348	±	0.06
13	28-13	4.0W	24-M	17	0.11128	75.134	±	0.563	Ma	6.715	±	0.05
14	28-14	4.5W	20kH	18	0.15775	73.268	±	0.518	Ma	6.545	±	0.05
15	28-15	4.5W	20kH	19	0.19968	71.484	±	0.539	Ma	6.382	±	0.05
16	28-16	4.5W	20kH	20	0.27999	75.635	±	0.324	Ma	6.761	±	0.03
17	28-17	4.5W	20kH	21	0.40870	75.552	±	0.398	Ma	6.753	±	0.04
18	28-18	4.5W	20kH	22	0.49581	73.075	±	0.381	Ma	6.527	±	0.03
19	28-19	4.5W	20kH	23	0.59547	81.066	±	0.379	Ma	7.257	±	0.03
20	28-20	4.5W	20kH	24	0.63552	79.554	±	0.325	Ma	7.119	±	0.03
21	28-21	4.5W	20kH	25	0.69581	84.940	±	0.281	Ma	7.612	±	0.03
22	28-22	4.5W	20kH	26	0.76886	83.661	±	0.240	Ma	7.495	±	0.02
23	28-23	4.5W	20kH	27	0.81369	85.897	±	0.333	Ma	7.700	±	0.03
24	28-24	4.5W	20kH	28	0.85213	87.690	±	0.405	Ma	7.865	±	0.04
25	28-25	4.5W	20kH	29	0.88105	96.334	±	0.397	Ma	8.661	±	0.04
26	28-26	4.5W	20kH	30	0.93537	103.601	±	0.246	Ma	9.333	±	0.02
27	28-27	5.0W	20kH	31	0.97045	148.802	±	0.540	Ma	13.576	±	0.05
28	28-28	6.0W	27-M	32	0.99909	196.376	±	0.552	Ma	18.158	±	0.05
29	28-29	7.0W	20kH	33	0.99989	2.090	±	0.013	Ga	344.973	±	3.62
30	28-30	6.0W	20kH	34	1.00000	3.050	±	0.049	Ga	698.295	±	23.32

DP10-2x P54-028 Sericite

No	Name			Cum 36S	40Ar / 36Ar			40ArAcc/g	37Ca / 39K			
1	28-01	1.5W	23-M	0.02021	5259.64	±	1294.57	1.6E-0012	22.261	±	95.036	m
2	28-02	1.5W	23-M	0.06923	3527.75	±	434.37	3.9E-0012	12.222	±	11.592	m
3	28-03	1.8W	23-M	0.11189	3373.05	±	257.08	3.4E-0012	21.269	±	6.958	m
4	28-04	2.0W	23-M	0.13116	2760.98	±	684.66	1.5E-0012	6.047	±	6.522	m
5	28-05	2.1W	23-M	0.15276	4242.53	±	1150.73	1.7E-0012	7.167	±	2.533	m
6	28-06	2.1W	23-M	0.16947	1834.29	±	649.33	1.3E-0012	8.364	±	7.553	m
7	28-07	2.2W	23-M	0.18349	2584.02	±	895.83	1.1E-0012	14.924	±	3.855	m
8	28-08	2.2W	23-M	0.19747	2863.20	±	915.43	1.1E-0012	9.946	±	5.363	m
9	28-09	2.5W	24-M	0.22494	4000.66	±	689.98	2.2E-0012	8.906	±	1.735	m
10	28-10	2.5W	24-M	0.23709	3113.96	±	1453.40	9.5E-0013	5.172	±	5.622	m
11	28-11	2.8W	24-M	0.25630	6848.61	±	1946.17	1.5E-0012	6.044	±	1.807	m
12	28-12	3.5W	24-M	0.26145	25785.11	±	16946.84	4.0E-0013	1.562	±	1.488	m
13	28-13	4.0W	24-M	0.30608	5412.61	±	614.23	3.5E-0012	2.917	±	1.327	m
14	28-14	4.5W	20kH	0.41845	3810.94	±	262.14	8.8E-0012	8.054	±	0.866	m
15	28-15	4.5W	20kH	0.49244	4992.50	±	555.95	5.8E-0012	2.140	±	1.176	m
16	28-16	4.5W	20kH	0.54087	14855.23	±	1856.39	3.8E-0012	1.264	±	0.317	m
17	28-17	4.5W	20kH	0.63269	12589.31	±	1025.52	7.2E-0012	1.067	±	0.221	m
18	28-18	4.5W	20kH	0.69360	12418.93	±	1629.75	4.8E-0012	1.138	±	0.300	m
19	28-19	4.5W	20kH	0.75504	15581.76	±	1511.73	4.8E-0012	1.842	±	0.515	m
20	28-20	4.5W	20kH	0.77010	24888.43	±	7568.54	1.2E-0012	2.459	±	2.463	m
21	28-21	4.5W	20kH	0.78033	58563.29	±	27759.95	8.0E-0013	1.425	±	0.579	m
22	28-22	4.5W	20kH	0.78913	81084.16	±	45147.73	6.9E-0013	1.464	±	0.395	m
23	28-23	4.5W	20kH	0.79248	134058.50	±	196599.62	2.6E-0013	1.806	±	0.676	m
24	28-24	4.5W	20kH	0.80359	35633.36	±	17944.13	8.7E-0013	1.917	±	0.458	m
25	28-25	4.5W	20kH	0.81287	35350.97	±	16026.80	7.3E-0013	4.076	±	0.873	m
26	28-26	4.5W	20kH	0.83366	31958.60	±	6743.71	1.6E-0012	4.856	±	0.430	m
27	28-27	5.0W	20kH	0.87372	15734.79	±	1392.19	3.1E-0012	4.883	±	0.668	m
28	28-28	6.0W	27-M	0.93117	12052.05	±	1093.06	4.5E-0012	12.220	±	0.858	m
29	28-29	7.0W	20kH	0.98493	6942.22	±	658.02	4.2E-0012	88.563	±	56.810	m
30	28-30	6.0W	20kH	1.00000	6980.17	±	1513.48	1.2E-0012	-45.812	±	166.152	m

DP10-2x P54-028 Sericite

No	38Cl / 39K	40Ar* Vol ccNTP/g		Atm Cont	F1	F2
1	27.807 ± 25.795 m	26.68 ± 0.42	E-12 (1.6%)	5.6183%	-0.000016	0.000174
2	5.892 ± 3.768 m	42.13 ± 0.52	E-12 (1.2%)	8.3764%	-0.000009	0.000194
3	7.945 ± 1.839 m	34.91 ± 0.32	E-12 (0.9%)	8.7606%	-0.000015	0.000931
4	2.898 ± 2.320 m	12.63 ± 0.38	E-12 (3.0%)	10.7027%	-0.000004	0.000482
5	1.797 ± 1.318 m	22.68 ± 0.48	E-12 (2.1%)	6.9652%	-0.000005	0.001079
6	2.238 ± 3.000 m	6.84 ± 0.47	E-12 (6.8%)	16.1097%	-0.000006	0.000664
7	2.492 ± 1.866 m	8.53 ± 0.39	E-12 (4.5%)	11.4357%	-0.000011	0.001859
8	5.409 ± 1.334 m	9.55 ± 0.36	E-12 (3.7%)	10.3206%	-0.000007	0.001305
9	4.178 ± 0.565 m	27.07 ± 0.40	E-12 (1.5%)	7.3863%	-0.000006	0.001574
10	5.517 ± 2.245 m	9.11 ± 0.45	E-12 (4.9%)	9.4895%	-0.000004	0.000708
11	1.925 ± 0.929 m	33.47 ± 0.46	E-12 (1.4%)	4.3147%	-0.000004	0.001846
12	2.716 ± 1.148 m	34.89 ± 0.32	E-12 (0.9%)	1.1460%	-0.000001	0.001749
13	1.969 ± 0.828 m	60.74 ± 0.52	E-12 (0.9%)	5.4595%	-0.000002	0.000619
14	2.375 ± 0.426 m	105.05 ± 0.86	E-12 (0.8%)	7.7540%	-0.000006	0.001202
15	1.362 ± 0.472 m	92.41 ± 0.81	E-12 (0.9%)	5.9189%	-0.000002	0.000438
16	2.147 ± 0.320 m	187.52 ± 1.17	E-12 (0.6%)	1.9892%	-0.000001	0.000759
17	1.411 ± 0.182 m	300.18 ± 1.86	E-12 (0.6%)	2.3472%	-0.000001	0.000542
18	1.524 ± 0.243 m	196.36 ± 1.31	E-12 (0.7%)	2.3794%	-0.000001	0.000590
19	1.362 ± 0.251 m	249.77 ± 1.56	E-12 (0.6%)	1.8964%	-0.000001	0.001082
20	1.671 ± 0.454 m	98.47 ± 0.62	E-12 (0.6%)	1.1873%	-0.000002	0.002366
21	1.601 ± 0.383 m	158.49 ± 0.90	E-12 (0.6%)	0.5046%	-0.000001	0.003037
22	1.879 ± 0.213 m	189.08 ± 1.06	E-12 (0.6%)	0.3644%	-0.000001	0.004390
23	1.238 ± 0.408 m	119.21 ± 0.73	E-12 (0.6%)	0.2204%	-0.000001	0.008688
24	1.948 ± 0.262 m	104.39 ± 0.70	E-12 (0.7%)	0.8293%	-0.000001	0.002399
25	3.365 ± 0.544 m	86.51 ± 0.55	E-12 (0.6%)	0.8359%	-0.000003	0.004586
26	1.183 ± 0.216 m	175.09 ± 0.96	E-12 (0.5%)	0.9246%	-0.000003	0.004578
27	2.239 ± 0.438 m	164.46 ± 0.93	E-12 (0.6%)	1.8780%	-0.000003	0.001546
28	3.025 ± 0.439 m	179.62 ± 1.00	E-12 (0.6%)	2.4519%	-0.000009	0.002197
29	27.411 ± 11.271 m	95.01 ± 0.63	E-12 (0.7%)	4.2566%	-0.000063	0.000413
30	8.635 ± 59.966 m	26.79 ± 0.29	E-12 (1.1%)	4.2334%	0.000033	0.000090

Integrated Results:

Age = 92.145 ± 0.335 MaWt. Mean Age = 88.220 ± 247.166 Ma (2825)

40Ar* / 39K = 8.275 ± 0.014

Total 39K Vol = 3.4535E-0010 ccNTP/g

Total 40Ar* Vol = 2.858 ± 0.004 E-9

(40Ar / 36Ar)sam = 11041.59 ± 328.64

Total Atm 40Ar Vol = 7.8580E-0011 ccNTP/g

(36Ar / 40Ar)sam = 0.00009057 ±0.00000376
(37Ar / 40Ar)sam = 0.00036895 ±0.00002281
(39Ar / 40Ar)sam = 0.11761865 ±0.00014432

Corr 36/40 & 39/40 ratios =-0.446581
Corr 36/40 & 37/40 ratios =-0.010557
Corr 37/40 & 39/40 ratios = 0.012315

37Ca / 39K = 3.137 ± 0.194 E-3
Ca / K = 5.756 ± 0.356 E-3
F1 = -2.238 E-6

38Cl / 39K = 1.923 ± 0.087 E-3
Cl / K = 4.038 ± 0.182 E-4
F2 = 1.135 E-3

DP10-4x P54-019 sericite

Fractions:

No	Name	Temp	Cum 39K	Age	40Ar* / 39K
1	19-01 1.5W 20-M	1	0.00113	-89.619 ± 114.186 Ma	-7.652 ± 9.51
2	19-02 2.5W 20-M	2	0.00461	26.054 ± 26.708 Ma	2.297 ± 2.37
3	19-03 1.7W 20-M	3	0.01100	57.087 ± 12.734 Ma	5.076 ± 1.15
4	19-04 2.5W NB 2	4	0.01288	66.885 ± 44.913 Ma	5.964 ± 4.08
5	19-05 2.7W 21-	5	0.01562	26.379 ± 41.154 Ma	2.326 ± 3.66
6	19-06 3.0W 21-M	6	0.02119	57.171 ± 16.391 Ma	5.084 ± 1.48
7	19-07 3.5W 21-M	7	0.03732	59.653 ± 4.972 Ma	5.308 ± 0.45
8	19-08 3.5W NB 2	8	0.06654	62.955 ± 3.300 Ma	5.607 ± 0.30
9	19-09 3.5W 20kH	9	0.08185	64.216 ± 5.402 Ma	5.722 ± 0.49
10	19-10 4.5W 20kH	10	0.28365	70.143 ± 0.683 Ma	6.260 ± 0.06
11	19-11 4.5W 20kH	11	0.33496	68.272 ± 2.377 Ma	6.090 ± 0.22
12	19-12 4.5W 20kH	12	0.54296	70.562 ± 0.716 Ma	6.298 ± 0.07
13	19-13 4.5W 20kH	14	0.64407	72.416 ± 0.801 Ma	6.467 ± 0.07
14	19-14 4.9W 20kH	15	0.98801	72.655 ± 0.269 Ma	6.489 ± 0.02
15	19-15 5.5W 20kH	16	1.00000	75.412 ± 7.998 Ma	6.740 ± 0.73

No	Name	Cum 36S	40Ar / 36Ar	40ArAcc/g	37Ca / 39K
1	19-01 1.5W 20-M	0.16856	151.36 ± 91.83	6.6E-0013	98.398 ± 213.435 m
2	19-02 2.5W 20-M	0.25960	542.54 ± 467.57	3.6E-0013	68.653 ± 36.690 m
3	19-03 1.7W 20-M	0.24859	-7983.28 ± 50546.37	-4.3E-0014	-0.585 ± 26.116 m
4	19-04 2.5W NB 2	0.22927	-1337.39 ± 5033.20	-7.6E-0014	-138.365 ± 166.421 m
5	19-05 2.7W 21-	0.30171	543.58 ± 716.86	2.8E-0013	-11.182 ± 58.839 m
6	19-06 3.0W 21-M	0.34078	2331.75 ± 4672.47	1.5E-0013	8.970 ± 30.900 m
7	19-07 3.5W 21-M	0.41190	3681.61 ± 3562.90	2.8E-0013	22.815 ± 16.092 m
8	19-08 3.5W NB 2	0.52903	4228.79 ± 2990.48	4.6E-0013	2.411 ± 8.477 m
9	19-09 3.5W 20kH	0.54558	15181.38 ± 64747.59	6.5E-0014	17.320 ± 16.940 m
10	19-10 4.5W 20kH	0.65823	31827.05 ± 30686.10	4.4E-0013	2.842 ± 1.177 m
11	19-11 4.5W 20kH	0.73604	11588.47 ± 15613.06	3.0E-0013	0.438 ± 3.418 m
12	19-12 4.5W 20kH	0.98739	14950.61 ± 7426.90	9.8E-0013	1.309 ± 0.750 m
13	19-13 4.5W 20kH	0.92209	-27862.62 ± 27265.41	-2.6E-0013	-1.064 ± 1.814 m
14	19-14 4.9W 20kH	1.00433	76602.12 ± 65782.45	3.2E-0013	406.544 ± 417.738 µ
15	19-15 5.5W 20kH	1.00000	-52179.24 ± 999176.17	-1.7E-0014	-29.597 ± 11.571 m

No	38Cl / 39K	40Ar* Vol ccNTP/g	Atm Cont	F1	F2
1	-195.801 ± 62.582 m	-321.91 ±-399.73 E-15 (124.2%)	195.2288%	-0.000070	0.000447
2	28.241 ± 24.844 m	297.96 ± 307.57 E-15 (103.2%)	54.4662%	-0.000049	0.002010
3	9.858 ± 8.567 m	1.21 ± 0.27 E-12 (22.7%)	-3.7015%	0.000000	0.000267
4	8.163 ± 55.384 m	418.02 ± 285.36 E-15 (68.3%)	-22.0952%	0.000099	0.010572
5	7.396 ± 27.379 m	238.11 ± 374.15 E-15 (157.1%)	54.3615%	0.000008	0.000325
6	2.393 ± 11.469 m	1.05 ± 0.31 E-12 (29.1%)	12.6729%	-0.000006	0.000996
7	-0.398 ± 4.656 m	3.19 ± 0.27 E-12 (8.5%)	8.0264%	-0.000016	0.004034
8	1.676 ± 3.154 m	6.10 ± 0.33 E-12 (5.3%)	6.9878%	-0.000002	0.000471
9	5.501 ± 9.200 m	3.26 ± 0.28 E-12 (8.5%)	1.9465%	-0.000012	0.012421
10	1.960 ± 0.934 m	47.06 ± 0.50 E-12 (1.1%)	0.9285%	-0.000002	0.003982
11	2.413 ± 1.390 m	11.64 ± 0.42 E-12 (3.6%)	2.5499%	-0.000000	0.000226
12	2.138 ± 0.493 m	48.80 ± 0.55 E-12 (1.1%)	1.9765%	-0.000001	0.000849
13	0.399 ± 1.023 m	24.36 ± 0.28 E-12 (1.2%)	-1.0606%	0.000001	0.001293
14	1.727 ± 0.347 m	83.15 ± 0.51 E-12 (0.6%)	0.3858%	-0.000000	0.001334
15	-1.827 ± 6.531 m	3.01 ± 0.33 E-12 (10.8%)	-0.5663%	0.000021	0.060506

DP10-4x P54-019 Sericite

Integrated Results:

Age = 70.219 ± 0.467 MaWt. Mean Age = 72.020 ± 0.761 Ma (3.202)

40Ar* / 39K = 6.267 ± 0.039

Total 39K Vol = 3.7254E-0011 ccNTP/g

Total 40Ar* Vol = 2.335 ± 0.014 E-10

(40Ar / 36Ar)sam = 17917.46 ± 6019.23

Total Atm 40Ar Vol = 3.9151E-0012 ccNTP/g

(36Ar / 40Ar)sam = 0.00005581 ±0.00002630
(37Ar / 40Ar)sam = 0.00021262 ±0.00012524
(39Ar / 40Ar)sam = 0.15693288 ±0.00089391

Corr 36/40 & 39/40 ratios =-0.681797
Corr 36/40 & 37/40 ratios =-0.007924
Corr 37/40 & 39/40 ratios = 0.009239

37Ca / 39K = 1.355 ± 0.798 E-3
Ca / K = 2.486 ± 1.464 E-3
F1 = -9.664 E-7

38Cl / 39K = 1.692 ± 0.390 E-3
Cl / K = 3.554 ± 0.819 E-4
F2 = 1.062 E-3

DP10-8x P54-034 Sericite

Fractions:

No	Name			Temp	Cum 39K	Age				40Ar* / 39K		
1	34-01c	1.5W	12-	2	0.00305	19.856	±	8.052	Ma	1.748	±	0.71
2	34-02	1.6W	12-M	3	0.00463	37.470	±	15.388	Ma	3.314	±	1.38
3	34-03	1.6W	12-M	4	0.00613	56.148	±	18.201	Ma	4.992	±	1.64
4	34-04	1.6W	NB 1	5	0.06053	61.934	±	0.876	Ma	5.515	±	0.08
5	34-05	1.6W	12-M	6	0.07288	61.947	±	2.661	Ma	5.516	±	0.24
6	34-06	1.6W	12-M	7	0.09602	61.748	±	1.967	Ma	5.498	±	0.18
7	34-07	1.6W	12-M	8	0.12064	68.441	±	1.022	Ma	6.105	±	0.09
8	34-08	2.0W	13-M	9	0.13545	71.906	±	1.909	Ma	6.421	±	0.17
9	34-09	2.0W	13-M	10	0.18965	72.731	±	0.691	Ma	6.496	±	0.06
10	34-10	2.0W	13-M	11	0.25588	69.348	±	0.685	Ma	6.188	±	0.06
11	34-11	2.5W	13-M	12	0.28735	68.093	±	0.742	Ma	6.074	±	0.07
12	34-12	2.7W	13-M	13	0.32202	69.122	±	0.726	Ma	6.167	±	0.07
13	34-13	3.0W	15-M	15	0.37184	71.594	±	0.653	Ma	6.392	±	0.06
14	34-14	3.0W	15-M	16	0.40899	71.477	±	0.753	Ma	6.382	±	0.07
15	34-15	3.2W	17-M	18	0.44147	72.817	±	0.784	Ma	6.504	±	0.07
16	34-16	3.2W	17-M	19	0.53646	73.743	±	0.442	Ma	6.588	±	0.04
17	34-17	3.4W	17-	20	0.57597	71.581	±	0.499	Ma	6.391	±	0.05
18	34-18	3.5W	19-M	21	0.61692	71.633	±	0.551	Ma	6.396	±	0.05
19	34-19	4.0W	19-M	22	0.66846	71.939	±	0.454	Ma	6.424	±	0.04
20	34-20	3.5W	20kH	23	0.70770	73.042	±	0.605	Ma	6.524	±	0.06
21	34-21	4.0W	20kH	24	0.85713	73.703	±	0.291	Ma	6.584	±	0.03
22	34-22	4.5W	20kH	25	0.95918	74.267	±	0.287	Ma	6.636	±	0.03
23	34-23	4.5W	20kH	26	1.00000	74.365	±	0.690	Ma	6.645	±	0.06

No	Name			Cum 36S	40Ar / 36Ar			40ArAcc/g	37Ca / 39K			
1	34-01c	1.5W	12-	0.17899	324.19	±	12.82	8.9E-0012	25.144	±	14.496	m
2	34-02	1.6W	12-M	0.27073	350.79	±	27.22	4.5E-0012	36.021	±	26.525	m
3	34-03	1.6W	12-M	0.30074	535.78	±	143.22	1.5E-0012	77.492	±	25.922	m
4	34-04	1.6W	NB 1	0.40331	3116.07	±	378.93	5.1E-0012	31.776	±	1.191	m
5	34-05	1.6W	12-M	0.43495	2372.11	±	717.14	1.6E-0012	33.413	±	3.123	m
6	34-06	1.6W	12-M	0.50203	2124.36	±	420.27	3.3E-0012	40.273	±	2.246	m
7	34-07	1.6W	12-M	0.53979	4134.99	±	802.33	1.9E-0012	33.154	±	1.950	m
8	34-08	2.0W	13-M	0.54513	17474.45	±	27238.08	2.6E-0013	22.588	±	6.075	m
9	34-09	2.0W	13-M	0.58777	8257.58	±	2092.05	2.1E-0012	16.764	±	0.882	m
10	34-10	2.0W	13-M	0.68809	4235.02	±	534.42	5.0E-0012	16.537	±	0.890	m
11	34-11	2.5W	13-M	0.73911	3907.69	±	514.05	2.5E-0012	20.021	±	3.332	m
12	34-12	2.7W	13-M	0.79342	4092.57	±	545.72	2.7E-0012	17.361	±	1.813	m
13	34-13	3.0W	15-M	0.82242	10887.36	±	3524.16	1.4E-0012	16.714	±	0.843	m
14	34-14	3.0W	15-M	0.84978	8650.69	±	2579.17	1.4E-0012	19.666	±	1.270	m
15	34-15	3.2W	17-M	0.85051	280255.62	±	2737120.24	3.6E-0014	18.753	±	2.158	m
16	34-16	3.2W	17-M	0.86930	32416.37	±	15609.39	9.3E-0013	17.765	±	0.586	m
17	34-17	3.4W	17-	0.87982	23427.40	±	12163.79	5.2E-0013	9.293	±	0.747	m
18	34-18	3.5W	19-M	0.89434	17693.85	±	7793.89	7.2E-0013	19.369	±	0.894	m
19	34-19	4.0W	19-M	0.91414	16422.79	±	5279.33	9.8E-0013	27.289	±	1.207	m
20	34-20	3.5W	20kH	0.93885	10285.61	±	2807.15	1.2E-0012	39.809	±	1.511	m
21	34-21	4.0W	20kH	0.99223	18071.35	±	2717.95	2.6E-0012	63.966	±	0.745	m
22	34-22	4.5W	20kH	0.99601	172940.53	±	209494.91	1.9E-0013	23.135	±	1.537	m
23	34-23	4.5W	20kH	1.00000	65856.34	±	129242.02	2.0E-0013	9.667	±	1.230	m

DP10-8x P54-034 sericite

Fractions

No	38Cl / 39K	40Ar* Vol ccNTP/g	Atm Cont	F1	F2
1	6.373 ± 8.977 m	860.67 ± 350.90 E-15 (40.8%)	91.1499%	-0.000018	0.000097
2	-102.399 ± 30.803 m	849.99 ± 352.63 E-15 (41.5%)	84.2393%	-0.000026	0.000142
3	3.741 ± 10.985 m	1.21 ± 0.40 E-12 (32.9%)	55.1535%	-0.000055	0.000986
4	2.427 ± 0.703 m	48.48 ± 0.70 E-12 (1.4%)	9.4831%	-0.000023	0.004498
5	-1.134 ± 2.244 m	11.01 ± 0.48 E-12 (4.3%)	12.4572%	-0.000024	0.003479
6	2.994 ± 1.680 m	20.56 ± 0.67 E-12 (3.2%)	13.9101%	-0.000029	0.003700
7	3.813 ± 0.847 m	24.29 ± 0.38 E-12 (1.6%)	7.1463%	-0.000024	0.005768
8	0.999 ± 3.211 m	15.37 ± 0.42 E-12 (2.7%)	1.6910%	-0.000016	0.016590
9	1.429 ± 0.616 m	56.91 ± 0.61 E-12 (1.1%)	3.5785%	-0.000012	0.005697
10	2.042 ± 0.391 m	66.23 ± 0.72 E-12 (1.1%)	6.9775%	-0.000012	0.002921
11	506.600 ± 977.864 µ	30.89 ± 0.37 E-12 (1.2%)	7.5620%	-0.000014	0.003302
12	4.252 ± 0.548 m	34.56 ± 0.40 E-12 (1.2%)	7.2204%	-0.000012	0.002965
13	1.911 ± 0.519 m	51.47 ± 0.54 E-12 (1.0%)	2.7142%	-0.000012	0.007667
14	513.965 ± 744.729 µ	38.31 ± 0.45 E-12 (1.2%)	3.4159%	-0.000014	0.007129
15	2.892 ± 1.263 m	34.14 ± 0.40 E-12 (1.2%)	0.1054%	-0.000013	0.184031
16	1.600 ± 0.314 m	101.14 ± 0.74 E-12 (0.7%)	0.9116%	-0.000013	0.023616
17	1.681 ± 0.426 m	40.81 ± 0.34 E-12 (0.8%)	1.2613%	-0.000007	0.009304
18	1.475 ± 0.553 m	42.33 ± 0.38 E-12 (0.9%)	1.6701%	-0.000014	0.014494
19	2.810 ± 0.471 m	53.51 ± 0.42 E-12 (0.8%)	1.7993%	-0.000019	0.018764
20	2.629 ± 0.855 m	41.37 ± 0.40 E-12 (1.0%)	2.8729%	-0.000028	0.016719
21	1.606 ± 0.186 m	159.02 ± 0.95 E-12 (0.6%)	1.6352%	-0.000046	0.045986
22	1.912 ± 0.517 m	109.45 ± 0.63 E-12 (0.6%)	0.1709%	-0.000017	0.143950
23	3.131 ± 0.579 m	43.84 ± 0.45 E-12 (1.0%)	0.4487%	-0.000007	0.025951

Integrated Results:

Age = 71.153 ± 0.289 Ma

Wt. Mean Age = 72.350 ± 2.410 Ma

(18.978) 40Ar* / 39K = 6.352 ± 0.016

Total 39K Vol = 1.6162E-0010 ccNTP/g

Total 40Ar* Vol = 1.027 ± 0.003 E-9

(40Ar / 36Ar)sam = 6421.23 ± 262.86

Total Atm 40Ar Vol = 4.9524E-0011 ccNTP/g

(36Ar / 40Ar)sam = 0.00015573 ±0.00000881
(37Ar / 40Ar)sam = 0.00420700 ±0.00004938
(39Ar / 40Ar)sam = 0.15018409 ±0.00031393

Corr 36/40 & 39/40 ratios =-0.619312
Corr 36/40 & 37/40 ratios =-0.111816
Corr 37/40 & 39/40 ratios = 0.157381

37Ca / 39K = 2.801 ± 0.032 E-2
Ca / K = 5.140 ± 0.060 E-2
F1 = -1.998 E-5

38Cl / 39K = 1.833 ± 0.154 E-3
Cl / K = 3.848 ± 0.322 E-4
F2 = 7.472 E-3

DP11-123 P57-004 biotite

Fractions:

No		Name		Temp	Cum 39K	Age				40Ar* / 39K		
1	4-01	1.5W	10-Fe	1	0.02522	89.598	±	72.014	Ma	8.578	±	7.07
2	4-02	3.5W	10-Fe	2	0.06775	489.522	±	40.965	Ma	52.513	±	5.02
3	4-03	4.5W	20kHz	3	0.13075	783.669	±	20.383	Ma	91.645	±	2.94
4	4-04	4.5W	20kHz	4	0.17460	832.691	±	34.265	Ma	98.810	±	5.08
5	4-05	4.5W	20kHz	5	0.30045	811.713	±	12.900	Ma	95.720	±	1.89
6	4-06	4.5W	20kHz	6	0.81568	677.600	±	4.444	Ma	76.793	±	0.60
7	4-07	4.5W	20kHz	7	0.91112	874.699	±	19.096	Ma	105.106	±	2.90
8	4-08	4.5W	20kHz	8	1.00000	614.276	±	19.162	Ma	68.334	±	2.52

No		Name		Cum 36S	40Ar / 36Ar		40ArAcc/g	37Ca / 39K	
1	4-01	1.5W	10-Fe	0.02815	905.07 ±	1532.30	1.9E-0013	685.247 ±	331.951 m
2	4-02	3.5W	10-Fe	0.08649	3332.23 ±	1970.00	3.9E-0013	741.413 ±	388.617 m
3	4-03	4.5W	20kHz	0.18164	5108.33 ±	2237.08	6.4E-0013	-4.032 ±	121.607 m
4	4-04	4.5W	20kHz	0.30395	3105.79 ±	1182.58	8.2E-0013	397.973 ±	223.930 m
5	4-05	4.5W	20kHz	0.31703	73326.94 ±	290244.12	8.8E-0014	-55.104 ±	53.405 m
6	4-06	4.5W	20kHz	0.53271	14847.24 ±	4179.37	1.4E-0012	39.852 ±	19.153 m
7	4-07	4.5W	20kHz	0.78782	3414.31 ±	815.75	1.7E-0012	285.694 ±	99.555 m
8	4-08	4.5W	20kHz	1.00000	2566.18 ±	655.05	1.4E-0012	288.145 ±	106.615 m

No	38Cl / 39K			40Ar* Vol				ccNTP/g	Atm Cont	F1	F2
1	-86.411 ±	94.510	m	388.68	±	319.36	E-15	(82.2%)	32.6494%	-0.000489	0.012941
2	12.094 ±	112.445	m	4.01	±	0.24	E-12	(5.9%)	8.8679%	-0.000529	0.011315
3	-16.918 ±	22.539	m	10.37	±	0.29	E-12	(2.8%)	5.7847%	0.000003	0.000056
4	35.030 ±	39.787	m	7.79	±	0.32	E-12	(4.1%)	9.5145%	-0.000284	0.002870
5	17.198 ±	14.951	m	21.64	±	0.37	E-12	(1.7%)	0.4030%	0.000039	0.011847
6	-4.975 ±	4.243	m	71.08	±	0.54	E-12	(0.8%)	1.9903%	-0.000028	0.002077
7	-19.276 ±	22.988	m	18.02	±	0.42	E-12	(2.3%)	8.6548%	-0.000204	0.002160
8	-54.463 ±	23.847	m	10.91	±	0.37	E-12	(3.4%)	11.5152%	-0.000206	0.002463

Integrated Results:

Age = 703.018 ± 5.159 Ma

40Ar* / 39K = 80.273 ± 0.724

(40Ar / 36Ar)sam = 6662.86 ± 951.22

(36Ar / 40Ar)sam = 0.00015009 ±0.00002964
(37Ar / 40Ar)sam = 0.00157728 ±0.00033961
(39Ar / 40Ar)sam = 0.01190496 ±0.00009973

37Ca / 39K = 1.325 ± 0.285 E-1
Ca / K = 2.431 ± 0.523 E-1
F1 = -9.451 E-5

Wt. Mean Age = 693.42 ± 195.6 Ma(50.26)

Total 39K Vol = 1.7965E-0012 ccNTP/g

Total 40Ar* Vol = 1.442 ± 0.010 E-10

Total Atm 40Ar Vol = 6.6926E-0012 ccNTP/g

Corr 36/40 & 39/40 ratios =-0.521936
Corr 36/40 & 37/40 ratios =-0.023506
Corr 37/40 & 39/40 ratios =0.020006

38Cl / 39K = -8.274 ± 7.156 E-3
Cl / K = -1.738 ± 1.503 E-3
F2 = 2.834 E-3

DP11-123 P57-007 whole rock Fractions:

No	Name			Temp	Cum 39K	Age				40Ar* / 39K		
1	7-01	1.5W	2-Fe	1	0.00623	624.975	±	22.425	Ma	69.743	±	2.96
2	7-02	1.6W	2-Fe	2	0.01167	189.093	±	30.199	Ma	18.616	±	3.13
3	7-03	3.5W	2-Fe	3	0.03230	131.284	±	7.878	Ma	12.716	±	0.79
4	7-04	4.5W	20kHz	4	0.07920	171.517	±	3.601	Ma	16.802	±	0.37
5	7-05	4.5W	20kHz	5	0.12880	186.920	±	4.397	Ma	18.390	±	0.46
6	7-06	4.5W	20kHz	6	0.15463	208.452	±	7.557	Ma	20.634	±	0.79
7	7-07	4.5W	20kHz	7	0.25537	232.266	±	1.547	Ma	23.146	±	0.16
8	7-08	4.5W	20kHz	8	0.36282	238.109	±	1.558	Ma	23.768	±	0.17
9	7-09	4.5W	20khz	9	0.56241	267.536	±	0.768	Ma	26.929	±	0.08
10	7-10	4.5W	20kHz	10	0.66372	247.064	±	1.528	Ma	24.725	±	0.16
11	7-11	4.5W	20kHz	11	0.72500	255.306	±	3.074	Ma	25.609	±	0.33
12	7-12	4.5W	20kHz	12	0.77166	262.870	±	3.855	Ma	26.425	±	0.42
13	7-13	4.5W	20kHz	13	0.93642	319.435	±	1.276	Ma	32.632	±	0.14
14	7-14	4.5W	20kHz	14	0.97119	441.110	±	3.832	Ma	46.662	±	0.46
15	7-15	5.5W	20kHz	15	1.00000	624.027	±	4.875	Ma	69.618	±	0.64

No	Name	Cum 36S	40Ar / 36Ar		40ArAcc/g	37Ca / 39K	
1	7-01 1.5W 2-Fe	0.32498	910.34 ±	74.92	5.7E-0012	3.356 ±	0.123
2	7-02 1.6W 2-Fe	0.29937	-1524.48 ±	1564.66	-4.5E-0013	3.606 ±	0.154
3	7-03 3.5W 2-Fe	0.35060	2651.81 ±	1308.87	8.9E-0013	12.512 ±	0.081
4	7-04 4.5W 20kHz	0.55160	2099.37 ±	257.69	3.5E-0012	27.723 ±	0.211
5	7-05 4.5W 20kHz	0.63352	5419.02 ±	2077.35	1.4E-0012	27.576 ±	0.283
6	7-06 4.5W 20kHz	0.72773	2898.05 ±	861.38	1.6E-0012	26.849 ±	1.082
7	7-07 4.5W 20kHz	0.81601	12449.13 ±	2825.72	1.5E-0012	21.901 ±	0.108
8	7-08 4.5W 20kHz	0.80986	-190764.36 ±	758190.51	-1.1E-0013	11.283 ±	0.041
9	7-09 4.5W 20khz	0.84425	72200.73 ±	40221.25	6.0E-0013	2.057 ±	0.013
10	7-10 4.5W 20kHz	0.91327	16993.74 ±	3204.50	1.2E-0012	261.666 ±	15.420 m
11	7-11 4.5W 20kHz	0.90930	-181712.16 ±	1313326.24	-6.9E-0014	248.713 ±	20.197 m
12	7-12 4.5W 20kHz	0.89654	-44176.46 ±	97728.63	-2.2E-0013	224.811 ±	18.062 m
13	7-13 4.5W 20kHz	0.91020	181469.55 ±	377089.11	2.4E-0013	322.521 ±	6.929 m
14	7-14 4.5W 20kHz	0.96294	14450.06 ±	4871.26	9.2E-0013	549.983 ±	19.578 m
15	7-15 5.5W 20kHz	1.00000	25199.90 ±	16385.77	6.4E-0013	712.504 ±	21.923 m

No	38Cl / 39K				40Ar* Vol			ccNTP/g			Atm Cont	F1	F2
1	16.030	±	17.604	m	11.76	±	0.47	E-12	(	4.0%)	32.4605%	-0.002394	0.005825
2	-31.799	±	22.621	m	2.74	±	0.46	E-12	(	16.7%)	-19.3837%	-0.002572	0.112131
3	2.773	±	4.758	m	7.10	±	0.44	E-12	(	6.2%)	11.1433%	-0.008925	0.387719
4	4.346	±	3.444	m	21.34	±	0.46	E-12	(	2.2%)	14.0756%	-0.019775	0.443237
5	7.398	±	1.618	m	24.70	±	0.60	E-12	(	2.4%)	5.4530%	-0.019670	0.675939
6	-4.079	±	6.822	m	14.43	±	0.50	E-12	(	3.5%)	10.1965%	-0.019152	0.476337
7	4.260	±	1.353	m	63.15	±	0.47	E-12	(	0.8%)	2.3737%	-0.015623	0.758940
8	0.106	±	1.045	m	69.16	±	0.55	E-12	(	0.8%)	-0.1549%	-0.008048	1.041414
9	1.765	±	0.899	m	145.56	±	0.81	E-12	(	0.6%)	0.4093%	-0.001467	0.604913
10	0.439	±	2.110	m	67.83	±	0.42	E-12	(	0.6%)	1.7389%	-0.000187	0.046876
11	0.335	±	1.944	m	42.50	±	0.54	E-12	(	1.3%)	-0.1626%	-0.000177	0.976207
12	0.592	±	3.040	m	33.40	±	0.52	E-12	(	1.6%)	-0.6689%	-0.000160	0.118390
13	1.110	±	0.673	m	145.59	±	0.89	E-12	(	0.6%)	0.1628%	-0.000230	0.333324
14	5.474	±	3.788	m	43.94	±	0.38	E-12	(	0.9%)	2.0450%	-0.000392	0.044163
15	8.286	±	2.961	m	54.32	±	0.50	E-12	(	0.9%)	1.1726%	-0.000508	0.066008

DP11-123 **P57-007** whole rock

Integrated Results:

Age = 273.749 ± 0.858 Ma Wt. Mean Age = 267.08 ± 380.33 Ma (762.1)

40Ar* / 39K = 27.603 ± 0.087

Total 39K Vol = 2.7081E-0011 ccNTP/g

Total 40Ar* Vol = 7.475 ± 0.021 E-10

(40Ar / 36Ar)sam = 12996.30 ± 1251.91

Total Atm 40Ar Vol = 1.7392E-0011 ccNTP/g

(36Ar / 40Ar)sam = 0.00007694 ±0.00001036
(37Ar / 40Ar)sam = 0.27028550 ±0.00115578
(39Ar / 40Ar)sam = 0.03540384 ±0.00009141

Corr 36/40 & 39/40 ratios =-0.591502
Corr 36/40 & 37/40 ratios =-0.379918
Corr 37/40 & 39/40 ratios =0.445701

37Ca / 39K = 7.634 ± 0.030
Ca / K = 1.401 ± 0.005 E 1
F1 = -5.446 E-3

38Cl / 39K = 1.947 ± 0.529 E-3
Cl / K = 4.088 ± 1.111 E-4
F2 = 4.926 E-1

DP11-125b P57-002 green muscovite

Fractions:

No		Name		Temp	Cum 39K	Age				40Ar* / 39K		
1	2-01	1.4W	6-Fe	1	0.00261	145.231	±	43.114	Ma	14.122	±	4.36
2	2-02	1.6W	6-Fe	2	0.04030	135.443	±	2.474	Ma	13.134	±	0.25
3	2-03	1.7W	6-Fe	3	0.08121	134.139	±	2.562	Ma	13.003	±	0.26
4	2-04	2.0W	6-Fe	4	0.11257	138.740	±	2.198	Ma	13.466	±	0.22
5	2-05	2.5W	6-Fe	5	0.16165	157.311	±	1.439	Ma	15.349	±	0.15
6	2-06	2.7W	6-Fe	6	0.17846	179.510	±	5.823	Ma	17.625	±	0.60
7	2-07	2.8W	6-Fe	7	0.22205	183.193	±	2.036	Ma	18.005	±	0.21
8	2-08	2.9W	6-Fe	8	0.24341	199.804	±	5.027	Ma	19.730	±	0.52
9	2-09	3.1W	6-Fe	9	0.26435	199.327	±	3.572	Ma	19.680	±	0.37
10	2-10	3.5W	6-Fe	10	0.29105	242.281	±	3.361	Ma	24.213	±	0.36
11	2-11	4.5W	20kHz	11	0.35934	293.572	±	1.628	Ma	29.769	±	0.18
12	2-12	4.5W	20kHz	12	0.41115	308.359	±	2.104	Ma	31.401	±	0.23
13	2-13	4.5W	20kHz	13	0.49091	308.620	±	1.597	Ma	31.430	±	0.18
14	2-14	4.5W	20kHz	14	0.60764	324.349	±	1.352	Ma	33.180	±	0.15
15	2-15	4.5W	20kHz	15	0.64513	321.535	±	3.241	Ma	32.866	±	0.36
16	2-16	4.5W	20kHz	16	0.72794	324.584	±	1.737	Ma	33.206	±	0.19
17	2-17	4.5W	20kHz	17	0.78906	328.022	±	1.606	Ma	33.591	±	0.18
18	2-18	4.5W	20kHz	18	0.84020	332.626	±	2.060	Ma	34.107	±	0.23
19	2-19	4.5W	20kHz	19	0.90159	395.253	±	1.730	Ma	41.263	±	0.20
20	2-20	4.5W	20kHz	20	0.94468	401.463	±	2.308	Ma	41.986	±	0.27
21	2-21	4.5W	20kHz	21	0.98005	409.832	±	3.076	Ma	42.965	±	0.36
22	2-22	5.0W	20kHz	22	1.00000	420.995	±	4.773	Ma	44.277	±	0.56

No		Name		Cum 36S	40Ar / 36Ar			40ArAcc/g	37Ca / 39K			
1	2-01	1.4W	6-Fe	0.03068	1043.84	±	811.31	6.0E-0013	-39.041	±	213.748	m
2	2-02	1.6W	6-Fe	0.21602	1962.53	±	180.95	3.6E-0012	46.068	±	9.730	m
3	2-03	1.7W	6-Fe	0.37580	2372.95	±	310.40	3.1E-0012	5.686	±	10.019	m
4	2-04	2.0W	6-Fe	0.39211	16453.06	±	14179.91	3.2E-0013	2.734	±	17.699	m
5	2-05	2.5W	6-Fe	0.44775	8743.73	±	2098.60	1.1E-0012	2.445	±	12.872	m
6	2-06	2.7W	6-Fe	0.44011	-23908.86	±	65831.74	-1.5E-0013	10.363	±	19.771	m
7	2-07	2.8W	6-Fe	0.55758	4464.93	±	672.25	2.3E-0012	12.276	±	9.534	m
8	2-08	2.9W	6-Fe	0.56078	82505.61	±	598637.08	6.3E-0014	52.345	±	19.088	m
9	2-09	3.1W	6-Fe	0.59742	7313.92	±	2708.40	7.2E-0013	4.681	±	16.496	m
10	2-10	3.5W	6-Fe	0.61623	21753.16	±	19619.37	3.7E-0013	10.221	±	11.528	m
11	2-11	4.5W	20kHz	0.68292	19316.37	±	5908.32	1.3E-0012	-3.787	±	5.547	m
12	2-12	4.5W	20kHz	0.71066	36892.96	±	29648.18	5.4E-0013	4.571	±	6.661	m
13	2-13	4.5W	20kHz	0.75080	39274.42	±	23012.99	7.9E-0013	1.049	±	4.723	m
14	2-14	4.5W	20kHz	0.81655	37052.99	±	10880.58	1.3E-0012	3.592	±	5.696	m
15	2-15	4.5W	20kHz	0.80486	-65491.64	±	101647.47	-2.3E-0013	1.095	±	17.813	m
16	2-16	4.5W	20kHz	0.86938	26891.22	±	8084.41	1.3E-0012	11.665	±	7.999	m
17	2-17	4.5W	20kHz	0.86536	-318050.11	±	1471413.77	-7.9E-0014	-3.341	±	6.537	m
18	2-18	4.5W	20kHz	0.86371	-659566.67	±	7835302.43	-3.2E-0014	7.540	±	5.628	m
19	2-19	4.5W	20kHz	0.88810	65098.02	±	48546.37	4.8E-0013	-3.567	±	6.210	m
20	2-20	4.5W	20kHz	0.93200	26013.63	±	10750.69	8.6E-0013	8.055	±	7.073	m
21	2-21	4.5W	20kHz	0.98595	17873.79	±	5846.40	1.1E-0012	3.967	±	9.631	m
22	2-22	5.0W	20kHz	1.00000	39520.60	±	52368.95	2.8E-0013	28.526	±	17.472	m

DP11-125b P57-002 green muscovite

No	38Cl / 39K				40Ar* Vol ccNTP/g					Atm Cont	F1	F2
1	-17.943	±	29.164	m	1.52	±	0.47	E-12	(30.7%)	28.3090%	0.000028	0.000551
2	0.027	±	3.796	m	20.48	±	0.37	E-12	(1.8%)	15.0571%	-0.000033	0.001598
3	5.521	±	1.917	m	22.00	±	0.43	E-12	(1.9%)	12.4529%	-0.000004	0.000250
4	0.069	±	2.467	m	17.47	±	0.29	E-12	(1.7%)	1.7960%	-0.000002	0.000914
5	0.874	±	1.907	m	31.16	±	0.31	E-12	(1.0%)	3.3796%	-0.000002	0.000374
6	2.572	±	4.266	m	12.26	±	0.42	E-12	(3.4%)	-1.2359%	-0.000007	0.004000
7	3.826	±	2.464	m	32.47	±	0.38	E-12	(1.2%)	6.6182%	-0.000009	0.000785
8	9.813	±	2.914	m	17.43	±	0.46	E-12	(2.7%)	0.3582%	-0.000037	0.057407
9	8.720	±	3.746	m	17.05	±	0.28	E-12	(1.7%)	4.0402%	-0.000003	0.000463
10	-3.916	±	2.882	m	26.75	±	0.36	E-12	(1.4%)	1.3584%	-0.000007	0.002517
11	0.739	±	1.341	m	84.10	±	0.59	E-12	(0.7%)	1.5298%	0.000003	0.000674
12	1.632	±	1.518	m	67.31	±	0.56	E-12	(0.8%)	0.8010%	-0.000003	0.001483
13	1.340	±	1.047	m	103.70	±	0.70	E-12	(0.7%)	0.7524%	-0.000001	0.000363
14	915.785	±	875.824	µ	160.23	±	0.89	E-12	(0.6%)	0.7975%	-0.000003	0.001108
15	0.359	±	2.214	m	50.98	±	0.45	E-12	(0.9%)	-0.4512%	-0.000001	0.000613
16	0.560	±	1.379	m	113.76	±	0.69	E-12	(0.6%)	1.0989%	-0.000008	0.002595
17	2.729	±	2.049	m	84.94	±	0.57	E-12	(0.7%)	-0.0929%	0.000002	0.008772
18	3.045	±	1.502	m	72.16	±	0.53	E-12	(0.7%)	-0.0448%	-0.000005	0.042497
19	3.854	±	1.476	m	104.79	±	0.64	E-12	(0.6%)	0.4539%	0.000003	0.001565
20	4.353	±	1.944	m	74.84	±	0.52	E-12	(0.7%)	1.1359%	-0.000006	0.001371
21	4.084	±	2.696	m	62.87	±	0.48	E-12	(0.8%)	1.6533%	-0.000003	0.000450
22	7.857	±	4.784	m	36.55	±	0.41	E-12	(1.1%)	0.7477%	-0.000020	0.006991

Integrated Results:

Age = 289.886 ± 0.751 Ma   Wt. Mean Age = 274.63 ± 790.31 Ma   (1719)

40Ar* / 39K = 29.365 ± 0.066   Total 39K Vol = 4.1370E-0011 ccNTP/g

Total 40Ar* Vol = 1.215 ± 0.002 E-9

(40Ar / 36Ar)sam = 18620.43 ± 1668.70   Total Atm 40Ar Vol = 1.9590E-0011 ccNTP/g

(36Ar / 40Ar)sam = 0.00005370 ±0.00000675   Corr 36/40 & 39/40 ratios =-0.548679
(37Ar / 40Ar)sam = 0.00022717 ±0.00007056   Corr 36/40 & 37/40 ratios =-0.006129
(39Ar / 40Ar)sam = 0.03351381 ±0.00006089   Corr 37/40 & 39/40 ratios =0.002917

37Ca / 39K = 6.778 ± 2.105 E-3   38Cl / 39K = 2.179 ± 0.432 E-3
Ca / K = 1.244 ± 0.386 E-2   Cl / K = 4.577 ± 0.907 E-4
F1 = -4.835 E-6   F2 = 1.176 E-3

DP11-125b P57-009 amphibole

Fractions:

No	Name			Temp	Cum 39K	Age			40Ar* / 39K		
1	9-01	1.5W	14-Fe	19	0.03904	217.503	± 10.342	Ma	21.585	±	1.09
2	9-02	1.7W	14-Fe	20	0.04616	121.937	± 41.222	Ma	11.780	±	4.12
3	9-03	2.0W	14-F	21	0.17701	173.720	± 3.067	Ma	17.028	±	0.32
4	9-04	2.1W	14-Fe	22	0.28562	204.476	± 2.993	Ma	20.218	±	0.31
5	9-05	3.5W	15-Fe	23	0.47750	384.476	± 1.604	Ma	40.014	±	0.19
6	9-06	4.5W	20kHz	24	0.63000	383.772	± 2.614	Ma	39.932	±	0.30
7	9-07	4.5W	20kHz	25	0.74356	340.223	± 3.513	Ma	34.962	±	0.40
8	9-08	4.5W	20kHz	26	0.80708	360.927	± 5.191	Ma	37.310	±	0.59
9	9-09	4.5W	20kHz	27	0.93391	362.512	± 2.860	Ma	37.491	±	0.33
10	9-10	5.0W	20kHz	28	1.00000	451.910	± 5.054	Ma	47.954	±	0.61

No	Name			Cum 36S	40Ar / 36Ar		40ArAcc/g	37Ca / 39K		
1	9-01	1.5W	14-Fe	0.21470	1064.11 ±	138.36	3.0E-0012	1.190 ±	0.045	
2	9-02	1.7W	14-Fe	0.24331	869.87 ±	581.63	3.9E-0013	1.346 ±	0.206	
3	9-03	2.0W	14-F	0.29271	9128.80 ±	4940.22	6.8E-0013	575.829 ±	12.093	m
4	9-04	2.1W	14-Fe	0.35620	7068.74 ±	2427.08	8.8E-0013	568.253 ±	21.851	m
5	9-05	3.5W	15-Fe	0.51132	9988.03 ±	1026.84	2.1E-0012	263.321 ±	21.343	m
6	9-06	4.5W	20kHz	0.59090	15282.79 ±	5434.80	1.1E-0012	711.537 ±	15.825	m
7	9-07	4.5W	20kHz	0.67609	9422.04 ±	2662.38	1.2E-0012	1.483 ±	0.021	
8	9-08	4.5W	20kHz	0.70598	15822.26 ±	10168.45	4.1E-0013	1.507 ±	0.035	
9	9-09	4.5W	20kHz	0.86017	6334.61 ±	910.31	2.1E-0012	1.877 ±	0.033	
10	9-10	5.0W	20kHz	1.00000	4734.07 ±	756.86	1.9E-0012	2.954 ±	0.042	

No	38Cl / 39K				40Ar* Vol			ccNTP/g			Atm Cont	F1	F2
1	6.418	±	7.293	m	7.70	±	0.39	E-12	(	5.0%)	27.7696%	-0.000849	0.010860
2	-12.359	±	57.291	m	766.87	±	264.76	E-15	(	34.5%)	33.9707%	-0.000960	0.017070
3	-8.166	±	2.602	m	20.36	±	0.38	E-12	(	1.9%)	3.2370%	-0.000411	0.076653
4	14.690	±	7.197	m	20.07	±	0.32	E-12	(	1.6%)	4.1804%	-0.000405	0.050121
5	1.993	±	1.276	m	70.16	±	0.44	E-12	(	0.6%)	2.9585%	-0.000188	0.017325
6	5.411	±	2.064	m	55.65	±	0.48	E-12	(	0.9%)	1.9335%	-0.000508	0.068963
7	2.152	±	2.417	m	36.28	±	0.38	E-12	(	1.0%)	3.1363%	-0.001058	0.096656
8	-7.445	±	7.420	m	21.66	±	0.29	E-12	(	1.3%)	1.8676%	-0.001075	0.148189
9	4.211	±	2.001	m	43.46	±	0.38	E-12	(	0.9%)	4.6648%	-0.001339	0.076648
10	17.004	±	8.558	m	28.96	±	0.34	E-12	(	1.2%)	6.2420%	-0.002107	0.069022

Integrated Results:

Age = 326.158 ± 1.277 Ma   Wt. Mean Age = 332.04 ± 774.96 Ma (790.5)

40Ar* / 39K = 33.383 ± 0.139   Total 39K Vol = 9.1389E-0012 ccNTP/g

Total 40Ar* Vol = 3.051 ± 0.012 E-10

(40Ar / 36Ar)sam = 6832.87 ± 498.80   Total Atm 40Ar Vol = 1.3790E-0011 ccNTP/g

(36Ar / 40Ar)sam = 0.00014635 ±0.00001479   Corr 36/40 & 39/40 ratios =-0.607422
(37Ar / 40Ar)sam = 0.03008023 ±0.00025269   Corr 36/40 & 37/40 ratios =-0.263470
(39Ar / 40Ar)sam = 0.02866029 ±0.00010281   Corr 37/40 & 39/40 ratios =0.340369

37Ca / 39K = 1.050 ± 0.008   38Cl / 39K = 3.327 ± 1.347 E-3
Ca / K = 1.926 ± 0.015   Cl / K= 6.986 ± 2.830 E-4
F1 = -7.487 E-4   F2 = 5.360 E-2

DP11-133 P57-041 muscovite

Fractions:

No	Name	Temp		Cum 39K		Age				40Ar* / 39K		
1	41-01	1.6W	1-F	1	0.01678	87.850	±	5.012	Ma	8.406	±	0.49
2	41-02	3.5W	1-F	2	0.07223	93.634	±	1.748	Ma	8.974	±	0.17
3	41-03	4.5W	20kH	3	0.12895	96.321	±	1.567	Ma	9.239	±	0.15
4	41-04	4.5W	20kH	4	0.44228	112.146	±	0.432	Ma	10.804	±	0.04
5	41-05	4.5W	20kH	5	0.53344	118.435	±	1.384	Ma	11.430	±	0.14
6	41-06	4.5W	20kH	6	0.61154	123.812	±	0.912	Ma	11.967	±	0.09
7	41-07	4.5W	20kH	7	0.66569	125.479	±	1.387	Ma	12.134	±	0.14
8	41-08	4.5W	20kH	8	0.70421	124.651	±	1.994	Ma	12.051	±	0.20
9	41-09	4.5W	20kH	9	0.71861	130.957	±	5.667	Ma	12.683	±	0.57
10	41-10	5.0W	20kH	10	0.95403	131.274	±	0.445	Ma	12.715	±	0.04
11	41-11	5.0W	20kH	11	0.97905	153.533	±	5.076	Ma	14.964	±	0.52
12	41-12	6.0W	20kH	12	1.00000	160.529	±	5.694	Ma	15.677	±	0.58

No	Name	Cum 36S	40Ar / 36Ar		40ArAcc/g	37Ca / 39K	
1	41-01 1.6W 1-F	0.34236	389.98 ±	7.25	1.7E-0011	27.368 ±	16.853 m
2	41-02 3.5W 1-F	0.50256	1007.78 ±	45.99	7.8E-0012	46.366 ±	4.378 m
3	41-03 4.5W 20kH	0.61137	1399.79 ±	85.54	5.3E-0012	23.188 ±	10.752 m
4	41-04 4.5W 20kH	0.84057	3682.32 ±	143.32	1.1E-0011	26.543 ±	0.928 m
5	41-05 4.5W 20kH	0.86075	12139.68 ±	5371.46	9.8E-0013	21.008 ±	6.950 m
6	41-06 4.5W 20kH	0.88372	9623.21 ±	2300.72	1.1E-0012	23.709 ±	6.381 m
7	41-07 4.5W 20kH	0.87926	-33469.33 ±	42215.69	-2.2E-0013	23.324 ±	10.021 m
8	41-08 4.5W 20kH	0.88106	59501.96 ±	189881.81	8.7E-0014	-7.875 ±	6.856 m
9	41-09 4.5W 20kH	0.88037	-60848.66 ±	557260.19	-3.3E-0014	-28.394 ±	20.053 m
10	41-10 5.0W 20kH	0.93073	13926.08 ±	1929.09	2.4E-0012	52.280 ±	1.329 m
11	41-11 5.0W 20kH	0.94945	4882.44 ±	2552.13	9.1E-0013	118.808 ±	13.146 m
12	41-12 6.0W 20kH	1.00000	1785.30 ±	320.79	2.5E-0012	88.082 ±	16.476 m

No	38Cl / 39K				40Ar* Vol ccNTP/g					Atm Cont	F1	F2
1	-6.932	±	6.099	m	5.32	±	0.31	E-12 (	5.8%)	75.7725%	-0.000020	0.000066
2	0.418	±	1.645	m	18.78	±	0.37	E-12 (	2.0%)	29.3220%	-0.000033	0.000994
3	0.013	±	1.389	m	19.77	±	0.34	E-12 (	1.7%)	21.1103%	-0.000017	0.000757
4	1.663	±	0.362	m	127.73	±	0.78	E-12 (	0.6%)	8.0248%	-0.000019	0.002301
5	-0.345	±	1.095	m	39.31	±	0.49	E-12 (	1.3%)	2.4342%	-0.000015	0.006031
6	3.799	±	0.438	m	35.26	±	0.32	E-12 (	0.9%)	3.0707%	-0.000017	0.005120
7	0.547	±	4.314	m	24.79	±	0.30	E-12 (	1.2%)	-0.8829%	-0.000017	0.018486
8	-0.724	±	2.481	m	17.52	±	0.29	E-12 (	1.7%)	0.4966%	0.000006	0.010922
9	-3.198	±	7.892	m	6.89	±	0.31	E-12 (	4.5%)	-0.4856%	0.000020	0.036858
10	1.934	±	0.618	m	112.94	±	0.66	E-12 (	0.6%)	2.1219%	-0.000037	0.015381
11	-6.081	±	7.112	m	14.13	±	0.48	E-12 (	3.4%)	6.0523%	-0.000085	0.009989
12	-2.412	±	4.279	m	12.39	±	0.45	E-12 (	3.6%)	16.5519%	-0.000063	0.002271

Integrated Results:

Age = 119.382 ± 0.428 Ma   Wt. Mean Age = 120.33 ± 39.38 Ma (146.19)

40Ar* / 39K = 11.525 ± 0.043

Total 39K Vol = 3.7730E-0011 ccNTP/g

Total 40Ar* Vol = 4.348 ± 0.016 E-10

(40Ar / 36Ar)sam = 2938.17 ± 75.39

Total Atm 40Ar Vol = 4.8622E-0011 ccNTP/g

(36Ar / 40Ar)sam = 0.00034035 ±0.00001174
(37Ar / 40Ar)sam = 0.00266172 ±0.00011104
(39Ar / 40Ar)sam = 0.07804351 ±0.00021574

Corr 36/40 & 39/40 ratios =-0.622419
Corr 36/40 & 37/40 ratios =-0.043877
Corr 37/40 & 39/40 ratios =0.058779

37Ca / 39K = 3.411 ± 0.142 E-2
Ca / K = 6.258 ± 0.261 E-2
F1 = -2.433 E-5

38Cl / 39K = 9.022 ± 4.318 E-4
Cl / K = 1.895 ± 0.907 E-4
F2 = 2.156 E-3

DP11-133 P57-036 garnet

Fractions:

No		Name		Temp	Cum 39K	Age		40Ar* / 39K	
1	#34	TF 3.5W	19-J	0	0.29657	452.271 ± 186.303	Ma	47.997 ±	22.35
2		#36 TF 5.0W 10-Feb-1		1	1.00000	332.904 ± 100.350 Ma		34.139 ±	11.27

No		Name	Cum 36S		40Ar / 36Ar	40ArAcc/g	37Ca / 39K	
1	#34	b 3.5W 19-J	0.74422	-249.53 ±	187.74	-3.5E-0013	640.208 ± 144.395	
2	#36	TF 10-Feb-1	1.00000	-2379.94 ±	7022.32	-1.2E-0013	186.075 ±	9.516

No	38Cl / 39K	40Ar* Vol ccNTP/g					Atm Cont	F1	F2
1	15.225 ± 299.410 m	647.73	±	284.53	E-15	(43.9%)	-118.4206%	-0.456672	2.412509
2	82.614 ± 74.615 m	1.09	±	0.36	E-12	(32.7%)	-12.4163%	-0.132730	1.368428

Integrated Results:

Age = 369.135 ± 88.754 Ma Wt. Mean Age = 357.71 88.34 Ma (0.306)

40Ar* / 39K = 38.249 ± 10.450

Total 39K Vol = 4.5505E-0014 ccNTP/g

Total 40Ar* Vol = 1.741 ± 0.457 E-12

(40Ar / 36Ar)sam = -794.45 ± 746.04

Total Atm 40Ar Vol = -4.718E-0013 ccNTP/g

(36Ar / 40Ar)sam =-0.00125874 ±0.00200651
(37Ar / 40Ar)sam =11.50531138 ±4.02226722
(39Ar / 40Ar)sam = 0.03586949 ±0.01283100

Corr 36/40 & 39/40 ratios =-0.789321
Corr 36/40 & 37/40 ratios =-0.807695
Corr 37/40 & 39/40 ratios =0.977221

37Ca / 39K = 3.208 ± 0.244 E 2
Ca / K = 5.886 ± 0.447 E 2
F1 = -2.288 E-1

38Cl / 39K = 0.626 ± 1.032 E-1
Cl / K = 1.315 ± 2.167 E-2
F2 = 1.791

DP11-136 P57-030 muscovite

Fractions:

No		Name	Temp	Cum 39K			Age		40Ar*	/ 39K
1	30-01	3.5W 16-J	1	0.01492	67.655	±	1.526	Ma	6.437 ±	0.15
2	30-02	4.5W 20kH	2	0.01896	68.397	±	3.347	Ma	6.509 ±	0.32
3	30-03	4.5W 20kH	3	0.03986	75.388	±	0.831	Ma	7.189 ±	0.08
4	30-04	4.5W 20kH	4	0.22526	96.679	±	0.445	Ma	9.274 ±	0.04
5	30-05	4.5W 20kH	5	0.28330	95.733	±	0.425	Ma	9.181 ±	0.04
6	30-06	4.5W 20kH	6	0.35618	101.132	±	0.422	Ma	9.713 ±	0.04
7	30-07	4.5W 20kH	7	0.43072	103.239	±	0.430	Ma	9.921 ±	0.04
8	30-08	4.5W 20kH	8	0.49371	100.343	±	0.501	Ma	9.635 ±	0.05
9	30-09	4.5W 20kH	9	0.67915	105.565	±	0.377	Ma	10.151 ±	0.04
10	30-10	4.5W 20kH	10	0.70454	108.067	±	0.715	Ma	10.399 ±	0.07
11	30-11	4.5W 20kH	11	0.74045	109.814	±	0.468	Ma	10.573 ±	0.05
12	30-12	4.5W 20kH	12	0.77026	112.869	±	0.445	Ma	10.876 ±	0.04
13	30-13	4.5W 20kH	13	0.80627	112.811	±	0.458	Ma	10.870 ±	0.05
14	30-14	5.0W 20kH	14	0.89685	121.025	±	0.299	Ma	11.689 ±	0.03
15	30-15	5.5W 20kH	15	0.99288	129.709	±	0.359	Ma	12.558 ±	0.04
16	30-16	5.5W 20kH	16	1.00000	168.251	±	2.274	Ma	16.467 ±	0.23

No		Name		Cum 36S	40Ar / 36Ar		40ArAcc/g		37Ca / 39K	
1	30-01	3.5W	16-J	0.09469	1854.24±	220.05	5.0E-0012	6.759 ±	3.789	m
2	30-02	4.5W	20kH	0.12721	1537.66±	320.14	1.7E-0012	17.228 ±	9.301	m
3	30-03	4.5W	20kH	0.16659	6160.29±	1297.76	2.1E-0012	2.272 ±	2.740	m
4	30-04	4.5W	20kH	0.37279	13110.67±	2052.59	1.1E-0011	2.438 ±	0.535	m
5	30-05	4.5W	20kH	0.43725	13001.27±	709.50	3.4E-0012	1.992 ±	1.996	m
6	30-06	4.5W	20kH	0.57138	8406.55±	457.05	7.0E-0012	3.810 ±	1.612	m
7	30-07	4.5W	20kH	0.66981	11842.03±	1178.08	5.2E-0012	1.635 ±	0.744	m
8	30-08	4.5W	20kH	0.76699	9894.09±	1424.39	5.1E-0012	5.652 ±	0.926	m
9	30-09	4.5W	20kH	0.91128	20346.51±	2883.69	7.6E-0012	1.715 ±	0.515	m
10	30-10	4.5W	20kH	0.92328	34119.28±	24765.65	6.3E-0013	1.047 ±	1.991	m
11	30-11	4.5W	20kH	0.94343	29249.33±	10977.11	1.1E-0012	3.359 ±	1.240	m
12	30-12	4.5W	20kH	0.94886	92047.10±	108277.04	2.8E-0013	0.397 ±	1.537	m
13	30-13	4.5W	20kH	0.95749	69976.41±	59669.53	4.5E-0013	-0.954 ±	1.306	m
14	30-14	5.0W	20kH	0.97771	80764.14±	29452.98	1.1E-0012	864.366 ±	579.138	µ
15	30-15	5.5W	20kH	0.99485	108441.60±	34722.53	9.0E-0013	2.689 ±	0.479	m
16	30-16	5.5W	20kH	1.00000	35318.79±	34776.63	2.7E-0013	12.925 ±	6.388	m

No	38Cl	/ 39K		40Ar*		Vol	ccNTP/g			Atm Cont	F1	F2
1	1.898 ±	1.586	m	26.14	±	0.60	E-12	(	2.3%)	15.9365%	-0.000005	0.000452
2	14.636 ±	3.291	m	7.15	±	0.36	E-12	(	5.0%)	19.2175%	-0.000012	0.000905
3	2.458 ±	1.176	m	40.90	±	0.48	E-12	(	1.2%)	4.7968%	-0.000002	0.000516
4	1.675 ±	0.215	m	467.91	±	3.02	E-12	(	0.6%)	2.2539%	-0.000002	0.000939
5	1.848 ±	0.474	m	145.03	±	0.80	E-12	(	0.6%)	2.2729%	-0.000001	0.000768
6	2.143 ±	0.416	m	192.65	±	1.17	E-12	(	0.6%)	3.5151%	-0.000003	0.000885
7	1.234 ±	0.651	m	201.25	±	1.18	E-12	(	0.6%)	2.4953%	-0.000001	0.000530
8	1.021 ±	0.759	m	165.17	±	1.13	E-12	(	0.7%)	2.9866%	-0.000004	0.001567
9	1.609 ±	0.230	m	512.31	±	2.94	E-12	(	0.6%)	1.4523%	-0.000001	0.000945
10	1.939 ±	1.215	m	71.86	±	0.59	E-12	(	0.8%)	0.8661%	-0.000001	0.000950
11	2.050 ±	0.669	m	103.32	±	0.66	E-12	(	0.6%)	1.0103%	-0.000002	0.002562
12	1.698 ±	0.536	m	88.24	±	0.56	E-12	(	0.6%)	0.3210%	-0.000000	0.000935
13	2.246 ±	0.503	m	106.50	±	0.66	E-12	(	0.6%)	0.4223%	0.000001	0.001711
14	1.899 ±	0.487	m	288.15	±	1.55	E-12	(	0.5%)	0.3659%	-0.000001	0.001659
15	1.987 ±	0.216	m	328.18	±	1.74	E-12	(	0.5%)	0.2725%	-0.000002	0.006427
16	2.817 ±	3.277	m	31.93	±	0.31	E-12	(	1.0%)	0.8367%	-0.000009	0.007613

DP11-136 P57-030 muscovite

Integrated Results:

Age = 106.085 ± 0.260 Ma   Wt. Mean Age = 108.95 ± 87.04 Ma (728.6)

40Ar* / 39K = 10.203 ± 0.022   Total 39K Vol = 2.7215E-0010 ccNTP/g

Total 40Ar* Vol = 2.777 ± 0.006 E-9

(40Ar / 36Ar)sam = 15976.35 ± 782.11   Total Atm 40Ar Vol = 5.2326E-0011 ccNTP/g

(36Ar / 40Ar)sam = 0.00006259 ±0.00000429   Corr 36/40 & 39/40 ratios =-0.468676
(37Ar / 40Ar)sam = 0.00023208 ±0.00002658   Corr 36/40 & 37/40 ratios =-0.007223
(39Ar / 40Ar)sam = 0.09619767 ±0.00012912   Corr 37/40 & 39/40 ratios =0.007456

37Ca / 39K = 2.413 ± 0.276 E-3   38Cl / 39K = 1.805 ± 0.127 E-3
Ca / K = 4.427 ± 0.507 E-3   Cl / K = 3.790 ± 0.266 E-4
F1 = -1.721 E-6   F2 = 1.033 E-3

DP11-137 P57-029 muscovite

Fractions:

No	Name	Temp	Cum 39K	Age			40Ar* / 39K	
1	29-01 3.5W 29-J	1	0.00277	69.400 ±	81.243	Ma	6.607 ±	7.88
2	29-02 4.5W 20kH	2	0.00971	18.838 ±	47.228	Ma	1.768 ±	4.46
3	29-03 4.5W 20kH	3	0.33551	107.083 ±	0.811	Ma	10.302 ±	0.08
4	29-04 4.5W 20kH	4	0.42669	121.086 ±	2.371	Ma	11.695 ±	0.24
5	29-05 4.5W 20kH	5	0.57260	123.224 ±	1.284	Ma	11.908 ±	0.13
6	29-06 4.5W 20kH	6	0.63974	125.489 ±	2.492	Ma	12.135 ±	0.25
7	29-07 4.5W 20kH	7	0.69764	126.653 ±	3.929	Ma	12.252 ±	0.39
8	29-08 4.5W 20kH	8	0.74202	127.195 ±	4.713	Ma	12.306 ±	0.47
9	29-09 4.5W 20kH	9	0.95247	135.892 ±	0.951	Ma	13.179 ±	0.10
10	29-10 4.5W 20kH	10	0.97211	126.565 ±	8.659	Ma	12.243 ±	0.87
11	29-11 5.0W 20kH	11	1.00000	143.733 ±	7.242	Ma	13.971 ±	0.73

No	Name	Cum 36S	40Ar / 36Ar		40ArAcc/g	37Ca / 39K		
1	29-01 3.5W 29-J	0.06807	1512.75 ±	7420.97	5.9E-0014	-0.771 ±	596.856	m
2	29-02 4.5W 20kH	0.46359	435.99 ±	522.35	3.5E-0013	-8.628 ±	183.019	m
3	29-03 4.5W 20kH	0.62595	93857.62 ±	227538.38	1.4E-0013	5.148 ±	2.335	m
4	29-04 4.5W 20kH	0.74163	42017.43 ±	117950.63	1.0E-0013	6.251 ±	5.884	m
5	29-05 4.5W 20kH	0.63480	-73310.43 ±	171790.39	-9.3E-0014	4.924 ±	5.753	m
6	29-06 4.5W 20kH	0.71009	49276.37 ±	164579.70	6.6E-0014	11.935 ±	6.770	m
7	29-07 4.5W 20kH	0.68831	-147155.96 ±	2334275.52	-1.9E-0014	-14.975 ±	11.945	m
8	29-08 4.5W 20kH	0.86432	14339.98 ±	25828.20	1.5E-0013	-2.658 ±	25.232	m
9	29-09 4.5W 20kH	0.75757	-117290.00 ±	326762.46	-9.3E-0014	20.804 ±	3.221	m
10	29-10 4.5W 20kH	1.0034	4721.61 ±	4975.88	2.1E-0013	11.090 ±	29.328	m
11	29-11 5.0W 20kH	1.00000	-508571.55 ±	45549478.61	-3.0E-0015	-24.548 ±	25.410	m

No	38Cl / 39K				40Ar* Vol ccNTP/g					Atm Cont	F1	F2
1	111.554	±	111.795	m	244.66 ±	291.52	E-15	(119.2%)		19.5339%	0.000001	0.000039
2	9.635	±	32.463	m	164.07 ±	413.49	E-15	(252.0%)		67.7765%	0.000006	0.000185
3	2.012	±	0.630	m	44.85 ±	0.41	E-12	(0.9%)		0.3148%	-0.000004	0.012892
4	2.508	±	1.429	m	14.25 ±	0.29	E-12	(2.1%)		0.7033%	-0.000004	0.006188
5	-0.768	±	1.361	m	23.22 ±	0.25	E-12	(1.1%)		-0.4031%	-0.000004	0.008580
6	2.272	±	1.764	m	10.89 ±	0.23	E-12	(2.1%)		0.5997%	-0.000009	0.013273
7	0.338	±	2.940	m	9.48 ±	0.31	E-12	(3.2%)		-0.2008%	0.000011	0.047954
8	-6.131	±	4.557	m	7.30 ±	0.28	E-12	(3.8%)		2.0607%	0.000002	0.000846
9	1.187	±	0.891	m	37.06 ±	0.32	E-12	(0.9%)		-0.2519%	-0.000015	0.054715
10	-2.858	±	7.372	m	3.21 ±	0.23	E-12	(7.1%)		6.2585%	-0.000008	0.001111
11	1.632	±	4.080	m	5.21 ±	0.27	E-12	(5.2%)		-0.0581%	0.000018	0.199908

Integrated Results:

Age = 120.785 ± 0.769 Ma   Wt. Mean Age = 120.47 ± 29.28 Ma (56.41)

40Ar* / 39K = 11.665 ± 0.077   Total 39K Vol = 1.3364E-0011 ccNTP/g

Total 40Ar* Vol = 1.559 ± 0.010 E-10

(40Ar / 36Ar)sam = 53089.49 ±58012.56   Total Atm 40Ar Vol = 8.7252E-0013 ccNTP/g

(36Ar / 40Ar)sam = 0.00001884 ±0.00002903   Corr 36/40 & 39/40 ratios =-0.691528
(37Ar / 40Ar)sam = 0.00056532 ±0.00025796   Corr 36/40 & 37/40 ratios =-0.011881
(39Ar / 40Ar)sam = 0.08525180 ±0.00052870   Corr 37/40 & 39/40 ratios =0.012802

37Ca / 39K = 6.631 ± 3.026 E-3   38Cl / 39K = 1.287 ± 0.631 E-3
Ca / K = 1.217 ± 0.555 E-2   Cl / K = 2.704 ± 1.325 E-4
F1 = -4.730 E-6   F2 = 8.311 E-3

DP11-146 P57-015 biotite

Fractions:

No		Name	Temp	Cum 39K			Age		40Ar*	/ 39K
1	15-01	1.7W 13-J	1	0.00127	682.836	±	42.975	Ma	77.506 ±	5.86
2	15-02	1.7W 13-J	2	0.00250	308.314	±	25.280	Ma	31.396 ±	2.80
3	15-03	1.8W 13-J	3	0.00759	248.456	±	9.996	Ma	24.874 ±	1.07
4	15-04	2.0W 13-J	4	0.01479	170.349	±	3.150	Ma	16.682 ±	0.32
5	15-05	2.6W 13-J	5	0.02289	167.410	±	2.981	Ma	16.381 ±	0.31
6	15-06	3.5W 13-J	6	0.11327	109.479	±	1.013	Ma	10.539 ±	0.10
7	15-07	3.7W 14-J	7	0.16194	99.567	±	0.655	Ma	9.559 ±	0.06
8	15-08	4.0W 14-J	8	0.25074	85.182	±	0.566	Ma	8.145 ±	0.06
9	15-09	4.5W 20kH	9	0.36458	101.283	±	0.168	Ma	9.728 ±	0.02
10	15-10	4.5W 20kH	10	0.80081	99.478	±	0.271	Ma	9.550 ±	0.03
11	15-11	4.5W 20kH	11	0.82670	98.679	±	1.358	Ma	9.471 ±	0.13
12	15-12	4.5W 20kH	12	1.00000	96.379	±	0.479	Ma	9.244 ±	0.05

No		Name	Cum 36S	40Ar / 36Ar		40ArAcc/g	37Ca / 39K		
1	15-01	1.7W 13-J	0.01898	7068.56 ±	12146.10	1.0E-0012	-54.464 ±	49.567	m
2	15-02	1.7W 13-J	0.04553	2184.77 ±	1220.90	1.4E-0012	-121.343 ±	48.309	m
3	15-03	1.8W 13-J	0.09604	3567.55 ±	1683.27	2.7E-0012	-3.975 ±	20.677	m
4	15-04	2.0W 13-J	0.11694	7803.00 ±	1928.65	1.1E-0012	9.222 ±	7.856	m
5	15-05	2.6W 13-J	0.13063	12934.70 ±	8914.41	7.4E-0013	9.731 ±	13.414	m
6	15-06	3.5W 13-J	0.20250	17591.79 ±	5372.99	3.9E-0012	2.164 ±	0.352	m
7	15-07	3.7W 14-J	0.22928	22959.02 ±	7323.22	1.4E-0012	4.533 ±	0.564	m
8	15-08	4.0W 14-J	0.38684	6285.87 ±	423.59	8.5E-0012	5.452 ±	0.374	m
9	15-09	4.5W 20kH	0.39336	221750.89 ±	227958.52	3.5E-0013	58.875 ±	0.522	m
10	15-10	4.5W 20kH	0.86358	11856.91 ±	960.03	2.5E-0011	7.618 ±	0.438	m
11	15-11	4.5W 20kH	0.86247	-287470.00±	3582083.22	-6.0E-0014	16.307 ±	8.001	m
12	15-12	4.5W 20kH	1.00000	15495.76±	2137.81	7.4E-0012	7.337 ±	0.922	m

No	38Cl		/ 39K		40Ar*		Vol	ccNTP/g			Atm Cont	F1	F2
1	19.434	±	9.921	m	23.52	±	1.77	E-12	(	7.5%)	4.1805%	0.000039	0.001293
2	17.266	±	7.812	m	9.18	±	0.81	E-12	(	8.8%)	13.5254%	0.000087	0.001958
3	10.941	±	2.467	m	30.25	±	1.30	E-12	(	4.3%)	8.2830%	0.000003	0.000143
4	4.685	±	5.398	m	28.71	±	0.37	E-12	(	1.3%)	3.7870%	-0.000007	0.001152
5	4.785	±	2.399	m	31.67	±	0.57	E-12	(	1.8%)	2.2846%	-0.000007	0.002087
6	3.580	±	0.600	m	227.49	±	2.04	E-12	(	0.9%)	1.6798%	-0.000002	0.000990
7	2.216	±	0.393	m	111.09	±	0.84	E-12	(	0.8%)	1.2871%	-0.000003	0.002991
8	2.524	±	0.331	m	172.72	±	1.25	E-12	(	0.7%)	4.7010%	-0.000004	0.001115
9	1.933	±	0.348	m	264.46	±	1.37	E-12	(	0.5%)	0.1333%	-0.000042	0.272421
10	2.262	±	0.205	m	994.89	±	5.53	E-12	(	0.6%)	2.4922%	-0.000005	0.002565
11	1.183	±	0.921	m	58.56	±	0.85	E-12	(	1.4%)	-0.1028%	-0.000012	0.160695
12	2.257	±	0.344	m	382.58	±	2.37	E-12	(	0.6%)	1.9070%	-0.000005	0.003354

Integrated Results:

Age = 101.790 ± 0.300 Ma   Wt. Mean Age = 99.98 ± 26.52 Ma (206.2)

40Ar* / 39K = 9.778 ± 0.032   Total 39K Vol = 2.3881E-0010 ccNTP/g

Total 40Ar* Vol = 2.335 ± 0.007 E-9

(40Ar / 36Ar)sam = 13055.27 ± 893.21   Total Atm 40Ar Vol = 5.4079E-0011 ccNTP/g

(36Ar / 40Ar)sam = 0.00007660 ±0.00000733   Corr 36/40 & 39/40 ratios =-0.505536

(37Ar / 40Ar)sam = 0.00125209 ±0.00003809   Corr 36/40 & 37/40 ratios =-0.036727

(39Ar / 40Ar)sam = 0.09995443 ±0.00021223   Corr 37/40 & 39/40 ratios =0.050160

37Ca / 39K = 1.253 ± 0.038 E-2   38Cl / 39K = 2.458 ± 0.142 E-3

Ca / K = 2.299 ± 0.070 E-2   Cl / K = 5.162 ± 0.298 E-4

F1 = -8.935 E-6   F2 = 4.538 E-3

DP11-146 P57-010 muscovite

Fractions:

No	Name	Temp	Cum 39K	Age				40Ar* / 39K		
1	10-01 1.6W 8-F	1	0.00248	50.612	±	61.833	Ma	4.793	±	5.94
2	10-02 2.5W 8-F	2	0.01066	73.201	±	18.001	Ma	6.976	±	1.75
3	10-03 3.5W 8-F	3	0.09824	88.951	±	1.648	Ma	8.514	±	0.16
4	10-04 4.5W 20kH	4	0.18228	91.540	±	2.093	Ma	8.768	±	0.21
5	10-05 4.5W 20kH	5	0.20817	89.618	±	6.363	Ma	8.580	±	0.62
6	10-06 4.5W 20kH	6	0.27471	96.517	±	2.214	Ma	9.258	±	0.22
7	10-07 4.5W 20kh	7	0.48658	101.499	±	0.734	Ma	9.749	±	0.07
8	10-08 5.0W 20kH	8	0.99013	114.996	±	0.446	Ma	11.088	±	0.04
9	10-09 5.5W 20kH	9	1.00000	155.251	±	23.227	Ma	15.139	±	2.36

No	Name	Cum 36S	40Ar / 36Ar		40ArAcc/g	37Ca / 39K		
1	10-01 1.6W 8-F	0.52965	331.82 ±	50.48	1.7E-0012	204.690 ± 199.063		m
2	10-02 2.5W 8-F	0.65533	1030.36 ±	640.52	4.1E-0013	263.655 ±	76.753	m
3	10-03 3.5W 8-F	0.75619	12267.43 ±	9267.22	3.3E-0013	3.759 ±	5.851	m
4	10-04 4.5W 20kH	0.91994	7581.46 ±	4321.57	5.3E-0013	24.730 ±	7.283	m
5	10-05 4.5W 20kH	0.91782	-169899.81 ±7069808.93		-6.9E-0015	17.191 ±	21.002	m
6	10-06 4.5W 20kH	0.84808	-14005.83 ±	15726.28	-2.3E-0013	21.484 ±	8.162	m
7	10-07 4.5W 20kh	0.90021	64450.38 ±	95731.53	1.7E-0013	3.068 ±	2.499	m
8	10-08 5.0W 20kH	0.85365	-193877.61 ± 442563.71		-1.5E-0013	26.120 ±	1.456	m
9	10-09 5.5W 20kH	1.00000	1949.05 ±	1690.37	4.8E-0013	141.118 ±	60.076	m

No	38Cl / 39K			40Ar* Vol ccNTP/g					Atm Cont	F1	F2
1	30.409 ±	51.777	m	212.05	±	262.65	E-15	(123.9%)	89.0552%	-0.000146	0.000287
2	30.742 ±	14.529	m	1.02	±	0.25	E-12	(25.0%)	28.6792%	-0.000188	0.007514
3	3.927 ±	1.206	m	13.31	±	0.26	E-12	(1.9%)	2.4088%	-0.000003	0.001472
4	3.513 ±	1.353	m	13.15	±	0.31	E-12	(2.4%)	3.8977%	-0.000018	0.005691
5	0.083 ±	3.513	m	3.97	±	0.29	E-12	(7.3%)	-0.1739%	-0.000012	0.105332
6	3.631 ±	2.213	m	11.00	±	0.26	E-12	(2.4%)	-2.1098%	-0.000015	0.009375
7	2.850 ±	0.820	m	36.87	±	0.32	E-12	(0.9%)	0.4585%	-0.000002	0.005607
8	2.305 ±	0.578	m	99.66	±	0.61	E-12	(0.6%)	-0.1524%	-0.000019	0.146556
9	9.134 ±	13.887	m	2.67	±	0.41	E-12	(15.5%)	15.1612%	-0.000101	0.004188

Integrated Results:

Age = 105.933 ± 0.565 Ma

Wt. Mean Age = 109.18 ± 24.98 Ma(69.42)

40Ar* / 39K = 10.188 ± 0.060

Total 39K Vol = 1.7850E-0011 ccNTP/g

Total 40Ar* Vol = 1.818 ± 0.010 E-10

(40Ar / 36Ar)sam = 16791.12 ± 4578.44

Total Atm 40Ar Vol = 3.2576E-0012 ccNTP/g

(36Ar / 40Ar)sam = 0.00005956 ±0.00002276

(37Ar / 40Ar)sam = 0.00213501 ±0.00016823

(39Ar / 40Ar)sam = 0.09642834 ±0.00048022

Corr 36/40 & 39/40 ratios =-0.675109

Corr 36/40 & 37/40 ratios =-0.044726

Corr 37/40 & 39/40 ratios =0.059183

37Ca / 39K = 2.214 ± 0.174 E-2

Ca / K = 4.063 ± 0.320 E-2

F1 = -1.579 E-5

38Cl / 39K = 3.064 ± 0.467 E-3

Cl / K = 6.435 ± 0.981 E-4

F2 = 9.902 E-3

DP11-161 P57-028 K-feldspar

Fractions:

No	Name	Temp	Cum 39K	Age			40Ar*	/	39K
1	28-01 1.5W 22-J	1	0.08805	490.503 ±	117.641	Ma	52.633	±	14.42
2	28-02 3.5W 22-J	2	0.53753	228.756 ±	10.787	Ma	22.774	±	1.14
3	28-03 4.5W 20kH	3	0.70381	285.289 ±	27.435	Ma	28.861	±	3.00
4	28-04 4.5W 20kH	4	0.89495	262.119 ±	28.972	Ma	26.343	±	3.13
5	28-05 4.5W 20kH	5	0.92953	218.426 ±	159.427	Ma	21.682	±	16.80
6	28-06 5.0W 20kH	6	1.00000	274.267 ±	77.063	Ma	27.660	±	8.38

No	Name	Cum 36S	40Ar / 36Ar		40ArAcc/g	37Ca / 39K		
1	28-01 1.5W 22-J	0.65189	719.98 ±	280.41	2.3E-0012	241.408 ±	464.127	m
2	28-02 3.5W 22-J	0.85071	3369.85 ±	1718.28	6.9E-0013	-13.926 ±	33.867	m
3	28-03 4.5W 20kH	0.81898	-8737.12 ±	27207.50	-1.1E-0013	32.488 ±	94.883	m
4	28-04 4.5W 20kH	0.85586	8448.52 ±	27060.68	1.3E-0013	80.325 ±	83.850	m
5	28-05 4.5W 20kH	1.01087	584.31 ±	437.08	5.4E-0013	573.180 ±	471.729	m
6	28-06 5.0W 20kH	1.00000	-10409.79 ±	113094.75	-3.8E-0014	31.759 ±	220.214	m

No	38Cl	/ 39K		40Ar* Vol ccNTP/g					Atm Cont	F1	F2
1	87.567 ±	48.158	m	3.24	±	0.88	E-12	(27.1%)	41.0426%	-0.000172	0.000372
2	16.428 ±	6.640	m	7.16	±	0.35	E-12	(4.9%)	8.7689%	0.000010	0.000516
3	37.478 ±	22.231	m	3.36	±	0.34	E-12	(10.2%)	-3.3821%	-0.000023	0.002872
4	26.178 ±	21.196	m	3.52	±	0.41	E-12	(11.6%)	3.4977%	-0.000057	0.006841
5	110.591 ±	121.358	m	524.74	±	401.70	E-15	(76.6%)	50.5723%	-0.000409	0.001721
6	54.439 ±	70.898	m	1.36	±	0.41	E-12	(30.0%)	-2.8387%	-0.000023	0.003469

Integrated Results:

Age = 271.914 ± 16.370 Ma

40Ar* / 39K = 27.404 ± 1.778

(40Ar / 36Ar)sam = 1931.84 ± 685.30

(36Ar / 40Ar)sam = 0.00051764 ±0.00024065
(37Ar / 40Ar)sam = 0.00178685 ±0.00166933
(39Ar / 40Ar)sam = 0.03090930 ±0.00170442

37Ca / 39K = 5.781 ± 5.392 E-2
Ca / K = 1.061 ± 0.989 E-1
F1 = -4.124 E-5

Wt. Mean Age = 240.50 ± 15.92 Ma (1.70)

Total 39K Vol = 6.9987E-0013 ccNTP/g

Total 40Ar* Vol = 1.918 ± 0.123 E-11

Total Atm 40Ar Vol = 3.4635E-0012 ccNTP/g

Corr 36/40 & 39/40 ratios =-0.635871
Corr 36/40 & 37/40 ratios =-0.039464
Corr 37/40 & 39/40 ratios =0.056518

38Cl / 39K = 3.399 ± 0.996 E-2
Cl / K = 7.138 ± 2.092 E-3
F2 = 9.224 E-4

DP11-161 P57-025 muscovite

Fractions:

No	Name		Temp	Cum 39K	Age				40Ar*		/ 39K
1	25-01	1.6W 21-J	1	0.00969	399.291	±	16.947	Ma	41.733	±	1.97
2	25-02	3.5W 21-J	2	0.02603	654.492	±	14.652	Ma	73.672	±	1.97
3	25-03	4.5W 20kH	3	0.06960	189.277	±	5.626	Ma	18.635	±	0.58
4	25-04	4.5W 20kH	4	0.08417	125.160	±	14.953	Ma	12.102	±	1.50
5	25-05	4.4W 20kH	5	0.10138	71.272	±	17.494	Ma	6.788	±	1.70
6	25-06	4.5W 20kH	6	0.69607	78.177	±	0.253	Ma	7.460	±	0.02
7	25-07	4.5W 20kH	7	0.71820	80.903	±	7.012	Ma	7.726	±	0.68
8	25-08	c 4.5W 20	8	0.74051	85.239	±	7.627	Ma	8.150	±	0.75
9	25-09	4.5W 20kH	9	0.81831	107.779	±	2.404	Ma	10.371	±	0.24
10	25-10	6.0W 20kH	10	0.85551	145.510	±	5.161	Ma	14.150	±	0.52
11	25-11	5.0W 20kH	11	0.95150	185.434	±	1.990	Ma	18.237	±	0.21
12	25-12	6.0W 20kH	12	1.00000	243.402	±	4.120	Ma	24.333	±	0.44

No	Name	Cum 36S	40Ar / 36Ar		40ArAcc/g		37Ca / 39K
1	25-01 1.6W 21-J	0.25071	580.43 ±	26.34	7.6E-0012	-14.930 ±	31.813 m
2	25-02 3.5W 21-J	0.41362	1600.97 ±	153.17	4.9E-0012	7.506 ±	49.195 m
3	25-03 4.5W 20kH	0.69811	799.51 ±	41.91	8.6E-0012	150.902 ±	18.592 m
4	25-04 4.5W 20kH	0.74688	934.25 ±	248.58	1.5E-0012	107.572 ±	34.727 m
5	25-05 4.4W 20kH	0.80804	632.99 ±	180.63	1.8E-0012	116.833 ±	41.727 m
6	25-06 4.5W 20kH	0.91432	7669.17 ±	568.99	3.2E-0012	79.458 ±	0.990 m
7	25-07 4.5W 20kH	0.92898	2355.52 ±	1445.04	4.4E-0013	233.516 ±	33.416 m
8	25-08 c 4.5W 20	0.93378	6989.32 ±	14186.36	1.4E-0013	192.871 ±	25.029 m
9	25-09 4.5W 20kH	0.99487	2628.10 ±	471.39	1.8E-0012	193.347 ±	7.537 m
10	25-10 6.0W 20kH	1.00305	11666.86 ±	16424.66	2.5E-0013	75.506 ±	15.553 m
11	25-11 5.0W 20kH	1.00628	96117.33 ±	308390.37	9.7E-0014	109.367 ±	9.555m
12	25-12 6.0W 20kH	1.00000	-32925.21 ±	64200.27	-1.9E-0013	72.091 ±	13.472m

No	38Cl / 39K				40Ar* Vol ccNTP/g					Atm Cont	F1	F2
1	33.362	±	7.612	m	7.29	±	0.35	E-12	(4.7%)	50.9103%	0.000011	0.000018
2	-0.980	±	7.708	m	21.69	±	0.48	E-12	(2.2%)	18.4575%	-0.000005	0.000032
3	6.950	±	3.663	m	14.62	±	0.46	E-12	(3.1%)	36.9600%	-0.000108	0.001032
4	6.366	±	8.998	m	3.18	±	0.39	E-12	(12.3%)	31.6296%	-0.000077	0.001507
5	20.740	±	8.111	m	2.11	±	0.53	E-12	(25.0%)	46.6834%	-0.000083	0.001537
6	2.284	±	0.424	m	79.93	±	0.47	E-12	(0.6%)	3.8531%	-0.000057	0.021416
7	19.108	±	6.436	m	3.08	±	0.27	E-12	(8.9%)	12.5450%	-0.000167	0.016935
8	8.622	±	6.741	m	3.27	±	0.30	E-12	(9.1%)	4.2279%	-0.000138	0.042251
9	4.011	±	2.184	m	14.53	±	0.34	E-12	(2.3%)	11.2439%	-0.000138	0.011869
10	0.464	±	3.778	m	9.48	±	0.35	E-12	(3.7%)	2.5328%	-0.000054	0.016618
11	-0.848	±	1.905	m	31.54	±	0.35	E-12	(1.1%)	0.3074%	-0.000078	0.138282
12	2.906	±	5.469	m	21.26	±	0.39	E-12	(1.8%)	-0.8975%	-0.000051	0.028331

Integrated Results:

Age = 121.808 ± 0.769 Ma Wt. Mean Age = 81.07 ± 140.08 Ma (563.3)

40Ar* / 39K = 11.767 ± 0.077

Total 39K Vol = 1.8015E-0011 ccNTP/g

Total 40Ar* Vol = 2.120 ± 0.014 E-10

(40Ar / 36Ar)sam = 2373.91 ± 101.14

Total Atm 40Ar Vol = 3.0138E-0011 ccNTP/g

(36Ar / 40Ar)sam = 0.00042125 ±0.00002385
(37Ar / 40Ar)sam = 0.00734379 ±0.00017582
(39Ar / 40Ar)sam = 0.07440552 ±0.00040431

Corr 36/40 & 39/40 ratios =-0.641885
Corr 36/40 & 37/40 ratios =-0.147641
Corr 37/40 & 39/40 ratios =0.218015

37Ca / 39K = 9.870 ± 0.231 E-2
Ca / K = 1.811 ± 0.042 E-1
F1 = -7.040 E-5

38Cl / 39K = 3.422 ± 0.585 E-3
Cl / K = 7.187 ± 1.229 E-4
F2 = 4.777 E-3

DP11-173 P57-023 whole rock

Fractions:

No	Name	Temp	Cum 39K	Age				40Ar* / 39K		
1	23-01 1.5W 31-D	1	0.00150	3.166	±	0.204	Ga	805.756	±	110.10
2	23-02 1.7W 31-D	2	0.00303	2.991	±	0.058	Ga	715.437	±	28.45
3	23-03 2.0W 31-D	3	0.00939	362.458	±	42.662	Ma	37.485	±	4.87
4	23-04 2.3W 2-J	4	0.01267	367.656	±	17.995	Ma	38.079	±	2.06
5	23-05 2.5W 3-J	5	0.01492	478.928	±	51.361	Ma	51.219	±	6.25
6	23-06 3.0W 5-J	6	0.02400	474.340	±	19.378	Ma	50.661	±	2.35
7	23-07 3.5W 5-J	7	0.08367	154.634	±	2.771	Ma	15.076	±	0.28
8	23-08 4.5W 20kH	8	0.35119	130.876	±	1.982	Ma	12.675	±	0.20
9	23-09 4.5W 20kH	9	0.45638	127.265	±	3.105	Ma	12.313	±	0.31
10	23-10 4.5W 20kH	10	0.58277	101.778	±	1.664	Ma	9.777	±	0.16
11	23-11 4.5W 20kH	11	0.60800	97.164	±	3.974	Ma	9.322	±	0.39
12	23-12 4.5W 20kH	12	0.65602	86.793	±	1.089	Ma	8.303	±	0.11
13	23-13 4.5W 20kH	13	0.72394	84.839	±	1.394	Ma	8.111	±	0.14
14	23-14 4.5W 20kH	14	0.79198	84.636	±	1.333	Ma	8.091	±	0.13
15	23-15 5.0W 20kH	15	0.93898	85.221	±	0.640	Ma	8.149	±	0.06
16	23-16 6.0W 20kH	16	0.99803	85.317	±	2.489	Ma	8.158	±	0.24
17	23-17 6.0W 20kH	17	1.00000	46.920	±	93.480	Ma	4.439	±	8.96

No	Name	Cum 36S	40Ar / 36Ar			40ArAcc/g	37Ca / 39K 1		
	23-01 1.5W 31-D	0.00373	167511.78	±	569405.98	9.8E-0014	3.065	±	1.337
2	23-02 1.7W 31-D	0.05282	11835.36	±	10507.67	1.3E-0012	11.336	±	0.491
3	23-03 2.0W 31-D	0.21587	1053.04	±	346.74	4.3E-0012	66.612	±	1.881
4	23-04 2.3W 2-J	0.23469	3724.33	±	2006.86	5.0E-0013	122.752	±	2.786
5	23-05 2.5W 3-J	0.24685	5209.38	±	10194.91	3.2E-0013	208.651	±	14.786
6	23-06 3.0W 5-J	0.26884	11118.85	±	18664.87	5.8E-0013	211.401	±	2.895
7	23-07 3.5W 5-J	0.40312	3763.20	±	768.78	3.5E-0012	49.841	±	0.665
8	23-08 4.5W 20kH	0.80755	4634.85	±	665.69	1.1E-0011	56.997	±	0.351
9	23-09 4.5W 20kH	0.77830	-22621.62	±	24153.41	-7.7E-0013	33.300	±	1.832
10	23-10 4.5W 20kH	0.77735	-669395.04	±	20894228.33	-2.5E-0014	8.002	±	1.098
11	23-11 4.5W 20kH	0.77064	-17865.00	±	45740.15	-1.8E-0013	14.640	±	0.419
12	23-12 4.5W 20kH	0.77097	628639.93	±	15919747.78	8.6E-0015	2.365	±	0.085
13	23-13 4.5W 20kH	0.82774	5318.43	±	1483.13	1.5E-0012	635.204	±	7.683 m
14	23-14 4.5W 20kH	0.88413	5348.28	±	1443.89	1.5E-0012	634.992	±	5.549 m
15	23-15 5.0W 20kH	0.96321	8136.35	±	1455.91	2.1E-0012	152.785	±	2.110 m
16	23-16 6.0W 20kH	0.98376	12423.19	±	14951.32	5.4E-0013	678.811	±	14.814 m
17	23-17 6.0W 20kH	1.00000	574.83	±	1096.36	4.3E-0013	1.817	±	0.315

DP11-173 P57-023 whole rock

No	38Cl / 39K				40Ar* Vol ccNTP/g					Atm Cont	F1	F2
1	-59.917	±	31.252	m	55.62	±	0.67	E-12	(1.2%)	0.1764%	-0.002186	0.149044
2	169.514	±	43.391	m	50.49	±	1.21	E-12	(2.4%)	2.4968%	-0.008087	0.040914
3	2.765	±	14.210	m	11.01	±	1.42	E-12	(12.9%)	28.0615%	-0.047516	0.238797
4	38.462	±	19.787	m	5.75	±	0.29	E-12	(5.1%)	7.9343%	-0.087561	0.733984
5	9.449	±	23.606	m	5.33	±	0.64	E-12	(12.0%)	5.6725%	-0.148834	0.825751
6	9.138	±	3.888	m	21.21	±	0.99	E-12	(4.6%)	2.6576%	-0.150796	0.915502
7	2.887	±	0.807	m	41.50	±	0.78	E-12	(1.9%)	7.8524%	-0.035553	0.753623
8	4.459	±	0.489	m	156.41	±	2.45	E-12	(1.6%)	6.3756%	-0.040657	0.838710
9	0.722	±	1.085	m	59.74	±	1.54	E-12	(2.6%)	-1.3063%	-0.023754	1.062740
10	1.495	±	0.560	m	57.00	±	0.90	E-12	(1.6%)	-0.0441%	-0.005708	1.006610
11	2.132	±	1.960	m	10.85	±	0.46	E-12	(4.2%)	-1.6541%	-0.010443	1.144983
12	0.205	±	1.987	m	18.39	±	0.24	E-12	(1.3%)	0.0470%	-0.001687	0.980366
13	2.970	±	1.046	m	25.41	±	0.44	E-12	(1.7%)	5.5561%	-0.000453	0.098614
14	2.853	±	0.904	m	25.39	±	0.42	E-12	(1.7%)	5.5251%	-0.000453	0.099334
15	1.948	±	0.588	m	55.25	±	0.48	E-12	(0.9%)	3.6318%	-0.000109	0.039351
16	-0.416	±	1.341	m	22.22	±	0.67	E-12	(3.0%)	2.3786%	-0.000484	0.219562
17	26.920	±	21.084	m	404.24	±	815.82	E-15	(201.8%)	51.4067%	-0.001296	0.029705

Integrated Results:

Age = 138.913 ± 0.932 Ma   Wt. Mean Age = 91.34 ± 66.92 Ma (156.1)

40Ar* / 39K = 13.484 ± 0.093   Total 39K Vol = 4.6127E-0011 ccNTP/g

Total 40Ar* Vol = 6.220 ± 0.041 E-10

(40Ar / 36Ar)sam = 7274.29 ± 907.80   Total Atm 40Ar Vol = 2.6336E-0011 ccNTP/g

(36Ar / 40Ar)sam = 0.00013747 ±0.00002331   Corr 36/40 & 39/40 ratios =-0.515491
(37Ar / 40Ar)sam = 1.89319864 ±0.02060073   Corr 36/40 & 37/40 ratios =-0.470794
(39Ar / 40Ar)sam = 0.07115018 ±0.00044032   Corr 37/40 & 39/40 ratios =0.493401

37Ca / 39K = 2.661 ± 0.025 E 1   38Cl / 39K = 2.822 ± 0.309 E-3
Ca / K = 4.882 ± 0.046 E 1   Cl / K = 5.926 ± 0.649 E-4
F1 = -1.898 E-2   F2 = 7.898 E-1

DP12-70 P59-017muscovite

No	Name		Temp	Fractions: Cum 39K	Age				40Ar* / 39K		
1	17-01	1.5W 19-O	1	0.02639	78.746	±	1.730	Ma	8.682	±	0.19
2	17-02	1.6W 19-O	2	0.05664	77.170	±	2.318	Ma	8.505	±	0.26
3	17-03	1.7W 19-O	3	0.17792	78.658	±	0.583	Ma	8.672	±	0.07
4	17-04	1.8W 26-O	4	0.26879	91.241	±	1.090	Ma	10.095	±	0.12
5	17-05	1.9W 26-O	5	0.41644	92.774	±	0.617	Ma	10.269	±	0.07
6	17-06	2.0W 26-O	6	0.46909	91.848	±	1.290	Ma	10.164	±	0.15
7	17-07	2.1W 26-O	7	0.55599	91.173	±	0.940	Ma	10.087	±	0.11
8	17-08	2.3W 26-O	8	0.60224	92.292	±	1.824	Ma	10.214	±	0.21
9	17-09	2.5W 26-O	9	0.75567	96.268	±	0.598	Ma	10.666	±	0.07
10	17-10	3.5W 26-O	10	0.80219	97.427	±	1.391	Ma	10.798	±	0.16
11	17-11	4.5W 20kH	11	0.83087	95.654	±	2.605	Ma	10.596	±	0.30
12	17-12	fuse 26-O	12	1.00000	99.510	±	0.430	Ma	11.035	±	0.05

No	Name			Cum 36S	40Ar /		36Ar	40ArAcc/g	37Ca/		39K	
1	17-01	1.5W	19-O	0.43970	913.07	±	41.20	4.7E-0012	8.137	±	9.475	m
2	17-02	1.6W	19-O	0.41901	-14447.92	±	21809.69	-2.2E-0013	-1.074	±	11.103	m
3	17-03	1.7W	19-O	0.56464	8856.34	±	1883.28	1.5E-0012	1.653	±	2.555	m
4	17-04	1.8W	26-O	0.66793	10821.88	±	4627.34	1.1E-0012	4.684	±	4.226	m
5	17-05	1.9W	26-O	0.83574	11006.02	±	2479.02	1.8E-0012	3.038	±	2.188	m
6	17-06	2.0W	26-O	0.86689	20660.15	±	19284.52	3.3E-0013	11.211	±	7.603	m
7	17-07	2.1W	26-O	0.94248	14040.44	±	6686.45	8.0E-0013	6.523	±	4.485	m
8	17-08	2.3W	26-O	0.96156	29637.03	±	59047.74	2.0E-0013	-4.912	±	6.165	m
9	17-09	2.5W	26-O	0.98409	86403.65	±	154042.26	2.4E-0013	1.776	±	1.734	m
10	17-10	3.5W	26-O	0.98398	-5460529.28	±	1430994162	-1.2E-0015	3.101	±	8.270	m
11	17-11	4.5W	20kH	0.99224	43907.32	±	179386.53	8.7E-0014	21.844	±	7.579	m
12	17-12	fuse	26-O	1.00000	285466.61	±	921802.76	8.2E-0014	38.311	±	1.176	m

No	38Cl		/ 39K		40Ar* Vol			ccNTP/g			Atm Cont	F1	F2
1	8.625	±	3.010	m	9.72	±	0.22	E-12	(	2.2%)	32.3634%	-0.000006	0.000156
2	-1.054	±	7.989	m	10.92	±	0.34	E-12	(	3.1%)	-2.0453%	0.000001	0.000521
3	462.022	±	953.431	µ	44.63	±	0.40	E-12	(	0.9%)	3.3366%	-0.000001	0.000455
4	0.005	±	2.959	m	38.92	±	0.51	E-12	(	1.3%)	2.7306%	-0.000003	0.001359
5	0.212	±	1.709	m	64.33	±	0.52	E-12	(	0.8%)	2.6849%	-0.000002	0.000882
6	6.724	±	4.378	m	22.71	±	0.33	E-12	(	1.4%)	1.4303%	-0.000008	0.006229
7	1.404	±	1.471	m	37.19	±	0.43	E-12	(	1.1%)	2.1046%	-0.000005	0.002472
8	0.643	±	1.432	m	20.05	±	0.41	E-12	(	2.1%)	0.9971%	0.000004	0.003954
9	1.118	±	0.590	m	69.44	±	0.55	E-12	(	0.8%)	0.3420%	-0.000001	0.003989
10	2.096	±	2.803	m	21.31	±	0.32	E-12	(	1.5%)	-0.0054%	-0.000002	0.779774
11	1.701	±	1.521	m	12.90	±	0.36	E-12	(	2.8%)	0.6730%	-0.000016	0.024489
12	1.709	±	0.560	m	79.19	±	0.48	E-12	(	0.6%)	0.1035%	-0.000027	0.216655

Integrated Results:

Age = 91.858 ± 0.483 Ma   Wt. Mean Age = 92.509 ± 21.490 Ma (90.74)

40Ar* / 39K = 10.165 ± 0.035

Total 39K Vol = 4.2429E-0011 ccNTP/g

Total 40Ar* Vol = 4.313 ± 0.014 E-10

(40Ar / 36Ar)sam = 12344.33 ± 1433.71

Total Atm 40Ar Vol = 1.0578E-0011 ccNTP/g

(36Ar / 40Ar)sam = 0.00008101 ±0.00001315

(37Ar / 40Ar)sam = 0.00093232 ±0.00010617

(39Ar / 40Ar)sam = 0.09602087 ±0.00028081

Corr 36/40 & 39/40 ratios =-0.663766

Corr 36/40 & 37/40 ratios =-0.019301

Corr 37/40 & 39/40 ratios =0.023320

37Ca / 39K = 9.710 ± 1.105 E-3

Ca / K = 1.782 ± 0.203 E-2

F1 = -6.926 E-6

38Cl / 39K = 1.396 ± 0.569 E-3

Cl / K = 2.932 ± 1.195 E-4

F2 = 3.198 E-3

DP11-77 P59-020muscovite

Fractions:

No	Name	Temp	Cum 39K	Age				40Ar* / 39K		
1	20-01 1.5W 30-O	1	0.02895	93.691	±	2.031	Ma	10.373	±	0.23
2	20-02 1.6W 30-O	2	0.05269	85.535	±	3.234	Ma	9.449	±	0.37
3	20-03 1.7W 30-O	3	0.27345	97.499	±	0.291	Ma	10.806	±	0.03
4	20-04 1.7W 30-O	4	0.42502	100.642	±	0.778	Ma	11.165	±	0.09
5	20-05 1.8W 30-O	5	0.47923	99.980	±	2.020	Ma	11.089	±	0.23
6	20-06 1.9W 30-O	6	0.59117	101.900	±	0.971	Ma	11.308	±	0.11
7	20-07 2.1W 30-O	7	0.68258	100.412	±	0.967	Ma	11.138	±	0.11
8	20-08 2.6W 30-O	8	0.73031	103.281	±	2.068	Ma	11.466	±	0.24
9	20-09 3.5W 30-O	9	0.87409	104.808	±	0.781	Ma	11.640	±	0.09
10	20-10 4.5W 20kH	10	0.99830	106.885	±	0.939	Ma	11.878	±	0.11
11	20-11 4.5W 20kH	11	1.00000	163.950	±	46.689	Ma	18.513	±	5.52

No	Name	Cum 36S	40Ar / 36Ar		40ArAcc/g	37Ca / 39K	
1	20-01 1.5W 30-O	0.15304	3974.61 ±	1072.78	9.4E-0013	5.512 ±	16.031 m
2	20-02 1.6W 30-O	0.19938	9368.65 ±	11016.97	2.8E-0013	27.868 ±	10.748 m
3	20-03 1.7W 30-O	0.44723	18339.40 ±	2005.66	1.5E-0012	10.010 ±	1.340 m
4	20-04 1.7W 30-O	0.57210	25702.38 ±	16668.87	7.6E-0013	3.572 ±	3.521 m
5	20-05 1.8W 30-O	0.56268	-119389.81 ±	930021.21	-5.8E-0014	-20.613 ±	12.487 m
6	20-06 1.9W 30-O	0.62750	36903.05 ±	42624.66	4.0E-0013	3.663 ±	3.005 m
7	20-07 2.1W 30-O	0.69525	28470.49 ±	25486.40	4.1E-0013	12.516 ±	3.478 m
8	20-08 2.6W 30-O	0.71149	63460.83 ±	277158.05	9.9E-0014	25.921 ±	6.338 m
9	20-09 3.5W 30-O	0.90905	16176.45 ±	6303.14	1.2E-0012	16.149 ±	2.156 m
10	20-10 4.5W 20kH	1.01366	26735.85 ±	20525.78	6.4E-0013	56.281 ±	2.891 m
11	20-11 4.5W 20kH	1.00000	-4011.11 ±	17155.39	-8.4E-0014	622.018 ±	439.672 m

No	38Cl / 39K				40Ar* Vol ccNTP/g				Atm Cont	F1	F2
1	4.093	±	6.009	m	11.67	±	0.26 E-12	(2.2%)	7.4347%	-0.000004	0.000542
2	5.770	±	2.420	m	8.72	±	0.34 E-12	(3.9%)	3.1541%	-0.000020	0.007402
3	1.774	±	0.990	m	92.69	±	0.49 E-12	(0.5%)	1.6113%	-0.000007	0.004641
4	1.099	±	1.443	m	65.75	±	0.60 E-12	(0.9%)	1.1497%	-0.000003	0.002264
5	-1.130	±	2.166	m	23.36	±	0.46 E-12	(2.0%)	-0.2475%	0.000015	0.058539
6	453.488	±	735.702	µ	49.18	±	0.52 E-12	(1.1%)	0.8007%	-0.000003	0.003300
7	1.764	±	1.579	m	39.56	±	0.42 E-12	(1.1%)	1.0379%	-0.000009	0.008760
8	-2.137	±	2.094	m	21.26	±	0.45 E-12	(2.1%)	0.4656%	-0.000018	0.038351
9	-0.214	±	1.015	m	65.03	±	0.58 E-12	(0.9%)	1.8267%	-0.000012	0.006107
10	555.139	±	837.032	µ	57.32	±	0.57 E-12	(1.0%)	1.1053%	-0.000040	0.033782
11	-105.990	±	101.991	m	1.22	±	0.36 E-12	(29.7%)	-7.3670%	-0.000444	0.042594

Integrated Results:

Age = 101.086 ± 0.545 Ma

40Ar* / 39K = 11.215 ± 0.042

Wt. Mean Age = 99.345 ± 4.496 Ma (19.59)

Total 39K Vol = 3.8854E-0011 ccNTP/g

Total 40Ar* Vol = 4.358 ± 0.016 E-10

(40Ar / 36Ar)sam = 21320.34 ± 4644.34

Total Atm 40Ar Vol = 6.1245E-0012 ccNTP/g

(36Ar / 40Ar)sam = 0.00004690 ±0.00001435

(37Ar / 40Ar)sam = 0.00137288 ±0.00013036

(39Ar / 40Ar)sam = 0.08792834 ±0.00028170

Corr 36/40 & 39/40 ratios =-0.661588

Corr 36/40 & 37/40 ratios =-0.024858

Corr 37/40 & 39/40 ratios =0.030017

37Ca / 39K = 1.561 ± 0.148 E-2

Ca / K = 2.865 ± 0.272 E-2

F1 = -1.114 E-5

38Cl / 39K = 7.209 ± 4.925 E-4

Cl / K = 1.514 ± 1.034 E-4

F2 = 8.101 E-3

DP12-80 P59-007 muscovite

Fractions:

No		Name	Temp	Cum 39K	Age				40Ar* / 39K		
1	7-01	1.5W 17-Oc	1	0.00087	322.369	±	81.180	Ma	38.074	±	10.47
2	7-02	1.6W 17-Oc	2	0.00722	126.955	±	10.822	Ma	14.188	±	1.25
3	7-03	1.7W 17-Oc	3	0.05204	102.116	±	1.454	Ma	11.333	±	0.17
4	7-04	1.8W 17-Oc	4	0.17010	114.253	±	0.719	Ma	12.723	±	0.08
5	7-05	1.8W 17-Oc	5	0.22692	112.367	±	1.660	Ma	12.506	±	0.19
6	7-06	2.0W 17-Oc	6	0.30447	111.900	±	0.794	Ma	12.453	±	0.09
7	7-07	2.5W 17-Oc	7	0.47241	121.727	±	0.527	Ma	13.584	±	0.06
8	7-08	3.5W 17-Oc	8	0.86546	122.972	±	0.337	Ma	13.727	±	0.04
9	7-09	4.5W 20kHz	9	0.98558	125.669	±	0.557	Ma	14.039	±	0.06
10	7-10	4.5W 20khz	10	0.99610	192.159	±	6.390	Ma	21.872	±	0.77
11	7-11	5.0W 20kHz	11	1.00000	518.057	±	14.350	Ma	64.732	±	2.06

No	Name	Cum 36S	40Ar / 36Ar			40ArAcc/g	37Ca / 39K			
1	7-01 1.5W 17-Oc	0.03299	1939.65	±	2932.45	2.6E-0013	78.123	±	157.445	m
2	7-02 1.6W 17-Oc	0.05756	6298.48	±	11190.49	1.9E-0013	168.174	±	85.907	m
3	7-03 1.7W 17-Oc	0.04959	-104097.70	±	521298.45	-6.2E-0014	33.219	±	4.933	m
4	7-04 1.8W 17-Oc	0.08016	80770.36	±	103840.02	2.4E-0013	28.876	±	10.470	m
5	7-05 1.8W 17-Oc	0.11468	34017.82	±	57940.16	2.7E-0013	21.437	±	3.205	m
6	7-06 2.0W 17-Oc	0.24467	12467.53	±	3322.30	1.0E-0012	23.996	±	2.709	m
7	7-07 2.5W 17-Oc	0.49719	15095.48	±	2640.02	2.0E-0012	16.008	±	1.159	m
8	7-08 3.5W 17-Oc	0.66875	51817.93	±	18805.51	1.3E-0012	38.406	±	2.954	m
9	7-09 4.5W 20kHz	0.67695	337041.84	±	1605430.68	6.4E-0014	566.160	±	4.757	m
10	7-10 4.5W 20khz	0.88792	2082.98	±	421.02	1.6E-0012	978.172	±	24.746	m
11	7-11 5.0W 20kHz	1.00000	3982.96	±	1382.77	8.7E-0013	1.255	±	0.091	

No	38Cl / 39K			40Ar* Vol		ccNTP/g		Atm Cont	F1	2
1	30.985±	50.809	m	1.43 ±	0.39	E-12	(27.2%)	15.2347%	-0.000056	0.000886
2	38.357±	20.466	m	3.89 ±	0.34	E-12	(8.8%)	4.6916%	-0.000120	0.019376
3	0.411±	1.280	m	21.94 ±	0.33	E-12	(1.5%)	-0.2839%	-0.000024	0.093519
4	-0.735±	2.614	m	64.85 ±	0.47	E-12	(0.7%)	0.3659%	-0.000021	0.048536
5	0.374±	1.234	m	30.68 ±	0.48	E-12	(1.6%)	0.8687%	-0.000015	0.015879
6	0.920±	2.077	m	41.70 ±	0.34	E-12	(0.8%)	2.3702%	-0.000017	0.006494
7	1.046±	0.983	m	98.50 ±	0.61	E-12	(0.6%)	1.9575%	-0.000011	0.004838
8	1.785±	0.821	m	232.97 ±	1.28	E-12	(0.5%)	0.5703%	-0.000027	0.038690
9	792.008±	907.472	µ	72.81 ±	0.48	E-12	(0.7%)	0.0877%	-0.000404	0.791339
10	-0.748±	5.202	m	9.94 ±	0.34	E-12	(3.4%)	14.1864%	-0.000698	0.021165
11	44.378±	30.967	m	10.89 ±	0.31	E-12	(2.9%)	7.4191%	-0.000895	0.018703

Integrated Results:

Age = 122.346 ± 0.597 Ma

Wt. Mean Age = 120.91 ± 28.30 Ma (126.58)

40Ar* / 39K = 13.655 ± 0.045

Total 39K Vol = 4.3179E-0011 ccNTP/g

Total 40Ar* Vol = 5.896 ± 0.018 E-10

(40Ar / 36Ar)sam = 22666.25 ± 3428.17

Total Atm 40Ar Vol = 7.7882E-0012 ccNTP/g

(36Ar / 40Ar)sam = 0.00004412 ±0.00000938
(37Ar / 40Ar)sam = 0.00795692 ±0.00014263
(39Ar / 40Ar)sam = 0.07227837 ±0.00016416

Corr 36/40 & 39/40 ratios =-0.609391
Corr 36/40 & 37/40 ratios =-0.081413
Corr 37/40 & 39/40 ratios =0.099963

37Ca / 39K = 1.101 ± 0.020 E-1
Ca / K = 2.020 ± 0.036 E-1
F1 = -7.853 E-5

38Cl / 39K = 1.432 ± 0.556 E-3
Cl / K = 3.008 ± 1.167 E-4
F2 = 4.790 E-2

DP12-81 P59-008 muscovite

Fractions:

No	Name	Temp	Cum 39K	Age				40Ar* / 39K		
1	8-01 1.5W 16-Oc	1	0.00663	56.274	±	2.719	Ma	6.166	±	0.30
2	8-02 1.6W 16-Oc	2	0.02044	76.737	±	1.282	Ma	8.456	±	0.14
3	8-03 1.7W 16-Oc	3	0.07955	90.574	±	0.485	Ma	10.019	±	0.06
4	8-04 1.8W 16-Oc	4	0.13883	111.387	±	0.534	Ma	12.394	±	0.06
5	8-05 1.8W 16-Oc	5	0.21934	130.817	±	0.318	Ma	14.635	±	0.04
6	8-06 1.9W 16-Oc	6	0.25703	115.891	±	1.031	Ma	12.911	±	0.12
7	8-07 1.9W 16-Oc	7	0.36284	124.278	±	0.459	Ma	13.878	±	0.05
8	8-08 2.0W 16-Oc	8	0.43815	116.675	±	0.553	Ma	13.001	±	0.06
9	8-09 2.5W 16-Oc	9	0.67945	129.031	±	0.429	Ma	14.428	±	0.05
10	8-10 4.4W 20kHz	10	0.75520	130.257	±	0.616	Ma	14.570	±	0.07
11	8-11 4.5W 20kHz	11	0.85076	131.081	±	0.475	Ma	14.666	±	0.06
12	8-12 4.5W 20kHz	12	0.89491	131.849	±	0.587	Ma	14.755	±	0.07
13	8-13 4.5W 20kHz	13	1.00000	129.762	±	0.501	Ma	14.513	±	0.06

No	Name		Cum 36S	40Ar / 36Ar		40ArAcc/g	37Ca / 39K		
1	8-01 1.5W	16-Oc	0.03442	1537.92±	315.61	1.3E-0012	1.888 ±	7.972	m
2	8-02 1.6W	16-Oc	0.05831	5409.05±	1568.96	9.1E-0013	11.832 ±	3.522	m
3	8-03 1.7W	16-Oc	0.19164	4944.02±	381.63	5.1E-0012	4.972 ±	1.610	m
4	8-04 1.8W	16-Oc	0.42568	3580.00±	127.69	8.9E-0012	14.910 ±	1.818	m
5	8-05 1.8W	16-Oc	0.49335	18515.02±	2372.25	2.6E-0012	2.872 ±	1.534	m
6	8-06 1.9W	16-Oc	0.51332	25794.27±	15779.47	7.6E-0013	-4.374 ±	3.341	m
7	8-07 1.9W	16-Oc	0.63247	13191.66±	1646.15	4.5E-0012	3.030 ±	0.871	m
8	8-08 2.0W	16-Oc	0.72220	11712.12±	1842.80	3.4E-0012	9.253 ±	1.184	m
9	8-09 2.5W	16-Oc	0.90858	19840.97±	1229.61	7.1E-0012	6.134 ±	1.307	m
10	8-10 4.4W	20kHz	0.91992	102190.62±	145575.27	4.3E-0013	8.806 ±	1.165	m
11	8-11 4.5W	20kHz	0.94166	67739.29±	46416.64	8.3E-0013	8.151 ±	0.852	m
12	8-12 4.5W	20kHz	0.98340	16623.23±	2424.72	1.6E-0012	26.283 ±	2.085	m
13	8-13 4.5W	20kHz	1.00000	96444.64±	102170.89	6.3E-0013	27.085 ±	0.487	m

No	38Cl / 39K			40Ar* Vol ccNTP/g				Atm Cont	F1	F2
1	3.307±	2.964	m	5.49 ±	0.27	E-12 (	4.9%)	19.2143%	-0.000001	0.000105
2	6.058±	2.260	m	15.70 ±	0.28	E-12 (	1.8%)	5.4631%	-0.000008	0.001987
3	4.329±	0.486	m	79.64 ±	0.56	E-12 (	0.7%)	5.9769%	-0.000004	0.000641
4	1.765±	0.720	m	98.78 ±	0.60	E-12 (	0.6%)	8.2542%	-0.000011	0.001092
5	-848.096±	578.783	µ	158.43 ±	0.87	E-12 (	0.6%)	1.5960%	-0.000002	0.000996
6	-0.198±	1.551	m	65.42 ±	0.57	E-12 (	0.9%)	1.1456%	0.000003	0.002416
7	744.518±	475.245	µ	197.44 ±	1.17	E-12 (	0.6%)	2.2401%	-0.000002	0.000784
8	740.972±	688.326	µ	131.65 ±	0.87	E-12 (	0.7%)	2.5230%	-0.000007	0.002259
9	1.438±	0.429	m	468.10 ±	2.55	E-12 (	0.5%)	1.4893%	-0.000004	0.002312
10	351.492±	491.716	µ	148.40 ±	0.97	E-12 (	0.7%)	0.2892%	-0.000006	0.016909
11	805.507±	466.583	µ	188.45 ±	1.12	E-12 (	0.6%)	0.4362%	-0.000006	0.010359
12	1.753±	0.701	m	87.58 ±	0.51	E-12 (	0.6%)	1.7776%	-0.000019	0.008042
13	988.752±	234.844	µ	205.07 ±	1.24	E-12 (	0.6%)	0.3064%	-0.000019	0.047725

DP12-81 P59-008 muscovite

Integrated Results:

Age = 123.258 ± 0.560 Ma	Wt. Mean Age = 122.43 ± 107.15 Ma 732.56)		
40Ar* / 39K = 13.760 ± 0.031		Total 39K Vol = 1.3445E-0010 ccNTP/g	
		Total 40Ar* Vol = 1.850 ± 0.004 E-9	
(40Ar / 36Ar)sam = 14693.75 ± 637.22		Total Atm 40Ar Vol = 3.7971E-0011 ccNTP/g	
(36Ar / 40Ar)sam = 0.00006806 ±0.00000413		Corr 36/40 & 39/40 ratios =-0.447266	
(37Ar / 40Ar)sam = 0.00066726 ±0.00003172		Corr 36/40 & 37/40 ratios =-0.014876	
(39Ar / 40Ar)sam = 0.07121103 ±0.00009636		Corr 37/40 & 39/40 ratios =0.016375	
37Ca / 39K = 9.370 ± 0.445 E-3		38Cl / 39K = 1.157 ± 0.175 E-3	
Ca / K = 1.719 ± 0.082 E-2		Cl / K = 2.429 ± 0.367 E-4	
F1 = -6.684 E-6		F2 = 2.725 E-3	

DP12-81 P59-209 Total-fusion garnets

No	Name	Temp	Cum 39K	Age			40Ar* / 39K		
1	214-00 fuse 26-	0	0.00000	260.057 ±	16.050	Ma	30.174	±	2.00
2	209a-00 29-Jan-	0	0.00000	135.170 ±	4.818	Ma	15.141	±	0.56
3	209b-00 29-Jan-	0	0.00000	629.949 ±	26.924	Ma	81.325	±	4.12
4	209c-00 fuse 29	0	0.00000	2.441 ±	0.042	Ga	558.197	±	17.47
5	209d-00 29-Jan-	0	0.00000	200.694 ±	7.472	Ma	22.899	±	0.90

No	Name	Cum 36S	40Ar / 36Ar			40ArAcc/g	37Ca / 39K	
1	214-00 fuse 26-	0.00000	2163.28 ±		884.13	7.5E-0013	**101.915 ± 304.858 m**	
2	209a-00 29-Jan-	0.00000	1832.20	±	349.50	1.6E-0012	21.096 ±	**0.169**
3	209b-00 29-Jan-	0.00000	9728.11	±	13196.80	2.1E-0013	56.240 ±	**2.080**
4	209c-00 fuse 29	0.00000	3141.92	±	323.75	2.8E-0012	63.315 ±	**2.695**
5	209e-00 29-Jan-	0.00000	2772.12	±	884.07	1.3E-0012	81.886 ±	0.694

No	38Cl / 39K			40Ar*	Vol ccNTP/g		Atm Cont	F1	F2
1	-2.746 ±	10.953	m	4.75 ±	0.31 E-12 (	6.5%)	13.6598%	-0.000073	0.001687
2	6.700 ±	2.743	m	8.25 ±	0.31 E-12 (	3.7%)	16.1282%	-0.015048	0.364897
3	-20.494 ±	37.242	m	6.61 ±	0.29 E-12 (	4.4%)	3.0376%	-0.040117	0.631501
4	20.244 ±	59.959	m	27.13 ±	0.40 E-12 (	1.5%)	9.4051%	-0.045164	0.041319
5	10.132 ±	7.693	m	10.55 ±	0.41 E-12 (	3.9%)	10.6597%	-0.058411	0.695384

DP12-87b P59-026 muscovite

Fractions:

No	Name		Temp	Cum 39K	Age			40Ar* / 39K		
1	26-01	1.5W 1-N	1	0.00028	64.268 ±	40.897	Ma	7.057	±	4.57
2	26-02	1.5W 1-N	2	0.00070	49.012 ±	32.593	Ma	5.359	±	3.61
3	26-03	1.5W 1-N	3	0.01244	68.812 ±	1.111	Ma	7.566	±	0.12
4	26-04	1.6W 1-N	4	0.01706	69.138 ±	2.377	Ma	7.603	±	0.27
5	26-05	1.7W 1-N	5	0.02626	71.577 ±	1.731	Ma	7.876	±	0.19
6	26-06	1.7W 1-N	6	0.05477	70.609 ±	0.537	Ma	7.767	±	0.06
7	26-07	3.5W 1-N	7	0.10911	71.282 ±	0.390	Ma	7.843	±	0.04
8	26-08	4.5W 20kH	8	0.15042	70.802 ±	0.419	Ma	7.789	±	0.05
9	26-09	4.5W 20kH	9	0.49725	71.892 ±	0.134	Ma	7.911	±	0.02
10	26-10	4.5W 20kH	10	0.60419	72.305 ±	0.154	Ma	7.958	±	0.02
11	26-11	4.5W 20kH	11	0.63672	71.134 ±	0.513	Ma	7.826	±	0.06
12	26-12	4.5W 20kH	12	0.84447	72.026 ±	0.105	Ma	7.926	±	0.01
13	26-13	4.5W 20kH	13	0.96762	72.707 ±	0.174	Ma	8.003	±	0.02
14	26-14	4.5W 20kH	14	0.98310	71.127 ±	0.736	Ma	7.826	±	0.08
15	26-15	4.5W 20kH	15	1.00000	72.909 ±	1.225	Ma	8.026	±	0.14

No	Name		Cum 36S	40Ar / 36Ar			40ArAcc/g	37Ca / 39K		
1	26-01	1.5W 1-N	0.00219	1735.11	±	5457.52	8.9E-0014	-97.899 ±	169.440	m
2	26-02	1.5W 1-N	0.00071	-2030.17	±	10750.53	-6.0E-0014	28.103 ±	85.731	m
3	26-03	1.5W 1-N	0.02570	5861.20	±	1792.36	1.0E-0012	4.425 ±	3.039	m
4	26-04	1.6W 1-N	0.02979	13717.84	±	21549.31	1.7E-0013	-3.341 ±	8.889	m
5	26-05	1.7W 1-N	0.05739	4404.80	±	1491.10	1.1E-0012	7.608 ±	4.738	m
6	26-06	1.7W 1-N	0.10593	7437.17	±	1291.21	2.0E-0012	9.950 ±	1.774	m
7	26-07	3.5W 1-N	0.17026	10664.97	±	1908.33	2.6E-0012	6.451 ±	0.770	m
8	26-08	4.5W 20kH	0.22142	10138.12	±	1961.02	2.1E-0012	10.307 ±	1.626	m
9	26-09	4.5W 20kH	0.74165	8550.83	±	334.53	2.1E-0011	5.771 ±	0.253	m
10	26-10	4.5W 20kH	0.75926	75965.00	±	25666.25	7.2E-0013	3.167 ±	0.592	m
11	26-11	4.5W 20kH	0.76842	43755.91	±	45463.03	3.7E-0013	4.276 ±	2.429	m
12	26-12	4.5W 20kH	0.90865	18675.68	±	1057.45	5.7E-0012	4.561 ±	0.330	m
13	26-13	4.5W 20kH	0.97052	25226.63	±	4557.39	2.5E-0012	5.556 ±	0.644	m
14	26-14	4.5W 20kH	0.98550	12945.91	±	5543.18	6.1E-0013	0.958 ±	6.122	m
15	26-15	4.5W 20kH	1.00000	14943.19	±	10701.60	5.9E-0013	-0.419 ±	8.945	m

No	38Cl / 39K				40Ar* Vol c cNTP/g				Atm Cont	F1	F2
1	32.644	±	27.733	m	435.69 ±	281.83	E-15	(64.7%)	17.0306%	0.000070	0.005541
2	29.319	±	25.035	m	476.01 ±	320.71	E-15	(67.4%)	-14.5555%	-0.000020	0.003439
3	1.706	±	0.960	m	19.25 ±	0.33	E-12	(1.7%)	5.0416%	-0.000003	0.000905
4	-1.228	±	2.312	m	7.60 ±	0.27	E-12	(3.5%)	2.1541%	0.000002	0.001649
5	1.201	±	1.301	m	15.70 ±	0.39	E-12	(2.5%)	6.7086%	-0.000005	0.001102
6	1.417	±	1.041	m	47.97 ±	0.42	E-12	(0.9%)	3.9733%	-0.000007	0.002543
7	1.549	±	0.537	m	92.33 ±	0.66	E-12	(0.7%)	2.7708%	-0.000005	0.002373
8	825.018	±	406.807	µ	69.68 ±	0.54	E-12	(0.8%)	2.9147%	-0.000007	0.003618
9	1.290	±	0.193	m	594.39 ±	3.12	E-12	(0.5%)	3.4558%	-0.000004	0.001676
10	778.967	±	305.823	µ	184.35 ±	0.96	E-12	(0.5%)	0.3890%	-0.000002	0.008341
11	1.253	±	0.613	m	55.15 ±	0.48	E-12	(0.9%)	0.6753%	-0.000003	0.006588
12	1.228	±	0.147	m	356.71 ±	1.84	E-12	(0.5%)	1.5823%	-0.000003	0.002943
13	1.410	±	0.261	m	213.49 ±	1.17	E-12	(0.5%)	1.1714%	-0.000004	0.004809
14	1.695	±	0.733	m	26.23 ±	0.30	E-12	(1.1%)	2.2826%	-0.000001	0.000432
15	-0.799	±	2.830	m	29.39 ±	0.46	E-12	(1.6%)	1.9775%	0.000000	0.000214

DP12-87b P59-026 muscovite

Integrated Results:

Age = 71.867 ± 0.326 Ma		Wt. Mean Age =	72.04 ± 0.40 Ma (3.87)
40Ar* / 39K =	7.909 ± 0.020	Total 39K Vol =	2.1662E-0010 ccNTP/g
		Total 40Ar* Vol =	1.713 ± 0.004 E-9
(40Ar / 36Ar)sam =	12673.77 ± 486.62	Total Atm 40Ar Vol =	4.0897E-0011 ccNTP/g
(36Ar / 40Ar)sam =	0.00007890 ±0.00000423	Corr 36/40 & 39/40 ratios =	-0.576718
(37Ar / 40Ar)sam =	0.00065070 ±0.00003450	Corr 36/40 & 37/40 ratios =	-0.014034
(39Ar / 40Ar)sam =	0.12349555 ±0.00013350	Corr 37/40 & 39/40 ratios =	0.015699
37Ca / 39K =	5.269 ± 0.279 E-3	38Cl / 39K =	1.218 ± 0.114 E-3
Ca / K =	9.668 ± 0.513 E-3	Cl / K =	2.558 ± 0.239 E-4
F1 =	-3.759 E-6	F2 =	2.295 E-3

DP12-94 P59-070 plagioclase

Fractions:

No	Name	Temp	Cum 39K	Age			40Ar* / 39K		
1	70-01 1.5W 23-J	1	0.29638	106.218 ±	17.447	Ma	11.802	±	2.00
2	70-02 1.6W 23-J	2	0.68351	95.372 ±	12.870	Ma	10.564	±	1.46
3	70-03 1.7W 23-J	3	0.76470	59.357 ±	61.598	Ma	6.509	±	6.87
4	70-04 2.0W 23-J	4	0.87286	101.343 ±	54.744	Ma	11.245	±	6.25
5	70-05 3.5W 23-J	5	0.99425	656.034 ±	37.154	Ma	85.344	±	5.77
6	70-06 4.5W 20kH	6	1.00000	357.636 ±	630.431	Ma	42.667	±	82.91

No	Name	Cum 36S		40Ar / 36Ar	40ArAcc/g		37Ca / 39K	
1	70-01 1.5W 23-J	0.32336	689.77 ±	154.64	1.1E-0012	1.292 ±	0.786	
2	70-02 1.6W 23-J	0.35059	5771.80±	14716.60	9.5E-0014	393.664 ±	251.640	m
3	70-03 1.7W 23-J	0.38251	898.95±	1929.26	1.1E-0013	2.572 ±	2.820	
4	70-04 2.0W 23-J	0.40867	1989.71±	6314.83	9.2E-0014	-88.400 ±	927.636	m
5	70-05 3.5W 23-J	0.47970	5612.21±	6088.69	2.5E-0013	-27.176 ±	924.576	m
6	70-06 4.5W 20kH	1.00000	312.70±	26.78	1.8E-0012	-26.656 ±	47.760	

No	38Cl		/ 39K		40Ar* Vc	l	ccNTP/g		Atm Cont	F1	F2
1	-17.571	±	32.560	m	1.51 ±	0.26	E-12	(16.9%)	42.8406%	-0.000922	0.011009
2	10.697	±	11.436	m	1.77 ±	0.24	E-12	(13.8%)	5.1197%	-0.000281	0.053676
3	37.537	±	86.080	m	228.52 ±	240.77	E-15	(105.4%)	32.8717%	-0.001835	0.060738
4	16.570	±	38.741	m	525.83 ±	291.51	E-15	(55.4%)	14.8514%	0.000063	0.003672
5	5.679	±	34.072	m	4.48 ±	0.27	E-12	(6.1%)	5.2653%	0.000019	0.000454
6	-1.046	±	3.125		106.16 ±	150.19	E-15	(141.5%)	94.4996%	0.019014	0.016060

Integrated Results:

Age = 175.965 ± 11.923 Ma Wt. Mean Age = 122.78 ± 313.35 Ma (32.26)

40Ar* / 39K = 19.937 ± 1.415

Total 39K Vol = 4.3237E-0013 ccNTP/g

Total 40Ar* Vol = 8.620 ± 0.603 E-12

(40Ar / 36Ar)sam = 1022.21 ± 175.50

Total Atm 40Ar Vol = 3.5053E-0012 ccNTP/g

(36Ar / 40Ar)sam = 0.00097827 ±0.00020603
(37Ar / 40Ar)sam = 0.02061068 ±0.01495920
(39Ar / 40Ar)sam = 0.03565753 ±0.00182235

Corr 36/40 & 39/40 ratios =-0.560712
Corr 36/40 & 37/40 ratios =-0.059682
Corr 37/40 & 39/40 ratios =0.060885

37Ca / 39K = 5.780 ± 4.188 E-1
Ca / K = 1.061 ± 0.768
F1 = -4.123 E-4

38Cl / 39K = -0.156 ± 2.137 E-2
Cl / K = -0.327 ± 4.487 E-3
F2 = 5.442 E-3

DP12-94 P59-072 biotite

Fractions:

No		Name	Temp	Cum 39K	Age			40Ar* / 39K	
1	72-01	1.5W 15-J	0	0.00075	28.435 ±	102.923	Ma	3.092 ±	11.28
2	72-02	1.6W 15-J	2	0.04130	72.926 ±	4.275	Ma	8.028 ±	0.48
3	72-03	1.7W 15-J	3	0.11754	108.082 ±	1.643	Ma	12.015 ±	0.19
4	72-04	1.8W 15-J	4	0.17405	113.150 ±	1.946	Ma	12.596 ±	0.22
5	72-05	1.8W 15-J	5	0.44378	105.621 ±	0.574	Ma	11.733 ±	0.07
6	72-06	1.9W 15-J	6	0.63995	102.202 ±	0.549	Ma	11.343 ±	0.06
7	72-07	2.0W 15-J	7	0.75286	102.138 ±	0.836	Ma	11.335 ±	0.10
8	72-08	2.1W 15-J	8	0.94059	102.623 ±	0.594	Ma	11.391 ±	0.07
9	72-09	3.5W 15-J	9	0.96559	105.648 ±	4.164	Ma	11.736 ±	0.48
10	72-10	4.5W 20kH	10	0.99322	106.156 ±	2.912	Ma	11.794 ±	0.33
11	72-11	4.5W 20kH	11	1.00000	81.924 ±	11.717	Ma	9.041 ±	1.32

No		Name	Cum 36S	40Ar / 36Ar		40ArAcc/g	37Ca / 39K		
1	72-01	1.5W 15-J	0.00073	391.18±	461.84	2.8E-0013	-1.118 ±	1.284	
2	72-02	1.6W 15-J	0.43859	317.68±	1.42	1.7E-0010	37.086 ±	20.863	m
3	72-03	1.7W 15-J	0.72872	389.70±	1.59	1.1E-0010	19.302 ±	36.266	m
4	72-04	1.8W 15-J	0.79491	616.33±	11.44	2.6E-0011	29.848 ±	40.689	m
5	72-05	1.8W 15-J	0.91561	1077.88±	14.24	4.7E-0011	14.561 ±	6.406	m
6	72-06	1.9W 15-J	0.94148	2861.59±	120.24	1.0E-0011	18.864 ±	7.180	m
7	72-07	2.0W 15-J	0.95129	4190.10±	427.00	3.8E-0012	-20.960 ±	19.127	m
8	72-08	2.1W 15-J	0.95850	9145.91±	1508.08	2.8E-0012	27.340 ±	10.138	m
9	72-09	3.5W 15-J	0.96623	1426.35±	217.82	3.0E-0012	76.139 ±	63.696	m
10	72-10	4.5W 20kH	0.98226	902.36±	51.53	6.3E-0012	184.633 ±	37.493	m
11	72-11	4.5W 20kH	1.00000	398.54±	20.06	6.9E-0012	22.035 ±	168.979	m

No	38Cl / 39K			40Ar* Vol ccNTP/g	Atm Cont	F1	F2
1	-268.056 ±	175.305	m	92.06 ± 335.78 E-15 (364.7%)	75.5409%	0.000797	0.008955
2	4.386 ±	2.642	m	12.85 ± 0.77 E-12 (6.0%)	93.0180%	-0.000026	0.000002
3	3.023 ±	2.575	m	36.17 ± 0.52 E-12 (1.4%)	75.8269%	-0.000014	0.000029
4	-0.809 ±	2.648	m	28.10 ± 0.50 E-12 (1.8%)	47.9455%	-0.000021	0.000191
5	1.842 ±	0.543	m	124.95 ± 0.90 E-12 (0.7%)	27.4148%	-0.000010	0.000261
6	1.811 ±	0.584	m	87.84 ± 0.62 E-12 (0.7%)	10.3264%	-0.000013	0.001178
7	-2.819 ±	3.137	m	50.53 ± 0.47 E-12 (0.9%)	7.0523%	0.000015	0.002001
8	1.468 ±	1.284	m	84.42 ± 0.63 E-12 (0.8%)	3.2310%	-0.000020	0.005881
9	5.283 ±	4.955	m	11.58 ± 0.47 E-12 (4.0%)	20.7172%	-0.000054	0.001991
10	1.584 ±	3.089	m	12.87 ± 0.36 E-12 (2.8%)	32.7476%	-0.000132	0.002516
11	-26.354 ±	15.856	m	2.42 ± 0.35 E-12 (14.6%)	74.1454%	-0.000016	0.000054

Integrated Results:

Age = 103.093 ± 0.588 Ma   Wt. Mean Age = 103.54 ± 3.385 Ma (11.34)

40Ar* / 39K = 11.444 ± 0.049   Total 39K Vol = 3.9480E-0011 ccNTP/g

Total 40Ar* Vol = 4.518 ± 0.019 E-10

(40Ar / 36Ar)sam = 636.97 ± 2.59   Total Atm 40Ar Vol = 3.9100E-0010 ccNTP/g

(36Ar / 40Ar)sam = 0.00156994 ±0.00000723   Corr 36/40 & 39/40 ratios =-0.374132

(37Ar / 40Ar)sam = 0.00100093 ±0.00026809   Corr 36/40 & 37/40 ratios =-0.013501

(39Ar / 40Ar)sam = 0.04684254 ±0.00010512   Corr 37/40 & 39/40 ratios =0.004336

37Ca / 39K = 2.137 ± 0.572 E-2   38Cl / 39K = 9.671 ± 5.848 E-4

Ca / K = 3.921 ± 1.050 E-2   Cl / K = 2.031 ± 1.228 E-4

F1 = -1.524 E-5   F2 = 1.629 E-4

DP12-94 P59-218 muscovite

Fractions:

No	Name			Temp	Cum 39K	Age				40Ar* / 39K		
1	218-01	1.6W	2-	1	0.00019	68.948	±	41.398	Ma	7.581	±	4.64
2	218-02	1.5W	2-	2	0.00252	61.097	±	2.787	Ma	6.703	±	0.31
3	218-03	1.5W	2-	3	0.01220	62.013	±	0.616	Ma	6.805	±	0.07
4	218-04	1.6W	2-	4	0.02217	64.873	±	0.688	Ma	7.125	±	0.08
5	218-05	1.7W	2-	5	0.04536	63.517	±	0.402	Ma	6.973	±	0.04
6	218-06	1.8W	2-	6	0.06280	64.322	±	0.499	Ma	7.063	±	0.06
7	218-07	1.9W	4-	7	0.08104	63.729	±	0.391	Ma	6.997	±	0.04
8	218-08	2.5W	4-	8	0.13125	71.762	±	0.218	Ma	7.897	±	0.02
9	218-09	3.5W	4-	9	0.23233	72.520	±	0.136	Ma	7.982	±	0.02
10	218-10	4.5W	20k	10	0.35521	71.852	±	0.232	Ma	7.907	±	0.03
11	218-11	4.5W	20k	11	0.64002	71.400	±	0.215	Ma	7.856	±	0.02
12	218-12	4.5W	20k	12	0.72240	71.072	±	0.136	Ma	7.819	±	0.02
13	218-13	4.5W	20k	13	0.78183	72.013	±	0.178	Ma	7.925	±	0.02
14	218-14	4.5W	20k	14	0.87575	72.313	±	0.117	Ma	7.959	±	0.01
15	218-15	4.5W	20k	15	0.91949	72.087	±	0.221	Ma	7.933	±	0.02
16	218-16	5.0W	20k	16	0.99765	73.982	±	0.154	Ma	8.146	±	0.02
17	218-17	5.5W	20k	17	1.00000	104.607	±	2.986	Ma	11.617	±	0.34

No	Name		Cum 36S	40Ar / 36Ar		40ArAcc/g	37Ca / 39K 1	
	218-01 1.6W	2-	-0.00222	-1282.22 ±	4169.66	-1.1E-0013	0.828 ±	1.086
2	218-02 1.5W	2-	0.02452	1732.60 ±	387.06	1.3E-0012	1.988 ±	51.100 m
3	218-03 1.5W	2-	0.17228	1394.33 ±	51.41	7.0E-0012	18.646 ±	10.633 m
4	218-04 1.6W	2-	0.20154	6272.98 ±	1298.53	1.4E-0012	25.793 ±	15.628 m
5	218-05 1.7W	2-	0.25098	8346.63 ±	1418.97	2.4E-0012	13.318 ±	6.457 m
6	218-06 1.8W	2-	0.26997	16276.74 ±	6638.16	9.0E-0013	8.440 ±	11.646 m
7	218-07 1.9W	4-	0.31984	6596.04 ±	745.09	2.4E-0012	45.062 ±	12.180 m
8	218-08 2.5W	4-	0.40584	11647.91 ±	951.60	4.1E-0012	29.387 ±	5.526 m
9	218-09 3.5W	4-	0.56778	12563.29 ±	783.31	7.7E-0012	7.950 ±	3.276 m
10	218-10 4.5W	20k	0.64394	31709.91 ±	5897.30	3.6E-0012	-12.411 ±	3.231 m
11	218-11 4.5W	20k	0.92862	19649.75 ±	3583.37	1.4E-0011	24.538 ±	3.581 m
12	218-12 4.5W	20k	0.93744	180037.74 ±	185210.76	4.2E-0013	18.625 ±	2.251 m
13	218-13 4.5W	20k	0.94783	111986.00 ±	90882.60	4.9E-0013	24.197 ±	3.196 m
14	218-14 4.5W	20k	0.96318	120166.65 ±	59647.55	7.3E-0013	15.525 ±	2.608 m
15	218-15 4.5W	20k	0.97027	120846.37 ±	135880.37	3.4E-0013	22.005 ±	5.498 m
16	218-16 5.0W	20k	0.99244	71015.89 ±	23130.87	1.1E-0012	20.678 ±	3.119 m
17	218-17 5.5W	20k	1.00000	9194.58 ±	7975.82	3.6E-0013	95.176 ±	98.249 m

DP12-94 P59-218 muscovite

No	38Cl / 39K				40Ar* Vol ccNTP/g				Atm Cont	F1	F2
1	-36.430	±	51.392	m	564.78 ±	345.30	E-15	(61.1%)	-23.0460%	-0.000591	0.051230
2	4.065	±	1.775	m	6.19 ±	0.29	E-12	(4.6%)	17.0553%	-0.000001	0.000118
3	2.649	±	0.795	m	26.16 ±	0.29	E-12	(1.1%)	21.1930%	-0.000013	0.000827
4	-1.105	±	0.796	m	28.18 ±	0.32	E-12	(1.1%)	4.7107%	-0.000018	0.005991
5	1.870	±	0.511	m	64.13 ±	0.52	E-12	(0.8%)	3.5404%	-0.000010	0.004268
6	1.680	±	0.475	m	48.89 ±	0.44	E-12	(0.9%)	1.8155%	-0.000006	0.005301
7	623.525	±	616.942	µ	50.63 ±	0.38	E-12	(0.7%)	4.4800%	-0.000032	0.011178
8	1.572	±	0.250	m	157.30 ±	0.86	E-12	(0.5%)	2.5369%	-0.000021	0.011645
9	1.107	±	0.285	m	320.09 ±	1.69	E-12	(0.5%)	2.3521%	-0.000006	0.003397
10	1.202	±	0.197	m	385.47 ±	2.12	E-12	(0.6%)	0.9319%	0.000009	0.013961
11	1.133	±	0.150	m	887.71 ±	5.13	E-12	(0.6%)	1.5038%	-0.000018	0.016593
12	1.132	±	0.183	m	255.57 ±	1.35	E-12	(0.5%)	0.1641%	-0.000013	0.106827
13	839.741	±	199.057	µ	186.86 ±	1.03	E-12	(0.5%)	0.2639%	-0.000017	0.086977
14	1.315	±	0.300	m	296.53 ±	1.54	E-12	(0.5%)	0.2459%	-0.000011	0.061316
15	1.953	±	0.354	m	137.67 ±	0.80	E-12	(0.6%)	0.2445%	-0.000016	0.085429
16	1.084	±	0.153	m	252.61 ±	1.34	E-12	(0.5%)	0.4161%	-0.000015	0.047749
17	4.243	±	9.942	m	10.84 ±	0.32	E-12	(2.9%)	3.2139%	-0.000068	0.019897

Integrated Results:

Age = 71.368 ± 0.324 Ma Wt. Mean Age = 71.69 ± 6.11 Ma (115.42)

40Ar* / 39K = 7.853 ± 0.017

Total 39K Vol = 3.9674E-0010 ccNTP/g

Total 40Ar* Vol = 3.115 ± 0.007 E-9

(40Ar / 36Ar)sam = 19631.60 ± 1199.58

Total Atm 40Ar Vol = 4.7610E-0011 ccNTP/g

(36Ar / 40Ar)sam = 0.00005094 ±0.00000437
(37Ar / 40Ar)sam = 0.00211368 ±0.00017242
(39Ar / 40Ar)sam = 0.12542998 ±0.00013626

Corr 36/40 & 39/40 ratios =-0.592865
Corr 36/40 & 37/40 ratios =-0.018921
Corr 37/40 & 39/40 ratios =0.009843

37Ca / 39K = 1.685 ± 0.137 E-2
Ca / K = 3.092 ± 0.252 E-2
F1 = -1.202 E-5

38Cl / 39K = 1.209 ± 0.078 E-3
Cl / K = 2.540 ± 0.163 E-4
F2 = 1.145 E-2

DP12-105 P63-055 muscovite

Fractions:

No	Name			Temp	Cum 39K	Age				40Ar* / 39K		
1	55-01	1.5W	-7 3	1	0.01669	87.130	±	3.957	Ma	24.165	±	1.12
2	55-02	1.5W	-7 3	2	0.19872	77.058	±	0.438	Ma	21.312	±	0.12
3	55-03	1.6W	-7 3	3	0.37402	78.252	±	0.529	Ma	21.649	±	0.15
4	55-04	1.6W	-7 3	4	0.53685	81.691	±	0.785	Ma	22.622	±	0.22
5	55-05	1.7W	-7 3	5	0.62443	83.486	±	1.473	Ma	23.131	±	0.42
6	55-06	1.8W	-7 3	6	0.66912	85.227	±	2.030	Ma	23.625	±	0.58
7	55-07	1.7W	-7	7	0.78304	86.264	±	0.695	Ma	23.919	±	0.20
8	55-08	1.7W	-7	8	0.80668	87.097	±	3.661	Ma	24.156	±	1.04
9	55-09	2.6W	20kH	9	0.99899	96.543	±	0.373	Ma	26.846	±	0.11
10	55-10	5.0W	20kH	10	1.00000	135.325	±	64.189	Ma	38.041	±	18.73

No	Name	Cum 36S	40Ar / 36Ar		40ArAcc/g	37Ca / 39K	
1	55-01 1.5W -7 3	0.02335	6960.73 ±	7161.81	2.1E-0013	-17.347 ±	37.650 m
2	55-02 1.5W -7 3	0.32646	5233.92 ±	459.67	2.8E-0012	24.130 ±	3.557 m
3	55-03 1.6W -7 3	0.71971	4019.43 ±	322.60	3.6E-0012	42.492 ±	3.575 m
4	55-04 1.6W -7 3	0.80298	17364.92 ±	9313.32	7.7E-0013	20.864 ±	8.164 m
5	55-05 1.7W -7 3	0.77578	-28443.56 ±	47867.44	-2.5E-0013	-0.292 ±	31.895 m
6	55-06 1.8W -7 3	0.76775	-50423.72 ±	203430.89	-7.4E-0014	-12.058 ±	32.053 m
7	55-07 1.7W -7	0.85992	11703.16 ±	3364.56	8.5E-0013	48.877 ±	4.890 m
8	55-08 1.7W -7	0.87923	11708.22 ±	19178.54	1.8E-0013	168.088 ±	24.120 m
9	55-09 2.6W 20kH	0.96424	23728.80 ±	6221.67	7.8E-0013	138.863 ±	3.659 m
10	55-10 5.0W 20kH	1.00000	710.98 ±	487.04	3.3E-0013	1.632 ±	0.710

No	38Cl / 39K				40Ar* Vol ccNTP/g					Atm Cont	F1	F2
1	7.087	±	6.760	m	4.84	±	0.22	E-12	(4.6%)	4.2452%	0.000012	0.001326
2	3.328	±	1.218	m	46.59	±	0.34	E-12	(0.7%)	5.6459%	-0.000017	0.001543
3	3.110	±	0.916	m	45.58	±	0.37	E-12	(0.8%)	7.3518%	-0.000030	0.002008
4	2.057	±	1.147	m	44.24	±	0.47	E-12	(1.1%)	1.7017%	-0.000015	0.004365
5	2.034	±	2.280	m	24.33	±	0.44	E-12	(1.8%)	-1.0389%	0.000000	0.000102
6	3.406	±	3.544	m	12.68	±	0.31	E-12	(2.4%)	-0.5860%	0.000009	0.007190
7	2.282	±	1.176	m	32.73	±	0.30	E-12	(0.9%)	2.5250%	-0.000035	0.006436
8	2.350	±	14.405	m	6.86	±	0.29	E-12	(4.3%)	2.5239%	-0.000120	0.021590
9	158.221	±	701.656	µ	62.01	±	0.37	E-12	(0.6%)	1.2453%	-0.000099	0.032661
10	0.357	±	107.991	m	462.41	±	225.45	E-15	(48.8%)	41.5623%	-0.001164	0.003796

Integrated Results:

Age = 84.224 ± 0.670 Ma

Wt. Mean Age = 85.64 ± 35.85 Ma (162.34)

40Ar* / 39K = 23.340 ± 0.094

Total 39K Vol = 1.2011E-0011 ccNTP/g

Total 40Ar* Vol = 2.803 ± 0.011 E-10

(40Ar / 36Ar)sam = 9301.72 ± 940.40

Total Atm 40Ar Vol = 9.1978E-0012 ccNTP/g

(36Ar / 40Ar)sam = 0.00010751 ±0.00001513
(37Ar / 40Ar)sam = 0.00216889 ±0.00015788
(39Ar / 40Ar)sam = 0.04148381 ±0.00014186

Corr 36/40 & 39/40 ratios =-0.653114
Corr 36/40 & 37/40 ratios =-0.033592
Corr 37/40 & 39/40 ratios =0.040995

37Ca / 39K = 5.228 ± 0.380 E-2
Ca / K = 9.593 ± 0.698 E-2
F1 = -3.729 E-5

38Cl / 39K = 2.281 ± 0.593 E-3
Cl / K = 4.790 ± 1.245 E-4
F2 = 5.568 E-3

DP12-110 P59-081muscovite

Fractions:

No		Name		Temp	Cum 39K	Age				40Ar* / 39K		
1	81-01	1.6W	16-J	0	0.00140	91.050	±	35.736	Ma	10.073	±	4.05
2	81-02	1.5W	16-J	0	0.00900	83.819	±	5.497	Ma	9.255	±	0.62
3	81-03	1.8W	16-J	0	0.05824	85.338	±	0.818	Ma	9.426	±	0.09
4	81-04	1.7W	16-J	0	0.09271	113.673	±	1.219	Ma	12.656	±	0.14
5	81-05	1.8W	16-J	0	0.11267	117.320	±	1.968	Ma	13.076	±	0.23
6	81-06	1.9W	16-J	0	0.16214	125.257	±	0.987	Ma	13.991	±	0.11
7	81-07	2.0W	16-J	0	0.21174	133.925	±	1.300	Ma	14.996	±	0.15
8	81-08	3.5W	16-J	0	0.26342	161.077	±	1.187	Ma	18.174	±	0.14
9	81-09	4.5W	20kh	0	0.49272	176.214	±	0.540	Ma	19.967	±	0.06
10	81-10	4.5W	20kH	0	0.66365	182.753	±	0.684	Ma	20.746	±	0.08
11	81-11	4.5W	18-J	0	0.75791	190.451	±	0.847	Ma	21.667	±	0.10
12	81-12	4.5W	20kH	0	0.78601	189.824	±	2.006	Ma	21.592	±	0.24
13	81-13	4.5W	20kH	0	0.88984	192.426	±	0.696	Ma	21.904	±	0.08
14	81-14	4.5W	20kH	0	0.93885	200.051	±	1.590	Ma	22.821	±	0.19
15	81-15	4.5W	20kH	0	0.98523	223.022	±	1.565	Ma	25.607	±	0.19
16	81-16	4.5W	20kH	0	1.00000	279.669	±	2.964	Ma	32.631	±	0.37

No		Name		Cum 36S	40Ar / 36Ar			40ArAcc/g	37Ca / 39K			
1	81-01	1.6W	16-J	0.00394	1123.76	±	1257.46	3.0E-0013	-1.067	±	0.414	
2	81-02	1.5W	16-J	0.05980	587.70	±	38.48	4.3E-0012	-64.904	±	93.434	m
3	81-03	1.8W	16-J	0.07461	7562.07	±	1600.64	1.1E-0012	9.522	±	20.698	m
4	81-04	1.7W	16-J	0.07723	38908.44	±	53058.78	2.0E-0013	-36.033	±	33.410	m
5	81-05	1.8W	16-J	0.09049	4863.54	±	1247.52	1.0E-0012	-64.239	±	40.060	m
6	81-06	1.9W	16-J	0.11248	7591.98	±	1245.91	1.7E-0012	5.399	±	16.523	m
7	81-07	2.0W	16-J	0.12306	16601.80	±	9001.51	8.1E-0013	25.381	±	19.968	m
8	81-08	3.5W	16-J	0.16015	6168.55	±	872.49	2.8E-0012	30.838	±	15.918	m
9	81-09	4.5W	20kh	0.21042	21415.60	±	2560.10	3.8E-0012	9.188	±	3.260	m
10	81-10	4.5W	20kH	0.33954	6664.22	±	297.66	9.8E-0012	26.215	±	3.880	m
11	81-11	4.5W	18-J	0.38994	9691.02	±	1150.83	3.8E-0012	5.054	±	13.914	m
12	81-12	4.5W	20kH	0.39063	204039.55	±	1462447.00	5.3E-0014	4.710	±	32.510	m
13	81-13	4.5W	20kH	0.40455	38183.34	±	16077.95	1.1E-0012	7.704	±	7.936	m
14	81-14	4.5W	20kH	0.41386	28144.39	±	19479.68	7.1E-0013	10.623	±	21.994	m
15	81-15	4.5W	20kH	0.64936	1465.16	±	40.35	1.8E-0011	20.135	±	23.377	m
16	81-16	4.5W	20kH	1.00000	614.16	±	6.81	2.7E-0011	107.790	±	36.508	m

No	38Cl / 39K			40Ar* Vol ccNTP/g					Atm Cont	F1	F2
1	-81.543	± 48.062	m	841.16	±	336.88	E-15	(40.0%)	26.2956%	0.000761	0.024346
2	8.880	± 26.132	m	4.21	±	0.28	E-12	(6.7%)	50.2806%	0.000046	0.000527
3	1.156	± 4.252	m	27.77	±	0.29	E-12	(1.0%)	3.9077%	-0.000007	0.002040
4	0.075	± 3.395	m	26.11	±	0.30	E-12	(1.2%)	0.7595%	0.000026	0.031663
5	-3.376	± 1.888	m	15.62	±	0.27	E-12	(1.7%)	6.0758%	0.000046	0.006264
6	0.292	± 1.597	m	41.42	±	0.36	E-12	(0.9%)	3.8923%	-0.000004	0.000782
7	2.767	± 1.250	m	44.51	±	0.49	E-12	(1.1%)	1.7799%	-0.000018	0.007634
8	933.066	± 973.901	µ	56.21	±	0.49	E-12	(0.9%)	4.7904%	-0.000022	0.002755
9	1.663	± 0.624	m	274.00	±	1.47	E-12	(0.5%)	1.3798%	-0.000007	0.002701
10	1.096	± 0.520	m	212.22	±	1.17	E-12	(0.6%)	4.4341%	-0.000019	0.002225
11	2.318	± 0.667	m	122.21	±	0.77	E-12	(0.6%)	3.0492%	-0.000004	0.000608
12	814.447	± 917.548	µ	36.32	±	0.42	E-12	(1.2%)	0.1448%	-0.000003	0.012261
13	446.182	± 558.947	µ	136.09	±	0.83	E-12	(0.6%)	0.7739%	-0.000005	0.003704
14	1.036	± 1.353	m	66.93	±	0.60	E-12	(0.9%)	1.0499%	-0.000008	0.003601
15	-0.527	± 1.408	m	71.08	±	0.61	E-12	(0.9%)	20.1684%	-0.000014	0.000243
16	1.502	± 3.180	m	28.84	±	0.33	E-12	(1.1%)	48.1146%	-0.000077	0.000217

Integrated Results:

Age = 171.920 ± 0.786 Ma	Wt. Mean Age = 163.44 ± 373.29 Ma (1444)		
40Ar* / 39K = 19.457 ± 0.048		Total 39K Vol = 5.9845E-0011 ccNTP/g	
		Total 40Ar* Vol = 1.164 ± 0.003 E-9	
(40Ar / 36Ar)sam = 4807.50 ± 96.53		Total Atm 40Ar Vol = 7.6259E-0011 ccNTP/g	

(36Ar / 40Ar)sam = 0.00020801 ±0.00000573 — Corr 36/40 & 39/40 ratios =-0.522703

(37Ar / 40Ar)sam = 0.00048835 ±0.00017410 — Corr 36/40 & 37/40 ratios =-0.010849

(39Ar / 40Ar)sam = 0.04823608 ±0.00007750 — Corr 37/40 & 39/40 ratios =0.001270

37Ca / 39K = 1.012 ± 0.361 E-2 — 38Cl / 39K = 1.051 ± 0.403 E-3

Ca / K = 1.858 ± 0.662 E-2 — Cl / K = 2.206 ± 0.847 E-4

F1 = -7.222 E-6 — F2 = 6.483 E-4

DP12-112 P59-068 muscovite

Fractions:

No	Name		Temp	Cum 39K	Age			40Ar* /		39K
1	68-01 1.5W	21-D	1	0.00181	225.119 ±	5.704	Ma	25.863	±	0.70
2	68-02 1.5W	21-D	2	0.00283	366.143 ±	9.896	Ma	43.788	±	1.31
3	68-03 1.5W	21-D	3	0.06979	138.329 ±	0.228	Ma	15.508	±	0.03
4	68-04 1.6W	21-D	4	0.09004	110.923 ±	0.572	Ma	12.341	±	0.07
5	68-05 1.7W	14-J	5	0.09535	120.560 ±	1.985	Ma	13.449	±	0.23
6	68-06 1.8W	14-J	6	0.22662	124.069 ±	0.203	Ma	13.854	±	0.02
7	68-07 1.9W	14-J	7	0.24929	123.132 ±	0.555	Ma	13.746	±	0.06
8	68-08 1.9W	14-J	8	0.28170	122.627 ±	0.463	Ma	13.687	±	0.05
9	68-09 2.0W	14-J	9	0.31806	123.651 ±	0.416	Ma	13.806	±	0.05
10	68-10 3.5W	flas	10	0.38155	143.869 ±	0.480	Ma	16.154	±	0.06
11	68-11 4.5W	20kH	11	0.49860	140.201 ±	0.476	Ma	15.726	±	0.06
12	68-12 4.5W	20kH	12	0.59537	140.006 ±	0.303	Ma	15.704	±	0.04
13	68-13 4.5W	10-6	13	0.83222	137.744 ±	0.246	Ma	15.440	±	0.03
14	68-14 4.5W	20kH	14	0.88084	135.922 ±	0.382	Ma	15.228	±	0.04
15	68-15 4.5W	20kH	15	0.92234	137.989 ±	0.368	Ma	15.469	±	0.04
16	68-16 4.5W	20kh	16	0.95319	137.110 ±	0.472	Ma	15.366	±	0.05
17	68-17 4.5W	20kH	17	0.99993	141.852 ±	0.351	Ma	15.919	±	0.04
18	68-18 4.5W	20kH	18	1.00000	158.621 ±	120.693	Ma	17.885	±	14.22

No	Name	Cum 36S	40Ar / 36Ar		40ArAcc/g	37Ca / 39K	
1	68-01 1.5W 21-D	0.22489	544.22 ±	11.95	1.8E-0011	-147.508 ±	541.088 m
2	68-02 1.5W 21-D	0.32114	851.39 ±	45.22	7.9E-0012	91.077 ±	53.608 m
3	68-03 1.5W 21-D	0.50854	6932.83 ±	213.85	1.5E-0011	10.254 ±	1.282 m
4	68-04 1.6W 21-D	0.53600	11194.79 ±	1750.50	2.2E-0012	28.709 ±	11.705 m
5	68-05 1.7W 14-J	0.51965	-4936.49 ±	1450.80	-1.3E-0012	-261.835 ±	165.571 m
6	68-06 1.8W 14-J	0.59430	29474.75 ±	2324.34	6.1E-0012	1.439 ±	5.326 m
7	68-07 1.9W 14-J	0.59244	-200404.49 ±	570018.14	-1.5E-0013	5.858 ±	12.619 m
8	68-08 1.9W 14-J	0.60945	31544.31 ±	10137.87	1.4E-0012	7.197 ±	8.420 m
9	68-09 2.0W 14-J	0.64632	16602.27 ±	2273.53	3.0E-0012	12.127 ±	7.558 m
10	68-10 3.5W flas	0.70413	21544.32 ±	2080.64	4.7E-0012	12.748 ±	4.738 m
11	68-11 4.5W 20kH	0.75862	40751.50 ±	19311.29	4.5E-0012	15.044 ±	2.844 m
12	68-12 4.5W 20kH	0.84390	21638.87 ±	1955.13	7.0E-0012	16.231 ±	1.441 m
13	68-13 4.5W 10-6	0.92007	57798.72 ±	11652.66	6.2E-0012	8.758 ±	1.546 m
14	68-14 4.5W 20kH	0.94679	33483.64 ±	7412.60	2.2E-0012	14.487 ±	4.486 m
15	68-15 4.5W 20kH	0.97081	32294.72 ±	7623.08	2.0E-0012	14.125 ±	5.202 m
16	68-16 4.5W 20kh	0.98550	38947.29 ±	13805.49	1.2E-0012	21.069 ±	7.468 m
17	68-17 4.5W 20kH	0.98775	396788.55 ±	660101.10	1.8E-0013	7.280 ±	2.357 m
18	68-18 4.5W 20kH	1.00000	414.39 ±	131.29	1.0E-0012	1.139 ±	2.509

DP12-112 P59-068 muscovite

No	38Cl / 39K				40Ar* Vol ccNTP/g					Atm Cont	F1	F2
1	-4.595	±	30.747	m	15.46	±	0.41	E-12 (	2.7%)	54.2979%	0.000105	0.000291
2	16.135	±	5.094	m	14.79	±	0.42	E-12 (	2.9%)	34.7080%	-0.000065	0.000258
3	1.982	±	0.266	m	343.88	±	1.79	E-12 (	0.5%)	4.2623%	-0.000007	0.001217
4	1.083	±	0.746	m	82.74	±	0.56	E-12 (	0.7%)	2.6396%	-0.000020	0.007014
5	3.875	±	1.943	m	23.64	±	0.41	E-12 (	1.7%)	-5.9860%	0.000187	0.027854
6	1.774	±	0.286	m	602.23	±	3.11	E-12 (	0.5%)	1.0026%	-0.000001	0.000845
7	2.217	±	0.746	m	103.16	±	0.68	E-12 (	0.7%)	-0.1475%	-0.000004	0.024489
8	913.685	±	439.686	µ	146.90	±	0.87	E-12 (	0.6%)	0.9368%	-0.000005	0.004565
9	1.657	±	0.580	m	166.23	±	0.95	E-12 (	0.6%)	1.7799%	-0.000009	0.003978
10	1.701	±	0.310	m	339.64	±	1.89	E-12 (	0.6%)	1.3716%	-0.000009	0.004654
11	961.417	±	241.498	µ	609.51	±	3.72	E-12 (	0.6%)	0.7251%	-0.000011	0.010687
12	1.494	±	0.248	m	503.25	±	2.63	E-12 (	0.5%)	1.3656%	-0.000012	0.006114
13	1.039	±	0.137	m	1.21	±	0.01	E-9 (	0.5%)	0.5113%	-0.000006	0.009025
14	1.044	±	0.351	m	245.16	±	1.38	E-12 (	0.6%)	0.8825%	-0.000010	0.008734
15	777.270	±	543.492	µ	212.57	±	1.18	E-12 (	0.6%)	0.9150%	-0.000010	0.008088
16	924.607	±	442.054	µ	157.00	±	0.92	E-12 (	0.6%)	0.7587%	-0.000015	0.014576
17	1.148	±	0.253	m	246.39	±	1.31	E-12 (	0.5%)	0.0745%	-0.000005	0.048212
18	309.835	±	129.317	m	402.62	±	317.36	E-15	(78.8%)	71.3091%	-0.000813	0.001301

Integrated Results:

Age = 135.438 ± 0.596 Ma   Wt. Mean Age = 133.48 ± 45.88 Ma (510.04)

40Ar* / 39K = 15.172 ± 0.029   Total 39K Vol = 3.3113E-0010 ccNTP/g

Total 40Ar* Vol = 5.024 ± 0.009 E-9

(40Ar / 36Ar)sam = 18466.37 ± 680.97   Total Atm 40Ar Vol = 8.1700E-0011 ccNTP/g

(36Ar / 40Ar)sam = 0.00005415 ±0.00000280   Corr 36/40 & 39/40 ratios =-0.508074
(37Ar / 40Ar)sam = 0.00060150 ±0.00011341   Corr 36/40 & 37/40 ratios =-0.013494
(39Ar / 40Ar)sam = 0.06485726 ±0.00005254   Corr 37/40 & 39/40 ratios =0.001489

37Ca / 39K = 9.274 ± 1.749 E-3   38Cl / 39K = 1.354 ± 0.101 E-3
Ca / K = 1.702 ± 0.321 E-2   Cl / K = 2.843 ± 0.211 E-4
F1 = -6.615 E-6   F2 = 3.087 E-3

DP12-125 P59-080 muscovite

Fractions:

No	Name		Temp		Cum 39K	Age			40Ar* / 39K		
1	80-01	1.5W	21-J	1	0.00163	21.809 ±	41.383	Ma	2.367	±	4.52
2	80-02	1.6W	21-J	2	0.00190	-60.240 ±	235.881	Ma	-6.391	±	24.61
3	80-03	1.7W	21-J	3	0.00642	44.959 ±	11.470	Ma	4.911	±	1.27
4	80-04	3.5W	21-J	4	0.00937	64.792 ±	18.568	Ma	7.116	±	2.08
5	80-05	4.4W	20kH	5	0.15108	67.513 ±	0.470	Ma	7.420	±	0.05
6	80-06	4.5W	20kH	6	0.26407	69.121 ±	0.431	Ma	7.601	±	0.05
7	80-07	4.5W	20kH	7	0.31340	70.765 ±	1.028	Ma	7.785	±	0.12
8	80-08	4.5W	30kh	8	0.49087	71.151 ±	0.385	Ma	7.828	±	0.04
9	80-09	4.5W	20kH	9	0.54511	69.407 ±	1.051	Ma	7.633	±	0.12
10	80-10	4.5W	20kH	10	0.57113	68.396 ±	1.914	Ma	7.519	±	0.21
11	80-11	4.5W	20kH	11	0.99572	72.871 ±	0.197	Ma	8.021	±	0.02
12	80-12	4.5W	20kH	27	1.00000	174.525 ±	15.533	Ma	19.766	±	1.85

No	Name			Cum 36S	40Ar / 36Ar		40ArAcc/g		37Ca / 39K	
1	80-01	1.5W	21-J	0.07264	299.67±	8.07	1.5E-0011	474.049 ±	514.885	m
2	80-02	1.6W	21-J	0.07827	271.90±	83.54	1.2E-0012	-1.943 ±	5.458	
3	80-03	1.7W	21-J	0.10380	363.61±	21.60	5.3E-0012	53.696 ±	318.902	m
4	80-04	3.5W	21-J	0.10703	804.92±	403.68	6.7E-0013	-43.281 ±	476.336	m
5	80-05	4.4W	20kH	0.18292	1381.56±	34.74	1.6E-0011	10.042 ±	10.004	m
6	80-06	4.5W	20kH	0.19155	8090.78±	1257.68	1.8E-0012	8.761 ±	6.853	m
7	80-07	4.5W	20kH	0.19282	23978.64±	27725.57	2.6E-0013	13.497 ±	10.834	m
8	80-08	4.5W	30kh	0.31730	1170.21±	17.10	2.6E-0011	25.755 ±	3.893	m
9	80-09	4.5W	20kH	0.32154	7955.57±	3048.36	8.8E-0013	53.518 ±	38.600	m
10	80-10	4.5W	20kH	0.32469	5151.88±	2365.19	6.6E-0013	145.916 ±	58.434	m
11	80-11	4.5W	20kH	0.53039	1593.17±	14.81	4.3E-0011	23.502 ±	3.747	m
12	80-12	4.5W	20kH	1.00000	309.63±	1.37	9.7E-0011	44.687 ±	157.152	m

No	38Cl		/ 39K		40Ar*	Vol		ccNTP/g		Atm Cont	F1	F2
1	46.751	±	25.646	m	212.60	± 405.83		E-15	(190.9%)	98.6091%	-0.000338	0.000105
2	-214.614	±	253.312	m	-93.26	±-358.76		E-15	(384.7%)	108.6781%	0.001386	0.000620
3	-42.160	±	22.549	m	1.22	±	0.32	E-12	(25.8%)	81.2689%	-0.000038	0.000170
4	-24.747	±	22.949	m	1.16	±	0.34	E-12	(29.1%)	36.7117%	0.000031	0.000836
5	2.920	±	0.520	m	57.87	±	0.49	E-12	(0.9%)	21.3889%	-0.000007	0.000403
6	1.402	±	0.711	m	47.27	±	0.37	E-12	(0.8%)	3.6523%	-0.000006	0.002498
7	0.487	±	1.049	m	21.14	±	0.32	E-12	(1.5%)	1.2323%	-0.000010	0.011333
8	1.356	±	0.383	m	76.46	±	0.54	E-12	(0.7%)	25.2518%	-0.000018	0.000785
9	1.362	±	2.097	m	22.79	±	0.36	E-12	(1.6%)	3.7144%	-0.000038	0.014747
10	3.322	±	3.114	m	10.77	±	0.31	E-12	(2.8%)	5.7358%	-0.000104	0.025554
11	1.296	±	0.310	m	187.44	±	1.03	E-12	(0.6%)	18.5479%	-0.000017	0.001044
12	5.603	±	11.379	m	4.66	±	0.43	E-12	(9.3%)	95.4373%	-0.000032	0.000023

Integrated Results:

Age = 71.159 ± 0.378 Ma Wt. Mean Age = 71.47 ± 2.86 Ma (18.88)

40Ar* / 39K = 7.829 ± 0.031

Total 39K Vol = 5.5037E-0011 ccNTP/g

Total 40Ar* Vol = 4.309 ± 0.017 E-10

(40Ar / 36Ar)sam = 909.10 ± 5.37

Total Atm 40Ar Vol = 2.0751E-0010 ccNTP/g

(36Ar / 40Ar)sam = 0.00109999 ±0.00000783

(37Ar / 40Ar)sam = 0.00214599 ±0.00038462

(39Ar / 40Ar)sam = 0.08621041 ±0.00018570

Corr 36/40 & 39/40 ratios =-0.484520

Corr 36/40 & 37/40 ratios =-0.019545

Corr 37/40 & 39/40 ratios =0.008483

37Ca / 39K = 2.489 ± 0.446 E-2

Ca / K = 4.568 ± 0.819 E-2

F1 = -1.776 E-5

38Cl / 39K = 1.327 ± 0.282 E-3

Cl / K = 2.787 ± 0.592 E-4

F2 = 5.271 E-4